VOLUME 35 | SUPPLEMENT 2 | MARCH 2022

MODERN PATHOLOGY

ABSTRACTS (522–659)

GENITOURINARY PATHOLOGY (INCLUDING RENAL TUMORS)

2022

USCAP 111TH ANNUAL MEETING

REAL INTELLIGENCE

MARCH 19–24, 2022 LOS ANGELES, CALIFORNIA

Published by
SPRINGER NATURE
www.ModernPathology.org

USCAP Creating a Better Pathologist
AN OFFICIAL JOURNAL OF THE UNITED STATES AND CANADIAN ACADEMY OF PATHOLOGY

EDUCATION COMMITTEE

Rhonda K. Yantiss
Chair

Kristin C. Jensen
Chair, CME Subcommittee

Laura C. Collins
Chair, Interactive Microscopy Subcommittee

Yuri Fedoriw
Short Course Coordinator

Ilan Weinreb
Chair, Subcommittee for Unique Live Course Offerings

Carla L. Ellis
Chair, DEI Subcommittee

Adebowale J. Adeniran
Kimberly H. Allison
Sarah M. Dry
William C. Faquin
Karen J. Fritchie
Jennifer B. Gordetsky
Levon Katsakhyan, Pathologist-in-Training
Melinda J. Lerwill
M. Beatriz S. Lopes
Julia R. Naso, Pathologist-in-Training
Liron Pantanowitz
Carlos Parra-Herran
Rajiv M. Patel
Charles "Matt" Quick
David F. Schaeffer
Lynette M. Sholl
Olga K. Weinberg
Maria Westerhoff

ABSTRACT REVIEW BOARD

Benjamin Adam
Oyedele Adeyi
Mariam Priya Alexander
Daniela Allende
Catalina Amador
Vijayalakshmi Ananthanarayanan
Tatjana Antic
Manju Aron
Roberto Barrios
Gregory R. Bean
Govind Bhagat
Luis Zabala Blanco
Michael Bonert
Alain C. Borczuk
Tamar C. Brandler
Eric Jason Burks
Kelly J. Butnor
Sarah M. Calkins
Weibiao Cao
Wenqing (Wendy) Cao
Barbara Ann Centeno
Joanna SY Chan
Kung-Chao Chang
Hao Chen
Wei Chen
Yunn-Yi Chen
Sarah Chiang
Soo-Jin Cho
Shefali Chopra
Nicole A. Cipriani
Cecilia Clement
Claudiu Cotta
Jennifer A. Cotter
Sonika M. Dahiya
Elizabeth G. Demicco
Katie Dennis
Jasreman Dhillon
Anand S. Dighe
Bojana Djordjevic
Michelle R. Downes
Charles G. Eberhart
Andrew G. Evans
Fang Fan
Julie C. Fanburg-Smith
Gelareh Farshid
Michael Feely
Susan A. Fineberg
Dennis J. Firchau
Gregory A. Fishbein
Agnes B. Fogo
Andrew L. Folpe
Danielle Fortuna
Billie Fyfe-Kirschner
Zeina Ghorab
Giovanna A. Giannico
Anthony J. Gill
Tamar A. Giorgadze
Alessio Giubellino
Carolyn Glass
Carmen R. Gomez-Fernandez
Shunyou Gong
Purva Gopal
Abha Goyal
Christopher C. Griffith
Ian S. Hagemann
Gillian Leigh Hale
Suntrea TG Hammer
Malini Harigopal
Kammi J. Henriksen
Jonas J. Heymann
Carlo Vincent Hojilla
Aaron R. Huber
Jabed Iqbal
Shilpa Jain
Vickie Y. Jo
Ivy John
Dan Jones
Ridas Juskevicius
Meghan E. Kapp
Nora Katabi
Francesca Khani
Joseph D. Khoury
Benjamin Kipp
Veronica E. Klepeis
Christian A. Kunder
Stefano La Rosa
Stephen M. Lagana
Keith K. Lai
Goo Lee
Michael Lee
Vasiliki Leventaki
Madelyn Lew
Faqian Li
Ying Li
Chieh-Yu Lin
Mikhail Lisovsky
Lesley C. Lomo
Fang-I Lu
aDeqin Ma
Varsha Manucha
Rachel Angelica Mariani
Brock Aaron Martin
David S. McClintock
Anne M. Mills
Richard N. Mitchell
Hiroshi Miyamoto
Kristen E. Muller
Priya Nagarajan
Navneet Narula
Michiya Nishino
Maura O'Neil
Scott Roland Owens
Burcin Pehlivanoglu
Deniz Peker Barclift
Avani Anil Pendse
Andre Pinto
Susan Prendeville
Carlos N. Prieto Granada
Peter Pytel
Stephen S. Raab
Emilian V. Racila
Stanley J. Radio
Santiago Ramon Y Cajal
Kaaren K Reichard
Jordan P. Reynolds
Lisa M. Rooper
Andrew Eric Rosenberg
Ozlen Saglam
Ankur R. Sangoi
Kurt B. Schaberg
Qiuying (Judy) Shi
Wonwoo Shon
Pratibha S. Shukla
Gabriel Sica
Alexa Siddon
Anthony Sisk
Kalliopi P. Siziopikou
Stephanie Lynn Skala
Maxwell L. Smith
Isaac H. Solomon
Wei Song
Simona Stolnicu
Adrian Suarez
Paul E. Swanson
Benjamin Jack Swanson
Sara Szabo
Gary H. Tozbikian
Gulisa Turashvili
Andrew T. Turk
Efsevia Vakiani
Paul VanderLaan
Hanlin L. Wang
Stephen C. Ward
Kevin M. Waters
Jaclyn C. Watkins
Shi Wei
Hannah Y. Wen
Kwun Wah Wen
Kristy Wolniak
Deyin Xing
Ya Xu
Shaofeng N. Yan
Zhaohai Yang
Yunshin Albert Yeh
Huina Zhang
Xuchen Zhang
Bihong Zhao
Lei Zhao

To cite abstracts in this publication, please use the following format: **Author A, Author B, Author C, et al. Abstract title (abs#). In "File Title."** ***Modern Pathology*** **2022; 35 (suppl 2): page#**

522 Clear Cell Adenocarcinoma of the Lower Urinary Tract: A Multi-Institutional Comprehensive Study with Emphasis on Unusual Pathological Features and Clinical Outcomes

Eman Abdulfatah[1], Khaleel Al-Obaidy[2], Roni Cox[3], Christopher Przybycin[3], Muhammad Idrees[4], Lakshmi Kunju[5], Angela Wu[1]

[1]Michigan Medicine, University of Michigan, Ann Arbor, MI, [2]Cleveland Clinic Foundation, Cleveland, OH, [3]Cleveland Clinic, Cleveland, OH, [4]Indiana University School of Medicine, Indianapolis, IN, [5]University of Michigan, Ann Arbor, MI

Disclosures: Eman Abdulfatah: None; Khaleel Al-Obaidy: None; Roni Cox: None; Christopher Przybycin: None; Muhammad Idrees: None; Lakshmi Kunju: None; Angela Wu: None

Background: Clear cell adenocarcinoma (CCA) of the lower urinary tract is a rare generally aggressive adenocarcinoma that arises in the bladder or urethra, more commonly in women. Here in, we report the immunomorphologic features and clinical findings/outcomes in a multi-institutional series of CCAs.

Design: All patients diagnosed with CCA (2000 -2020) at three institutions were identified. H&E and previously performed IHC slides were reviewed by 3 GU pathologists. Clinical and follow-up data were obtained.

Results: 24 CCA patients (16 biopsies/TURs and 8 resections, median age 62(range 37-89) years, F:M 3:1) were included. Primary sites included urethra and urinary bladder(6), urethra only(12) and bladder only(6). Bladder neck was the most common site involved in the bladder; 2 involved a diverticulum and 2 involved the prostatic urethra. Gross hematuria was the most common presenting symptom(80%) and on cystoscopy 70% had a polypoid mass. 2 patients(8%) had a history of endometriosis; none had a history of urothelial carcinoma(UC). Histologically, none of the cases showed concurrent UC; only 1 had concurrent endometriosis. Nine tumors(38%) exhibited the classical triad of tubulocystic, papillary and solid architecture. Unusual features included micropapillary architecture (4,17%), prominent cherry red nucleoli (FH-like nucleoli) (14,58%), and nephrogenic adenoma-like foci (6,25%). Other histologic features included eosinophilic cells (24,100%), clear cells (23,95%) and hobnail cells (15,63%), marked nuclear pleomorphism (12,50%), mucinous background (7,29%), necrosis (7,29%) and mitotic figures (average 7, range 1-32/10 HPF). For cases with available IHC (17,71%), all (100%) expressed CK7, PAX-8 and Napsin A and all were negative for GATA-3 and p63. Additional IHC and sequencing are currently being performed. Clinical stages were stage II(37%), stage III(37%) and stage IV(26%). Of the 23 patients with follow up (mean 27 months), the majority underwent resection only(n=9) or chemotherapy only(n=7), and 9(37.5%) recurred after therapy. 9(39%) are ANED, 5(22%) are AWD and 9(39%) are DOD.

Conclusions: CCA share similar immunohistologic features with CCAs of the female genital tract but are not frequently associated with endometriosis. None of our cases were associated with prior/concurrent UC. A subset(25%) showed nephrogenic adenoma-like foci. Unusual morphologic features included prominent cherry-red nucleoli. The majority presented at high stage and a high proportion recurred and/or DOD.

523 Comprehensive Profiling of Neuroendocrine Carcinomas of the Bladder with Expanded Neuroendocrine Markers ASCL1, NEUROD1, POU2F3, YAP1 and DLL3

Dilara Akbulut[1], Liwei Jia[2], Gamze Gokturk Ozcan[1], Jatin Gandhi[3], Rayan Rammal[4], Jie-Fu Chen[1], Judy Sarungbam[1], Bin Xu[1], S. Joseph Sirintrapun[1], Samson Fine[1], Ying-Bei Chen[1], Marina Baine[1], Natasha Rekhtman[1], Anuradha Gopalan[1], Satish Tickoo[1], Victor Reuter[1], Hikmat Al-Ahmadie[1]

[1]Memorial Sloan Kettering Cancer Center, New York, NY, [2]UT Southwestern Medical Center, Dallas, TX, [3]University of Washington, Seattle, WA, [4]University of Pittsburgh Medical Center, Pittsburgh, PA

Disclosures: Dilara Akbulut: None; Liwei Jia: None; Gamze Gokturk Ozcan: None; Jatin Gandhi: None; Rayan Rammal: None; Jie-Fu Chen: None; Judy Sarungbam: None; Bin Xu: None; S. Joseph Sirintrapun: None; Samson Fine: None; Ying-Bei Chen: None; Marina Baine: None; Natasha Rekhtman: None; Anuradha Gopalan: None; Satish Tickoo: None; Victor Reuter: None; Hikmat Al-Ahmadie: None

Background: Distinct subtypes of small cell carcinoma (SmCC) of the lung have been recently identified by expression of transcriptional regulators (NEUROD1, ASCL1, POU2F3, YAP1). DLL3 overexpression in neuroendocrine (NE) carcinomas has been suggested as a potential therapeutic target. We aimed to analyze the expression of these novel NE markers and that of traditional NE markers CD56, synaptophysin (SYP) and chromogranin (CHR) in a large cohort of NE carcinoma of the bladder.

Design: We identified 98 SmCC and 19 large cell neuroendocrine carcinomas (LCNEC), 34 of which co-existed with a non-NE component (24 NOS, 2 micropapillary, 1 glandular, 3 squamous, 3 plasmacytoid, 1 sarcomatoid). Cases were assembled in tissue

microarray blocks. IHC for NE markers CD56, SYP, CHR, INSM1, NEUROD1, ASCL1, POU2F3, YAP1 and DLL3 was performed. Co-expression patterns and morphologic correlations were analyzed.

Results: Detailed results are in Table 1. Based on the expression of ASCL1, NEUROD1 and POU2F3, SmCC of bladder can be divided into five patterns: ASCL1+/NEUROD1- (n=31; 32%), ASCL1-/NEUROD1+ (n=20; 20%), ASCL1+/NEUROD1+ (n=20; 20%), POU2F3+ (n=19, 20%), and ASCL1-/NEUROD1-/POU2F3- (n=8, 8%). POU2F3+ tumors were mutually exclusive of ASCL1 and NEUROD1 and were enriched with round cell morphology compared to a more spindle or oval cell morphology in POU2F3- cases (p=0.022). Expression of traditional NE markers was positively correlated with ASCL1 and NEUROD1 expression, and negatively correlated with POU2F3 expression (p<0.05). Compared to SmCC, LCNEC was rarely POU2F3+ but showed similar expression of ASCL1 and NEUROD1. DLL3 expression was high in both SmCC (n=77, 79%) and LCNEC (n=16, 84%). The non-NE components were negative for all the markers except for YAP1 which showed strong expression in 33 of 34 cases (97%). YAP1 expression in SmCC and LCNEC (n=29, 30% and n=10, 53%, respectively) was negatively correlated with all NE markers (p<0.05).

Pattern	SmCC n=98 (%)	LCNEC n=19 (%)	Non-NE components n=34 (%)
ASCL1+/NEUROD1-	31 (32%)	5 (26%)	0
ASCL1-/NEUROD1+	20 (20%)	7 (37%)	0
ASCL1+/NEUROD1+	20 (20%)	3 (16%)	0
POU2F3+ (ASCL1-/NEUROD1-)	19 (20%)	1 (5%)	0
ASCL1-/NEUROD1-/POU2F3-	8 (8%)	3 (16%)	34 (100%)
SYN	89 (90%)	18 (95%)	0
CHR	65 (66%)	14 (74%)	0
CD56	91 (93%)	17 (90%)	0
INSM1	81 (83%)	15 (79%)	0
YAP1	29 (30%)	10 (53%)	33 (97%)
DLL3	77 (79%)	16 (84%)	0

Conclusions: SmCC of bladder can be divided into distinct subgroups based on the expression of ASCL1 followed by NEUROD1 and POU2F3. POU2F3+ tumors represent an ASCL1-/NEUROD1- subset with lower expression of traditional NE markers. Except for YAP1, the expression of these markers is restricted to NE components in mixed tumors. The expression of these markers is similar in SmCC and LCNEC. DLL3, a potential therapeutic target, is expressed at high levels in both SmCC and LCNEC. Clinical correlation with these expression patterns is underway.

524 Challenges In Classifying Renal Cell Carcinomas: A Single Institution Experience

Adesola Akinyemi[1], Ansa Mehreen[2], Hussein Alnajar[3]
[1]University of Chicago Medical Center/NorthShore University HealthSystem, Evanston, IL, [2]University of Chicago NorthShore, Evanston, IL, [3]NorthShore University HealthSystem, Evanston, IL

Disclosures: Adesola Akinyemi: None; Ansa Mehreen: None; Hussein Alnajar: None

Background: The classification of renal cell carcinoma(RCC) has been going through continual changes driven by genomic profiling and morphological correlation that have provided valuable insights into tumor biology. Nevertheless, some RCCs remain difficult to subtype and are diagnosed as unclassified RCC(uRCC). uRCCs are a histologically heterogeneous category of tumors, many of which are high-grade and high-stage tumors with poor outcomes. Although all none clear-cell RCCs(cRCC) are commonly categorized under one therapeutic category, the treatment and prognosis of the specific subtypes vary. This study attempts to retrospectively examine uRCCs using our current knowledge and identify some of the challenges encountered in classifying them.

Design: Our records were reviewed for renal specimens diagnosed as uRCC between January 2009 and January 2021. IHC for cytokeratin AE1/AE3, CK7, CD10, CAIX, AMACR, Melan-A, HMB45, PAX8, Fumarate hydratase, Succinate dehydrogenase-B, and TFE3 were then performed as necessary to further categorize these cases. The results of the IHCs were evaluated along with the morphology and the cases were reclassified, when possible.

Results: 27 uRCCs cases were identified (4% of total RCCs). 59% of the cases showed high-grade morphology and the low-grade cases were predominantly eosinophilic (55%) and cystic (45%). We were able to reclassify 16 cases, while 11 remained unclassifiable. Most of the cases were reclassified into one of the traditional subtypes, while 4 fell under one of the emerging novel and provisional entities (Figure.1). The majority of cases (59%)were stage 1, (4%)were stage 2, and 10 (37%)were stage 3. The majority of the reclassified cases were stage 1 (69%) and showed low-grade histology (69%). Of the cases that remained uRCC, 45% were stage 1 and 55% were stage 3 and they all showed high-grade histology.

Table 1. Characteristics of RCCs Following Reclassification

Case number	Age (years)	Gender (F = Female; M = Male)	Diagnosis	Histology: Eosinophilic = e; Cystic = c; High grade = h	Stage (1-4)
2	69	M	Chromophobe Renal Cell Carcinoma	e	1
34	47	M	Chromophobe Renal Cell Carcinoma	e	1
3	67	F	Clear Cell Papillary Renal Cell Carcinoma	c	1
8	65	M	Clear Cell Renal Cell Carcinoma	h	1
19	52	M	Clear Cell Renal Cell Carcinoma	h	3
27	47	M	Clear Cell Renal Cell Carcinoma	h	3
10	54	F	Eosinophilic Solid and Cystic Renal Cell Carcinoma	e	2
32	73	M	Hybrid Oncocytic/Chromophobe Tumors	e	1
28	78	F	Low-grade Oncocytic Tumor	e	1
30	81	M	Malignant Mixed Epithelial Stromal Tumor	c	3
25	43	M	Multilocular Cystic Renal Neoplasm of Low Malignant Potential	c	1
18	50	F	Papillary Renal Cell Carcinoma	e	1
4	69	F	Papillary Renal Cell Carcinoma	h	1
39	58	M	Papillary Renal Cell Carcinoma	h	1
7	69	M	Renal Cell Carcinoma with Leiomyomatous Stroma	c	1
11	75	M	Renal Cell Carcinoma with Leiomyomatous Stroma	c	3
23	60	M	Unclassified Renal Cell Carcinoma	h	1
26	66	M	Unclassified Renal Cell Carcinoma	h	1
31	63	F	Unclassified Renal Cell Carcinoma	h	1
33	63	M	Unclassified Renal Cell Carcinoma	h	1
36	45	M	Unclassified Renal Cell Carcinoma	h	1
9	72	F	Unclassified Renal Cell Carcinoma	h	3
13	57	M	Unclassified Renal Cell Carcinoma	h	3
16	66	F	Unclassified Renal Cell Carcinoma	h	3
21	66	M	Unclassified Renal Cell Carcinoma	h	3
37	37	M	Unclassified Renal Cell Carcinoma	h	3
38	77	M	Unclassified Renal Cell Carcinoma	h	3

Figure 1 - 524

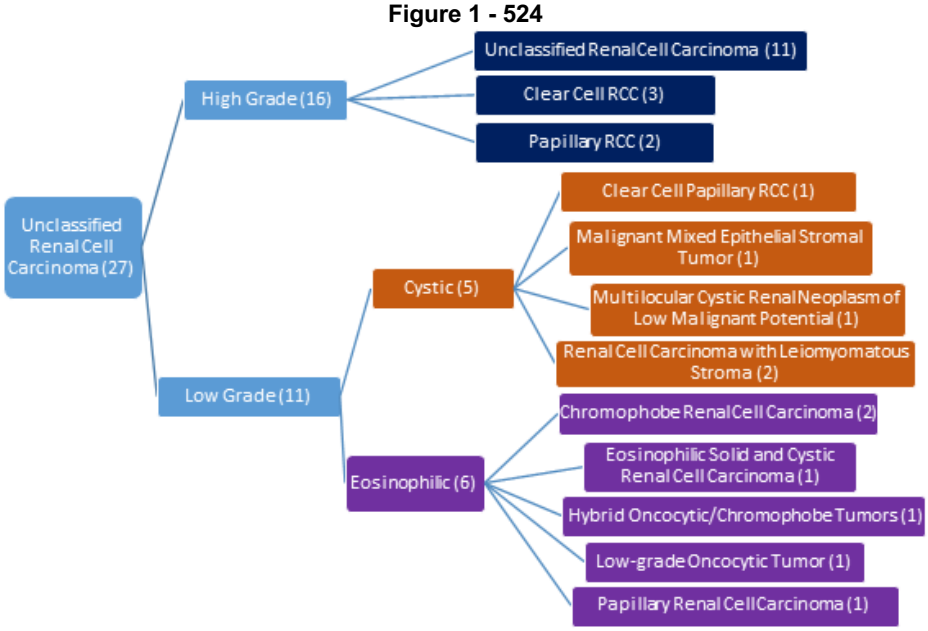

Conclusions: Our limited study suggests that similar to previous studies, challenges in subtyping renal tumors often involve tumors with cystic, eosinophilic and high grade/sarcomatoid histology. However, recognizing the major morphologic patterns and cell types across the tumor aided by judicious use of a broader range of IHCs may help classify all low-grade tumors into a more definitive category. This can be more challenging in high-grade tumors and the focus should be on finding a minor component of conventional cRCC which can affect future treatment choices. More advanced techniques (FISH or sequencing) might be needed to further classify these cases.

525 Acquired Cystic Disease-Associated Renal Cell Carcinoma: A Clinicopathologic and Molecular Study of 30 Cases

Khaleel Al-Obaidy[1], Ahmad Alkashash[2], Sean Williamson[3], Liang Cheng[2], Muhammad Idrees[4]
[1]Cleveland Clinic Foundation, Cleveland, OH, [2]Indiana University, Indianapolis, IN, [3]Cleveland Clinic, Cleveland, OH, [4]Indiana University School of Medicine, Indianapolis, IN

Disclosures: Khaleel Al-Obaidy: None; Ahmad Alkashash: None; Sean Williamson: None; Liang Cheng: None; Muhammad Idrees: None

Background: Acquired cystic disease-associated renal cell carcinoma (ACD-RCC) is a distinct renal tumor reported exclusively in patients with end-stage kidney disease & the incidence increases with dialysis duration. Recent studies documented the presence of mTOR and/or TSC mutations in these tumors. We studied the clinicopathologic and molecular characteristics of ACD-RCC

Design: 30 ACD-RCC were included in this study. The H&E stained slides were reviewed, and 8 tumors underwent next-generation sequencing. Follow-up information was obtained from patients' electronic records

Results: The cohort comprised 25 men, and 5 women, with an age range of 24-84 yrs (median 58 yrs.) and tumor size range of 5-40 mm (median 16 mm). All patients had a clinical diagnosis of end-stage kidney disease and histologic evidence of acquired cystic disease and calcium oxalate crystals, meeting our minimum criteria. Seven patients had multiple tumors of similar or different histology, including renal oncocytoma, clear cell RCC, papillary RCC, unclassified RCC or multifocal ACD-RCC. Histologically, most tumors showed dominant sieve-like architecture, with few areas showing mixed sieve-like and papillary architectures. Papillary and microcystic architectures were predominant in few tumors, while one showed papillary renal cell carcinoma morphology with no sieve-like architecture. The cells had invariably abundant eosinophilic cytoplasm with cytoplasmic vacuolization and nuclear atypia with prominent nucleoli in the majority of cases (WHO/ISUP grades 2-3). One tumor had areas of significant nuclear atypia (WHO/ISUP grades 4). NGS showed no recurrent mutations in our analyzed tumors, and none was found to have mTOR or TSC mutations. Interestingly, however, one case showed frameshift deletion in SMARCB1 and duplication in NF1 genes. One tumor also had frameshift duplication in the BRCA2 gene, leading to truncated proteins with predicated loss of function. No other pathogenic mutations were detected. Copy number alterations (CNAs) showed gains in ch.16 in 5 tumors, followed by gains in ch.17(n=2) and ch.8(n=2). No CNAs were identified in 2 tumors. One tumor had complex CNAs. No correlation between CNA and histology was identified. No evidence of disease at 29 months of median follow-up

Conclusions: ACD-RCC is heterogeneous with frequent gains of ch.16; however, no histologic/ molecular correlation was identified. Additional studies are still needed to further characterize its molecular nature.

526 Low-grade Oncocytic Tumor (LOT) of The Kidney: Histomorphologic, Immunohistochemical, and Molecular Characterization of 53 Cases

Mohammed Alghamdi[1], Jie-Fu Chen[1], Judy Sarungbam[1], S. Joseph Sirintrapun[1], Anuradha Gopalan[1], Hikmat Al-Ahmadie[1], Samson Fine[1], Satish Tickoo[1], Victor Reuter[1], Ying-Bei Chen[1]
[1]Memorial Sloan Kettering Cancer Center, New York, NY

Disclosures: Mohammed Alghamdi: None; Jie-Fu Chen: None; Judy Sarungbam: None; S. Joseph Sirintrapun: None; Anuradha Gopalan: None; Hikmat Al-Ahmadie: None; Samson Fine: None; Satish Tickoo: None; Victor Reuter: None; Ying-Bei Chen: None

Background: Renal low-grade oncocytic tumor (LOT) has been regarded as a provisional entity in the most recent genitourinary pathology society (GUPS) update on renal neoplasia, and few case series demonstrated consistent histologic and immunohistochemical (IHC) findings.

Design: We retrospectively reviewed 330 consecutive nephrectomies between 2000-2021 with a diagnosis of eosinophilic chromophobe (E-chRCC) or oncocytic unclassified renal cell carcinomas and identified 42 LOT tumors (41 patients). 11 cases were separately identified from other diagnosis categories or personal consults. CK7 and CD117 IHC were performed in 47 tumors with available material and molecular analysis in a subset of cases.

Results: Patients' median age was 66 years (36-89) and M:F ratio was 1:2.3. All patients had localized disease (92% pT1) with a median tumor size of 3.5 cm (1.0-12.0). No recurrence or metastasis was observed during a median follow-up period of 9.8 years (0.2-24). One patient had a second tumor excised from the contralateral kidney 10 years after the initial diagnosis. We noted variations in cytoplasmic quality, including densely eosinophilic (predominant), markedly vacuolated, and variably amphophilic.

Densely packed small nests, perinuclear halos, and negative CD117 were present in all cases, while diffuse and strong CK7 positivity, an abrupt transition to central stromal edema, and smooth nuclear membranes, were present in most cases (Fig. 1). 5 of 6 tumors had a flat genome by copy number analysis; one case showed chromosome 7 gain. Mutations of *MTOR* (3), *RHEB* (2), and *TSC1* (1) genes were identified in these 6 tumors. Applying the current histologic and IHC criteria, 36 out of 115 (31%) E-chRCC cases were reassigned as LOT in our analysis, emphasizing a need to revisit the diagnostic criteria of E-chRCC. Review of digital slides from the TCGA chRCC cohort suggested that E-chRCC with characteristic chromosomal losses (n=11) exhibited mostly solid sheet/tubular/trabecular patterns, whereas 7 cases with small compact nests were consistent with LOT (n=4) or had atypical molecular features. Additional molecular analysis to compare LOT to E-chRCC and other cases with overlapping morphology is ongoing.

Figure 1 - 526

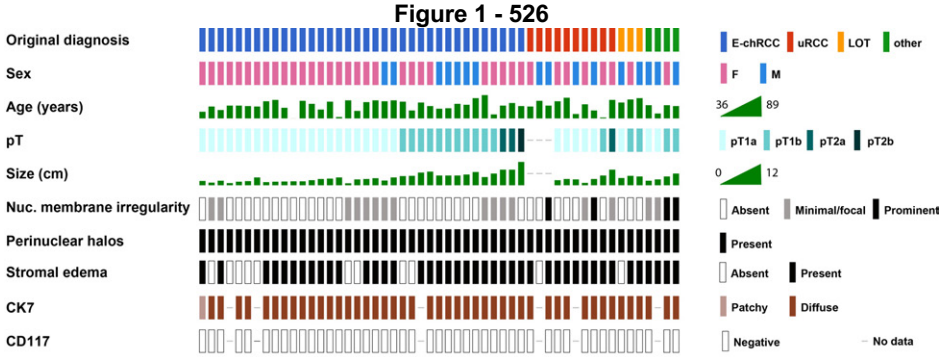

Figure 1. Clinical, morphologic, and immunohistochemical features of 53 low-grade oncocytic tumors (LOT).
E-chRCC: eosinophilic variant of chromophobe renal cell carcinoma; uRCC: unclassified renal cell carcinoma.

Conclusions: Our study analyzed the largest cohort of LOT to date and further delineated the histologic, IHC, and molecular features. The indolent behavior of these tumors highlights a need to refine the diagnostic criteria to distinguish them from E-chRCC and other oncocytic tumors with overlapping histology.

527 Malignant Germ Cell Tumors: A Large Academic Center Experience of 47 Cases in Men Aged 50 Years and Over

Fawaz Almutairi[1], Rayan Rammal[1], Sheldon Bastacky[1], Rajiv Dhir[2], Gabriela Quiroga-Garza[1]
[1]University of Pittsburgh Medical Center, Pittsburgh, PA, [2]UPMC Shadyside Hospital, Pittsburgh, PA

Disclosures: Fawaz Almutairi: None; Rayan Rammal: None; Sheldon Bastacky: None; Rajiv Dhir: None; Gabriela Quiroga-Garza: None

Background: Germ cell tumors (GCT) are the most common malignancy in men in the third and fourth decades of life, and their incidence have been increasing over the last 40 years in the United States. The occurrence of malignant GCT in men aged 50 years or over is rare, and their histopathologic characteristics and outcome is insufficiently characterized in the medical literature. Hence, we report the histopathologic features and clinical outcome of 47 cases of malignant germ cell tumors in men aged 50 years or over diagnosed at our institution.

Design: We performed a retrospective search of our database from 2005-2021 to identify men aged 50 years or older with malignant GCT. Cases of spermatocytic tumor were excluded. Clinical and histopathologic features of the tumors were reviewed and follow up data were extracted from electronic medical record (EMR).

Results: Forty-seven cases were identified. Median patient age was 56 years (range 50-79 years). Median tumor size was 4.6 cm (range 0.3-14 cm). Thirty-nine (83%) tumors were testicular while eight (17%) were non-testicular in presentation. Twenty-six (55%) of the tumors were seminomas, thirteen (28%) of the tumors were mixed GCT and two (4%) of the tumors were teratomas and five (11%) were regressed testicular germ cell tumors. Of note, one (2%) patient showed only germ cell neoplasia in situ (GCNIS) without evidence of invasive GCT component. The most common component in the mixed malignant germ cell tumors was embryonal carcinoma (77%) followed by seminoma and yolk sac tumor (62% each). GCNIS accompanied 57% of the cases. Aggressive features including lymphovascular invasion, retroperitoneal/lymph node involvement and higher stage at presentation were identified in a significant proportion of cases. Clinical follow up was available for 42 patients (89%, ranging from 1-104

months) and showed thirty-three (79%) patients had no evidence of disease, six (14%) died of disease and three (7%) died of unrelated causes.

Table 1: Histopathologic characteristics of malignant germ cell tumors in men aged 50 years or older

Diagnosis	Seminoma-26 (55%)
	Mixed germ cell tumor-13 (28%)
	Regressed germ cell tumor-5 (11%)
	Mature teratoma-2 (4%)
	Germ cell neoplasia in situ-1 (2%)
Laterality	Right-23 (49%)
	Left-20 (43%)
Adverse pathologic features:	
1.Rete Testis invasion	10 (21%)
2. Epididymis involvement	5 (11%)
3.Tunica albuginea invasion	4 (9%)
4. Lymphovascular invasion	22 (47%)
5. Spermatic cord invasion	5 (11%)
6. Margin status	Positive-3 (6%)
Associated Germ cell neoplasia in situ (GCNIS)	27 (57%)
Mixed germ cell tumor patterns	Embryonal carcinoma: present-10 (77%), predominant-7 (54%) Seminoma: present-8 (62%), predominant-2 (15%) Yolk Sac tumor: present-8 (62%), predominant-2 (15%) Teratoma: present-5 (38%), predominant-2 (15%)
Pathologic Stage	pT0-5 (11%) pTis-1 (2%) pT1-11 (23%) pT2-19 (40%) pT3-3 (6%) pN1-6 (13%) pN2-5 (11%) pM-9 (19%)

Conclusions: Conclusion: Our findings expand and corroborate the previously reported data on the malignant GCT in older men. Unique characteristics include tendency for higher stage at presentation with adverse pathologic features and more aggressive clinical course. GCT in this age group can represent a challenging entity both from the diagnostic and management standpoint and should be kept as part of the differential diagnosis for these patients.

528 Gradual and Synergistic Correlation between Tumor Thickness and Histological Grade in Penile Invasive Carcinomas. An Outcome Study of 147 Mexican Patients

Isabel Alvarado-Cabrero[1], Diego F Sanchez[2], Raquel Valencia-Cedillo[3], María José Fernandez-Nestosa[4], Sofia Canete-Portillo[5], Antonio Cubilla[2]

[1]Mexican Oncology Hospital SXXI, IMSS, Mexico City, Mexico, [2]Instituto de Patologia e Investigacion, Asuncion, Paraguay, [3]Mexican Oncology Hospital IMSS, Mexico City, Mexico, [4]Universidad Nacional de Asunción, San Lorenzo, Paraguay, [5]The University of Alabama at Birmingham, Birmingham, AL

Disclosures: Isabel Alvarado-Cabrero: None; Diego F Sanchez: None; Raquel Valencia-Cedillo: None; María José Fernandez-Nestosa: None; Sofia Canete-Portillo: None; Antonio Cubilla: None

Background: Histological grade is among the best outcome pathological predictor in penile cancer. The TNM system is based on the combination of grade and depth of infiltration of penile anatomical levels. It is assumed in general that higher grade and deep tumors carries the worst prognosis and the contrary occur with superficially invading and low-grade neoplasms. However, there is no systematic evaluation of the phenomenon.

Design: 147 patients diagnosed, treated, and followed at the Hospital de Oncologia - Instituto Mexicano del Seguro Social, from January 2000 to August 2013 were selected. All patients were treated either by total or partial penectomies. Lymph node involvement was evaluated by bilateral inguinal node dissection (126 cases) or ultrasonography (21 cases). Thickness was measured in mm from tumor surface to deepest invasion point and were classified as superficial (≤5 mm) or deep (>10 mm)

tumors. Histological grade evaluation was made according to WHO 2016 and AFIP 2020 criteria [low-grade: grades 1 (G1) and 2 (G2); high-grade: grade 3(G3)]. Correlation between grade and thickness was explored using Spearman's rank correlation test. Comparative outcome was evaluated using Fisher's exact test.

Results: Average age was 62 (26 to 98) years old. Thickness average was 15 mm (2 to 30 mm). G1, G2 and G3 tumors corresponded to 19 (13%), 48 (33%), and 80 (54%) cases, respectively. Distribution according to thickness, histological grade, positive lymph nodes, and outcome is shown in Table. Follow-up ranged from 10 to 82 months (median: 57 months). Fifty-three (36%) patients died of disease. There was a positive correlation between grade and thickness (Spearman's rho: 0.72, p-value < 2.2e-16) (Figure).

Thickness (mm)	# of cases	Low-grade (%)	High-grade (%)	Positive nodes (%)	DOD (%)
≤5	13	12 (92)	1 (8)*	0	0
5.1 – 10	37	31 (84)**	6 (16)	4 (11)	0
10.1 – 15	35	19 (54)***	16 (46)	14 (40)	10 (29)
>15	62	5 (8)****	57 (92)	55 (89)	43 (69)
Total	**147**	**67 (46)**	**80 (54)**	**73 (50)**	**53 (36)**

* negative nodes, not evidence of disease. ** 1 case with positive inguinal nodes and retroperitoneal metastasis.

*** 5 cases with positive inguinal nodes, all alive. **** 2 cases with positive inguinal nodes; 1 died of the disease (DOD).

Figure 1 - 528

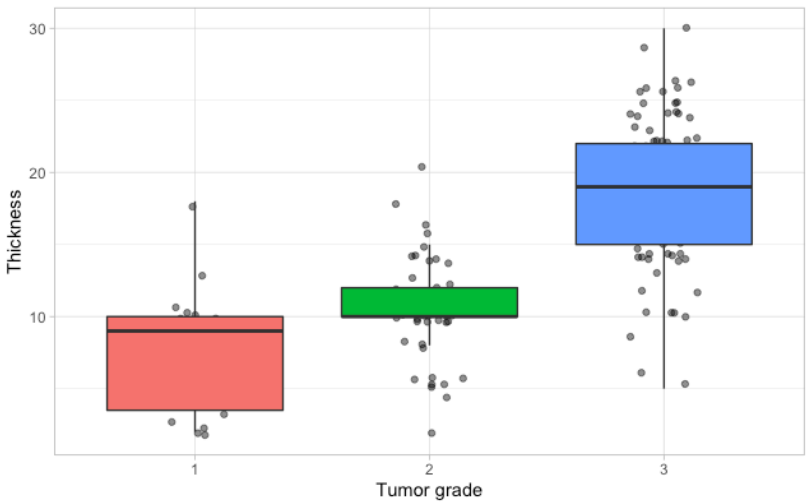

Conclusions: There was an overall correlation between thickness and grade in most of the cases. Low-grade tumors were encountered in 92% (12/13) of superficial tumors. Deep tumors showed high-grade in 75% of cases (73/97 cases, p-value = 1.879e-12). Superficial tumors with low histological grade had negative inguinal nodes and no mortality whereas deep tumors showing high histological grade were associated with a higher metastatic risk to lymph nodes (69/73 cases, 94%, p-value = 9.063e-14) and mortality (53/73 cases, 73%, p-value = 1.443e-12). Of 24 deep tumors with low histological grade, 7 had nodal spread (29%) but only 1 died of disease. Thickness and grade are important synergistic and predictive pathological factors in relation to prognosis.

529 Lymphovascular Invasion (LVI) and Perineural Invasion (PNI) According to Tumor Thickness in Invasive Penile Carcinomas

Isabel Alvarado-Cabrero[1], Diego F Sanchez[2], María José Fernandez-Nestosa[3], Raquel Valencia-Cedillo[4], Ingrid Rodríguez Servín[5], Sofia Canete-Portillo[6], Antonio Cubilla[2]

[1]Mexican Oncology Hospital SXXI, IMSS, Mexico City, Mexico, [2]Instituto de Patologia e Investigacion, Asuncion, Paraguay, [3]Universidad Nacional de Asunción, San Lorenzo, Paraguay, [4]Mexican Oncology Hospital IMSS, Mexico City, Mexico, [5]Universidad Nacional de Asuncion, Asunción, Paraguay, [6]The University of Alabama at Birmingham, Birmingham, AL

Disclosures: Isabel Alvarado-Cabrero: None; Diego F Sanchez: None; María José Fernandez-Nestosa: None; Raquel Valencia-Cedillo: None; Ingrid Rodríguez Servín: None; Sofia Canete-Portillo: None; Antonio Cubilla: None

Background: Lymphovascular invasion (LVI) and perineural invasion (PNI) were considered adverse prognostic factors in superficially invasive carcinomas in the 8th edition of the TNM staging manual, hence responsible for the pT1b category. pT1 refers to tumors invading into lamina propria (LP). We would like to challenge this view, since in our experience LVI and PNI tend to occur in deeply invasive and not in superficial tumors

Design: 147 patients with invasive carcinoma treated by partial or total penectomies were studied. Lymph node involvement was evaluated by bilateral inguinal node dissection (126 cases) or ultrasonography (21 cases). Tumor thickness was measured in mm from tumor surface to deepest invasion point and were classified as superficial (≤5 mm) or deep (>10 mm) tumors. Follow-up ranged from 10 to 82 months (median: 57 months). Statistical analysis was done using Fisher's exact test

Results: Average tumor thickness was 15 mm (2 to 30 mm). LVI was identified in 87 (59%) and PNI in 58 (39%) cases, respectively. No LVI was detected in superficial tumors (1-5mm) and only 2 of these had PNI. There was a gradual and synergistic increase in the rate of LVI and PNI in deeper tumors (LVI p-value < 2.2e-16, PNI p-value = 5.701e-12). Unfavorable outcome was present only in tumors with thickness greater than 10mm (LVI p-value = 1.17e-14, PNI p-value = 2.435e-09) (Table)

Thickness mm	# of cases	LVI	Positive nodes LVI (%)*	DOD LVI (%)*	PNI	Positive nodes PNI (%)**	DOD PNI (%)**
1-3 (LP)	6	0	0	0	0	0	0
3.1-5 (LP-superficial CS)	7	0	0	0	2 (29)	0	0
5.1-10 (CS)	37	7 (19)	4 (57)	0	1 (3)	0	0
10.1-15 (deep CS, CC)	35	18 (51)	13 (72)	9 (50)	11 (31)	6 (55)	6 (55)
>15 (CC)	62	62 (100)	55 (89)	43 (69)	43 (69)	40 (93)	32 (74)
TOTAL	**147**	**87 (59)**	**72 (83)**	**52 (60)**	**57 (39)**	**46 (81)**	**38 (67)**

LVI: Lymphovascular invasion. PNI: Perineural invasion. LP: Lamina propria. CS: Corpus spongiosum. CC: Corpora cavernosa. DOD: Died of Disease. *Percentage referred to the number of LVI positive cases in the thickness category. ** Percentage referred to the total of PNI positive cases in the thickness category.

Conclusions: Only 2 patients with superficial tumors (1-5mm) had PNI, with no regional spread or mortality. LVI was not detected in this category. Nodal metastasis was noted in 4 carcinomas invading 5 to 10 mm and none died from disease. There was a gradual increase of metastasis and mortality rate for tumors with LVI or PNI invading more than 10 mm with highest rate for those invading more than 15 mm. Tumors invading superficial CS behaved as those invading only LP and tumors invading into deep CS behaved as those invading CC. Tumor thickness may be a better prognostic indicator than anatomical levels. We found no evidence for supporting the category pT1b in the current TNM staging model.

530 Prostate Cancer in Patients on Gender Affirming Hormonal Therapy: Highlighting Diagnostic Issues in an Underserved Patient Population

Ezra Baraban[1], Chien-Kuang Cornelia Ding[2], Marissa White[3], Poonam Vohra[2], Jeffry Simko[2], Jonathan Epstein[4]
[1]Johns Hopkins Hospital, Baltimore, MD, [2]University of California, San Francisco, San Francisco, CA, [3]Johns Hopkins University School of Medicine, Baltimore, MD, [4]Johns Hopkins Medical Institutions, Baltimore, MD

Disclosures: Ezra Baraban: None; Chien-Kuang Cornelia Ding: None; Marissa White: None; Poonam Vohra: None; Jeffry Simko: *Stock Ownership*, lightspeed Biosciences Inc.; *Stock Ownership*, Protean biodiagnostics, AbbVie, Gilead; *Consultant*, 3D Biopsy; Jonathan Epstein: None

Background: Transgender individuals face well-established barriers to routine cancer screening and treatment. For individuals assigned male sex at birth, gender affirming therapies include hormonal and/or surgical approaches which typically leave the prostate gland intact. Therefore Male-to-Female (MtF) transgender individuals remain at risk for PCA. Due to the lack of specific guidelines, current MtF PCA screening should follow cisgender male guidelines. However, PCA risk factors, clinical features, and relevant PSA thresholds are unclear in MtF patients. Moreover, gender-affirming therapy alters the morphology of benign prostate tissue and PCA, but to date, there has been no report dedicated to describing the histologic changes in prostate tissue from transgender patients. These issues represent a significant diagnostic challenge at the time of prostate sampling.

Design: Archives of 3 large academic institutions were searched to identify MtF transgender patients who had undergone prostate sampling. Slides and clinical data were reviewed.

Results: Patients were identified from all 3 institutions. In one institution, 3 of 580 transgender patients age >35 underwent prostate sampling. Of these, 2 were benign and the report from the third was unavailable. 5 additional cases with available slides were identified from the other 2 institutions, including 2 radical prostatectomies (RPs) for PCA, 1 bone biopsy of metastatic PCA, and 2 benign prostate biopsies. Both patients who underwent RP presented with abnormal DRE or local symptoms. In 1 patient who underwent RP, the PSA declined from 6.5 to <1.0 ng/mL following initiation of gender-affirming hormone therapy the year before PCA diagnosis. One RP showed Grade Group 5 PCA with intraductal carcinoma and extra-prostatic extension, and the other showed Grade Group 2 PCA. Both RPs showed focal hormone therapy effect in invasive carcinoma and in benign prostate tissue.

Figure 1 - 530

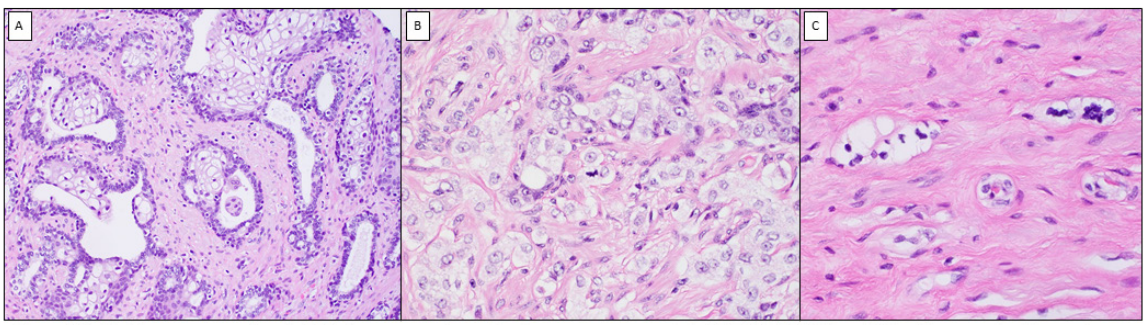

Figure 1: Radical Prostatectomy, Case 1. A. Benign prostate tissue showing squamous metaplasia (H&E 40x). B. High grade invasive prostatic adenocarcinoma without hormone therapy effect (H&E, 40x). C. Subtle foci of invasive carcinoma show nuclear pyknosis and cytoplasmic vacuolization, indicative of hormone therapy effect (H&E 40x).

Conclusions: We describe histologic features of PCA and benign prostate tissue in patients receiving gender-affirming therapy. Prominent squamous metaplasia in benign tissue should suggest the possibility of hormone therapy and prompt a search for subtle foci of prostate cancer with hormone therapy effect, which, if not suspected, may be overlooked. PCA should not be graded if altered by hormone therapy because this can overestimate tumor aggressiveness. 2 patients in our study were diagnosed later in their disease with symptoms or abnormal DRE, with one patient having an elevated PSA that decreased significantly after initiating gender-affirming hormone therapy. Awareness of these clinical and histologic features is important as we continue to see prostate biopsies from aging transgender patients and as barriers to their healthcare are dismantled.

531 Genetic Profiling of African American Patients with Prostatic Adenocarcinoma Metastatic to the Lymph Node

Samuel Bidot[1], Jun Yin[2], Linsheng Zhang[3], Kristin Deeb[1], Charles Hill[1], Joanne Xiu[2], Mehmet Bilen[1], Katherine Case[1], Lara Harik[1]
[1]Emory University School of Medicine, Atlanta, GA, [2]Caris Life Sciences, Phoenix, AZ, [3]Emory University Hospital, Atlanta, GA

Disclosures: Samuel Bidot: None; Jun Yin: *Employee*, Caris Life Sciences; Linsheng Zhang: None; Kristin Deeb: None; Charles Hill: None; Joanne Xiu: *Employee*, Caris Life Sciences; Mehmet Bilen: None; Katherine Case: None; Lara Harik: None

Background: *Prostatic adenocarcinoma (PCa)* is characterized by substantial molecular heterogeneity. Members of the E26 transformation specific (ETS), which are androgen regulated promoters, represent 50% of genetic alterations, while 25% harbor a somatic point mutation, most often involving *SPOP*, *TP53*, *FOXA1* and *PTEN*.

Genetic profiling of PCa data is derived from predominantly white patient cohorts. Reports suggest PCa in African American patients (AA) have higher mortality rate, histologic grade at presentation, and poorer prognosis, raising the possibility of distinct genetic alterations in AA. Our goal is to investigate the differential genomic alterations of PCa metastatic to regional lymph node (LN) in AA.

Design: We retrospectively reviewed pN1 AA with PCa managed with radical prostatectomy and LN dissection (2011- 2019). Nineteen PCa patients had comprehensive molecular profiling, including next generation sequencing of DNA and RNA (whole exome and transcriptome sequencing). Neuroendocrine PCa (NEPC) and androgen receptor (AR) signaling scores were calculated. Disease-free survival curves were derived from the Kaplan-Meier method.

Results: Genetic profiling showed that *SPOP* mutations (5/19, 29%), *TP53* mutations (4/19, 24%) and *TPMRSS2–ETS* gene fusions (4/19, 24%) are the most frequent alterations (Tab.1, Fig.1). While most alterations were associated with high levels of AR activity (*TPMRSS2–ETS*, 4/4; *TP53*, 3/4), *SPOP* mutations were exclusively associated with low levels of AR activity (Fig.1). *SPOP* mutant tumors' gene expression suggests a trend toward a higher expression of *SPOP* RNA levels (versus *SPOP* wild-type tumors, 50.26 vs 48.78 transcripts per million, p=0.33), with patients showing a tendency toward a better prognosis (Fig. 2, p=0.51).

Demographics, staging and follow-up findings in our 19 prostatic adenocarcinoma African American patients at baseline

	n (%) or median [IQR], n=19
Demographics	
Age, years	62 [53–63.5]
pT staging	
pT2	0 (0%)
pT3a	7 (37%)
pT3b	12 (63%)
pT4	0 (0%)
Histopathologic grade	
1	0 (0%]
2	1 (5%)
3	6 (32%)
4	0 (0%)
5	12 (63%)
Lymph nodes	
Type of dissection	
Limited	10 (53%)
Extended	9 (47%)
Including pM1a (n=9)	4/9 (44%)
Number of positive lymph nodes	
1	2 (11%)
2–3	12 (63%)
>3	5 (26%)
Follow-up	
Duration, month	27 (21–37)
Outcome	
No evidence of disease	5 (26%)
Alive with disease	14 (74%)
Died of disease or other cause	0 (0%)

IQR: interquartile range

Figure 1 - 531

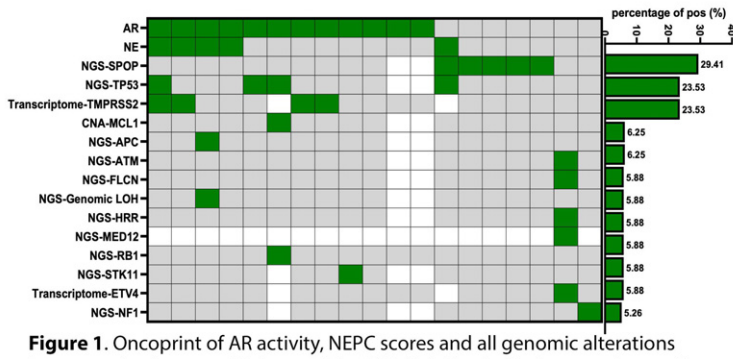

Figure 1. Oncoprint of AR activity, NEPC scores and all genomic alterations (green: mutant; grey: wild-type; white: NA). Side bar indicates prevalence of individual alterations.

Figure 2 - 531

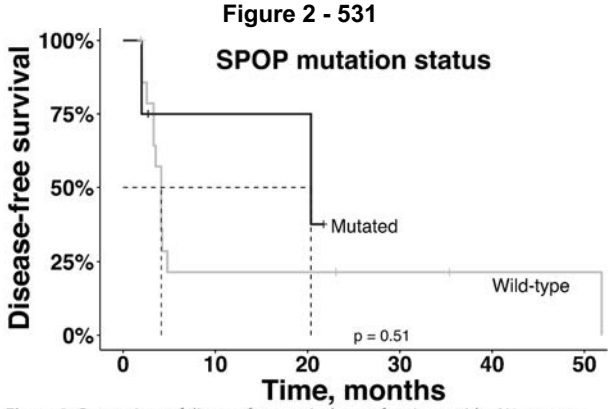

Figure 2: Comparison of disease-free survival rate of patients with pN1 prostate adenocarcinoma stratified by SPOP mutation status.

Conclusions: African American patients have higher *SPOP* mutations (30%), compared to ~10% in a predominantly Caucasian cohort (TCGA data). *SPOP* gene has a tumor suppressive role in PCa by promoting the degradation of oncoproteins, including AR. *SPOP* mutations (loss-of-function) are usually associated with increased AR activity, resulting from decreased degradation of AR. Our data suggests that *SPOP* mutations in AA could be associated with decreased AR activity (possibly resulting from gain-of-function mutation), raising concern for suboptimal efficacy of androgen deprivation in this subset of patients. Better genetic understanding of the mutational milieu of PCa in AA is critical to improving choices of targeted treatment.

532 Renal Cell Carcinoma with TFEB Gene Alterations: Comparison of Different Analysis for the Diagnosis

Anna Calio'[1], Stefano Marletta[1], Matteo Brunelli[1], Serena Pedron[1], Lisa Marcolini[2], Lavinia Stefanizzi[2], Guido Martignoni[3]
[1]University of Verona, Verona, Italy, [2]Ospedale Pederzoli, Peschiera del Garda, Italy, [3]University of Verona, Ospedale Pederzoli, Peschiera del Garda, Italy

Disclosures: Anna Calio': None; Stefano Marletta: None; Matteo Brunelli: None; Serena Pedron: None; Lisa Marcolini: None; Lavinia Stefanizzi: None; Guido Martignoni: None

Background: Renal cell carcinoma with TFEB gene alterations comprise renal tumors harboring translocation and/or amplification of the TFEB gene. Despite the current knowledge on such tumors, it is still challenging to reach the proper diagnosis in the clinical practice, which relies on time-consuming molecular techniques, like FISH, often not available among institutions. Thus, we sought to extensively investigate a series of renal cell carcinoma with TFEB gene alterations by additional more affordable methods, namely immunohistochemistry and RNA-ISH.

Design: Fourteen cases were retrieved, including 10 tumors with *MALAT1/TFEB* rearrangement, 1 case with *ACTB/TFEB* fusion, 1 lesion with *TFEB* rearrangement and amplification and 2 neoplasms with *TFEB* amplification. Sections from tissue blocks of each tumor were immunohistochemically stained for cathepsin K (clone 3F9, dilution 1:2000, Abcam) and *TFEB* by using 3 different assays: *TFEB* policlonal rabbit antibodies (dilution 1:1500, Invitrogen; dilution 1:1000 BETHYL) and C-6 (dilution 1:800, Santa Cruz). TFEB and TRIM63 mRNA expression levels were scored with RNA-ISH according to ACD guideline for semiquantitative assessment of RNAscope staining intensity as 0, 1, 2, 3, 4. A positive result was considered when the neoplastic cells showed 3 or 4 intensity staining.

Results: All tumors labelled for cathepsin K, albeit focally in two samples. Overall, by using policlonal antibody of TFEB (Bethyl), roughly 30% of tumors showed a clear nuclear staining, with even lower rates when considering the other clones. TFEB mRNA overexpression was found in a noteworthy proportion of the neoplasms (80%, 11/14), except for the *ACTB/TFEB* fused tumor, one TFEB-amplified renal cell carcinoma and the case carrying both *TFEB* rearrangement and amplification. Regarding TRIM63, either TFEB-rearranged and TFEB-amplified renal cell carcinomas revealed enriched mRNA levels (overall 85%); interestingly *ACTB/TFEB* rearranged renal cell carcinoma showed focal immunostaining for cathepsin K, and low level of TFEB and TRIM63 mRNA expression.

Conclusions: As for immunohistochemistry, our results confirm cathepsin K as the most useful marker for the diagnosis of renal cell carcinoma with *TFEB* gene alterations; conversely, assays for *TFEB* are less reliable. On the other hand, the higher accuracy

of TFEB and TRIM63 RNA-ISH suggests the combination of those methods with immunohistochemistry for improving the efficiency of the diagnosis of those tumors.

533 GATA3 expression in Metastatic Prostatic Adenocarcinoma

Sofia Canete-Portillo[1], Maria Del Carmen Rodriguez Pena[2], Aysha Mubeen[3], Anna Posey[1], Cristina Magi-Galluzzi[1]
[1]The University of Alabama at Birmingham, Birmingham, AL, [2]Clinical Center, National Institutes of Health, Bethesda, MD, [3]Brigham and Women's Hospital, Boston, MA

Disclosures: Sofia Canete-Portillo: None; Maria Del Carmen Rodriguez Pena: None; Aysha Mubeen: None; Anna Posey: None; Cristina Magi-Galluzzi: None

Background: GATA3 is a useful immunohistochemical (IHC) marker to confirm urothelial origin, commonly utilized to distinguish the nature of a poorly differentiated tumor involving the bladder neck (urothelial vs. prostatic origin). However, recent literature has reported GATA3 expression in high-grade prostatic adenocarcinoma with potential for misdiagnosis. The aim of this study was to explore GATA3 expression in metastatic prostatic adenocarcinoma (mPCa).

Design: After IRB approval, our pathology database was searched for cases of metastatic prostatic adenocarcinoma diagnosed between 2010 and 2020. Patients' clinicopathologic data were recorded. GATA3 IHC stains were performed in all cases; nuclear staining was interpreted as positive.

Results: 32 cases met the search criteria: 12 were African American, 17 Caucasian, 1 was recorded as "other"; 2 had no available data. Mean age was 71 years (range: 55-88). Tumor grading on initial biopsy or prostatectomy was available for 16 patients and corresponded to Grade Group (GG) 4/5 in 12 (75%), GG3 in 1 (6%), and GG1 in 3 (19%). mPCa involved bone (n=14, 44%), liver (n=8, 25%), lung (n=4, 12%), soft tissue (n=4, 12%), ureter (n=1%), and rectum (n=1%). At least one prostate-specific IHC stain (NKX3.1, PSA, PSAP) was used in each case to confirm the diagnosis. Morphologically, glandular differentiation was seen in 18 (56%) cases, 7 of which showing cribriform pattern; 14 metastases (44%) showed no convincing gland formation. GATA3 was positive in 2 (6%) cases of mPCa to the liver (Table 1) (Figure 1). Time from initial prostate cancer diagnosis to metastasis ranged from 1 to 224 months (mean: 99.7). Treatment modality received before metastatic disease was available for 16 patients (50%) and consisted in combination of radiotherapy, androgen deprivation therapy, and prostatectomy; 10 patients presented with metastatic disease. Genetic testing (Strata®) was available for one of the cases with positive GATA3 staining and detected MSH2 deletion, high TMB, and TP53 mutation; this patient was treated with immunotherapy and gonadotropin-releasing hormone agonists.

Table 1. Clinicopathologic features in metastatic prostatic adenocarcinoma.

Age	Metastasis site	Gland formation	NKX3.1	PSA	PSAP	GATA3	Initial Gleason (Grade Group)	Treatment before metastasis	Time from initial diagnosis to metastasis (months)
60	Bone	No	+	-		-	NA	RT, RP	130
79	Lung	Yes σ	+	+		-	4+4=8 (4) a	RT, HT	66
56	ST	No	+			-	NA	None**	NA
69	Liver	Yes	+			-	4+5=9 (5) b	RT, RP, ADT	68
87	Bone	Yes	+			-	NA	NA	NA
76	Bone	Yes	+	+		-	NA	None**	NA
82	ST	Yes	+	+*		-	5+4=9 (5) a	SRP, ADT	195
66	ST	No	+	-	-	-	NA	None**	NA
80	Liver	No	+	+	+	-	4+5=9 (5) b	RT, RP	17
74	Bone	No	+	-	+	-	NA	None**	NA
73	Lung	Yes	+	+		-	NA	RT, RP	208
84	Bone	Yes σ	+	+	+	-	5/10 (1) b	RT, RP	224
55	ST	No	-	+		-	5+4=9 (5) a	ADT	66
71	Lung	Yes σ			+	-	4+3=7 (3) b	RT, RP	71
63	Bone	Yes σ		+	+	-	NA	None**	NA
74	Bone	No	+	+	+*	-	NA	None**	NA
71	Bone	No	+		-	-	4+4=8 (4) a	RT, ADT	147
62	Liver	Yes		+		-	4+5=9 (5) b	None**	NA
76	Liver	Yes σ		+		+	4+4=8 (4) b	RT, ADT	13
71	Rectum	Yes		+	-	-	4+4=8 (4) a	ADT	121
73	Ureter	No		+		-	5/10 (1) a	RT	188
64	Bone	Yes		+	-	-	NA	None**	NA

80	Bone	Yes		+		-	NA	None**	NA
67	Liver	Yes		+	-	-	NA	RT	35
56	Bone	No		+		-	NA	NA	NA
84	Lung	Yes σ		+			NA	NA	NA
67	Liver	Yes σ		+		-	NA	RT	167
62	Bone	No		+	+	-	4+5=9 (5) b	RT, RP, ChT	45
88	Bone	No		+	-	-	6/10 (1) b	NA	NA
66	Bone	Yes		+	+	-	NA	NA	NA
71	Liver	No	+	+		-	4+4=8 (4) a	NA	33
65	Liver	No	+			+	4+5=9 (5) c	None**	1

C: Caucasian, AA: African American, ST; soft tissue, NA: not available/not applicable; RT: radiotherapy; ADT: androgen deprivation therapy; ChT: chemotherapy; RP: radical prostatectomy; SRP: simple retropubic prostatectomy; FU: follow-up, AWD: alive with disease, DOD: dead of disease, σ cribriform pattern; * focal; ** patients that presented with metastasis; a biopsy; b radical prostatectomy, c transurethral resection.

Figure 1 - 533

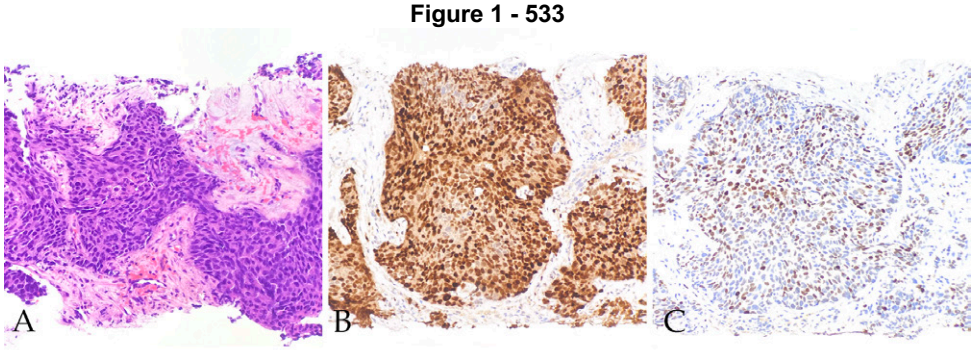

Figure 1. Metastatic prostatic adenocarcinoma to the liver (**A**) showing positive NKX3.1 (**B**) and GATA 3 (**C**) staining.

Conclusions: To our knowledge, this is the first study exploring GATA3 expression in mPCa. Although only 6% of our cases showed positive GATA3 staining, our findings provide evidence of aberrant GATA3 expression in mPCa. Pathologists should be aware of this potential diagnostic pitfall and use a panel-based approach in the distinction of urothelial vs. prostatic origin.

534 How Closely Related are Juxtaglomerular Cell Tumors to Other Pericytic Tumors, Molecularly?

Sofia Canete-Portillo[1], Jesse McKenney[2], Chin-Chen Pan[3], Manju Aron[4], Brandon Wilk[1], Felipe Massicano[1], Manavalan Gajapathy[1], Donna Brown[1], Dilek Baydar[5], Andres Matoso[6], Maria Del Carmen Rodriguez Pena[7], Maria Tretiakova[8], Kiril Trpkov[9], Sean Williamson[2], Alexander Mackinnon[1], Shuko Harada[1], Elizabeth Worthey[1], Cristina Magi-Galluzzi[1]
[1]The University of Alabama at Birmingham, Birmingham, AL, [2]Cleveland Clinic, Cleveland, OH, [3]Taipei Veterans General Hospital, Taipei, Taiwan, [4]Keck School of Medicine of USC, Los Angeles, CA, [5]Koç University, Istanbul, Turkey, [6]Johns Hopkins Medical Institutions, Baltimore, MD, [7]Clinical Center, National Institutes of Health, Bethesda, MD, [8]University of Washington, Seattle, WA, [9]University of Calgary, Calgary, Canada

Disclosures: Sofia Canete-Portillo: None; Jesse McKenney: None; Chin-Chen Pan: None; Manju Aron: None; Brandon Wilk: None; Felipe Massicano: None; Manavalan Gajapathy: None; Donna Brown: None; Dilek Baydar: None; Andres Matoso: None; Maria Del Carmen Rodriguez Pena: None; Maria Tretiakova: None; Kiril Trpkov: None; Sean Williamson: None; Alexander Mackinnon: None; Shuko Harada: None; Elizabeth Worthey: None; Cristina Magi-Galluzzi: None

Background: Juxtaglomerular cell tumors (JGCT) are rare tumors arising from modified smooth muscle cells (pericytes) of juxtaglomerular afferent renal arteriole. Pericytic tumors (PT) comprise a group of mesenchymal neoplasms arising from perivascular myoid cells and include glomus tumors/glomangiomas (GT) and myopericytomas (MP). Limited literature is available on the molecular features of JGCT, mostly describing chromosomal abnormalities and expression profile. *BRAF*, *KRAS* and *NOTCH* gene mutations have been previously described in PT. The aim of this study was to compare gene alterations in JGCT to PT to evaluate their possible relationship at a molecular level.

Design: JGCT, GT and MP diagnosed by subspecialty pathologists were retrospectively collected from 9 institutions. DNA was extracted from formalin-fixed paraffin embedded tissue sections and whole exome sequencing (WES) was performed. Following

base calling, sequences were aligned to genome reference GRCh38 with BWA-MEM. Aligned sequences were processed via GATK for base quality score recalibration, indel realignment and duplicate removal. Variant analysts performed interpretation and classification of variants according to ACMG-AMP criteria. Cross cohort analyses were performed to ensure consistency in variant selection and classification across the cohort.

Results: Ten JGCT and 10 PT were included in the study. Four PT were from kidney (2GT, 2MP) and 6 PT were of non-kidney origin (5GT, 1MP) from upper and lower extremities. WES identified 406 alterations in 106 genes of JGCT compared to 374 alterations in 94 genes of PT. Table 1 summarizes alterations identified in more than one case according to tumor type. *KMT2C* alterations were found in all tumor types irrespective of tumor site. *ATR* alterations were found in JGCT, GT (non-kidney) and MP (non-kidney). *TGFBR2* alterations were present in JGCT, GT (non-kidney) and MP (kidney). Gene alterations found in more than 1 tumor were common to JGCT and GT (7/9) and JGCT and MP (4/9). *NOTCH2* alterations, previously described in glomus tumor, were found in one JGCT and one GT.

Table 1. Alterations (pathogenic/likely pathogenic) found in according to tumor type.

	JGCT (n=10)	**GT (n=7)**		**MP (n=3)**	
		Kidney (n=2)	*Non-kidney (n=5)*	*Kidney (n=2)*	*Non-kidney (n=1)*
ATR	5 frameshift (n=5)	-	1 frameshift (n=1)		1 frameshift (n=1)
TGFBR2	6 frameshift (n=5)	-	5 frameshift (n=4)	1 frameshift (n=1) 1 missense (n=1)	-
KMT2C	4 missense (n=4)	1 missense (n=1)	4 missense (n=4)	2 missense (n=2)	1 missense (n=1)
GNAQ	5 missense (n=5) 5 nonsense (n=5)	-	3 missense (n=3) 3 nonsense (n=3)	-	-
SDHA	5 frameshift (n=5)	-	1 frameshift (n=1)	-	-
MSH6	3 frameshift (n=3)	-	2 frameshift (n=2)	-	-
NPHS2	2 missense (n=2)	-	2 missense (n=2)	-	-
NOTCH2	1 missense (n=1)	1 missense (n=1)		-	-
POLE	1 frameshift (n=1)	-	1 frameshift (n=1)	-	-

Conclusions: This is the first study comparing molecular features of JGCT vs PT. *KMT2C* alterations were found in all tumor types. A more similar gene profile was found between JGCT and GT. Our findings are in keeping with the common origin (pericytes) shared between JGCT and PT, suggested by the resemblance in gene alterations found in JGCT and GT and supporting the close phenotypic-genotypic relation of JGCT and PT.

535 Molecular Characterization of Juxtaglomerular Cell Tumors

Sofia Canete-Portillo[1], Jesse McKenney[2], Manju Aron[3], Brandon Wilk[1], Felipe Massicano[1], Manavalan Gajapathy[1], Donna Brown[1], Dilek Baydar[4], Andres Matoso[5], Maria Del Carmen Rodriguez Pena[6], Chin-Chen Pan[7], Maria Tretiakova[8], Soroush Rais-Bahrami[1], Alexander Mackinnon[1], Shuko Harada[1], Elizabeth Worthey[1], Cristina Magi-Galluzzi[1]
[1]The University of Alabama at Birmingham, Birmingham, AL, [2]Cleveland Clinic, Cleveland, OH, [3]Keck School of Medicine of USC, Los Angeles, CA, [4]Koç University, Istanbul, Turkey, [5]Johns Hopkins Medical Institutions, Baltimore, MD, [6]Clinical Center, National Institutes of Health, Bethesda, MD, [7]Taipei Veterans General Hospital, Taipei, Taiwan, [8]University of Washington, Seattle, WA

Disclosures: Sofia Canete-Portillo: None; Jesse McKenney: None; Manju Aron: None; Brandon Wilk: None; Felipe Massicano: None; Manavalan Gajapathy: None; Donna Brown: None; Dilek Baydar: None; Andres Matoso: None; Maria Del Carmen Rodriguez Pena: None; Chin-Chen Pan: None; Maria Tretiakova: None; Soroush Rais-Bahrami: None; Alexander Mackinnon: None; Shuko Harada: None; Elizabeth Worthey: *Advisory Board Member*, AbbVie; *Advisory Board Member*, Hermansky-Pudliak Foundation; Cristina Magi-Galluzzi: None

Background: Juxtaglomerular cell tumors (JGCT), also known as reninomas, are rare tumors arising from modified smooth muscle cells (pericytes) of the afferent renal arteriole of the juxtaglomerular apparatus. Limited literature is available on molecular features

of JGCT, with most studies describing chromosomal abnormalities and expression profile of various genes, including renin. Our study aims to expand the mutational landscape of JGCT to find potential driver pathways by whole exome sequencing (WES).

Design: JGCT diagnosed by genitourinary pathologists were retrospectively collected from 8 institutions. Clinicopathologic data was obtained. DNA was extracted from formalin-fixed paraffin embedded tissue sections and WES was performed. Following base calling, sequences were aligned to current genome reference (hg19) with BWA-mem. Aligned sequences were processed via GATK for base quality score recalibration, indel realignment and duplicate removal. A variant calling pipeline was run to call and genotype variants; interpretation to identify pathogenic (PV), likely pathogenic (LPV), and variants of unknown significance (VUS) was then conducted.

Results: Ten JGCT were included in the study. WES identified 406 alterations (range: 31-51) in 106 different genes (range: 29-45). A high number of alterations were found in two patients with unusual features (45 and 42, respectively): one was incidentally discovered during workup for hepatocellular carcinoma (HCC); one had prominent rhabdoid differentiation and renal vein involvement. PV/LPV are summarized in Table 1 according to frequency: 11 PV were identified in 9 cases; 8 LPV in all cases. Most of the PV/LPV are described to interact with known oncogenic pathways including DNA repair and MAPK. Various VUS (range: 8-16) were detected including *ATM, BRAF, BRCA1, MSH2, MSH6, NF1, NOTCH1/3* and *SMAD.* At least one deleterious molecular alterations in the *RAS* pathway was present in 50% of cases.

Table 1. Alterations found in pathogenic and likely pathogenic variants in JGCT (n=10).

Gene	# Cases	Missense	Nonsense	Frameshift
Pathogenic				
GNAQ **	5	5	5	-
TGFBR2 *	4	-	-	4
MSH6	3	-	-	3
CYP21A2 **	2	2	-	-
NPHS2 *	2	2	-	-
CYP7B1	1	-	1	-
KRAS	1	1	-	-
NOTCH2	1	1	-	-
POLE	1	-	-	1
SETD2	1	1	-	-
*APOB**	1	-	1	-
Likely pathogenic				
ATR **	5	-	-	5
SDHA	5	-	-	5
KMT2C *	4	4	-	-
ROS1	2	2	-	-
TGFBR2	2	-	-	2
BRAF	1	1	-	-
KIT	1	-	1	-
TLR4	1	-	1	-

*: patient with HCC, **: patient with rhabdoid features and renal vein involvement

Conclusions: This is the largest series of JGCT characterized by WES. Most of the PV/LPV identified are involved in oncogenic pathways such as DNA repair or MAPK. Alterations involving the RAS pathway were present in all cases when well-supported candidate VUS is included. Tumors from patients with unusual clinicopathologic features harbored a high number of gene alterations. More studies are necessary to establish a definite association of these genes and their role in JGCT.

536 Primary Renal Synovial Sarcoma (PRSS): A Multi-institutional Clinicopathologic and Molecular Study of 14 Cases

Bindu Challa[1], Sambit Mohanty[2], Nakul Sampat[2], Ruhani Sardana[3], Anandi Lobo[4], Shilpy Jha[2], Niharika Pattnaik[2], Shivani Sharma[5], Ekta Jain[5], Mohit Kumar[6], Anil Parwani[7]

[1]The Ohio State University Wexner Medical Center, Columbus, OH, [2]Advanced Medical and Research Institute, Bhubaneswar, India, [3]Advanced Medical Research Institute and Hospital, Bhubaneswar, India, [4]Kapoor Centre of Urology and Pathology, Raipur, India, [5]Core Diagnostics, Gurgaon, India, [6]Core Diagnostics, Gurugram, India, [7]The Ohio State University, Columbus, OH

Disclosures: Bindu Challa: None; Sambit Mohanty: None; Nakul Sampat: None; Ruhani Sardana: None; Anandi Lobo: None; Shilpy Jha: None; Niharika Pattnaik: None; Shivani Sharma: None; Ekta Jain: None; Mohit Kumar: None; Anil Parwani: None

Background: PRSS is a rare aggressive mesenchymal neoplasm of the kidney that accounts for less than 1% of renal sarcomas. These neoplasms resemble sarcomatoid and spindle cell tumors of the kidney and need immunohistochemical (IHC) work up for therapeutic decision-making and prognostication. Herein, we describe the clinicopathologic and molecular findings of PRSS in one of the largest case series to date and to our knowledge, the only PRSS series to use novel SS18-SSX IHC.

Design: PRSS cases were identified from the pathology files of collaborating academic institutions. Clinicopathologic, IHC, molecular, treatment, and follow up data were analyzed.

Results: There were 9 males and 5 females, ranging from 17 to 72 years (median 40.5 years). The tumor size ranged from 3.0 cm to 14.0 cm in maximum dimension. Grossly, the tumors (n=10) showed solid and homogeneous (n=3), solid and variegated (n=1), and solid and cystic with variegated appearance (n=6). Spindle cell (n=10), round cell (n=3), and round to epithelioid morphologies (n=1) were observed. SS18-SSX IHC was positive in all 14 tumors (diffuse, n=10; multifocal, n=2; focal, n=2). All the tumors harbored SS18-SSX gene rearrangement (Figure 1, Table 1). All 14 tumors exhibited TLE1 immunoreactivity. Other positive immunostains included were CD99 (n=14/14) and BCL2 (n =13/13). NKX2.2, BCOR, and STAT6 immunostains were negative in 13/13 tumors. Surgical resections included were as follows: radical nephrectomy (n=11); radical nephrectomy and inferior vena cava (IVC) thrombectomy (n=2) and radical nephrectomy with IVC repair; liver resection and diaphragm repair (n=1). Metastases to the liver, brain, and lung (n=1); liver and bone (n=1); liver and diaphragm (n=1) was identified. Adjuvant chemotherapy was instituted in 11/12 patients. Follow up was available for 10 patients (range: 5 months to 24 months), 4 patients died of disease, and 6 patients are alive with no recurrence or metastasis.

Case #	Histologic cell type	Mitoses (/10 HPF)	Necrosis (%)	SS18-SSX IHC (up to 25% = focal; 25% to 75% = Multifocal; greater than equal to 75% = Diffuse), Positive +, negative -	SS18 % of Break-apart signals (counting 200 tumor nuclei), FISH result (Positive:+, negative: -)	Metastasis (at the time of diagnosis)	Status
1	Spindle cell	17	20	Positive, Diffuse and Strong	45%, +	NA	Alive with no recurrence or metastasis
2	Spindle cell	9	0	Positive, Diffuse and Strong	73%, +	NA	NA
3	Spindle cell	20	0	Positive, Diffuse and Strong	48%, +	Liver, Brain and Lungs	Dead
4	Round cell	40	50	Positive, Diffuse and Strong	55%, +	None	Dead with multiorgan failure-metastasis in liver, lung, lymph nodes and brain
5	Spindle cell	23	10	Positive, Diffuse and Strong	39%, +	None	NA
6	Round cell	7	0	Positive, Diffuse and strong	70%, +	None	Alive with no recurrence or metastasis
7	Spindle cell	18	20	Positive, Diffuse and Strong	43%, +	None	Alive with no recurrence or metastasis
8	Spindle cell	25	40	Positive, Diffuse and Strong	60%, +	None	Alive with no recurrence or metastasis
9	Spindle cell	11	10	Positive, Multi-focal and Strong	28%, +	None	Dead with liver and lung metastasis
10	Round cell	19	0	Positive, Diffuse and Strong	35%, +	None	Alive with no recurrence or metastasis

11	Spindle cell	9	30	Positive, Focal and Strong	19%, +	Liver and Bone	Dead
12	Spindle cell	18	50	Positive, Focal and Strong	23%, +	None	NA
13	Round to epithelioid	13	20	Positive, Diffuse and Strong	80%, +	None	NA
14	Spindle cell	12	20	Positive, Diffuse and Strong	80%, +	Liver and Diaphragm	Alive with no recurrence or metastasis

NA: Not Available

Figure 1 - 536

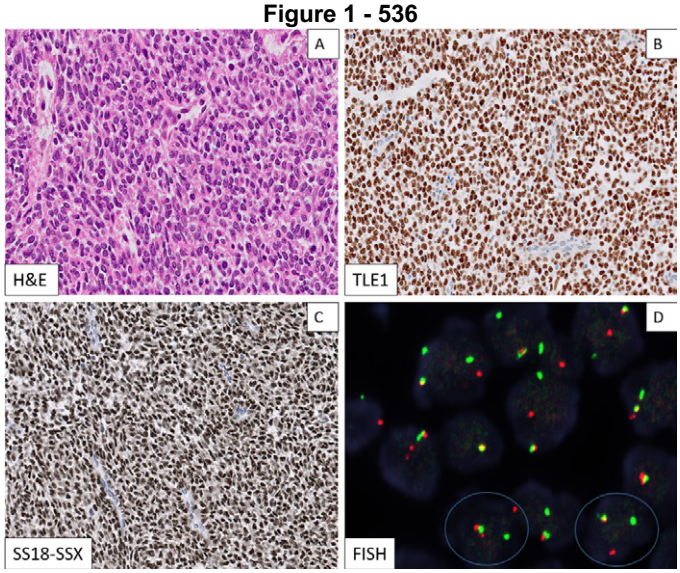

Conclusions: PRSS has poor prognosis, especially in patients presenting with metastasis at the time of diagnosis. In our series, 67% patients who had metastasis at diagnosis, died. As SS18-SSX IHC showed an excellent concordance with the FISH results, this may reliably be used in the IHC panel of spindle/round cell sarcomas of the kidney and as a molecular surrogate for PRSS, particularly in a resource-limited setting. Also, the tumors with focal SS18-SSX expression had lower break-apart signals in the FISH assay (19% & 23% in 2 tumors with focal SS18-SSX IHC+).

537 Tumor Volume is a Risk Factor of Biochemical Recurrence: a 20-year Retrospective Case Series

Meagan Chambers[1], Funda Vakar-Lopez[1], Maria Tretiakova[1], Nicholas Reder[1], Lawrence True[2]
[1]University of Washington, Seattle, WA, [2]University of Washington Medical Center, Seattle, WA

Disclosures: Meagan Chambers: None; Funda Vakar-Lopez: None; Maria Tretiakova: None; Nicholas Reder: *Employee*, Lightspeed Microscopy, Inc.; Lawrence True: *Stock Ownership*, LightSpeed Microscopy, Inc.

Background: The volume of prostate cancer in prostatectomies is not included as a risk factor for biochemical recurrence (BCR) in current prostate cancer nomograms. This may be due to conflicting reports in the literature and lack of a standardized method for estimating volume of cancer. We undertook a large study to assess the relationship of prostate cancer volume to the risk for BCR.

Design: We reviewed 20 years (1991 – 2021) of pathology records at our university medical center for prostatectomy specimens with adenocarcinomas of the prostate. Inclusion criteria included tumor volume and at least two post-operative (baseline) serum prostate specific antigen (PSA) values. Exclusion criteria included cases with incomplete resection or metastatic disease. Tumor volume (in cc) has routinely been reported as a mandatory item in our radical prostatectomy templates since 1991. Tumor volume is measured by overlaying a grid with 0.1 cm^2 grid marks onto areas of cancer on slides of entirely submitted prostate. Biochemical recurrence was defined as two post-operative PSA measurements $\geq$0.2 ng/ml.

Results: 2,984 cases met inclusion criteria. Series characteristics include age, pre- and post-operative serum PSA values, prostate volume, tumor volume, grade, and stage (Table 1). There were 398 cases of BCR (13.3%). Median time to BCR was 2.5 years (*Med* = 30.8 ± 46.5 months, range = 2 - 22.5 years). Median PSA at time of biochemical recurrence was 0.31 ± 12.8 ng/mL (range = 0.2 – 220 ng/mL). The median tumor volume of BCR-negative cases was 1.50 ± 2.6 cc (range = 0 – 33.8 cc). The median tumor volume of BCR-positive cases was 2.65 ± 4.2 cc (range = 0.05 – 30 cc). The size of tumors was significantly larger in BCR cases compared to those without recurrence (p = <0.0001). Cases with ≥5 cc of tumor were 2.5 times more likely to recur compared to those with <5.0 cc of tumor. In addition, previously validated risk factors for recurrence were significant in our data set except for age at diagnosis [Table 1].

	All cases (n = 2984)	Disease free (n = 2586)	BCR cases (n = 398)	p-value
Age (median, SD, years)	61.2 (7.3)	61 (7.2)	61.6 (7.6)	0.99
Age <50 yo		163 (6%)	26 (6%)	0.87
Gleason grade sum (average, SD)				
Gleason grade, presence of 4 or 5		1772 (68.5%)	336(84%)	<0.0001
6 (n, %)	849 (28%)	792 (31%)	57 (14%)	
7 (n, %)	1698 (57%)	1474 (57%)	224 (56%)	
8 (n, %)	70 (2%)	53 (2%)	17 (4%)	
9 (n, %)	187 (6%)	136 (5%)	51 (13%)	
10 (n, %)	1 (<0.1%)	1 (<0.1%)	0 (0%)	
Prostate volume (mean, SD, grams)	47.7 (20.7)	48.0 (20.5)	45.6 (22.1)	0.44
Cancer volume (mean, SD, cc)	2.5 (2.9)	2.3 (2.6)	4.0 (4.2)	<0.0001
Positive margins (n, %)*	619 (21%)	447 (17%)	132 (33%)	<0.0001
Extracapsular extension (n, %)	765 (26%)	608 (24%)	157 (39%)	<0.0001
Seminal vesicle invasion (n, %)	224 (8%)	154 (6%)	70 (18%)	<0.0001
Vascular invasion (n, %)	82 (3%)	59 (2%)	23 (6%)	<0.0001
Pre-operative PSA (mean, SD, ng/mL)	6.9 (5.8)	6.6 (5.3)	8.5 (8.3)	<0.0001
Post-operative PSA (mean, SD, ng/mL)	0.05 (0.04)	0.05 (0.04)	0.07 (0.03)	<0.0001

Conclusions: In our series of almost 3,000 cases, tumor size was a significant predictor of biochemical recurrence. A multivariate analysis to assess the relative importance of this variable in relation to other known risk factors is required to further characterize the relationship between tumor size and biochemical recurrence.

538 Validation of the Commercial Fumarate Hydratase (FH) and 2SC Antibodies for Immunohistochemistry in Diagnosing Molecularly Confirmed FH-Deficient Renal Cell Carcinoma

Hsin-Yi Chang[1], Jen-Fan Hang[1], Paul Chen[1], Chin-Chen Pan[1]
[1]Taipei Veterans General Hospital, Taipei, Taiwan

Disclosures: Hsin-Yi Chang: None; Jen-Fan Hang: None; Paul Chen: None; Chin-Chen Pan: None

Background: Fumarate hydratase (FH)-deficient renal cell carcinoma (RCC) is characterized by mutation in the *FH* gene, which results in complete loss or reduction of the FH expression and overexpression of S-(2-succino)-cysteine (2SC). Previous immunohistochemistry (IHC) studies using a laboratory developed 2SC antibody highlighted its utility in diagnosing FH-deficient RCC and differential with other eosinophilic RCCs with papillary feature, especially in cases without FH loss. Recently, the 2SC antibody has been commercially available. This study aimed to validate the commercial FH and 2SC antibodies for IHC in diagnosing FH-deficient RCCs and investigate the correlation between IHC and *FH* mutation.

Design: Consecutive cases diagnosed as papillary RCC and FH-deficient RCC between 2010 and 2021 were retrieved and reviewed. FH and 2SC IHC were performed on tissue microarrays. IHC results were scored with the H-score. Localization of 2SC immunoreactivity (nuclear, cytoplasmic, or both) was also recorded. Cases with aberrant IHC staining pattern were subtyped based on the definition as followed, type 1: FH complete loss (H-score 0) and 2SC overexpression (H-score ≧200), type 2: FH intact (H-score ≧200) and 2SC overexpression. Mutation analysis of *FH* was performed by PCR and Sanger sequence for the above 2 types.

Results: A total of 149 RCCs were selected. Aberrant IHC staining pattern were identified in 22 cases (14.8%) as type 1 and 26 cases (17.4%) as type 2. For type 1, the localization of 2SC overexpression was in both nuclei and cytoplasm in all cases (Figure 1). For type 2, the 2SC overexpression was in the cytoplasm in 23 cases (Figure 2) and in both nuclei and cytoplasm in 3. By Sanger sequencing, 17 (77.3%) of type 1 cases were confirmed to be *FH* mutated, while no truncating mutation was detected in

type 2. Nuclear and cytoplasmic overexpression of 2SC alone showed 100% sensitivity and 74.2% specificity in diagnosing molecularly confirmed FH-deficient RCC and the specificity increased to 83.9% when accompanied with complete loss of FH. Overexpression of 2SC in the cytoplasm alone did not predict *FH* mutation.

Figure 1 - 538

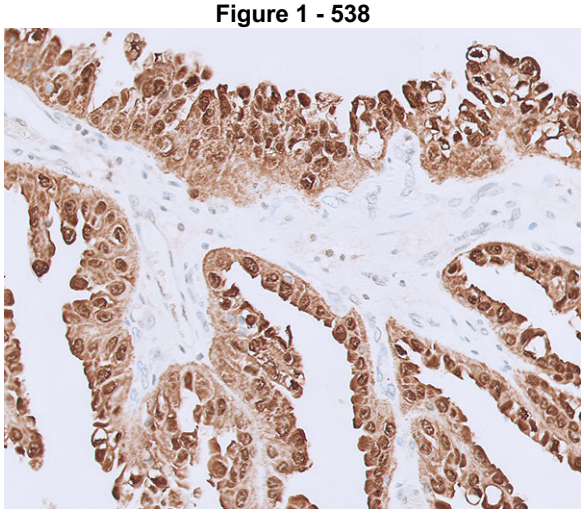

Figure 2 - 538

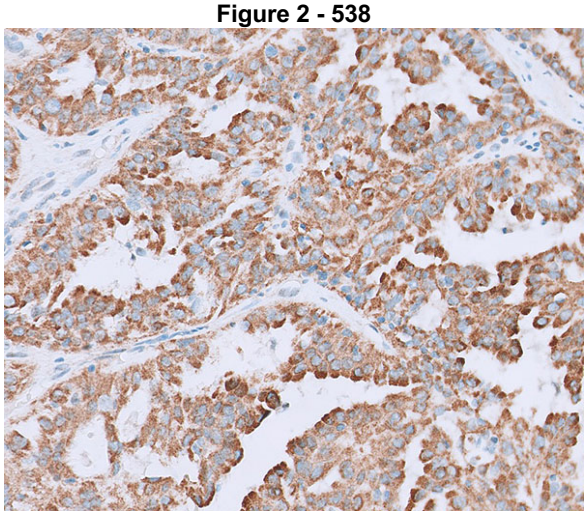

Conclusions: By Sanger sequencing, 77.3% of type 1 aberration cases were confirmed to be *FH* mutated. Complete FH loss accompanied with nuclear and cytoplasmic overexpression of 2SC is sensitive (100%) and specific (83.9%) for diagnosis of FH-deficient RCC. Further next-generation sequencing will be performed for Sanger negative cases to exclude mutations of lower frequency.

539 Diagnostic Utility of FH and 2-succinocysteine (2SC) Immunohistochemistry for Fumarate Hydratase-Deficient Renal Cell Carcinoma: Comparison and Validation of a New (Commercially Available) 2SC Antibody

Jie-Fu Chen[1], Jatin Gandhi[2], Achim Jungbluth[1], Max Kong[3], Hikmat Al-Ahmadie[1], Samson Fine[1], Anuradha Gopalan[1], Judy Sarungbam[1], S. Joseph Sirintrapun[1], Satish Tickoo[1], Victor Reuter[1], Ying-Bei Chen[1]
[1]Memorial Sloan Kettering Cancer Center, New York, NY, [2]University of Washington, Seattle, WA, [3]Kaiser Permanente, Sacramento, CA

Disclosures: Jie-Fu Chen: None; Jatin Gandhi: None; Achim Jungbluth: None; Max Kong: None; Hikmat Al-Ahmadie: *Consultant*, AstraZeneca, Janssen Biotech, Paige.ai; Samson Fine: None; Anuradha Gopalan: None; Judy Sarungbam: *Consultant*, Janssen Research & Development, LLC; S. Joseph Sirintrapun: None; Satish Tickoo: None; Victor Reuter: None; Ying-Bei Chen: None

Background: Diagnosis of Fumarate hydratase-deficient renal cell carcinoma (FHD-RCC) is challenging as its morphologic spectrum has been greatly expanded. Loss of FH by immunohistochemistry (IHC) is highly specific for FHD-RCC but lacks sensitivity in cases with retained defective FH protein. 2SC detects aberrant protein succination in FHD-RCC and showed higher sensitivity than FH, but the availability of antibody was limited. Recently, a new rabbit polyclonal 2SC (Discovery, crb2005017e) antibody became commercially available; however, its performance in diagnosing FHD-RCC remains to be explored.

Design: We performed FH and 2SC IHC on tissue sections and tissue microarrays from 47 molecularly confirmed FHD-RCC and a range of non-FHD renal tumors (237 clear cell, 11 clear cell papillary, 97 papillary [pRCC], 26 classic chromophobe, 12 eosinophilic chromophobe, 93 high grade unclassified, 19 low-grade unclassified RCC [uRCC-LGE], and 10 oncocytoma) to assess the sensitivity, specificity, and staining patterns.

Results: Of the molecularly-confirmed 47 FHD-RCC, FH was lost in 32 (71%), partially lost in 7 (16%), and retained in 6 (13%); 2SC exhibited diffuse, strong cytoplasmic staining and granular to diffuse nuclear reactivity (positive; pattern 1) in all 47 tumors (100%). In non-FHD renal tumors, we identified 4 2SC staining patterns: Pattern 2 (equivocal) – patchy to diffuse cytoplasmic staining and focal nuclear reactivity; pattern 3 (negative) – patchy to diffuse cytoplasmic staining only; pattern 4 (negative) – patchy to diffuse nuclear staining only; pattern 5 (negative) – rare scattered cytoplasmic/nuclear staining or completely non-reactive

(Figures 1 & 2). Pattern 1 was not seen in non-FHD tumors. Pattern 2 was seen in 1 pRCC (1%), 2 uRCC-LGE (11%), and 1 oncocytoma (10%); all 4 retained FH. Pattern 3 was observed in 120 cases (24%) with enrichment of tumors with eosinophilic cytoplasm. Overall, 2SC stain had sensitivity and specificity approaching 100%. Loss of FH was only seen in 1 case of pRCC (specificity 99.8%), which showed pattern 5 (negative) 2SC staining.

Figure 1 - 539

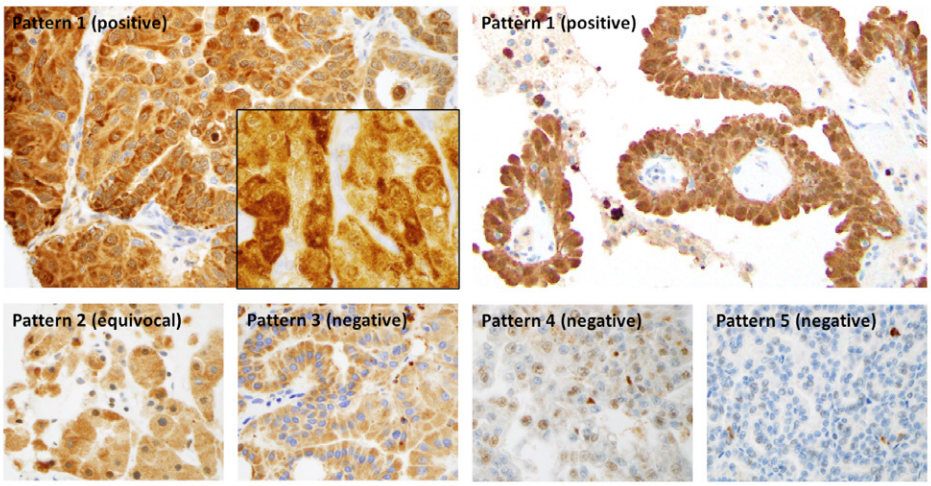

Figure 2 – 539

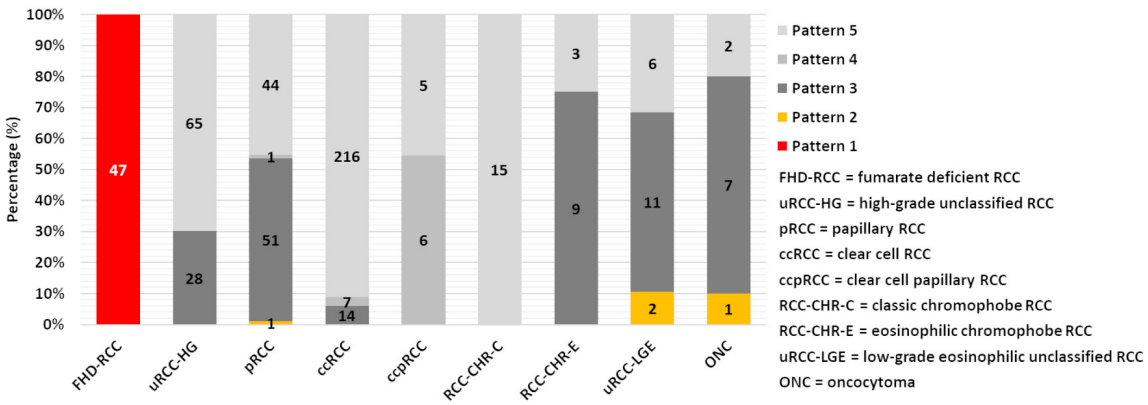

Conclusions: The 2SC IHC stain using the new commercial 2SC antibody for diagnosing FHD-RCC requires recognizing the pattern correlated with FH-deficiency: 1) nuclear staining at variable intensity, 2) diffuse staining in tumor cells. The relatively common cytoplasmic-only 2SC staining (pattern 3) does not correlate with FH deficiency. Combination of FH and 2SC or molecular testing can help achieve high sensitivity and specificity.

540 Molecular Cytogenetic and Clinical-Pathologic Analysis of Papillary Renal Cell Carcinoma Type 2: A Single Institution Experience

Zhengshan Chen[1], Yipeng Geng[1], Anica Wandler[2], Brian Cone[3], Fabiola Quintero-Rivera[4], Anthony Sisk[5]
[1]University of California, Los Angeles, Los Angeles, CA, [2]David Geffen School of Medicine at UCLA, Los Angeles, CA, [3]Affiliated Pathologist Medical Group, Los Angeles, CA, [4]University of California, Irvine, Orange, CA, [5]The Regents of the University of California, Los Angeles, Los Angeles, CA

Disclosures: Zhengshan Chen: None; Yipeng Geng: None; Anica Wandler: None; Brian Cone: None; Fabiola Quintero-Rivera: None; Anthony Sisk: None

Background: Papillary renal cell carcinoma (pRCC) is the most common non-clear cell RCC and is classified into 2 types by morphology. pRCC type 2 is heterogeneous with diverse histology and genetic changes. Currently 3 cytogenetic groups have been proposed (Linehan et al, 2016). Each group is characterized by specific aberrations as describe in Table 1 legend below. Limited data is available about the correlation between cytogenetic groups and clinicopathologic features. In this study we report the molecular cytogenetic analysis of pRCC type 2 and analyze its association with adverse pathological features.

Design: All cases with a diagnosis of pRCC type 2 between January 2002 and August 2017 were retrieved per IRB approval. Tissue microarray cores containing only tumor were used for SNP chromosome microarray (CMA) testing. Tumors were classified into 3 cytogenetic groups based on G-band karyotyping and CMA results. The pathologic, demographic and clinical variables were compared between those groups.

Results: From 160 cases with a diagnosis of pRCC type 2, 135 (84%) cases had pure pRCC type 2 and the rest had mixed pRCC type 1 and type 2. 88 out of 135 cases had abnormal karyotyping results, 16 of those cases with inconclusive results were chosen for additional CMA analysis for further characterization. CMA detected 1q loss in 3 cases, reflex IHC for FH confirmed FH deficient RCC in one case and suggested this diagnosis in the other 2 cases, thus all 3 cases) were excluded from this study. For the remaining 85 cases, 68 cases were classified into cytogenetic group 1, 8 cases into group 2 and 9 cases into group 3 (Table 1). Compared to group 1, tumors in group 2 and 3 had a much larger size ($p = 0.002$), a higher nuclear grade ($p = 0.038$), a higher pT stage ($p < 0.00001$) and a higher chance for metastasis ($p < 0.00001$). There was no significant difference between group 2 and group 3 regarding the analyzed pathologic parameters.

Table 1. Clinicopathologic features of molecular cytogenetic subgroups of pure pRCC type 2

	Group1 (n = 68)	Group 2 (n = 8)	Group 3 (n = 9)	P value
Age (mean, y)	64	58	68	0.727
Gender M F	58 (85.3%) 10 (14.7%)	8 (100.0%) 0	7 (77.8%) 2 (22.2%)	0.755
Tumor size (mean, cm)	5.1	7.3	10.3	0.002
ISUP/WHO Grade 1-2 3-4	26 (38.2%) 42 (61.8%)	2 (25.0%) 6 (75.0%)	0 9 (100.0%)	0.038
Stage (pT) 1-2 3	53 (77.9%) 15 (22.1%)	1 (12.5%) 7 (87.5%)	1 (11.1%) 8 (88.9%)	< 0.00001
Metastasis	2 (3.1%)	4 (50.0%)	4 (44.4%)	< 0.00001

Group 1: cytogenetic profile similar to type 1 pRCC with mostly gain of chromosomes 7, 16, and 17 as well as less frequent gain of chromosomes 3 and 12 and loss of chromosome 22; Group 2: cytogenetic subgroup with fewer chromosome alterations that typically have gain of chromosomes 16 and 17q and less frequent gain of chromosome 12 and loss of chromosome 14; Group 3: genome unstable subgroup with multiple chromosomal losses including 1p, 3p, 4, 9p, 14, 18, and 22. Group 2 and 3 are combined together to be compared with group 1 and p value is calculated by statistical analysis. Metastasis includes local lymph node and remote metastasis.

Conclusions: Cytogenetic group 1 pRCC type 2 has a similar cytogenetic profile as pRCC type 1 and presents with a smaller tumor size, a lower pT stage and rare metastasis. However cytogenetic group 2 and 3 pRCC type 2 are more aggressive with a higher pT stage and higher chance for metastasis. CMA is more conclusive than karyotyping to characterize genetic alterations in

kidney tumors. Patients with group 2 and 3 cytogenetic features may require a closer follow up and alternative treatment after surgery.

541 Deep Learning-based Automated Detection of Prostate Cancer Lesions in Hematoxylin Only Visualized Images

Joonyoung Cho[1], Tae-Yeong Kwak[2], Sun Woo Kim[1], Hyeyoon Chang[1]
[1]Deep Bio Inc., Seoul, South Korea, [2]Deep Bio Inc., Guro-gu, South Korea

Disclosures: Joonyoung Cho: *Employee*, Deep Bio Inc.; Tae-Yeong Kwak: *Employee*, Deep Bio Inc.; Sun Woo Kim: *Stock Ownership*, DeepBio; Hyeyoon Chang: *Employee*, Deep Bio Inc.

Background: Hematoxylin and eosin (H&E) stain is a technique widely used in pathology for recognizing various tissue morphologies. Hematoxylin is one of the most commonly used counterstains to enable visualization of nuclei when employing an enzyme/chromogen detection system including immunohistochemical (IHC) staining. Most research for deep learning on whole slide images (WSIs) has been focused on analyzing H&E stained images. In this study, we introduce a deep learning algorithm that can identify cancerous regions on artificially generated hematoxylin only (H-only) visualized WSIs of prostate needle biopsies.

Design: We generated 1,219,451 patches from 2,955 H&E stained prostate needle biopsy and resection WSIs to train the model. During patch generation, we used the color deconvolution method to separate the stain into Hematoxylin and other stains. (Figure 1) Cancer lesion annotations were applied to the generated H-only patches. The cancer lesions in the patches were annotated by an experienced pathologist. We split these data into 2,376 slides for training and 579 slides for tuning. After training, the checkpoint with the best intersection over union (IoU) value for cancer detection (0.6902) was selected. For evaluation, we generated 12,942 patches from 1,032 H&E stained prostate needle biopsy WSIs. Sample patches were transformed to H-only patches and analyzed for detection of cancerous regions. The semantic segmentation model was trained to segment cancer lesion regions at the pixel-level. In addition, we performed a slide-level evaluation for H&E and high molecular weight cytokeratin (HMW-CK) staining using the same set of WSIs. The model diagnoses a slide as cancer if the cancer lesion is detected in patches from the slide.

Results: In the slide-level evaluation, the model achieved sensitivity 87.67% and specificity 86.52% for H&E stained WSIs. For HMW-CK stained WSIs, it achieved 84.98% and 91.47% respectively. An example of the cancer detection model run on the original H&E stained patch (Figure 2, first row) and HMW-CK stained patch (Figure 2, second row) are shown. The model demonstrated a cancer patch detection accuracy, sensitivity, and specificity of 93.03%, 85.22%, 96.07% respectively (Table 1). Compared with the ground truth established by a pathologist, the model's total IoU of cancer is 0.5657.

		Label	
		Cancer	Benign
Model	Cancer	3079	367
	Benign	534	8962
Accuracy		93.03%	
Sensitivity		85.22%	
Specificity		96.07%	
Cancer IoU		0.5657	

Figure 1 - 541

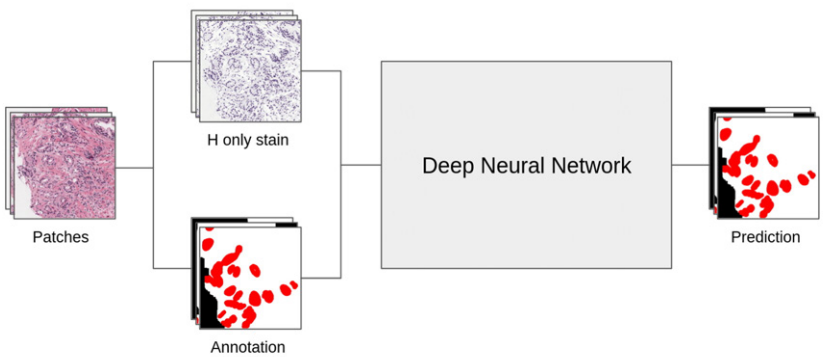

Figure 2 – 541

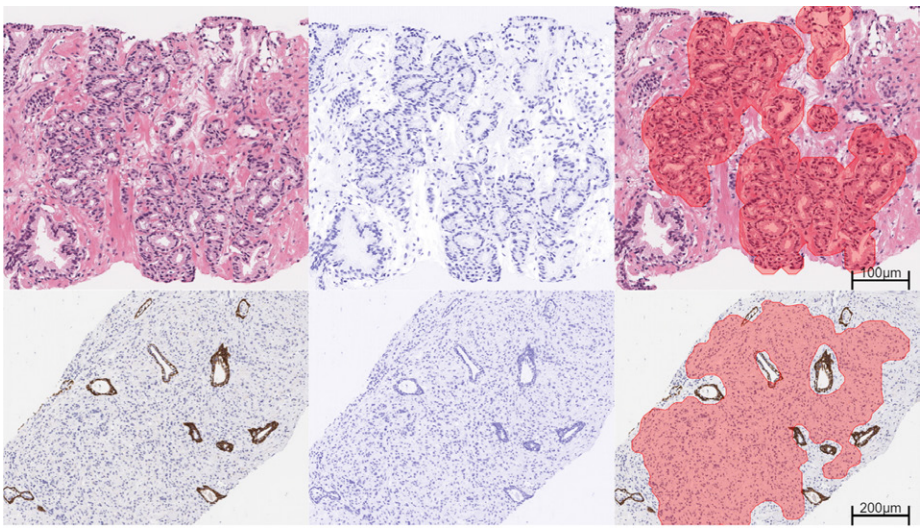

Conclusions: Although the performance could be refined, our study suggests the potential of applying deep learning models to detect cancerous regions other than H&E stains.

542 Analysis of Pathological Risk Factors for Metastatic Behaviour in 88 Pure Testicular Seminomas After Total Embedding of the Spermatic Cord and Hilar Soft Tissue

Maurizio Colecchia[1], Biagio Paolini[2], Giacomo Pini[3], Barbara Avuzzi[2], Stefano Andreani[2], Laura Carpenito[4], Anna Maria Paganoni[5], Nicola Nicolai[4]

[1]University Vita-Salute San Raffaele, Milan, Italy, [2]Fondazione IRCCS Istituto Nazionale Tumori Milano, Milan, Italy, [3]University of Insubria, Italy, [4]Fondazione IRCCS Istituto Nazionale Tumori Milano, Milano, Italy, [5]MOX - Modeling and Scientific Computing Dipartimento di Matematica, Milan, Italy

Disclosures: Maurizio Colecchia: None; Biagio Paolini: None; Giacomo Pini: None; Barbara Avuzzi: None; Stefano Andreani: None; Laura Carpenito: None; Anna Maria Paganoni: None; Nicola Nicolai: None

Background: Clinical stage I (no evidence of metastasis) is the most common presentation for pure seminoma (PS) (90%). A small proportion of clinical stage I PS will develop distant metastases, usually within 3 years since diagnosis. Identification of factors associating with metastatic disease is a clinical need to orient post-orchiectomy management in clinical stage I. Available studies are however prone to methodological limitations concerning sampling.

Design: In this monoinstitutional prospective study, we have extensively sampled 88 consecutive orchiectomies consisting of pure seminoma performed between 2017 and 2020 at Istituto Nazionale dei Tumori . We have processed at least 1 block for centimeter of tumor size. Additional blocks were submitted for the entire embedding of the spermatic cord and of hilar soft tissues (Figure 1). Every patient was followed up at the same institution (range 16-53 months). The following clinical and pathologic features were evaluated for potential association with metastatic disease: age, tumor size, peritumoral and spermatic cord lymphovascular invasion (LVI), pagetoid and stromal rete testis (RT) invasion, tumor extension into tunica vaginalis, hilar soft tissue invasion (HSTI), epididymal invasion (EI), infiltration of spermatic cord soft tissue. Studied parameters were correlated with the clinical stage.

Results: Mean age was 38 years (range 21-70). Mean tumor size was 3.6 cm(range 0.4-16). Metastatic disease was documented in 16 patients. RT pagetoid invasion only did not significantly associate with presence of metastasis. At multivariate logistic regression analysis, the most performing model includes vascular invasion and epididymal infiltration (Table 1). The size of the tumor was associated as a continuous variable with metastatic disease, while a distinct cut-off didn't reveal statistical significance as categorical variable in multivariate analysis. The extensive sampling of the spermatic cord (cord sections range 5-12) did not improve the detection of further foci of invasion.

Table1 Multivariate analysis with p-values and area under the curve (ROC curve)

Covariate	OR	IC (95%)	P-value	AUC
Vascular Infiltration	6.687	[1.872; 23.884]	0.003	0.778
Epididymis Infiltration	8.522	[1.239; 58.574]	0.029	

Figure 1 - 542

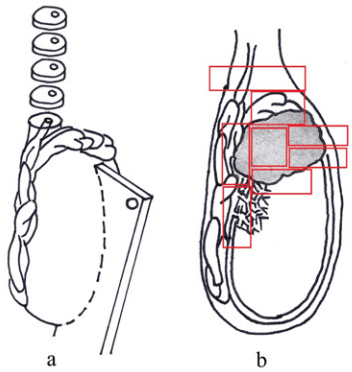

Figure 1 – Thorough sampling of the spermatic cord (a), hilar soft tissue and head of the epididymis (b)

Conclusions: Extensive sampling of paratesticular soft tissue and entire embedding of spermatic cord did not outperform standard protocol of testicular sampling, adopted for tumor staging. Although all factors, but pagetoid RT infiltration, were significantly correlated to metastasis in univariate analysis, in multivariate analysis LVI and EI only were associated with metastatic disease based on logistic regression model.

543 Evaluation of Clinicopathologic Characteristics Influencing the Spontaneous Regression of Germ Cell Tumors

Katrina Collins[1], Omer Saeed[1], Muhammad Idrees[1]
[1]*Indiana University School of Medicine, Indianapolis, IN*

Disclosures: Katrina Collins: None; Omer Saeed: None; Muhammad Idrees: None

Background: Spontaneous regression of a primary testicular germ cell tumor (GCT) is an uncommon phenomenon and refers to partial or complete disappearance of a GCT in the absence of treatment that commonly manifests as metastatic disease. Depending on the histologic type, tumor markers may be elevated. We evaluated a cohort of partially and completely regressed GCTs to assess factors influencing regression poorly understood at present time.

Design: By retrospective review, 156 cases (83 in house and 72 consultation) with evidence of partial or complete tumor regression were identified from January 1993 to August 2021. We analyzed clinical information and histopathological characteristics of testicular lesions and metastasis, and highlight the main findings.

Results: Cases presented between 18 and 77 yrs (mean, 39 yrs). Clinical presentations are as follows: 33 with retroperitoneal mass (2 also with abdominal pain and 1 also with testicular swelling), 21 with testicular mass, 19 with abdominal pain, 17 with back/flank pain (1 also with scrotal swelling), 7 with symptoms of metastases, 10 with testicular pain or swelling, 4 with a neck mass and 3 with an abdominal mass. Clinical presentation was unknown in 42 cases. One or more serum tumor markers (bHCG, AFP, LDH) were elevated in 73 cases, while 10 were not, and unknown in 73 cases. Microscopically, all cases showed a scar. Partial regression was seen in 54 cases (35%) and complete regression in 102 cases (65%). Germ cell neoplasia in situ (GCNIS) was present in 64 cases (41%), more common with partial regression compared to complete regression (66.7% and 27.5%, respectively, $p<0.001$). Ninety-one patients received chemotherapy, while 34 had no treatment prior to orchiectomy or retroperitoneal lymph node dissection. Treatment was unknown in 31 cases. GCT metastases in 50 cases were seminoma (18), teratoma (17), yolk sac tumor (8), mixed GCT (5), embryonal carcinoma (1), and choriocarcinoma (1). Follow-up data were available for 76 patients, 44 with complete regression and 29 with partial regression; the majority had no evidence of disease (96%) while 3 with complete regression died of disease (4%). There was no statistically significant difference in clinical outcome between patients with complete and partial regression. Clinical follow-up duration ranged from 0 to 283 mos (mean, 29 mos). Older patients

were found to be less likely to have complete regression compared with younger patients (odds ratio 0.9, 95% C.I. 0.002-0.055, *p*=0.037).

Conclusions: This is the largest series of cases with regressed GCTs to date. GCNIS was more common in cases with partial regression compared to complete. Increasing age reduced the odds of complete regression. Post-therapy follow-up showed the majority of our subjects had no evidence of disease. Despite metastasis as initial presentation and higher stage, the cure rate is comparable to non-regressed GCTs.

544 Spectrum of Morphologic Findings in Orchiectomy Specimens from Individuals Undergoing Gender-Affirming Surgery

Katrina Collins[1], Micheal Andry[1], Joshua Roth[1], Liang Cheng[2], Muhammad Idrees[1]
[1]Indiana University School of Medicine, Indianapolis, IN, [2]Indiana University, Indianapolis, IN

Disclosures: Katrina Collins: None; Micheal Andry: None; Joshua Roth: None; Liang Cheng: None; Muhammad Idrees: None

Background: The incidence of gender dysphoria and those seeking surgical procedures to address gender dysphoria is increasing. We provide a histologic review of morphologic features observed in orchiectomy specimens from individuals who have undergone hormonal therapy prior to gender-affirming surgery.

Design: Orchiectomy specimens from 47 patients (bilateral, 45; unilateral, 2) who underwent gender- affirming surgery between 2017 and 2021 were examined for histopathologic alterations of germinal epithelium and interstitial cells, changes to germ cell morphology including germ cell neoplasia in situ (GCNIS) and hormone therapy-associated changes.

Results: The average age was 38 years (range 19-70 years). The average testis size was 4 cm (range 2-11 cm). The majority of cases showed seminiferous tubules with basement membrane thickening in 41/47 (86%) cases (mild, 22; moderate, 10; severe, 9) and 12/47 (26%) cases with full maturation. No cases of maturation arrest. Sertoli cell only profiles were observed in 6/47 (13%) cases. The most unusual finding was the presence of large atypical germ cells (3x size of normal germ cell) with clear cytoplasm and prominent nucleoli. Occasional bi-nucleated forms and mitotic figures were seen. These atypical germ cells were present in 43/47 (91%) cases. Although these atypical germ cells were basally aligned and displayed features resembling germ cell neoplasia in situ, on closer scrutiny they displayed regular nuclear borders and lacked markedly hyperchromatic and stippled chromatin, additionally confirmed with CD117 and SALL4 immunostains. Scattered mast cells were present in all cases. Leydig cells were present in all cases, frequently showed degenerated changes and were markedly reduced in 24/47 (51%), normal in number in 16/47 (34%), and abundant in 7/47 (57%) cases. GCNIS was present in 1 testis. The interstitium was edematous in 19/47 (40%), fibrotic in 10/47 (21%), and mixed in 18/47 (38%) cases. Various stages of maturation and regression were seen despite patients being on hormonal therapy.

Conclusions: Pathologists must be aware of the histologic changes related to treatment in patients undergoing gender-affirming surgery including reduction of germ cells with frequently encountered atypical germ cell forms. In rare cases, especially in the absence of maturation, GCNIS may be overlooked on routine H&E stain alone. Proper utilization of immunohistochemistry may aid to distinguish GCNIS from potential mimics.

545 Clinicopathologic Features and Proposed Grossing Protocol of Orchiectomy Specimens Performed for Gender Affirmation Surgery

Kristine Cornejo[1], Esther Oliva[2], Rory Crotty[1], Peter Sadow[2], Kyle Devins[1], Anton Wintner[2], Chin-Lee Wu[1]
[1]Massachusetts General Hospital, Boston, MA, [2]Massachusetts General Hospital, Harvard Medical School, Boston, MA

Disclosures: Kristine Cornejo: None; Esther Oliva: None; Rory Crotty: None; Peter Sadow: None; Kyle Devins: None; Anton Wintner: None; Chin-Lee Wu: None

Background: Gender affirmation surgery performed for gender dysphoria is increasing in order to instigate changes in secondary sex characteristics more closely approximating gender identity. We investigated the clinicopathologic features of gender affirming orchiectomies to devise a grossing protocol for these increasingly encountered specimens.

Design: We obtained 35 orchiectomies from 18 patients and reviewed clinical characteristics and morphologic features. The number of sections obtained per case were noted and reviewed to devise an optimal grossing protocol to assess pathologic findings.

Results: 17 patients had bilateral orchiectomy with 1 unilateral. Average patient age was 41.2 (23-71) years; all received hormone therapy with variations of estradiol (n=17), spironolactone (n=12) and Lupron (n=7), for a mean of 72.8 (12-348) months. The average number of slides per orchiectomy was 6.77 (1-11) slides.

The mean gonad size was 4.08 (2-5.5) cm and weighed 30.6 (19-46) grams. Seminiferous tubules were small in diameter 0.192 (0.11-0.43) mm with peritubular fibrosis and wall thickness of 0.014 (0.006-0.036) mm. Aspermatogenesis occurred in 24 (51.5%) testes, of which 18 and 6 displayed maturation arrest at the level of spermatogonia and spermatocytes, respectively; some with Sertoli-only appearance (Figure 1). 5 showed hypospermatogenesis with complete maturation. 18 (51.5%) testes exhibited scattered cells with cytomegaly (≥3x Sertoli cell nuclei), concerning for germ cell neoplasia in situ (GCNIS), but OCT3/4 negative, and 6 (17%) had multinucleated stromal cells (Figure 2). Leydig cells were markedly reduced/absent in 26 (74%) and hyperplastic in 1 (3%) testis. Epithelial hyperplasia with stratification and micropapillae/cribriform formation was identified in 15 (44%) rete testes and 17 (52%) epididymides and 11 (33%) showed peri-epididymal muscular hyperplasia. All findings were identified in the initial 1-2 slides reviewed per case which included rete testis/epididymis, except for 2 in which focal tubular sclerosis would have been missed.

Figure 1 - 545

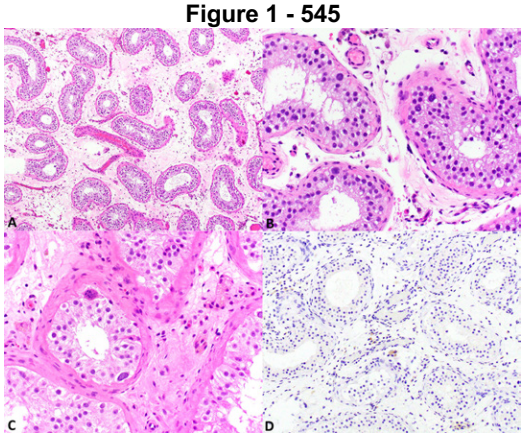

Figure 2 - 545

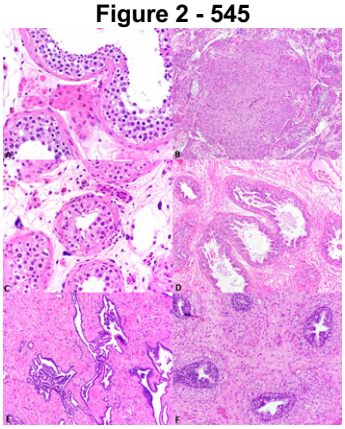

Conclusions: Although all patients received hormone therapy, only a subset had changes consistent with exogenous hormone exposure including testicular atrophy, hypo/aspermatogenesis, Leydig cell hypoplasia and rete testis/epididymal hyperplasia. The presence of cytomegaly which can mimic GCNIS in some cases, may be a potential pitfall. Overall, 2 sections (including rete testis/epididymis) appear to be sufficient to identify the relevant pathology.

546 p53 Immunohistochemistry Identifies High-Risk Prostate Cancer: A Prospective Study with Three Decades of Follow-up

Daniela Correia Salles[1], Konrad Stopsack[2], Bailey Vaselkiv[3], Sydney Grob[3], Lorelei Mucci[3], Tamara Lotan[4]
[1]Johns Hopkins Medical Institutions, Baltimore, MD, [2]Harvard T.H. Chan School of Public Health, Boston, MA, [3]Harvard University, Boston, MA, [4]Johns Hopkins University School of Medicine, Baltimore, MD

Disclosures: Daniela Correia Salles: None; Konrad Stopsack: None; Bailey Vaselkiv: None; Sydney Grob: None; Lorelei Mucci: *Consultant*, Bayer; *Grant or Research Support*, Astra Zeneca, Janssen; Tamara Lotan: *Grant or Research Support*, Roche/Ventana, DeepBio, Myriad

Background: Given heterogeneous clinical outcomes and the increase in active surveillance, there is a growing need for inexpensive and widely available tissue-based biomarkers to guide clinical decision making in prostate cancer. Among genomic biomarkers of tumor aggression, *TP53* inactivation has emerged as the most consistently associated with adverse outcomes in primary and metastatic prostate cancer. Here, we evaluated an inexpensive and genetically validated immunohistochemical assay that detects *TP53* missense mutations with high sensitivity in population-based cohorts with long-term follow-up.

Design: To evaluate prevalence, clinical and molecular features, and long-term outcomes of p53 expression, we studied participants of two cohort studies, the Health Professionals Follow-up Study (HPFS) and the Physicians' Health Study (PHS),

diagnosed with prostate cancer 1982–2009 during prospective follow-up and followed through 2019 (HPFS) or 2014 (PHS). Prostate cancer diagnoses and development of metastases were confirmed by the participating health professionals, their treating physicians, and a review of medical and pathology records. Cause of death was adjudicated by physicians. To assess p53 expression, we performed immunohistochemistry on 14 tissue microarrays using the BP53-11 antibody and a genetically validated automated staining and scoring protocol on the Ventana BenchMark system.

Results: p53 was expressed in 36 tumors (3.7%) characterized by higher Gleason scores, increased proliferation, more frequent PTEN loss, and greater aneuploidy (Table 1). 949 men with nonmetastatic disease were followed for up to 31 years (median: 17 years) for the development of metastases and prostate cancer death (Figure 1). p53 nuclear accumulation was associated with lethality before (hazard ratio [HR] 6.2; 95% CI 3.6–10.8) and after adjusting for age and Gleason score (HR 3.8; 95% CI 2.2–6.7). Over 20 years, men with p53-positive cancers lost, on average, 5.6 years due to lethal prostate cancer, compared to 1.0 years among those with p53-negative cancers (difference, 4.6 years; 95% CI 2.1–7.0).

Table 1. Characteristics of men diagnosed with primary prostate cancer 1982–2009 during prospective follow-up of the HPFS and PHS cohorts, by p53 status.[1]

	p53-negative	**p53-positive**
Participants/tumors	926	36
Cohort		
HPFS	712 (77%)	24 (68%)
PHS	214 (23%)	12 (32%)
Age at diagnosis (years)	65.6 (61.6, 69.0)	64.6 (60.0, 69.8)
Gleason score		
5-6	166 (18%)	0 (0%)
3+4	330 (36%)	7 (19%)
4+3	236 (26%)	7 (19%)
8	73 (8%)	9 (25%)
9–10	120 (13%)	13 (36%)
Unknown	1	0
Clinical stage		
T1/T2	870 (95%)	29 (81%)
T3	30 (3%)	3 (8%)
T4/N1	7 (1%)	1 (3%)
M1	9 (1%)	3 (8%)
Unknown	10	0
Prostatectomy stage		
pT1/T2	606 (70%)	16 (59%)
pT3/T3a	168 (19%)	4 (15%)
pT3b	66 (8%)	4 (15%)
pT4/N1	30 (3%)	3 (11%)
Unknown/No prostatectomy	56	9
PTEN expression status		
PTEN intact	650 (84%)	18 (60%)
PTEN loss	120 (16%)	12 (40%)
Not assessed	156	6
Ki67 (positive nuclei)		
<1%	462 (86%)	14 (58%)
1 to <5%	62 (12%)	6 (25%)
≥5%	12 (2%)	4 (17%)
Not assessed	390	12

1. HPFS, Health Professionals Follow-up Study; PHS, Physicians Health Study. Values are count (percent) or median (interquartile range).

Figure 1 - 546

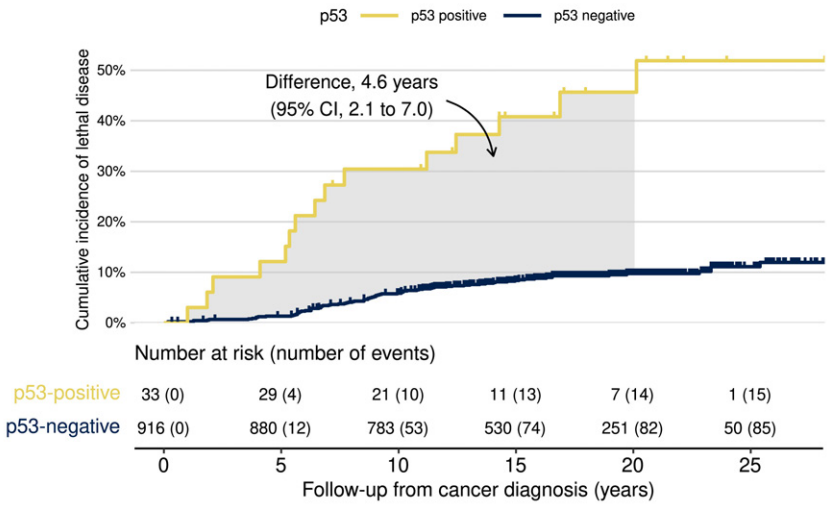

Conclusions: These results support clinical implementation of this robust and inexpensive assay to identify alterations in p53, the "guardian of the genome." p53 alterations are rare in primary prostate cancer, but associated with a very high risk of poor long-term outcomes.

547 Distribution of Tumor Infiltrating Lymphocytes and Tertiary Lymphoid Structures in Chemo-Naive Bladder Cancer Across Stages pT1 and pT2

Reba Daniel[1], Sahar Farahani[2], Geetika Goyal[1], Anna Budina-Kolomets[3], Maria Smith[3], Kyle Devins[4], Aileen Grace Arriola[5], Anupma Nayak[6], Priti Lal[1]

[1]University of Pennsylvania, Philadelphia, PA, [2]Renaissance School of Medicine at Stony Brook University, Stony Brook, NY, [3]Hospital of the University of Pennsylvania, Philadelphia, PA, [4]Massachusetts General Hospital, Boston, MA, [5]Temple University Hospital, Philadelphia, PA, [6]Perelman School of Medicine at the University of Pennsylvania, Philadelphia, PA

Disclosures: Reba Daniel: None; Sahar Farahani: None; Geetika Goyal: None; Anna Budina-Kolomets: None; Maria Smith: None; Kyle Devins: None; Aileen Grace Arriola: None; Anupma Nayak: None; Priti Lal: None

Background: Tumor infiltrating lymphocytes (TILs) and tertiary lymphoid structures (TLS) play a critical role in cancer outcomes and response to treatment (1-3) and are well studied in many solid tumors. However, literature on TLS and TILS on treatment naive primary bladder cancer (BC) is sparse. In this study, we sought to review patterns of TILs and TLS formation in primary, chemo-naive trans urethral resection (TUR) specimens staged as pT1 and pT2.

Design: Under institutional IRB approval, we reviewed 103 chemo-naïve TURBT specimens (Table 1) including 56 pT1 (non-muscle invasive bladder cancers/ NMIBC) and 47 stage pT2 (muscle invasive bladder cancers/ MIBC including chemo responsive MIBC-R and non-responsive MIBC-NR) for TIL density & presence or absence of TLS (with and without germinal centers/ GC). Indepth review of EMR to ensure identification of index chemo naive TUR and systematic documentation of recurrences by date was done. Depth of invasion for NMIBC was collected in mm, as number of invasive foci and with reference to involvement of MM or its surrogate vascular plexus (VP). Chi-square and Mann-Whitney tests were used to evaluate the association of TILs and TLS with depth of invasion and recurrence (in NMIBC) & response to treatment (in MIBC). Furthermore, a comparison of TILs/TLS between NMIBC and MIBC was also performed. Cox-proportional hazard ratio models was used for association of TILs/TLS formation in NMIBC recurrence/ progression to MIBC

Results: (1) In NMIBC, moderate TIL density (HR 0.38; p value: 0.03) and presence of TLSGC (HR 0.15; p value: 0.04) were associated with reduced risk of recurrence. (2) NMIBC show no significant difference in TLS distribution in association with depth, size or number of invasive foci. (3) While the distribution of TIL density between MIBC and NMIBC was significantly different (p value: 0.018), no significant difference in TLS was identified. (4) Both NMIBC as well as MIBC reveal TLS with GC. (5) TLSNGC are the most common pattern of TLS in BC

Table 1	NMIBC	MIBC with Response (MIBC-R)	MIBC No Response (MIBC-NR)
Number of patients	56	16	31
Mean Age (Range)	69.3 (39-94)	66.6 (52-82)	
Total number of TLS identifiable by H&E	35 (62.5%)	13 (81.3%)	22 (70.9%)
TLS with GC (TLSGC)	12 (21.4%)	4 (25.0%)	5 (16.1%)
TLS with NO GC (TLSNGC)	23 (41.1%)	9 (56.3%)	17 (54.8%)
TIL Density			
Absent	2 (3.6%)	0	0
Sparse	23 (41.1%)	2 (12.5%)	9 (29.0%)
Intermediate	26 (46.4%)	8 (50%)	14 (45.2%)
Dense band like	5 (8.9%)	6 (37.5%)	8 (25.8%)

Conclusions: 1)Our data suggests a reduced risk of recurrence in NMIBC in the presence of moderate TIL density and TLS with GC. 2)Unlike some of the recent studies, we saw no difference in TLS with GC between NMIBC and MIBC. We however did not use immunohistochemical stains to identify GC. 3)An expanded cohort with more detailed evaluation of TIL density and TLS will be undertaken to follow up on the above findings.

548 Bilateral Testicular Germ Cell Tumors in Post-Pubertal Males: Clinicopathologic Features and Important Prognostic Factors

Kingsley Ebare[1], Joe Rodriguez[1], Ahmed Shehabeldin[2], Niki Milward[1], Marcos Estecio[1], Aron Joon[1], Shi-Ming Tu[1], Miao Zhang[1]

[1]The University of Texas MD Anderson Cancer Center, Houston, TX, [2]The University of Texas MD Anderson Cancer Center, TX

Disclosures: Kingsley Ebare: None; Joe Rodriguez: None; Ahmed Shehabeldin: None; Niki Milward: None; Marcos Estecio: None; Aron Joon: None; Shi-Ming Tu: None; Miao Zhang: None

Background: Bilateral testicular germ cell tumor (TGCT) is rare, comprising 1-3% of adult germ cell tumors. Understanding the clinical and pathologic factors influencing evolution, progression and survival from these tumors is crucial for the management and prediction of outcomes. We aim to provide an insight into clinical and pathologic features that may influence survival and development of contralateral TGCT.

Design: Our study cohort comprised 33 patients with bilateral TGCT who underwent first orchiectomy between January 1984 and March 2019 and the second orchiectomy between August 1997 and August 2020. Hematoxylin and eosin-stained slides were reviewed, and the corresponding relevant blocks were retrieved and marked for DNA and RNA extractions. RNA Epigenomic assays and genomic assays are currently being performed on HiSeq 3000 (Illumina, Inc SanDiego) to evaluate the concordance between the first and second tumors. We also reviewed the pathologic reports and retrieved pertinent histologic and clinical information. All statistical analyses were conducted with SAS 9.4 (SAS, Cary NC USA). Cox proportional hazard model was utilized to calculate overall survival. Model parameters included age, presence/absence of mixed tumor, tumor size, and synchronous vs metachronous tumors.

Results: The mean age of our cohort is 33 years (range 24.2-44.2 years) with majority of the patients developing metachronous tumors (87.8%). Overall, 18 patients died and 10 were lost to follow-up. Tumors were predominantly mixed with seminoma (50%) and embryonal carcinoma (33%) comprising the majority. For metachronous TGCT, the median time to develop a second testicular malignancy was 47 months. Patients with synchronous TGCT (mean 33 years) were significantly younger vs. metachronous (mean 38 years, p value 0.04). Older patients were more likely to develop TGCT in the second testis (p value = 0.015). Larger tumor size was statistically associated with shorter overall survival (p =0.008; hazard ratio 1.021 (1.049, 1.381). DNA and RNA seq analysis show similar genomic abnormality between bilateral tumors and provide information on possible targetable genes for treatment.

Conclusions: Our findings re-emphasize the important factors that lead to the development of a second testicular malignancy and suggests that tumor size, age and histologic types are important prognostic factors in the development of a second testicular tumor as well as overall survival. Our study identifies targetable genes for future treatment.

549 MAGE Family of Cancer Testis Antigen Genes are Associated with Resistance to Immune Checkpoint Inhibitors in Sarcomatoid Renal Cell Carcinomas

Kingsley Ebare[1], Yong Lee[2], Pieretti Christian[3], Cameron Noorbakhsh[1], Xiangjun Tian[1], Jing Wang[1], Kasthuri Kannan[1], Krishna Bhat[1], Jose Karam[1], Kanishka Sircar[1]

[1]The University of Texas MD Anderson Cancer Center, Houston, TX, [2]HTG Molecular Diagnostics, Inc., Tucson, AZ, [3]The University of Texas MD Anderson Cancer Center, University of Texas MD Anderson Cancer Center, TX

Disclosures: Kingsley Ebare: None; Yong Lee: None; Pieretti Christian: None; Cameron Noorbakhsh: None; Xiangjun Tian: None; Jing Wang: None; Kasthuri Kannan: None; Krishna Bhat: None; Jose Karam: *Consultant*, Merck, Pfizer, Johnson and Johnson; *Grant or Research Support*, Mirati, Merck, Elypta, Roche/Genentech; *Stock Ownership*, MedTek, RomTech; Kanishka Sircar: None

Background: Sarcomatoid renal cell carcinoma (sRCC), traditionally refractory to treatment and associated with an aggressive clinical course, has recently shown response to immune checkpoint inhibitor (ICI) therapy in a subset of patients. Given the lack of predictive biomarkers to ICI therapy in RCC generally, including in sRCC, our aim was to evaluate potential tissue based immune related biomarkers in sRCC patients treated with ICI therapy.

Design: The study cohort consisted of patients with surgically resected sarcomatoid RCC of clear cell subtype(sccRCC), with no neoadjuvant therapy and who subsequently received an ICI therapy regimen (ipilimumab/nivolumab) after resection. The epithelioid (E-) and sarcomatous (S-) components of sccRCC were macrodissected from FFPE tissues. Thirty-two (32) samples from 17 patients (median age (63 yrs), tumor size (8.5 cm), stage group III/IV) were interrogated by the Precision Immuno-Oncology Panel (HTG EdgeSeq) which assays the RNA expression of 1392 immune related genes. Gene expression was correlated to response to ICI therapy as defined by clinical/radiological parameters. RNA-seq expression data from TCGA sccRCC (n=31) and control ccRCC cases (n=494) and HTG EdgeSeq ccRCC (n=24) cases were also analyzed.

Results: Nine (9) patients responded to ICI therapy whereas 8 were resistant with no significant differences in clinicopathologic variables between the 2 groups. While traditional markers such as CD274 (PDL1) were not associated with response, our most striking finding was that the MAGE family of cancer-testis antigen (CTA) genes constituted 4 of the top 10 genes associated with therapy resistance (Figure 1). Moreover, other CTA genes (XAGE2, XAGE5, CT47) that were differentially expressed between responders and non-responders, also showed significantly higher expression in therapy resistant cases (Table 1). Notably, this differential expression in CTA genes was not related to: E-versus S- histology within tumors; or to sccRCC vs ccRCC phenotype.

Table 1: Cancer Testis Antigens Associated with ICI Resistance in sRCC

Probe	Fold Change	Resistance to ICI (p value)	S vs E (p value)	sccRCC vs ccRCC HTG (p value)	sccRCC vs ccRCC TCGA (p value)
MAGEC2	2.40	4.13E-04	NA	0.21	0.23
MAGEA3_A6	2.03	1.30E-03	0.17	0.98	NA
MAGEA4	2.12	1.40E-03	0.42	0.03	0.04
MAGEA1	2.16	2.10E-03	0.28	0.67	0.75
MAGEA10	2.15	2.30E-03	NA	0.89	9.10E-14
MAGEA12	2.06	2.50E-03	0.19	0.08	0.65
CT47_family	1.86	5.80E-03	0.67	0.53	NA
XAGE2	1.63	1.82E-02	0.65	0.89	0.58
MAGEC1	1.78	2.16E-02	0.63	0.62	0.10
XAGE5	1.57	3.31E-02	0.72	0.59	0.95

Figure 1 - 549

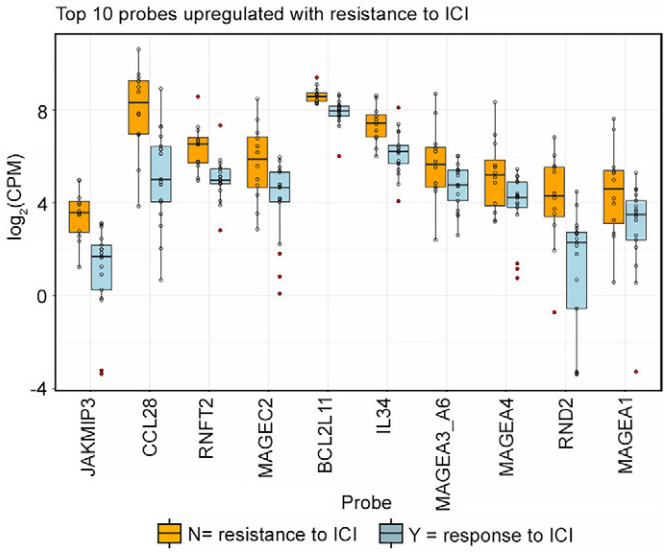

Conclusions: Our data suggest that some cancer-testis antigen genes, particularly MAGE family genes, may serve as biomarkers of resistance to ICI based therapy in sccRCC. These findings warrant validation using orthogonal assays and in broader RCC patient cohorts.

550 Utilization of NKX3.1, P501S, PSA and SF-1 to Distinguish Malignant Leydig Cell Tumor From Metastatic Adenocarcinoma of the Prostate to the Testis

Eric Erak[1], Tamara Lotan[2], Jonathan Epstein[3]
[1]Johns Hopkins Hospital School of Medicine, Baltimore, MD, [2]Johns Hopkins University School of Medicine, Baltimore, MD, [3]Johns Hopkins Medical Institutions, Baltimore, MD

Disclosures: Eric Erak: None; Tamara Lotan: *Grant or Research Support*, Roche/Ventana; *Grant or Research Support*, DeepBio; *Grant or Research Support*, Myriad; Jonathan Epstein: None

Background: A recent study has demonstrated that NKX3.1 positive staining can be uncommonly seen in testicular Sertoli cell tumors (1 out of 4 cases). Also, it was reported that two out of three Leydig cell tumors of the testis showed diffuse cytoplasmic staining for P501S, although it is unclear if it was the specific granular staining that defined true positivity. However, Sertoli cell tumors do not typically pose a diagnostic dilemma with metastatic prostate carcinoma to the testis. In contrast, malignant type Leydig cell tumors can closely resemble Gleason Score 5+5=10 prostatic carcinomas metastatic to the testis. No data is currently published regarding the expression of prostate markers in malignant Leydig cell tumors of the testis.

Design: Cases for this study were gathered from two large genitourinary pathology consult services, one of them specializing in testicular pathology. The cases were gathered from 1990 to 2019. 15 cases of malignant Leydig tumors with available blocks or unstained slides were collected. We are in the process of staining a TMA of high grade prostate adenocarcinoma with SF-1.

Results: All 15 cases of malignant Leydig cell tumors were negative for NKX3.1. PSA and P501S were also performed in 9 cases with available material, with negative staining for both markers in all the cases. SF-1 staining on the same 9 cases that we performed PSA and P501S showed positive nuclear staining in all 9 cases.

TMA from 77 cases showing high grade prostate adenocarcinoma with primary Gleason pattern 5 demonstrated no staining for SF-1.

Figure 1 - 550

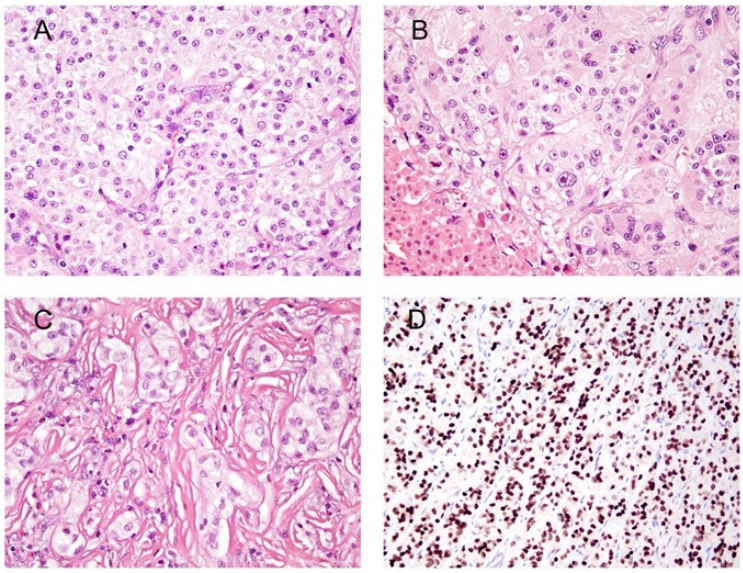

Legend: A) Sheets of malignant Leydig cell tumor mimicking prostate cancer; B) Malignant Leydig cell tumor with atypia and necrosis (lower left) mimicking high grade prostate cancer; C) Nests of malignant Leydig cell tumor; D) Diffuse SF-1 staining in malignant Leydig cell tumor.

Conclusions: Malignant Leydig tumors are extremely rare tumors and can closely resemble metastatic prostate cancer to the testis, which is the most common metastasis to the testis. Prostatic markers have not been reported in malignant Leydig cell tumor, and only very recently has a series been published on SF-1 staining in these tumors. In our study, all malignant Leydig cell tumors were negative for prostate markers and showed positivity for SF-1, which can be used to distinguish metastatic prostate cancer to the testis from malignant Leydig Cell tumor.

551 Nested Variant of Urothelial Carcinoma (NVUC) of the Upper Urinary Tract

Aisha Fatima[1], Daniel Russell[2], Jonathan Epstein[1]
[1]Johns Hopkins Medical Institutions, Baltimore, MD, [2]Jackson Memorial Hospital/University of Miami Hospital, Miami, FL

Disclosures: Aisha Fatima: None; Daniel Russell: None; Jonathan Epstein: None

Background: NVUC of the upper urinary tract is rare. While this variant has an aggressive behavior in the urinary bladder, little is known about this variant in the renal pelvis and ureter. Additionally, due to NVUC's bland morphology and resemblance to von Brunn's nests proliferation which can be florid in the renal pelvis and ureter, establishing a diagnosis of NVUC in these sites can be difficult, especially on small biopsies

Design: 15 cases of NVUC of the renal pelvis and the ureter were identified. 1 was in-house and 14 cases were sent to our genitourinary pathology consult service. Four cases were excluded due difficulty in obtaining the slides from other institutions. Of the remaining 11 cases, 6 six were nephrouretectomies, 1 nephrectomy, 2 ureterectomies, 1 ureter biopsy, and 1 kidney biopsy. We are in the process of obtaining and reviewing any prior biopsies of the resection specimens.

Results: 4/11 (36%) cases showed large nested morphology, 4/11 (36%) cases showed mixed large and small nested morphology, and only 2 (18%) cases showed predominantly small nested morphology. In 4/11 cases there was the presence of an overlying low grade papillary urothelial carcinoma. An associated desmoplastic stromal reaction was none/minimal in 8/11 (73%) cases, with a prominent reaction in the remaining 3/11 (27%) cases. Pathological stages for the resections were pT1 (n=1), pT2 (n=2), pT3 (n=5), and pT4 (n=1). There was only 1 case with a lymph node metastasis at the time of resection who had pT4 disease. Follow-up was available in 7/15 cases and we are in the process of trying to obtain information on the remainder of the cases. 5/7 cases showed no recurrences or metastases, and the remaining 2/7 cases later developed urothelial carcinoma of the bladder.

Figure 1 - 551

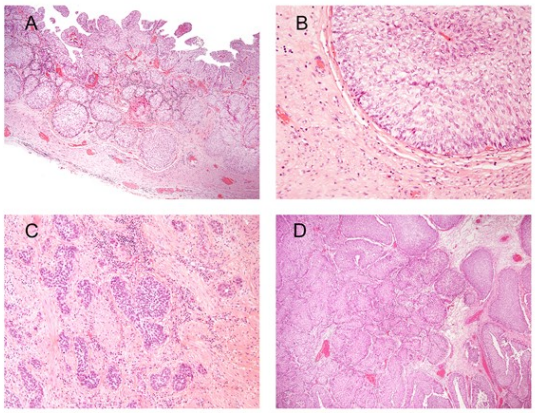

A)NVUC in ureter with overlying papillary low grade urothelial carcinoma; B) Higher magnification of A with bland nest of large nested UC in muscularis propria; C) Small nested UC in arising in renal pelvis; D) Irregular crowded nests of large nested UC (center) associated with round lobules of inverted growth pattern of noninvasive papillary urothelial carcinoma (lower right) arising in renal pelvis

Conclusions: In contrast to NVUC of the urinary bladder, NVUC in the upper urothelial tract is: 1) more frequently associated with an overlying papillary urothelial carcinoma; 2) more commonly has a large nested pattern; and 3) appears to behave less aggressively. Similar to NVUC in the urinary bladder, NVUC in the upper tract lacks an associated desmoplastic reaction and has by definition bland cytology. These findings make large nested carcinoma of the upper tract difficult to distinguish from an inverted growth pattern of non-invasive low grade papillary urothelial carcinoma, and small nested carcinoma difficult to distinguish from florid proliferation of von Brunn nests.

552 Fumarate Hydratase-Deficient Renal Cell Carcinoma: A Comprehensive Study of 59 Patients and Comparative Analysis of Germline and Sporadic Cases

Jatin Gandhi[1], Jie-Fu Chen[2], Chuanyong Lu[3], Max Kong[4], Renzo DiNatale[2], Hikmat Al-Ahmadie[2], Samson Fine[2], Anuradha Gopalan[2], Judy Sarungbam[2], S. Joseph Sirintrapun[2], Maria Carlo[2], Satish Tickoo[2], Victor Reuter[2], Ying-Bei Chen[2]
[1]University of Washington, Seattle, WA, [2]Memorial Sloan Kettering Cancer Center, New York, NY, [3]Montefiore Medical Center, Bronx, NY, [4]Kaiser Permanente, Sacramento, CA

Disclosures: Jatin Gandhi: None; Jie-Fu Chen: None; Chuanyong Lu: None; Max Kong: None; Renzo DiNatale: None; Hikmat Al-Ahmadie: None; Samson Fine: None; Anuradha Gopalan: None; Judy Sarungbam: None; S. Joseph Sirintrapun: None; Maria Carlo: None; Satish Tickoo: None; Victor Reuter: None; Ying-Bei Chen: None

Background: Fumarate hydratase-deficient RCC (FHD-RCC) are characterized by pathogenic alterations in the *FH* gene which are commonly germline but can also be somatic. The diagnosis of familial cases - hereditary leiomyomatosis and renal cell carcinoma (HLRCC) syndrome – has crucial implications for patients and family members, and requires an integration of clinical/family history, morphology, FH and/or 2SC immunohistochemistry (IHC), and genetic counseling/testing. Meanwhile, limited info is available regarding the incidence, clinicopathological, and molecular features of sporadic FHD-RCC.

Design: We retrospectively identified 59 patients (72 tumors; primary-55, metastasis-17) who had a diagnosis of FHD-RCC based on FH and 2SC IHC or were found to carry germline pathogenic *FH* alterations. Somatic mutations and copy number analyses were conducted in 46 tumors (43 patients) with available material.

Results: Based on tumor characterization and *FH* mutation status, the 59 patients could be divided into 4 categories: germline FHD-RCC/HLRCC (n=33), somatic FHD-RCC (n=11), IHC-only FHD-RCC (n=13), and non-FHD RCC in 2 patients carrying germline *FH* c.1431_1433dupAAA mutation. All FHD-RCC cases had IHC evidence of FH deficiency. Sporadic (somatic) cases were proven to have biallelic somatic *FH* alterations and accounted for 25% of the molecularly characterized subset (n=44). The clinicopathologic features of HLRCC and somatic FHD-RCC largely overlapped (Table), with germline cases showed a trend to have higher frequencies of pertinent family/personal history, clinical evidence of metastatic disease including lymph node

involvement. Interestingly, 5/11 (45%) sporadic cases occurred in patients ≤ 45 years old who had negative *FH* germline testing. Recurrent *NF2* mutations occurred in both germline (4/29, 14%) and somatic (3/11, 27%) cases. One case in the IHC-only FHD-RCC group had molecular analysis and surprisingly showed a lack of either germline or somatic *FH* alterations despite a loss of FH expression and diffuse positivity for 2SC staining.

	Somatic	Germline	p-value
Patient	**11 (100%)**	**33 (100%)**	
Age (y/o) [Median (range)]	47 (25-74)	42.5 (20-73)	
Gender (M : F)	2.7 : 1	1.5 : 1	
Pertinent family/personal history	2 (18%)	17 (52%)	p = 0.08
Primary tumor (pT)			
pT1/2	2 (14%)	5 (15%)	
pT3/4	9 (64%)	19 (58%)	
Clinical metastatic disease	5 (45%)	25 (76%)	p = 0.06
Lymph node (cN1)	3 (27%)	21 (64%)	p = 0.08
Distant metastasis (cM1)	4 (36%)	14 (42%)	
Duration of follow-up (months)[Median (range)]	31 (1-75)	22 (1-72)	
Outcome			
Metastatic disease	11 (100%)	32 (97%)	
Died of disease	6 (55%)	19 (58%)	
Alive with metastatic disease	4 (44%)	7 (21%)	
Alive with no evidence of disease	0 (0%)	5 (15%)	
Tumor	**14 (100%)**	**39 (100%)**	
Primary	11 (79%)	28 (72%)	
Tumor size (cm) [Median (range)]	8 (3-16)	8 (3-19)	
Growth pattern			
Multi-nodular	5 (45%)	8 (24%)	
Solid/sheet-like	11 (79%)	22 (56%)	p = 0.09
Papillary	11 (79%)	17 (44%)	p = 0.08
Tubular	8 (57%)	20 (51%)	
Tubulopapillary	8 (57%)	16 (41%)	
Tubulocystic	3 (21%)	7 (18%)	
Cystic	3 (21%)	5 (13%)	
Collecting duct carcinoma-like	3 (21%)	6 (15%)	
Cribriform/sieve-like	1 (7%)	5 (13%)	
Low-grade oncocytic	0 (0%)	2 (5%)	
Sarcomatoid/rhabdoid features	3 (21%)	11 (28%)	
Tumor-infiltrating lymphocytes	5 (36%)	13 (33%)	
FH IHC			
Retained	3 (27%)	3 (9%)	
Partially lost	1 (9%)	6 (18%)	
Completely lost	7 (64%)	24 (71%)	
2SC IHC			
Positive	13 (100%)	38 (100%)	

Conclusions: Somatic/sporadic cases represent approximately 25% of FHD-RCC in a molecularly characterized cohort and have overlapping clinical, pathological, and molecular features as HLRCC. Mechanisms other than *FH* alterations may lead to FH deficiency in rare cases. Germline *FH* c.1431_1433dupAAA mutation likely is not associated with FHD-RCC and other types of RCC should be considered in the differential diagnosis for patients carrying this variant.

553 High-Grade Desmoplastic Foamy Gland Prostate Adenocarcinoma – A Study of 24 Cases

Guofeng (George) Gao[1], Jonathan Epstein[2], Tamara Lotan[3]
[1]Stanford University School of Medicine, Stanford, CA, [2]Johns Hopkins Medical Institutions, Baltimore, MD, [3]Johns Hopkins University School of Medicine, Baltimore, MD

Disclosures: Guofeng (George) Gao: None; Jonathan Epstein: None; Tamara Lotan: None

Background: After the first report of the foamy prostatic adenocarcinoma, a unique subset with an extensive desmoplasia was noted in our expanded report include 55 high grade tumors. Subsequently, we received more consultation cases of foamy gland adenocarcinoma with prominent desmoplasia, where many contributors have expressed difficulty in diagnosing cancer or assigning an accurate grade even when recognizing malignancy.

Design: 24 cases of high grade desmoplastic foamy gland prostatic adenocarcinoma sent in consultation to the senior author from 2010 to 2021 were analyzed. In all cases, basal cell markers (p63, HMWCK), PTEN and TP53 IHC labelling submitted with the case or performed at our institution were evaluated.

Results: Of the 24 patients, 4 lost to follow-up, 2 diagnosed recently with only 1-2 months follow-up, 2 died at 1 and 6 years with no further information, and 4 had no evidence of disease with follow-ups of 7-15 months. Of the remaining 12 patients, 6 were alive with metastatic disease (2 to bone, 2 to lymph node, 1 to the lung and 1 to the liver), 5 died of cancer with metastases to bone or lung, and 1 had spread to the bone and without information if he was alive. Overall, of the 16 patients with meaningful follow-up, 12 (75%) either had metastases or died of prostate cancer.

Observed in all our cases was a prominent desmoplastic stroma (with aberrant HMWCK staining of cancer cells in a non-basal cell pattern), its defining feature, which often obscured poorly-formed glands (Figure 1). The large glands with infolding were often disrupted, causing difficulty in diagnosing malignancy and assigning grade. All cases showed foamy gland with 7 cases showing prominent foamy gland morphology (Figure 2). Consistent with high grade, 20 cases were Grade Group 5, while the remaining 4 cases were Grade Group 4. Tumor necrosis as a component of Gleason pattern 5 was observed in 21 cases, extensive necrosis observed in 5 cases. PTEN loss was observed in 9 cases, and p53 nuclear accumulation was observed in 8 cases.

Figure 1 - 553

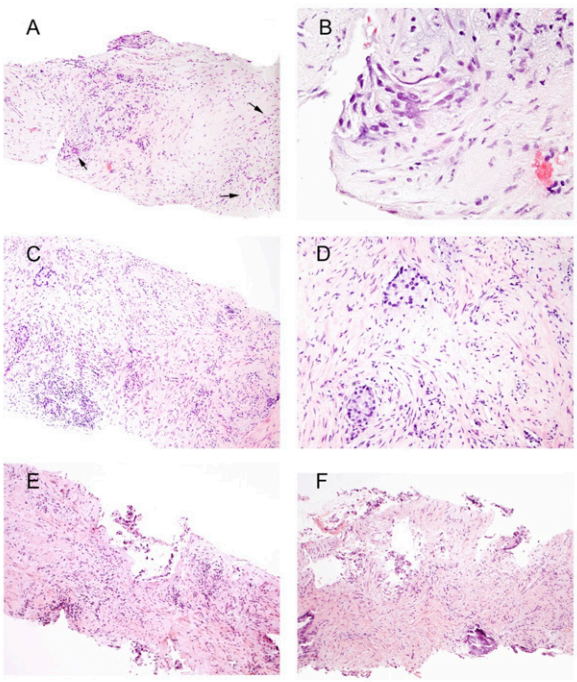

Figure 1. A: Scattered poorly-formed glands of prostatic adenocarcinoma (arrows) in a dense desmoplastic stroma. B: Higher magnification of poorly-formed gland in Figure 1A. C: Widely dispersed poorly-formed glands of adenocarcinoma (Left) in abundant desmoplastic stroma. D: Higher magnification of poorly-formed gland in Figure 1C. E: Disrupted of prostatic adenocarcinoma, difficult to diagnose and grade, in desmoplastic stroma. F: Same case as Figure 1E with another core showing fragmented and disrupted glands with desmoplastic stroma.

Figure 2 - 553

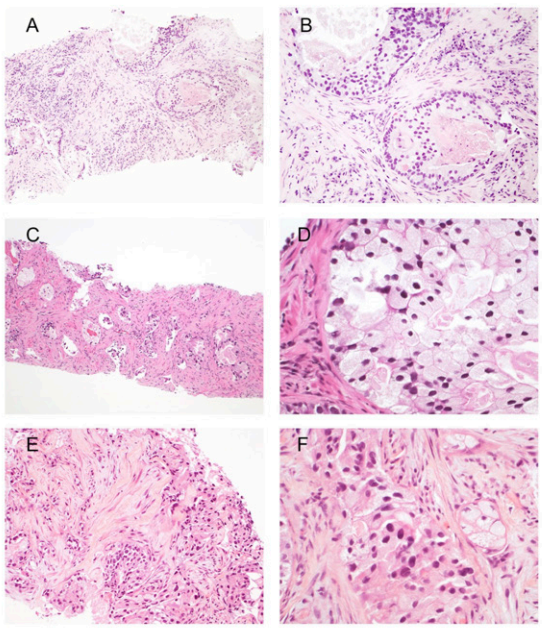

Figure 2. A: Cribriform foamy gland adenocarcinoma with necrosis within dense desmoplastic stroma. B: Higher magnification of Figure 2A showing cribriform foamy gland adenocarcinoma with mild-moderate nuclear atypia. C: Well-formed and poorly-formed glands of foamy gland carcinoma in desmoplastic stroma. D: Same case as Figure 2C with high-grade cribriform foamy gland adenocarcinoma with relatively bland nuclei and indistinct nucleoli. E: High grade foamy gland adenocarcinoma composed of solid nests, poorly-formed glands, and cords of cells embedded in dense fibrous stroma. F: Same case as Figure 2E with solid nests of foamy gland adenocarcinoma with variable cytological atypia, lacking prominent nucleoli.

Conclusions: High-grade desmoplastic foamy gland adenocarcinoma is difficult to diagnose and grade due to foamy cytoplasm, prominent desmoplastic stroma, disrupted glands and nonspecific staining for HMWCK. Only 1/3 contributing pathologists were able to definitively diagnose and grade the tumor as Gleason score 8-10 prostate cancer accurately. It is important to recognize this variant and its high-grade nature given its aggressive clinical course with frequent metastases and death.

554 Morphometric Performance, Extraprostatic Extension Estimation and Prostatic Adenocarcinoma Grade Group Concordance in Prostatectomies Following Magnetic Resonance Imaging Guided Core Needle Biopsies

Rose George[1], Mahmut Akgul[1], Richard Pacheco[1], Arkar Htoo[1], Andrea Lightle[1], Tipu Nazeer[2], Michael Schuster[1], Badar Mian[1]

[1]Albany Medical Center, Albany, NY, [2]Albany Medical College, Albany, NY

Disclosures: Rose George: None; Mahmut Akgul: None; Richard Pacheco: None; Arkar Htoo: None; Andrea Lightle: None; Tipu Nazeer: None; Michael Schuster: None; Badar Mian: None

Background: Multiparametric magnetic resonance imaging (MRI) of the prostate is increasingly used to guide core needle biopsy (CNB) procedure. This study compares morphometric performance and PCa characteristics of the MRI targeted CNB on the detected main lesion with the largest PCa nodule (PCaN) identified by microscopic examination.

Design: Patients whom underwent prostatectomy following MRI guided CNB-proven PCa in years between 2017 and 2019 were selected. Multiparametric MRI of the prostate was performed in accordance with the PI-RADS 2.1 recommendations. Axial T2 axial images (3-mm thickness) with the support of apparent diffusion coefficient and kinetic data from multiple exam were used to locate lesion. Prostatectomy specimens were entirely submitted using whole mount, and hematoxylin eosin stained slides were subsequently digitized. All PCa foci were manually annotated. Greatest surface area (cm^2), linear measurement (cm) of extraprostatic extension (EPE), and PCa grade group (GG) of the PCaN were collected. GG of the target core of the MRI guided CNB, MRI-estimated surface area and EPE interpretation of the main lesion were recorded. For GG between MRI-targeted CNB and PCaN, concordance (same GG), minor discrepancy (GG difference of 1), and major discrepancy (GG discrepancy >1) was noted. Student's t-test and Mann-Whitney U test (MRI and histologic estimates comparison); Chi-square and Fisher's exact tests (categorical variables); Spearman's rank correlation coefficients (GG and EPE) were performed when indicated. A *p*-value <0.05 was considered statistically significant.

Results: Table 1 includes summary of the findings. Sixty-four patients with median age of 63 years (51-71) were included. GG2 was the most common in both MRI targeted CNB (n=28, 44%) and in PCaN (n=30, 47%). The mean MRI targeted CNB GG and PCaN were 2.1 and 2.4, respectively, although the difference was not significant (p=0.09). GG between MRI targeted CNB and PCaN was concordant in 26 (41%) cases, minor and major discrepancy were present in 25 (39%) and 13 (20%) cases. In 6 (9%) patients, MRI did not detect a distinct lesion, although PCaN (range 0.27-2.5 cm^2) were found histologically. The MRI surface area (mean 1.0; 0.0-8.2 cm^2) underestimated the PCaN surface area (1.8, 0.01-10.4 cm^2)(<0.001). MRI interpreted EPE in 34 (59%), whereas it was present in 20 (33%) cases, with the sensitivity and specificity of 58% and 41%, respectively.

	Total patients (n=64)		
Age (years)			
Mean (median, range)	63.7 (63.3, 50.8-71.3)		
Highest ISUP Grade Group	**Targeted biopsy**	**Largest nodule**	*p*-value
No malignancy	8 (13%)	0	N/A
GG1	7 (11%)	10 (16%)	
GG2	28 (44%)	30 (47%)	
GG3	17 (27%)	17 (27%)	
GG4	8 (13%)	4 (6%)	
GG5	4 (6%)	3 (5%)	
Mean (median, range)	2.1 (2.0, 0.0-5.0)	2.4 (2.0, 1.0-5.0)	0.09
Measurements	**Histology**	**MRI**	
Largest cross section (cm^2) mean (median, range)	1.8 (1.5, 0.01-10.4)	1.0 (0.6, 0.0-8.2)	**<0.001**
Extra-prostatic extension recognition	20 (33%)	34 (59%)	**0.012**
N/A=Not applicable Bold values indicate statistical significance			

Conclusions: Our study suggests underestimation of the PCaN by MRI morphometrics with low-level accuracy in EPE, and major GG disagreement in a subset of cases. Studies with more patients with additional variables should be performed to evaluate multiparametric MRI.

555 TRPS1 Expression in Morphologic Variants of Urothelial Carcinoma

Benjamin Gertsen[1], Moises Velez[1], Hiroshi Miyamoto[1], Ying Wang[1]
[1]University of Rochester Medical Center, Rochester, NY

Disclosures: Benjamin Gertsen: None; Moises Velez: *Speaker*, Roche; Hiroshi Miyamoto: None; Ying Wang: None

Background: Currently there is no highly specific and sensitive marker for urothelial carcinoma (UC). Gata3 is the most widely used tumor marker to determine the urothelial origin while expressing in most of breast cancers and some of others. A recent study suggested that trichorhinophalangeal syndrome type 1 (TRPS1) was a highly sensitive and specific marker for breast carcinoma and showed no or little expression in conventional UCs. However, the status of TRPS1 expression in the morphologic variants of UC, some of which share similar morphologic features to breast carcinoma, remains to be determined. The current study aims to determine if TRPS1 is expressed in non-conventional bladder cancers.

Design: Immunohistochemistry for TRPS1 was performed in surgical specimens from patients with histologically confirmed variants of UC including plasmacytoid (n=13), sarcomatoid (n=15), micropapillary (n=24), nested (n=15), squamous (n=13), as well as small cell carcinoma (n=8), with or without admixed conventional UC. A quantitative score was calculated based on both the intensity (0, 1+, 2+, 3+) and the percentage of positive cells. A final score was assigned: negative, low positive, intermediate positive, or high positive for TRPS1 expression.

Results: 4 (30.8%) of 13 plasmacytoid tumors are positive, including 2 (15.4%) cases with high positivity, 1 (7.6%) case with intermediate positivity, and 1(7.6%) case with low positivity. 10 (66.7%) of 15 sarcomatoid tumors are positive, including 3 (13.3%) cases with high positivity, 6 (40.0%) cases with intermediate positivity, and 1 (6.7%) case with low positivity. 1 (4.2%) of 24 micropapillary tumors are intermediately positive, while all 15 nested tumors are negative. 11 (84.6%) of 13 squamous cell tumors are positive, including 6 (46.2%) cases with high positivity, 3 (23.1%) cases with intermediate positivity, and 2 (15.4%) cases with low positivity. 3 (37.5%) of 8 small cell carcinomas are positive, including 2 (25.0%) cases with intermediate positivity and 1 (12.5%) case with low positivity. Finally, TRPS1 show low positivity in concurrent conventional UC component in 2 (6.8%) of 29 cases.

Table 1 TRPS1 expression in UC morphological variants and small cell carcinoma.

			Positive			
	Negative	Positive	Low	Intermediate	High	Total
Plasmacytoid	9 (69%)	4 (31%)	1 (8%)	1 (8%)	2 (15%)	13
Sarcomatoid	5 (33%)	10 (67%)	1 (7%)	6 (40%)	3 (20%)	15
Micropapillary	23 (96%)	1 (4%)	0	1 (4%)	0	24
Nested	15 (100%)	0	0	0	0	15
Squamous	2 (15%)	11 (85%)	2 (15%)	3 (23%)	6 (46%)	13
Small cell	5 (63%)	3 (38%)	1 (13%)	2 (25%)	0	8

Conclusions: TRPS1 is found to be expressed in conventional UC components and UC variants particularly squamous, sarcomatoid, plasmacytoid tumors, and small cell carcinoma. These findings have diagnostic implications when using TRPS1 immunohistochemistry as a marker for breast cancer.

556 HPV-independent Penile Squamous Cell Lesions Mimicking HPV-associated PeIN

Jose Guerrero Pineda[1], Isabel Trias[2], Inmaculada Ribera[2], María Teresa Rodrigo[2], Sherley Diaz-Mercedes[1], Luis Veloza Cabrera[3], Rafael Parra-Medina[4], Jaume Ordi[5], Natalia Rakislova[2]
[1]Hospital Clinic, University of Barcelona, Barcelona, Spain, [2]Hospital Clinic, Barcelona, Spain, [3]CHUV and University of Lausanne, Lausanne, Switzerland, [4]Fundacion Universitaria de Ciencias de la Salud, Bogotá, Colombia, [5]University of Barcelona, Barcelona, Spain

Disclosures: Jose Guerrero Pineda: None; Isabel Trias: None; Inmaculada Ribera: None; María Teresa Rodrigo: None; Sherley Diaz-Mercedes: None; Luis Veloza Cabrera: None; Rafael Parra-Medina: None; Jaume Ordi: None; Natalia Rakislova: None

Background: Most human papillomavirus (HPV)-independent penile squamous cell carcinomas (PSCC) originate from a differentiated penile intraepithelial neoplasia (dPeIN), characterized by abnormal maturation with basal atypia. Previous studies in

vulvar cancer, which has a similar etiopathogenesis to PSCC, showed that about one fifth of HPV-negative precursors are morphologically indistinguishable from HPV-associated lesions. However, such unusual lesions have not been described in PSCC.

Design: From 2000 to 2021, 55 PSCC having at least 1 cm of skin adjacent to the invasive tumor were identified. In all cases, thorough morphological evaluation, HPV DNA detection and p16 and p53 immunohistochemical staining were performed. HPV-independent status was assigned based on both negative p16 staining and negative HPV detection.

Results: Thirty-eight out of the 55 PSCC (69%) were classified as HPV-independent. PeIN was identified in 26/38 cases (68%). Five of them (19%) showed basaloid features, morphologically indistinguishable from HPV-associated PeIN. Median age of the five patients was 73 years. All five cases were p16- and HPV-negative. Three cases showed an abnormal p53 pattern and the other two showed wild-type-p53 staining. The associated invasive carcinoma showed basaloid/warty features in four cases and was of conventional, keratinizing type in one.

Case	Age	Location	Tumor size (mm)	Invasive carcinoma	p53 pattern	Staging
1	70	Glans	28	Usual type	Abnormal (basal overexpression)	pT2N1M0
2	72	Glans	23	Basaloid	Abnormal (null)	pT1aN0M0
3	67	Foreskin	11	Warty-basaloid	Abnormal (basal overexpression)	pT1aN0M0
4	76	Glans	5	Basaloid	Wild-type (scattered)	pT1aN0M0
5	83	Glans and foreskin	20	Basaloid	Wild-type (mid-epithelial)	pT1aN0M0

Figure 1 - 556

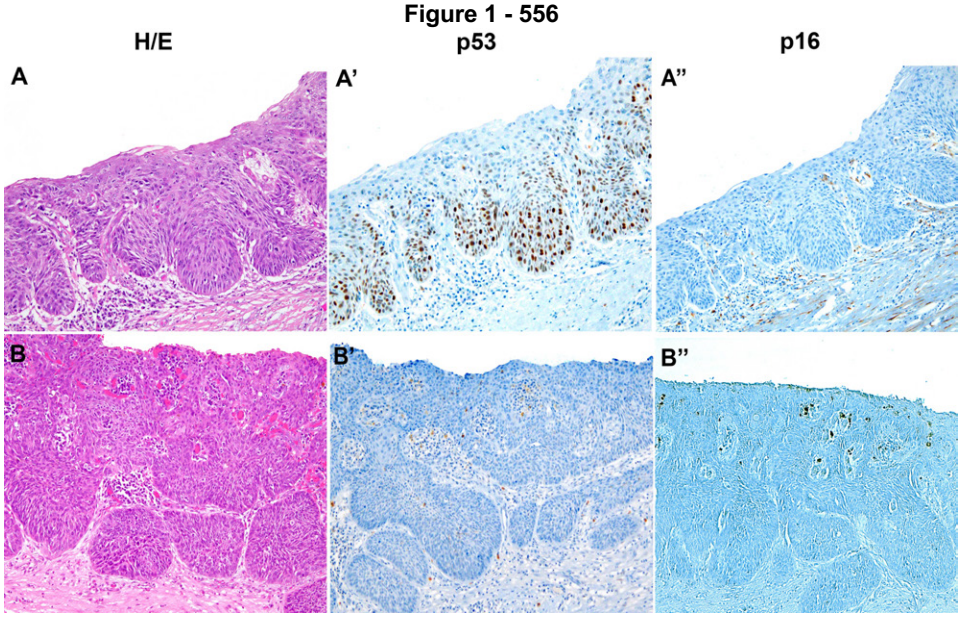

Conclusions: A small proportion of HPV-independent PSCC may arise on adjacent dPeIN morphologically identical to HPV-associated PeIN. Although some HPV-independent PeIN with mixed basaloid and differentiated features have been occasionally mentioned, this unusual histological pattern has not been previously reported and characterized in detail in PSCC.

557 Clear Cell Adenocarcinoma of the Genitourinary Tract: A Clinicopathologic Study of 31 Cases

Nihar Hotchandani[1], Bogdan Czerniak[1], Charles Guo[1]
[1]*The University of Texas MD Anderson Cancer Center, Houston, TX*

Disclosures: Nihar Hotchandani: None; Bogdan Czerniak: None; Charles Guo: None

Background: Clear cell adenocarcinoma (CCA) is a rare disease in the genitourinary tract. There have been limited studies on this disease. Herein we study the clinicopathologic, immunohistochemical, and gene mutational features in a large cohort of CCA from a single institute.

Design: We searched our pathology files from 2000 to 2021 and identified 31 cases of CCA of the genitourinary tract. Pathological features were analyzed, and clinical data was collected from the medical records. Whenever available, immunohistochemical and next-generation sequencing (NGS) results were also evaluated.

Results: The patients included 29 females and 2 males with a mean age of 60.4 years (range, 37-76 years). The most common presentations were hematuria (18) and urinary obstructive symptoms (8). The tumor involved the urethra (22), urethra and bladder neck (8) and anterior bladder wall (1). In more than half of the cases, the tumor involved a diverticulum (16). The mean tumor size was 4.3 cm (range, 2-6.6 cm). Immunohistochemical stains showed the tumor was positive for PAX8 (35/35), CK7 (30/33), p504s (18/19) and HNF1B (4/5). Next-generation sequencing data was available for 7 cases. The most common mutations were TP53, CDKN2A, ATM and GNAS (2/6 each). Four cases presented with a clinical stage T1, twenty-one cases presented with a higher clinical stage (T2-4). The tumor spread to the lymph nodes in 11 cases, while distant metastases (lung, liver, bone and brain) were identified in 8 cases. The patients were treated with surgery (21), chemotherapy (24), radiation (15) and immunotherapy (4). The mean follow-up time was 42.3 months (range 1-125 months). At last follow-up, fourteen patients were alive with no evidence of disease and five patients were alive with disease. Seven patients died with confirmed metastatic disease; three patients died with cause of death unknown. Clinical outcome was analyzed in relation to clinical stage, tumor location, mutation status, and diverticulum (Table 1).

Table 1

	Patient status at last follow-up	
	Number of patients alive	Number of patients dead
Clinical stage		
T1	3	1
T2-4	13	8
Tumor location		
Urethra	16	6
Urethra and bladder neck	3	5
Anterior bladder wall	0	1
Gene mutations		
Present	4	2
Absent	1	-
Tumor involving a diverticulum		
Yes	13	4
No	7	7

Conclusions: CCA commonly involves the urethra and bladder neck with a female predominance. It is an aggressive disease, and the clinical outcome is closely associated with cancer stage. CCA frequently arises from a diverticulum, which may be associated with favorable outcome. CCA shows distinct mutations in several oncogenes and tumor suppressor genes, which may contribute to the development of this rare disease.

558 Mutant Pattern p53 and SMARCA4 and SMARCB1 SWI/SNF Subunit Inactivation by Immunohistochemistry in Sarcomatoid and Rhabdoid Renal Cell Carcinoma and Matched Differentiated Renal Cell Carcinoma

Robert Humble[1], Alexandra Isaacson[1], Andrew Bellizzi[1]
[1]*University of Iowa Hospitals & Clinics, Iowa City, IA*

Disclosures: Robert Humble: None; Alexandra Isaacson: None; Andrew Bellizzi: None

Background: SWI/SNF subunit inactivation has been identified in tumors with rhabdoid morphology across multiple organ systems, including renal cell carcinoma (RCC). Inactivation in sarcomatoid RCC is poorly characterized. We recently observed a dedifferentiated RCC with mutant-pattern p53 in the dedifferentiated component.

Design: SMARCA4 (clone EPR-3912), SMARCB1 (clone 25/BAF47), and p53 (clone DO-7) immunohistochemistry (IHC) was performed on tissue microarrays (TMAs) constructed from 73 nephrectomies demonstrating sarcomatoid (sRCC) and/or rhabdoid (rRCC) features and matched differentiated tumors: clear cell RCC (ccRCC; n=58), chromophobe RCC (ChRCC; n=6), papillary RCC (pRCC; n=4) and unclassified RCC (RCCu; n=5). Sarcomatoid features only were present in 45% of cases

(n=33), rhabdoid features only were present in 27% of cases (n=20), and both were identified in 27% of cases (n=20). SMARCA4 and SMARCB1 IHC was assessed as intact or lost; p53 was assessed as wild-type (WT), missense, or null pattern.

Results: Among sRCC cases 83% yielded an interpretable p53 result (n=44); 90% of cases were WT (n=40) and 10% were missense (n=4). Of the missense cases 3 of 4 occurred in a background of ChRCC. The matched differentiated components in all p53 missense cases showed WT p53. In one of the cases missense pattern p53 was also detected in the rhabdoid component. SMARCA4 loss was seen in one sRCC case with simultaneous loss in the differentiated ccRCC component. SMARCB1 loss was also seen in one sRCC case, again with simultaneous loss in the RCCu differentiated component (possibly a renal medullary carcinoma). Among rRCC cases 75% yielded an interpretable p53 result (n=30); 87% of cases were WT (n=26) and 13% were missense (n=4). Of the missense cases 3 of 4 occurred in a background of ccRCC. Again, the matched differentiated components showed WT p53. One of the missense p53 cases had a simultaneous sRCC component with WT p53. SMARCA4 loss was seen in one rRCC with intact expression in the differentiated ccRCC component. SMARCB1 was intact in 100% of rRCC cases. Findings are summarized in the Table.

	Sarcomatoid RCC	Sarcomatoid RCC differentiated match	Rhabdoid RCC	Rhabdoid RCC differentiated match
Freq p53 missense	10% (4/40)	0% (0/3)	13% (4/30)	0% (0/3)
Freq BRG1 loss	2% (1/53)	100% (1/1)	2.5% (1/40)	0% (0/1)
Freq INI1 loss	2% (1/53)	100% (1/1)	0% (0/0)	0% (0/0)

Conclusions: Mutant-pattern p53 is detected in approximately 10% of sRCC and rRCC and appears to underlie transformation, as the matched differentiated components do not show mutant-pattern staining. 3 of 6 ChRCC had a mutant-pattern s/rRCC component. SMARCA4 and SMARCB1 inactivation is infrequent, seen in ~2% of both sRCC and rRCC, which may or may not be seen in the matched differentiated component.

559 Radical Prostatectomy Findings in Men with Grade Group 1 Cancer on Biopsy Significantly Differ Between Those with PI-RADS 4-5 and PI-RADS 3 Radiologic Lesions and are Worse in White Hispanic and Black Men

Oleksii Iakymenko[1], Merce Jorda[1], Oleksandr Kryvenko[1]
[1]*University of Miami Miller School of Medicine, Miami, FL*

Disclosures: Oleksii Iakymenko: None; Merce Jorda: None; Oleksandr Kryvenko: None

Background: The prostate imaging reporting and data system (PI-RADS) 4-5 lesions are actionable findings for biopsy and often associated with higher grade cancer. However, no studies have described the radical prostatectomy (RP) outcomes in men with PI-RADS 4-5 and multiparametric MRI-ultrasound fusion biopsy showing Grade Group 1 (GG1) prostate cancer.

Design: We assess RP findings in men who had PI-RADS 4-5 (n=87) and PI-RADS 3 (n=43) lesions with MRI-ultrasound fusion biopsy showing GG1 cancer. We also assembled a group of men who had no preoperative MRI (n=57), had GG1 on template biopsy, and proceeded to RP. The outcomes at RP were assessed for upgrading and cancer aggressiveness that was ranked into 4 groups factoring in cancer grade, volume, and local extent. Multivariable analysis was performed to assess the independent effects of high PI-RADS and patient race/ethnicity on upgrading at RP.

Results: Preoperatively, the 3 groups only differed by the number of biopsy cores taken but were comparable by age, prostate weight, PSA and PSA density, number of positive cores, percent of involved cores, racial/ethnic distribution, and number of MRI lesions. At RP, the number of tumor nodules did not differ between the 3 groups. The correlations of the dominant tumor nodule location with radiologic findings did not differ between the 2 groups with preoperative MRI. The incidence of upgrading was significantly higher in PI-RADS 4-5 (68/87, 78%) vs. no MRI (38/57, 67%) vs. PI-RADS 3 (24/43, 56%), p=0.03. The cancer grade and level of cancer aggressiveness at RP also varied significantly between the 3 groups (Table). In multivariable analysis, PSA density (OR=186, p=0.038), White Hispanic race/ethnicity (OR=3.4, p=0.013), Black race/ethnicity (OR=4.4, p=0.024), and PI-RADS 4-5 (OR=2.9; p=0.014) significantly correlated with the upgrading at RP. Patient age, percent of involved cores, and number of MRI lesions did not independently correlate with the upgrading at RP.

Finding / Classifier		PI-RADS 4-5 (n=87)	PI-RADS 3 (n=43)	No MRI (n=57)	p-value
Grade Group	1	19 (22%)	19 (44%)	19 (33%)	0.04
	2	48 (55%)	23 (54%)	29 (51%)	
	3	6 (7%)	0	3 (5%)	
	4	8 (9%)	0	1 (2%)	
	5	6 (7%)	1 (2%)	5 (9%)	
Cancer aggressiveness	Insignificant cancer	7 (8%)	13 (30%)	14 (25%)	0.01
	1	10 (12%)	6 (14%)	5 (9%)	
	2	34 (39%)	18 (42%)	24 (42%)	
	3	20 (23%)	5 (12%)	7 (12%)	
	4	16 (18%)	1 (2%)	7 (12%)	

Conclusions: In men with prostate MRI and targeted biopsy showing GG1 cancer, the RP outcomes are significantly worse in those patients with PI-RADS 4-5 than PI-RADS 3 lesions. Men with PI-RADS 4-5 lesions and GG1 on biopsy may possibly benefit from an immediate re-biopsy for accurate cancer grading. Men considering active surveillance with PI-RADS 4-5 lesions should also be counseled accordingly. White Hispanic and Black men had higher chances of upgrading at RP than White non-Hispanic men when other factors were accounted for.

560 Is Accurate Morphological Diagnosis of Eosinophilic Renal Tumors Possible? A Study of Histomorphology versus Immunohistochemistry Variability

Aiswarya Irri[1], Swati Bhardwaj[1], George Haines III[2], Qiusheng Si[1]
[1]Icahn School of Medicine at Mount Sinai, New York, NY, [2]Mount Sinai Hospital, New York, NY

Disclosures: Aiswarya Irri: None; Swati Bhardwaj: None; George Haines III: None; Qiusheng Si: None

Background: Eosinophilic renal tumors are a diverse group of entities with similar, overlapping morphologic features, making their diagnosis challenging. The issue is complicated by the existence of both benign and malignant entities sharing the common feature of eosinophilic cytoplasm.

Design: We performed a retrospective review of all eosinophilic renal tumors diagnosed from January 2020 to August 2021 (20 months). Those cases with diagnostic immunohistochemical staining (IHC) were selected for further study, and were independently reviewed by 2 residents and 2 attending pathologists. On the basis of hematoxylin and eosin (H&E) stained slides alone, a consensus opinion was reached. This was then compared to the final diagnosis rendered using IHC as an adjunct.

Results: A total of 356 clear cell renal cell carcinomas (CC-RCC), 55 chromophobe RCC (Ch-RCC), 161 papillary RCC (PRCC), 117 renal oncocytomas (RO), 3 acquired cystic disease-associated RCC (ACD-associated RCC), and one each of MiT family translocation (MITF) RCC and mucinous tubular and spindle cell carcinoma (MTSC) were diagnosed. In this timeframe, 71 cases had IHC as part of the diagnostic workup and were included in the study, including 13 eosinophilic CC-RCC, 20 Ch-RCC, 17 PRCC, 11 RO, 5 unclassifiable RCC, 3 ACD-associated RCC, 1 MITF RCC, and 1 MTSC. The overall consensus diagnosis on H&E was concordant with the final diagnosis in 70% (50/71) of cases. Maximum discordance between H&E and final diagnosis was seen in Ch-RCC (40%, 8/20), eosinophilic CC-RCC (38%, 5/13), and PRCC (18%, 3/17). Ch-RCC were most likely to be misdiagnosed as RO on H&E alone, while eosinophilic CC-RCC was often diagnosed as chromophobe RCC, and PRCC was misdiagnosed as unclassifiable RCC. Neither MITF RCC nor MTSC were diagnosed without IHC. Conversely, RO, unclassifiable RCC, and ACD-associated RCC had high concordance rates of 82% (9/11), 80% (4/5), and 100% (3/3), respectively, between H&E and the final diagnosis.

Conclusions: Considering a high likelihood of making a correct diagnosis on H&E alone, RO and ACD-associated RCC may not always require IHC. However, Ch-RCC, eosinophilic CC-RCC, and PRCC are often confused with the entities mentioned above due to factors such as eosinophilic variations seen in CC-RCC, and focal loss of papillary architecture in PRCC. For these reasons, the accurate diagnosis of eosinophilic renal tumors is challenging, necessitating immunohistochemical studies.

561 Homologous Recombination Deficiency (HRD) Mutations in Advanced Prostate Cancer: A Clinicopathologic Study of 17 Cases from an Indian Perspective

Ekta Jain[1], Shivani Sharma[1], Aditi Aggarwal[1], Deepika Jain[2], Mallika Dixit[2], Gauri Munjal[2], Sambit Mohanty[3]
[1]Core Diagnostics, Gurgaon, India, [2]Core Diagnostics, Gurugram, India, [3]Advanced Medical and Research Institute, Bhubaneswar, India

Disclosures: Ekta Jain: None; Shivani Sharma: None; Aditi Aggarwal: None; Deepika Jain: None; Mallika Dixit: None; Gauri Munjal: None; Sambit Mohanty: None

Background: Ninety percent of metastatic castration-resistant prostate cancer (mCRPC) harbor at least one actionable molecular alteration with androgen receptor (AR) pathways being the most commonly affected. Somatic or Germline defects in the Homologous Recombination DNA Repair (HRR) pathway account for around 20-25% of advanced Prostate cancers (PCs). Thus, therapies (platinum derivatives and PARP inhibitors) targeting this pathway is the present area of interest showing promising results in patients with mCRPC. As there is paucity of HRD testing in PCs from an Indian perspective, we studied the correlation of clinicopathologic profile and HRD mutations in these patients.

Design: Samples from 17 advanced PC patients were studied for HRD germline or somatic mutations. The complete coding region and splice junctions of HRR pathway genes (including *ATM, MRE11, BARD1, NBN, BRCA1, PALB2, BRCA2, PPP2R2A, BRIP1, RAD51B, CDK12, RAD54L, CHEK2, TP53, FANCD2, RAD51C and RAD51D*) were sequenced by Next Generation Sequencing on Illumina sequencing platform at ≥1000X mean depth and HRD mutations were analyzed for association with various clinicopathologic features.

Results: HRD mutation was seen in 6 (5 somatic and 1 germline) of 17 cases (35.3%). Somatic mutations included *TP53* mutations in 4 (23.5%) patients and *BRCA2* mutation in 1 (5.9%) patient, while *ATM* germline mutation was seen in 1 (5.9%) patient. The median age was 64.5 years with more prevalence in primary (4/6, 66.7%) than metastatic (2/6, 33.4%) cases. Five of 6 patients had higher serum PSA levels (>40ngml) while 1 patient had normal level (4.48ng/ml). The prevalence of HRD mutation was 3/6 (50%), 2/6 (33.3%) and 1/6 (16.7%) for Gleasons score 9, 8 and 7 and grade groups 5, 4 and 2, respectively. Perineural invasion (PNI) was seen in 5/6 (83.3%) HRD positive cases (Table 1 and Figure 1).

Table 1: Correlation of HRD mutations with various parameters (n=6)

S.No	Age (yrs)	Gleasons score	Prognostic Group Grade	Germline mutation	Somatic mutation	Variant	Location	Variant Classification	Mutant allele %
1	50	4+5=9	5	-	TP53	c.743G>A	Exon 7	Pathogenic	31.02%
2	59	3+4=7	2	ATM	NA	c.7502A>G	Exon 50	VUS	48.75%
3	58	4+5=9	5	-	TP53	c.701A>G	Exon 7	Pathogenic	23.78%
4	70	4+4=8	4	NA	BRCA2	c.8523delT	Exon 20	Pathogenic	65.71%
5	75	5+4=9	5	NA	TP53	c.638G>A	Exon 6	Pathogenic	54.29%
6	75	4+4=8	4	NA	TP53	c.559+1G>A	Intron 5	Pathogenic	54.48%

Figure 1 - 561

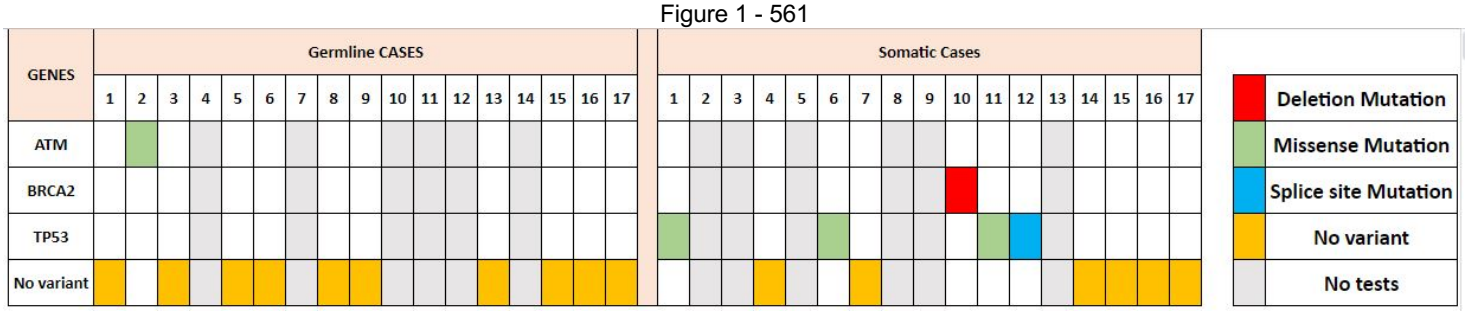

Conclusions: 1. Ours is the first Indian study evaluating HRD mutations in PC demonstrating the same in about one-third of the patients. 2. HRD mutations were more prevalent in tumors with high Gleasons score and group grade. 3. Given the recent FDA approval for two PARP inhibitors, the presence of defects in HRR pathway suggest that these patients could benefit from targeted therapy and can be included in the neoadjuvant clinical trials. However, further studies with a large cohort of patients with clinical follow-up data are warranted to evaluate their utility in PC, particularly in the advanced stage.

562 Epithelioid Angiosarcoma of the Urinary Bladder: A Multi-institutional Study of Twenty-three Cases with Literature Review

Shilpy Jha[1], Anil Parwani[2], Anandi Lobo[3], Chiu-Hsiang Liao[4], Daniel Luthringer[5], Ekta Jain[6], Hikmat Al-Ahmadie[4], Kiril Trpkov[7], Manju Aron[8], Nakul Sampat[1], Shivani Sharma[6], Sean Williamson[9], Sambit Mohanty[1]
[1]Advanced Medical and Research Institute, Bhubaneswar, India, [2]The Ohio State University, Columbus, OH, [3]Kapoor Centre of Urology and Pathology, Raipur, India, [4]Memorial Sloan Kettering Cancer Center, New York, NY, [5]Cedars-Sinai Medical Center, West Hollywood, CA, [6]Core Diagnostics, Gurgaon, India, [7]University of Calgary, Calgary, Canada, [8]Keck School of Medicine of USC, Los Angeles, CA, [9]Cleveland Clinic, Cleveland, OH

Disclosures: Shilpy Jha: None; Anil Parwani: None; Anandi Lobo: None; Chiu-Hsiang Liao: None; Daniel Luthringer: None; Ekta Jain: None; Hikmat Al-Ahmadie: *Consultant*, AstraZeneca, Janssen Biotech, Paige.ai; Kiril Trpkov: None; Manju Aron: None; Nakul Sampat: None; Shivani Sharma: None; Sean Williamson: None; Sambit Mohanty: None

Background: Epithelioid angiosarcoma (eAS) of the urinary bladder is a rare malignancy that may be easily confused with urothelial carcinoma. Approximately 21 cases have been reported as case reports and small case series, with prior radiation history as a commonly associated risk factor.

Design: We add a series of 23 patients to the collection of bladder eAS where the clinicopathologic parameters including clinical presentation, prior radiation history, histopathology, immunohistochemistry (IHC), management and follow-up data were analyzed comprehensively.

Results: The results are illustrated in Table 1 and Figure 1 as follows. Table 1 shows the demographics, histopathologic, prior radiation, staging, treatment, and follow-up data on the cases of eAS, including the present cohort of 23 cases (abbreviations used: Ca: Carcinoma; CT: Chemotherapy; NA: Not available. Figure 1 shows a case of bladder eA(a,b: Hematoxylin and Eosin stain; c: CD31; d: ERG). Variable combinations of vascular endothelial markers were positive in all these tumors that included CD31, CD34, D2-40, TLE1, FLI1, and ERG. The case 22 (1/7) expressed cMYC. Urothelial markers including GATA3 and Uroplakin 2 were negative. Keratin was positive in 11 cases (focal). The follow-up data was available for 32 patients and 18 (56.2%) succumbed to death within 1 to 32 months.

Age/ Gender	Clinical history	Time from RT	Location	Size	Type of specimen	Histopathology	Pathologic Stage	Site of metastasis	Treatment	Follow-up duration	Vital status
51yr/F	Hematuria	Ca cervix (11)	Trigone	5 cm	TURBT	Epithelioid	T2	Right lung	CT	LTF	NA
74yr/F	Hematuria	Ca cervix (20)	Trigone and urethra	9 cm	TURBT	Epithelioid	T2	NA	NA	LTF	NA
66yr/F	Hematuria	None	Posterior wall	NA	TURBT	Epithelioid	T2	Liver and bone	CT	LTF	NA
53yr/F	Hematuria	None	Right lateral wall	3 cm	TURBT	Epithelioid	T2	NA	NA	LTF	NA
68yr/F	Hematuria	Ca cervix (60)	Trigone	1.7 cm	TURBT	Epithelioid	T2	NA	NA	LTF	NA
58yr/F	Hydronephrosis and hematuria	Ca cervix (72)	Left lateral wall and trigone	4.8 cm	TURBT	Epithelioid	T2	Lungs, pelvis and liver	CT	4 months	Dead
51yr/F	Hematuria	Ca cervix (43)	Trigone	7 cm	TURBT	Epithelioid	T2	None	no	1 month	Dead
56yr/F	Hematuria	Ca cervix (17)	Trigone	NA	TURBT	Epithelioid	T2	None	CT	1 year	NA
73yr/F	Hematuria	None	Posterior wall	NA	TURBT	Epithelioid	T2	Peritoneum	None	3 months	Dead
58yr/F	Hydronephrosis and hematuria	Ca cervix (48)	Trigone	NA	TURBT	Epithelioid	T2	None	None	2 months	Dead
41yr/F	Hematuria	Ca cervix (84)	Trigone	7 cm	Radical cystectomy	Epithelioid	T3a	Lungs, liver and lymph node	CT	7 months	Dead
80yr/M	Hematuria and flank pain	None	Trigone and urethra	2.8 cm	Radical cystectomy	Epithelioid	T3a	Lungs, pelvis and liver	CT	5 months	Dead
57yr/M	Hydronephrosis and hematuria	None	Right lateral wall	4.2 cm	TURBT	Epithelioid	T2	B/L lungs	CT	LTF	Dead

52yr/M	Hematuria	None	Posterior wall	3 cm	Radical cystectomy	Epithelioid	T2	None	CT	LTF	NA
57yr/M	Hematuria and flank pain	None	Trigone and urethra	NA	Radical cystectomy	Epithelioid	T2	NA	NA	LTF	NA
44yr/M	Hematuria	None	Trigone	NA	TURBT	Epithelioid	T2	None	CT	18 months	Alive
70yr/M	Hematuria	Ca prostate (36)	Posterior wall	3 cm	Radical cystectomy	Epithelioid	T2	None	CT	20 months	Alive
44yr/M	Hematuria	None	Right lateral wall and bladder neck	8 cm	TURBT	Epithelioid	T2	None	CT	11 months	Alive
87yr/M	Hematuria	Ca prostate (28)	Right lateral wall	2.2 cm	Radical cystectomy	Epithelioid	T2	None	CT	75 months	Alive
49yr/M	Low back ache	None	Left lateral wall	7.3 cm	Radical cystectomy	Epithelioid	T3b	None	CT	12 months	Alive
72yr/M	Hematuria	None	Posterior wall	0.7 cm	TURBT	Epithelioid	T2	None	None	LTF	NA
72yr/M	Hematuria and flank pain	None	Posterior wall	1.2 cm	TURBT	Epithelioid	T2	None	None	3 months	Alive
89yr/M	Hematuria	Ca colon (31)	Trigone	6 cm	TURBT	Epithelioid	T2	None	None	LTF	NA

Figure 1 - 562

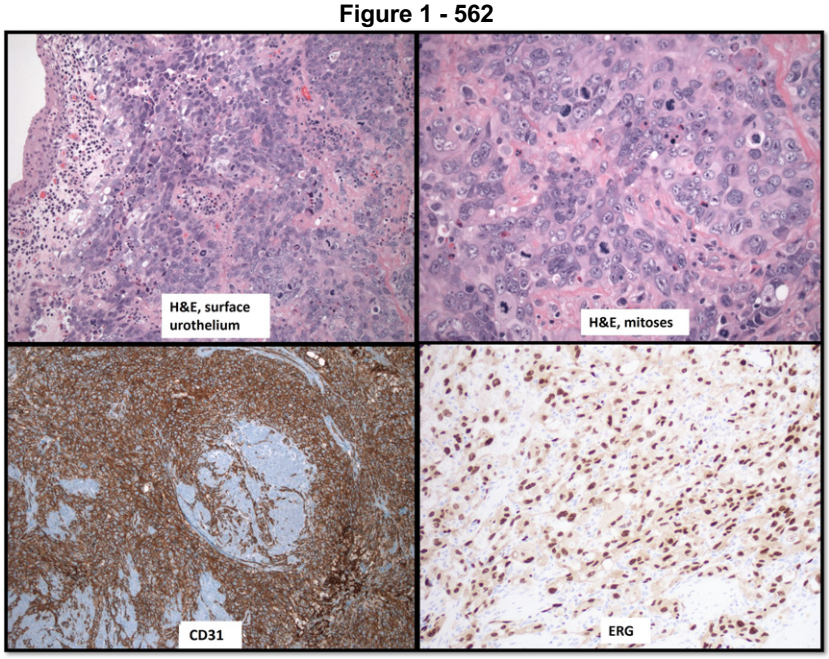

Conclusions: Based on our experience with the largest multi-institutional series of eAS to date and aggregate of the published data, eAS of bladder is an aggressive neoplasm with commonly associated radiation exposure and frequent metastasis. Owing to its rarity at this location, careful attention to morphology and vascular and urothelial IHC markers are helpful to render a correct diagnosis, as this distinction has significant therapeutic and prognostic ramification.

563 Comprehensive Scoring System of Non-Neoplastic Kidney Tissue at Time of Tumor Nephrectomy Predicts Post-Operative Renal Function Outcomes

Yong Jia[1], Seyed Mohammad Mohaghegh Poor[1], Brenden Dufault[2], Miao Lu[1], Jasmir Nayak[1], Deepak Pruthi[3], Ian Gibson[2]
[1]Shared Health Manitoba/University of Manitoba, Winnipeg, Canada, [2]University of Manitoba, Winnipeg, Canada, [3]The University of Texas at San Antonio, San Antonio, TX

Disclosures: Yong Jia: None; Seyed Mohammad Mohaghegh Poor: None; Brenden Dufault: None; Miao Lu: None; Jasmir Nayak: None; Deepak Pruthi: None; Ian Gibson: None

Background: Impaired renal function is a significant post-operative complication from renal cancer surgery. Currently, we are limited in our ability to predict post-operative renal function and rely on serological and urinary investigations to monitor. The histological evaluation of non-neoplastic kidney (NNK) at the time of surgery provides a unique opportunity to evaluate an individual's predisposition to develop post-operative renal dysfunction.

Design: This study was performed as a combined prospective pathologic review and retrospective clinical chart review. Patients were included if they underwent a nephrectomy from January 2016 to December 2017 in a tertiary facility. Patients were excluded if they had a solitary kidney, history of obstructive nephropathy, bilateral renal tumors, prior renal surgery, known hereditary renal cell carcinoma syndromes, or known preexisting renal disease. A blinded, expert nephropathologist assessed H&E, PAS and trichrome stained sections of NNK, using a standardized scoring scheme (0-3) of four elements: glomerular sclerosis, chronic tubulointerstitial damage, arteriosclerosis and hyaline arteriolosclerosis. The individual scores were combined to form the non-neoplastic chronic kidney damage pathology score (NNCKDPS). Multivariate logistic regression models were created to assess the effect of NNK pathology and other factors on renal function at 24 months.

Results: 156 patients were included with a median of 24 months follow up. 70% patients underwent radical nephrectomy (RN) and the remainder had partial nephrectomy (PN). The mean age at time of surgery was 60 years old and there was a 2.1:1 male to female preponderance. History of hypertension and diabetes was present in 55.8% and 22.1%, respectively. Pre-operatively, 3.8% had chronic kidney disease stage 3b or greater disease, compared with 23.3% post-operatively at 24 months. Higher NNCKDPS was associated with worsening renal function in univariate analysis at 24 months. Multivariate models revealed that higher NNCKDPS (greater than median score 6), RN and reduced baseline eGFR were found to be predictive for worsening eGFR and CKD stage. Glomerular sclerosis and arteriosclerosis were found to be adversely associated with eGFR.

Conclusions: Systematic assessment of NNK at the time of surgery can help identify patients at risk of post-operative renal dysfunction. A combined NNCKDPS represents a standardized and prognostically relevant histologic reporting system for NNK tissue.

564 Spectrum of Hormone Therapy Related Changes in Orchiectomy Specimens of Patients Seeking Male to Female Physical Adaptation

Christopher Jurief[1], Sabika Sadiq[2], Ameer Hamza[3]
[1]University of Kansas Health System, KS, [2]Bradenton, FL, [3]University of Kansas Medical Center, Kansas City, KS

Disclosures: Christopher Jurief: None; Sabika Sadiq: None; Ameer Hamza: None

Background: Hormonal therapy followed by orchiectomy is the standard of care in management of gender dysphoria in patients seeking male to female physical adaptation. The orchiectomy specimens from these patients are routinely subjected to histopathologic evaluation. We discuss the spectrum of histopathologic findings and cost analysis of processing these specimens.

Design: Orchiectomy specimens from patients seeking male to female transition received at our institution from January 2019 to June 2021 were included in the study. Data including patient age, history of hormonal therapy, testicular weight, histopathologic findings, number of tissue sections, and processing cost were collected.

Results: A total of 79 specimens were identified. Mean age of the patients was 36.7±14.5 years. Mean testicular weight (including weight of spermatic cord) was 28.0±8.3 grams (right) and 27.8±9.1 grams (left). Histologic evaluation showed fibrosis of seminiferous tubules and diminished or absent spermatogenesis in 96.2% and 100% of cases, respectively (Figure 1A, 1B). Additional findings within the testicular parenchyma included either the reduction or complete absence of Leydig cells (n=40 of 79; 50.63% and n=17 of 79; 21.5%, respectively) (Figure 1A, 1B). Sections from the epididymis were submitted in 67 cases and showed peri-epididymal fibrosis in 54 (80.6%) (Figure 1C) and hyperplastic epididymal epithelium in 11 (16.4%) cases (Figure 1D).

Benign, incidental findings were present in 6 (7.6%) cases and included benign cysts (n=2; 2.5%) (Figure 1E), ectopic adrenal tissue (n=2; 2.5%), adenomatoid tumor (n=1; 1.3%) (Figure 1F), and lipoma (n=1; 1.3%). For most cases, 3 sections per testis were submitted. This resulted in a mean of 5.8±1.1 tissue sections per case. The estimated cost of tissue processing, including technician labor, was $41.50 per specimen. Table 1 summarizes the results.

Table 1: Summary of Results Including Histologic Findings

Patient Age Range and Mean	19-77 years (36.7±14.5 years)
Right Testis Weight	28.0±8.3
Left Testis Weight	27.8±9.1
Mean Number of Tissue Sections per Case	5.8±1.1
Reduced/Absent Spermatogenesis	79 (100%)
Hyalinization of Seminiferous Tubules	76 (96.2%)
Reduced Leydig Cells	40 (50.6%)
Absence of Leydig Cells	17 (21.5%)
Peri-epididymal Fibrosis*	54 (80.6%)
Hyperplastic Epididymal Epithelium*	11 (16.4%)
Cases with Incidental Findings	6 (7.6%)

*Sections of epididymis were submitted in 67 cases

Figure 1 - 564

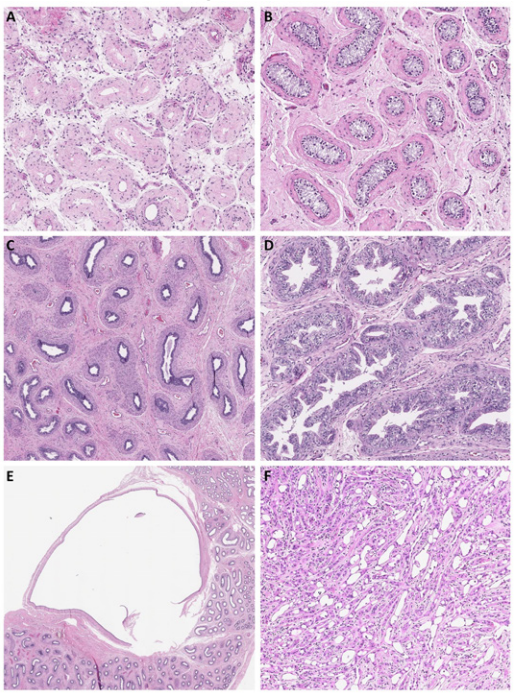

Figure 2 - 564

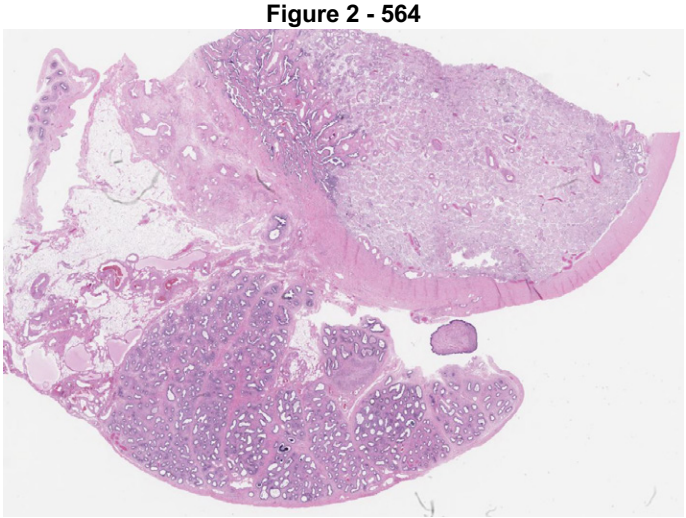

Conclusions: Orchiectomy specimens from patients with gender dysphoria demonstrate consistent hormone therapy related changes and chances of discovering incidental findings of clinical significance are negligible. Histologic findings in these orchiectomy specimens can be evaluated with minimal tissue sampling, specially by taking a strategic tissue section showing the major structures as shown in the whole mount image from one of our cases (Figure 2). Additional sampling can be reserved for gross abnormalities. This can potentially bring the processing cost to one-third of the current cost in these specimens.

565 Renal Cell Carcinoma with Low-Copy TFE3 Amplification

Maria Kamal[1], Michael Quinton[1], Xianfu Wang[1], Shibo Li[1], Zoran Gatalica[1], Wenyi Luo[1]
[1]*University of Oklahoma Health Sciences Center, Oklahoma City, OK*

Disclosures: Maria Kamal: None; Michael Quinton: None; Xianfu Wang: None; Shibo Li: None; Zoran Gatalica: None; Wenyi Luo: None

Background: Some renal cell carcinomas (RCCs) have aberrant expression of melanogenesis-associated transcription factors (MiTFs) including TFE3 and TFEb. Overexpression of these proteins, detectable by immunohistochemistry (IHC), was initially discovered in RCCs harboring *TFE3* or *TFEb* translocations. Recent findings show RCCs containing *TFE3* or *TFEb* amplification or *MITF* mutation as in familial MITF-related renal cell carcinoma. The response of these tumors to immune checkpoint inhibitors and the emerging availability of targeted therapies necessitate a better understanding of the histologic and molecular spectrum for accurate diagnosis.

Design: A MediTech search for RCCs with *TFE3* amplification or translocation between 2019 to 2021 was conducted. Clinicopathologic data including results of IHCs and FISH with break-apart *TFE3* probe (Xp11.2) were retrieved. CGH was performed using archived paraffin tissue blocks.

Results: Three RCCs with *TFE3* amplification were identified among a total of 698 RCCs diagnosed, two diagnosed in radical nephrectomy and one in a liver biopsy for metastatic tumor (Table 1). All three tumors occurred in male patients who presented with large tumors and distant metastasis. These tumors were composed of rhabdoid or pleomorphic tumor cells in solid growth (Figure 1A). Although predominantly high-grade with geographic necrosis (Figure 1B), one of them had an area of lower-grade papillary morphology (Figure 1C). TFE3 IHC was diffusely positive (Figure 2A) except in the low-grade area (Figure 2B). Other IHCs were variable with focal and weak cytokeratin and negative CAIX in some cases. FISH demonstrated 1-2 extra copies of the *TFE3* gene (Figure 2C) as a result of the segmental amplification of X chromosomes in both high-grade and low-grade areas. Among the genes in the amplified segment, only *TFE3* has been associated with RCC. No other copy number changes were identified by CGH.

Case #	Clinical	Morphology	IHC	FISH	Grade	TNM Stage	Metastasis
1	41 year-old male, flank pain, hematuria, weight loss	7.5 cm; predominantly solid and papillary growth with rhabdoid features and abundant necrosis (50%), no calcification	**Positive:** TFE3 Fumarate hydratase PanCK (diffuse, strong) CAIX (diffuse, strong) CD10 (patchy) **Negative:** CK7 (weak positive in papillary component) AMACR (weak positive in papillary component)	Approximately 34% of the cells analyzed showed one extra copy of the TFE3 gene	G4	T3N1M1	Lung metastasis; vena cava thrombus
2	40 year-old male, renal mass	Liver biopsy shows metastasis with nests of atypical cells with eosinophilic and vacuolated cytoplasm and high-grade nuclei	**Positive:** TFE3 Fumarate hydratase PanCK (weak) Pax-8 (diffuse, strong) CD10 (patchy) **Negative:** HepPar-1, CAIX, CD117, CK7, ALK	Approximately 64% of the cells analyzed showed one or two extra copies of the TFE3 gene	G4	NA	Liver metastasis; patient died within 2 years of diagnosis
3	65 year-old male, flank pain	13.5 cm; predominantly solid growth with sarcomatoid and rhabdoid features and necrosis (70%), no calcification	**Positive:** TFE3 Fumarate hydratase PanCK (scattered) CK 8/18 (scattered) CAIX(patchy) CD10 (patchy) S100 (rare, weak) **Negative:** PAX8, GATA3, HMB45	Approximately 45% of the cells analyzed showed one or two extra copies of the TFE3 gene.	G4	T3N1M1	Lung and cerebral metastasis, left supraclavicular LN level 4 metastasis

Figure 1 - 565

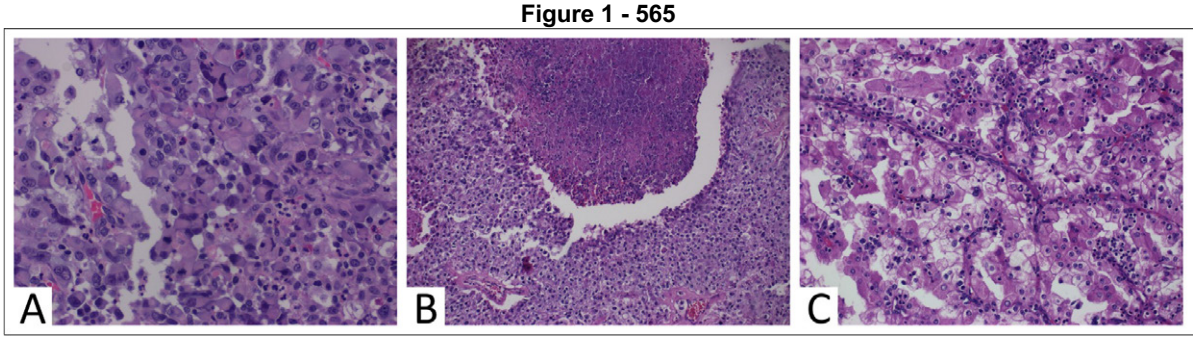

Figure 2 – 565

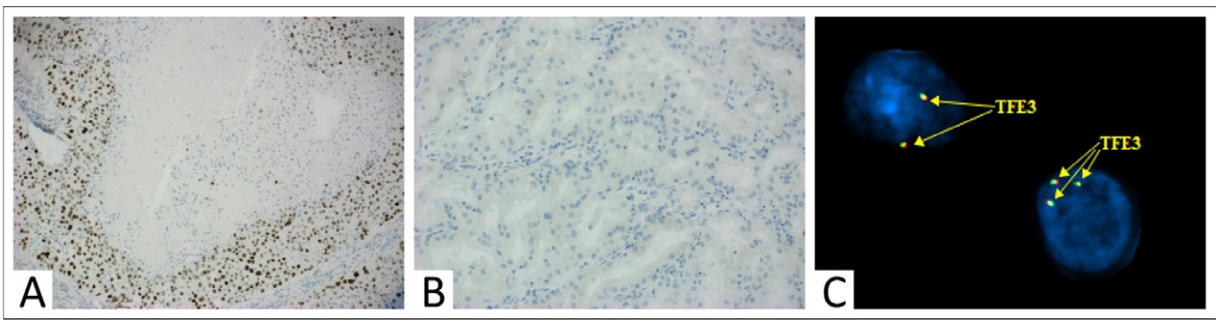

Conclusions: RCCs with *TFE3* amplification are high-grade and aggressive with frequently reduced cytokeratin expression. The absence of other known RCC-related CGH alterations is suggestive of a pathogenic role of TFE3 and the potential efficacy of TFE3 targeted therapies. TFE3 IHC was able to detect low-copy *TFE3* amplification and therefore can be used for screening. Additional factors, potentially promoted by TFE3, may be needed for high-grade transformation based on the presence of *TFE3* amplification in the low-grade area which was only very focally and rarely present.

566 Urethra Sparing in Women at the Time of Cystectomy Does Not Compromise Oncological Outcomes

Sonia Kamanda[1], Sunil Patel[2], Shirley Wang[3], Armine Smith[2], Andres Matoso[4]
[1]James Buchanan Brady Urological Institutions, Johns Hopkins Hospital, Johns Hopkins Medical Institutions, Baltimore, MD, [2]Johns Hopkins Hospital, Baltimore, MD, [3]Johns Hopkins University School of Medicine, Baltimore, MD, [4]Johns Hopkins Medical Institutions, Baltimore, MD

Disclosures: Sonia Kamanda: None; Sunil Patel: None; Shirley Wang: None; Armine Smith: None; Andres Matoso: None

Background: Unlike its male equivalent, female cystectomy usually involves urethrectomy when orthotopic bladder is not a consideration. The aim of this study is to evaluate urethral involvement and urethral recurrence of cancer in women who have undergone radical cystectomy.

Design: A retrospective review was conducted of the electronic medical records from 1999 to 2020 at The Johns Hopkins Medical Institutes. Clinicopathologic reports of cystectomies were examined noting surgical procedure (radical vs partial), size and type of cancer, involvement of urethra as well as subsequent urethrectomies. Hematoxylin and eosin (H&E) stained slides were examined by GU trained pathologists to confirm urethra involvement.

Results: A total of 329 radical cystectomy specimens were evaluated over a 20 year time period. These cases were grouped into patients with a neobladder, ileal conduit and continent cutaneous diversion. The cases were comprised of variants of bladder carcinoma and sarcoma with 64% being urothelial carcinoma. Most of the patients were Caucasians (85%) with a mean age of 67 (60-73) years and a significant history of smoking (61%). The tumor ranged in size from 1.5-4.5cm and was mostly multifocal. Eighteen patients (6%) were found to have a positive urethra margin involved by either invasive or in-situ carcinoma (CIS). Majority of the patients (81%) had an ileal conduit which ordinarily necessitates a cystourethrectomy. One patient with a

neobladder had a recurrence out of 41 patients studied. Overall, there were no subsequent urethrectomies performed for local recurrence. Comparing the overall survival, recurrence free survival and time to recurrence, there was no statistical significance in the three groups (0.209, 0.645 and 0.636) respectively.

Conclusions: Given the low rate of urethra involvement, urethra-sparing radical cystectomies should be highly considered when there is no clinical evidence of involvement. If in doubt, frozen section during surgery may provide guidance on the necessity of urethrectomy. Radical cystectomy is a highly morbid procedure, and sparing the urethra benefits both the surgeon and the patient by simplifying the surgery and preventing the postoperative complications of sexual dysfunction and perineal wound healing complications.

567 Cribriform Pattern Identification is Unreliable in Predicting Prognosis in Prostate Cancer Diagnostic Needle Biopsies. A Trans-Atlantic Prostate Group Study

Solene-Florence Kammerer-Jacquet[1], Kim Chu[2], Luis Beltran[2], Jack Cuzick[2], Theodorus Van Der Kwast[3], Jesse McKenney[4], Daniel Berney[2]

[1]University Hospital, Rennes, France, [2]Queen Mary University of London, London, United Kingdom, [3]University Health Network, Toronto, Canada, [4]Cleveland Clinic, Cleveland, OH

Disclosures: Solene-Florence Kammerer-Jacquet: None; Kim Chu: None; Luis Beltran: None; Jack Cuzick: None; Theodorus Van Der Kwast: None; Jesse McKenney: None; Daniel Berney: None

Background: Cribriform prostate cancer is associated with a poor prognosis in radical prostatectomy specimens but its utility in biopsies is not fully elucidated. A previous study (*Histologic grading of prostatic adenocarcinoma can be further optimized*. McKenney et al. Am J Surg Pathol. 2016) has divided cribriform lesions graded Gleason 4 as 'small cribriform', 'expansile cribriform' and 'cribriform with irregular contours'.

Design: Cribriform *patterns were morphologically reported in a retrospective cohort of patients with prostate cancer of grade groups (GG) 2-4 (n=563). The outcome was death from disease. Univariate and multivariate analysis were performed using Cox models. Other clinicopathologic parameters such as PSA and extent of disease were integrated to the multivariate model.*

Results: Cribriform patterns identified in biopsies from GG 2 (n=299), 3 (n=208) and 4 (n=56) were mainly small cribriform glands (n=236) and rarely expansile cribriform glands (n=57) and cribriform glands with irregular contours (n=22). Cribriform patterns (taken separately or together) were not significantly associated with the prognosis in grade groups 2, 3 and 4 (taken separately or together) in univariate (p=0,09, Table 1) or multivariate analysis (p=0.52, Table 2) along with other relevant clinicopathologic variables.

		Univariate analysis			Multivariate analysis		
Variables	n	HR	95% CI	p-value	HR	95% CI	p-value
Cribriform	564						0.52
No	279	1.00	(reference)		1.00	(reference)	
Yes	285	1.34	0.96, 1.88	0.09	1.12	0.79, 1.59	0.52
Baseline PSA	564						0.02
<=16.9	282	1.00	(reference)		1.00	(reference)	
>16.9	282	2.02	1.43, 2.85	<0.001	1.55	1.06, 2.26	0.02
Extent of disease	564						0.02
x<=25%	96	1.00	(reference)		1.00	(reference)	
25%<x<=50%< span=""></x<=50%<>	158	1.22	0.69, 2.17	0.49	1.17	0.66, 2.09	0.59
50%<x<=75%< span=""></x<=75%<>	115	1.14	0.61, 2.13	0.68	0.95	0.50, 1.81	0.87
x>75%	195	2.52	1.49, 4.25	<0.001	1.90	1.08, 3.35	0.03
Gleason grade group	564						0.003
2	299	1.00	(reference)		1.00	(reference)	
3	209	2.03	1.42, 2.92	<0.001	1.73	1.19, 2.49	0.004
4	56	2.22	1.30, 3.79	0.003	2.13	1.25, 3.65	0.01

Conclusions: Contrary to previous studies, cribriform architecture was not significantly associated with poor prognosis whatever the type of cribriform pattern. We suggest that although its presence may be associated with poor behaviour, absence may be due to sampling errors and extreme caution should be undertaken in active surveillance programmes for GG2 if the disease is poorly sampled.

568 Molecular Characterization of High-Risk Human Papilloma Virus-Positive Carcinomas of the Urethra and Urothelial Tract

Neslihan Kayraklioglu[1], Walter Devine[1], Bradley Stohr[1], Emily Chan[1]
[1]*University of California, San Francisco, San Francisco, CA*

Disclosures: Neslihan Kayraklioglu: None; Walter Devine: None; Bradley Stohr: None; Emily Chan: None

Background: Human Papilloma Virus (HPV) is a sexually-transmitted infection and well-known cause for squamous cell carcinomas (SCCa) of anogenital and oropharyngeal regions, where treatment strategies and prognosis depend on HPV status. While HPV has been detected in tumors arising along the urothelial tract, the significance of HPV status is not well-established, as these tumors are rare and poorly understood. In this study, we provide detailed molecular analysis in a series of HPV-positive (HPV+) urethral and urothelial tract carcinomas (UUTCa).

Design: 10 UUTCa with HPV+ by in situ hybridization were included; cases showing direct extension from outside the UUT were excluded. All cases were analyzed using a clinically validated targeted DNA sequencing panel that includes 529 cancer-related genes and genome-wide copy number alterations. For comparison, 10 recent UUT HPV-negative (HPV-) SCCa or squamous predominant carcinomas were also reviewed. Additional clinical and pathologic data were extracted from medical records.

Results: The 10 HPV+ UUTCa were located in: urethra (4/10 penile, 2/10 female, 1/10 prostatic) and urinary bladder (3/10). On histology, HPV+ UUTCa were basaloid with hybrid squamous and urothelial features (9/10); well-differentiated squamous areas were only focally present (6/10). Immunohistochemical workup showed positive GATA3 (5/6), p63 (4/4) and negative uroplakin II (0/6). On molecular analysis, the most frequently altered genes were *KMT2C* (40%) and *PIK3CA* (30%).
No *TERT, TP53* or *CDKN2A* aberrations were observed. In contrast, the HPV- cases showed mutational profiles similar to that more commonly reported in urothelial carcinomas with most frequently altered genes: *TERT (70%)*, *TP53 (50%)*, *PIK3CA (40%), CDKN2A (40%) and KMT2D (40%).* Interestingly, while HPV+ cases presented with more lymph node metastasis (5/10 HPV+ vs 2/10 HPV-), no HPV+ deaths occurred; whereas 2 HPV- patients died of disease (median follow up time: HPV+ 36 vs HPV- 15 months).

Figure 1 - 568

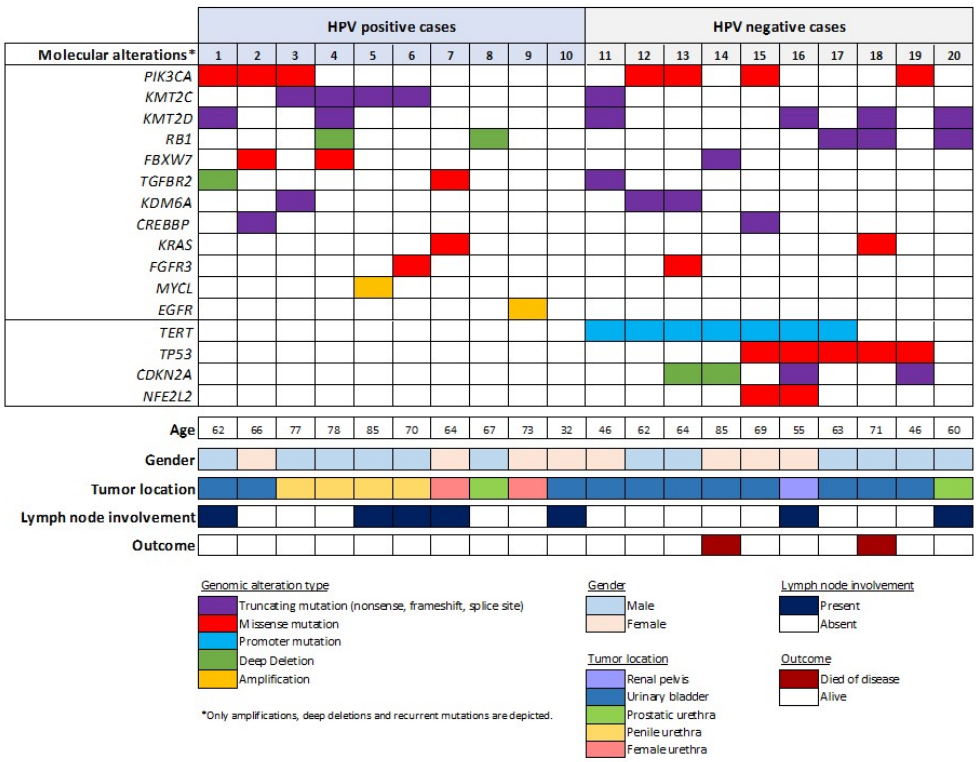

Conclusions: HPV+ UUTCa have an overall molecular profile distinct from HPV- UUT SCCa/squamous predominant carcinomas. Our HPV+ UUTCa also presented with more advanced nodal stage but had better outcomes. Though limited by sample size and

site specific differences in the comparison group, our findings show similarities to that of head and neck HPV+ cancers, suggesting an important role for HPV in UUTCa. Further investigation is warranted.

569 Fibroblast Growth Factor Receptor-3 (FGFR3) Expression is Associated with HPV-driven Penile Squamous Cell Carcinoma

Brian Keller[1], Elena Pastukhova[2], Paul Borowy-Borowski[3], Kevin Hogan[3], Harmanjatinder Sekhon[4], Trevor Flood[5]
[1]Ottawa Hospital, University of Ottawa, Ottawa, Canada, [2]University of Ottawa/The Ottawa Hospital, Ottawa, Canada, [3]The Ottawa Hospital, Eastern Ontario Regional Laboratory Association, Ottawa, Canada, [4]The Ottawa Hospital, University of Ottawa, Eastern Ontario Regional Laboratory Association, Ottawa, Canada, [5]The Ottawa Hospital, Ottawa, Canada

Disclosures: Brian Keller: *Grant or Research Support*, Turnstone Biologics; *Consultant*, Amplitude Ventures; Elena Pastukhova: None; Paul Borowy-Borowski: None; Kevin Hogan: None; Harmanjatinder Sekhon: None; Trevor Flood: None

Background: Penile squamous cell carcinoma (PSCC) represents approximately 0.5% of all male malignancies and approximately half of PSCC cases are associated with infection by human papilloma virus (HPV). FGFR3 is a receptor tyrosine kinase whose downstream signaling pathways include PI3K/AKT and RAS-MEK-ERK, both of which are involved in oncogenesis. Increased FGFR3 expression has been observed in multiple cancer subtypes and has been proposed as a potential therapeutic target. In this study we examined the immunohistochemical expression of FGFR3 in both HPV-positive and HPV-negative PSCCs.

Design: A search of our database from 2011-2020 identified 38 patients diagnosed with PSCC. The cohort consisted of 19 partial penectomies, 7 total penectomies, 10 biopsies, and 2 circumcisions. A semi-quantitative scoring system was used to assess FGFR3 immunostaining: 0, all tumor cells negative; 1+, faint but detectable expression in some or all cells; 2+, weak to intermediate expression; 3+, strong positivity. All samples were also stained with p16 which acted as a surrogate marker for HPV infection. Expression of p16 was scored as either positive (strong and diffuse positivity) or negative (absence of strong and diffuse positivity).

Results: FGFR3 expression was identified in 22/38 (58%) cases (12 cases of 1+, 8 cases of 2+, and 2 cases of 3+ staining). The FGFR3 immunostain frequently showed a unique spatial distribution with increased expression intensity observed at the periphery and leading edges of tumors (Figure 1). Tumors were divided into four groups based on FGFR3 and p16 expression: 17/22 (77%) of cases were +FGFR3/+p16, 5/17 (29%) were +FGFR/-p16, 4/16 (25%) were -FGFR3/+p16, and 12/16 (75%) were -FGFR3/-p16. FGFR3 positivity was significantly associated with p16 expression (p=.001). Of note, both cases of 3+ staining were observed in p16 negative tumors arising in a background of lichen sclerosis.

Figure 1 - 569

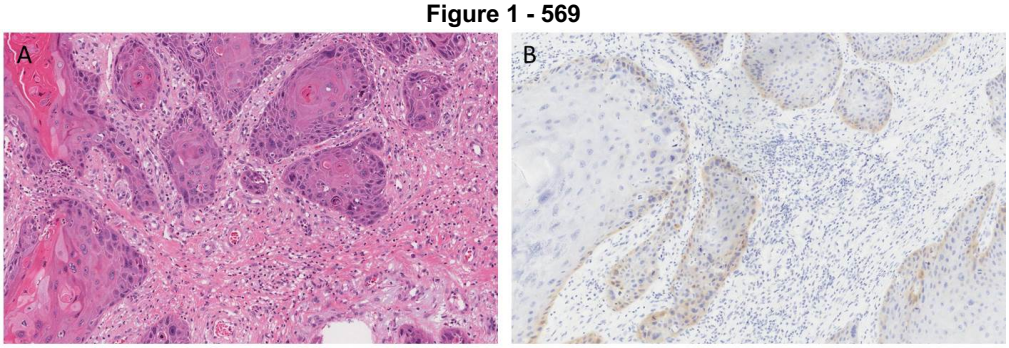

Figure 1: A) H&E showing PSCC with large invasive tumor nests. B) FGFR3 expression by immunohistochemistry shows positivity within the periphery of the tumor nests.

Conclusions: To our knowledge, this is the first study to characterize FGFR3 immunohistochemical expression in PSCC. Positive staining of FGFR3 localized exclusively towards the periphery or leading edge of tumor nests. FGFR3 expression was significantly associated with p16 positive tumors which suggests that this phenomenon occurs preferentially in the setting of HPV induced carcinogenesis. FGFR3 is a potential target for novel therapies in the treatment of PSCC, particularly in HPV-driven cases.

570 Mixed Lineage Kinase Domain-like Protein (MLKL) in Primary Resected Bladder Cancer: Expression, Prognostic Role and Correlations with the Immune Environment

Eva C. Keller[1], Philipp J. Jost[2], Kristina Schwamborn[1], Wilko Weichert[1], Thomas Horn[3], Julia Slotta-Huspenina[1]
[1]Institute of Pathology, Technical University Munich, Munich, Germany, [2]Medical University of Graz, Graz, Austria, [3]Klinikum Rechts der Isar, Technical University Munich, München, Germany

Disclosures: Eva C. Keller: None; Philipp J. Jost: *Speaker*, Abbvie, Ariad, Bayer, Böhringer, Janssen, MSD, BMS Celgene, Pierre Fabre, Roche, Servier, Novartis; Kristina Schwamborn: *Speaker*, Roche, MSD; *Advisory Board Member*, MSD, BMS; *Speaker*, Merck; Wilko Weichert: *Speaker*, Roche, MSD, BMS, AstraZeneca, Pfizer, Merck, Lilly, Boehringer, Novartis, Takeda, Bayer, Amgen, Astellas, Eisai, Illumina, Siemens, Agilent, ADC, GSK, Molecular Health.; *Grant or Research Support*, Roche, MSD, BMS, AstraZeneca; Thomas Horn: None; Julia Slotta-Huspenina: None

Background: Mixed lineage kinase domain-like protein (MLKL) is a critical executioner of necroptosis, a form of regulated necrosis which is characterized by its immunogenic effects through the release of damage-associated molecular patterns (DAMPs), chemokines and cytokines. The necroptotic pathway has been shown to be implicated in a variety of cancer entities but its role in bladder cancer remains unclear. Thus, the aim of our study was to determine the tumoral protein expression levels of MLKL and its relationship with the prognosis and the immune environment in bladder cancer.

Design: Tissue microarrays of formalin-fixed paraffin-embedded (FFPE) invasive bladder cancer specimens of 145 patients (pT1-pT4) who received cystectomy without neoadjuvant treatment and lacked distant metastasis were analyzed. The expression of MLKL, MHC I, MHC II, CD3, CD8, FOXP3 and CD45 was determined by immunohistochemistry. MLKL, MHC I and MHC II levels on tumor cells were semi-quantitatively scored (immunoreactivity score, IRS 0– 12). Infiltration densities of intratumoral immune cells (CD3, CD8, FOXP3 and CD45) were analyzed with an automated image analysis system. MLKL expression levels were correlated with the above-named markers and clinicopathological parameters (pT, pN, overall survival).

Results: MLKL was expressed in 55.2% (80/145) of cases (MLKL IRS 1-12) while 44.8% (65/145) were completely negative (IRS 0). In MLKL positive cases expression levels showed a wide range with low expression (IRS 1-4) in 80% (64/80) and high expression (IRS 5-12) in 20% of cases (16/80). MLKL was positively correlated with the abundance of intratumoral CD3-positive T-cells ($p=0.032$) and high expression of MHC I and MHC II ($p<0.001$, $p=0.009$). High MLKL expression significantly correlated with higher tumor stage ($p=0.04$). However, no significant associations of MLKL with N status, overall survival or infiltration density of CD8-, FOXP3- or CD45-positive cells were found.

Conclusions: To the best of our knowledge, we are the first to show that the executioner of necroptosis, MLKL, is expressed in a substantial proportion of invasive bladder cancer and is significantly associated with tumor stages and lymphocytic infiltration. MLKL might serve as a marker for an immune enhanced expression profile in bladder cancer.

571 Discriminative Significance of Prostate Biopsy Decipher Score to Predict Adverse Pathology and Pathological Discordance at Radical Prostatectomy

Ghazal Khajir[1], Deepika Kumar[2], Syed Rahman[2], Michael Leapman[3], Angelique Levi[4], Peter Humphrey[3], Preston Sprenkle[3]
[1]Yale School of Medicine, Yale New Haven Hospital, New Haven, CT, [2]Yale New Haven Hospital, New Haven, CT, [3]Yale School of Medicine, New Haven, CT, [4]Yale University, New Haven, CT

Disclosures: Ghazal Khajir: None; Deepika Kumar: None; Syed Rahman: None; Michael Leapman: None; Angelique Levi: None; Peter Humphrey: None; Preston Sprenkle: None

Background: The predictive value of Decipher test in Grade Group (GG) 3-5, pT3b-T4, or lymph node involvement at radical prostatectomy (RP) is well established. However, little is known about its prognostic significance in other pathological surrogates for metastatic potential, including positive surgical margin (PSM), and extraprostatic extension (EPE), as well as pathologic concordance between biopsy and RP. Therefore, we sought to determine if Decipher score was associated with the presence of those pathological characteristics at RP and biopsy-RP pathological discordance.

Design: We retrospectively queried an IRB-approved institutional MRI-ultrasound fusion prostate biopsy database of 283 men with Decipher testing on their biopsy tissues. Patients who underwent RP between February 2017 and May 2021 were included in the final analysis. Binary logistic regression was performed to identify biopsy Decipher score and clinical features associated with pT3a or higher staging, and the presence of PSM, EPE, as well as upgrading and downgrading of biopsy pathology on RP.

Results: Our cohort included 74 men with biopsy Decipher testing who underwent RP. GG1, GG2 and GG3 was identified on the final pathology in 3 (4.1%), 66 (89.1)% and 5 (6.8%) patients, respectively. Presence of pT3a or higher, PSM, EPE, upgrading, and downgrading of biopsy pathology on RP was reported in 29 (39.1%), 35 (47.3%), 30 (40.5%), 7 (9.5%), and 11 (14.9%) patients, respectively. Four patients (5.4%) had positive lymph nodes on pathology. No studied variables were associated with the presence of EPE, pT3a and higher staging, or upgrading. Among variables entered multivariate analysis (age, PSA density, and Decipher risk category), PSA density remained significantly associated with an increased risk of PSM at RP (OR 1.93, 95% CI 1.04-3.57, p=0.03, Table 1). Moreover, low-intermediate Decipher risk category (Decipher score <0.60) was associated with more than threefold increased odds of downgrading, although this association did not reach conventional levels of statistical significance (OR 3.37, p=0.051, Table 1).

Table 1. Univariate and multivariate logistic regression models for the prediction of positive surgical margin and downgrading in men undergoing radical prostatectomy

	Variable	**Univariate**		**Multivariate**	
		OR (95% CI)	*P value*	*OR (95% CI)*	*P value*
Positive surgical margin	Age	0.91 (0.84-0.99)	0.03	0.92 (0.84-1.00)	0.06
	PSA density (per 0.1 increase in unit)	2.12 (1.18-3.82)	0.01	1.93 (1.04-3.57)	0.03
	Decipher risk category Low risk (score <0.45) Intermediate/high risk (score ≥0.45)	1.00 (Ref) 2.64 (0.65-10.73)	0.07	1.00 (Ref) 0.73 (0.24-2.17)	0.57
Downgrading	Age	0.97 (0.87-1.08)	0.65		
	PSA density (per 0.1 increase in unit)	0.64 (0.29-1.43)	0.28		
	Decipher risk category Low risk/intermediate (score <0.60) High risk (score ≥0.60)	1.00 (Ref) 0.29 (0.66-1.10)	0.051		

Conclusions: No significant association was found between biopsy Decipher score or risk categories and biopsy-RP pathological discordance or any of the studied pathological features (PSM, EPE, and pT3a or higher staging). Nevertheless, our study might provide some clues to further investigate the noted higher rate of downgrading in the low-intermediate vs high-risk Decipher risk category.

572 Molecular Characterization of Urachal Neoplasms

Osama Khan[1], Christian Kunder[1], Chia-Sui (Sunny) Kao[1], Ankur Sangoi[2]
[1]Stanford Medicine/Stanford University, Stanford, CA, [2]El Camino Hospital, Mountain View, CA

Disclosures: Osama Khan: None; Christian Kunder: None; Chia-Sui (Sunny) Kao: None; Ankur Sangoi: None

Background: Urachal neoplasms are rare and include a spectrum of lesions from mucinous cystadenoma to adenocarcinoma. Urachal carcinomas account for <1% of all bladder-associated malignancies, and amongst adenocarcinomas involving the bladder, account for approximately 10% of cases; the outcomes of urachal adenocarcinomas remain poor as these malignancies present at advanced stages and are detected late into their disease course. In this study, we aim to characterize the molecular features of urachal neoplasms.

Design: Eighteen total cases of urachal glandular neoplasms were retrospectively identified from 2004 to 2017 from the pathology archives of Stanford University and four from outside facilities. Patients ranged in age from 32 to 78 (median 48), and males and females were equally affected. Formalin-fixed archival samples of urachal glandular neoplasms were available from 12 patients and analyzed using the STanford Actionable Mutation Panel for Solid Tumors (STAMP) next generation sequencing platform.

Results: Eleven urachal cases yielded molecular results as one of the cases had poor DNA quality. We identified seven cases yielding oncogenic *KRAS* mutations with 3 of these cases harboring the uncommon *KRAS* c.436G>A, p.A146T variant. Nine of the cases had *TP53* alterations. Five cases had both *KRAS* and *TP53* mutations. Other oncogenic variants included 2 cases each with *PIK3CA* and *GNAS* mutations. Case 11 showed a somewhat distinct pattern with variants generally associated with urothelial carcinoma.

No	Diagnosis	*TP53*	*KRAS*	*PIK3CA*	*GNAS*	Other variants
1	Adenocarcinoma NOS	c.818G>A p.R273H	c.33_35delinsAGA p.G12D			**AR* c.1849C>T, p.L617F
2	Mucinous Adenocarcinoma	c.524G>A p.R175H	c.35G>T p.G12V			
3	Mucinous Adenocarcinoma	c.1024C>T p.R342*	c.436G>A p.A146T			
4	Mucinous Adenocarcinoma	c.437G>A p.W146*	c.436G>A p.A146T			
5	Villous adenoma	c.524G>A p.R175H	c.436G>A p.A146T		c.602G>A p.R201H	*FBXW7* c.1513C>T, p.R505C **KRAS* c.538_540del, p.C180del **NF2* c.628G>A, p.A210T
6	Mucinous Adenocarcinoma	c.533A>C p.H178P			c.602G>A p.R201H	*ERBB2* c.2033G>A, p.R678Q *CTNNB1* c.110C>G, p.S37C **KIT* c.1918G>C, p.E640Q **NTRK3* c.1782C>A, p.N594K
7	Mucinous Adenocarcinoma	c.626_627del p.R209fs				
8	Enteric-type Adenocarcinoma	c.637C>T p.R213X				**HGF* c.152T>C, p.I51T
9	Mucinous Cystadenoma		c.35G>A p.G12D			
10	Enteric-type Adenocarcinoma		c.38G>A p.G13D	c.3140A>G p.H1047R		
11	Mucinous Adenocarcinoma	c.853G>A p.E285K		c.1624G>A p.E542K		*TERT* promoter mutation C228T *PLEKHS1* promoter mutation c.-20+73C>T *CDKN1B* c. 487C>T, p.Q163* *ARID1A* c.1543C>T, p.Q515* *5 additional VUS

Conclusions: We investigated the complex molecular signature of 11 urachal neoplasms in this series and the majority had either a KRAS or TP53 oncogenic variant and presence of both variants is common. These results further elucidate the genomic landscape and biology of urachal tumors and provide possible targets of treatment for these rare neoplasms.

573 Do All Seminomas Originate from Germ Cells: A Short Tandem Repeat (STR) Study

Deepika Kumar[1], Minghao Zhong[2], Tong Sun[2], Pei Hui[3], Peter Humphrey[2]
[1]Yale New Haven Hospital, New Haven, CT, [2]Yale School of Medicine, New Haven, CT, [3]Yale University School of Medicine, New Haven, CT

Disclosures: Deepika Kumar: None; Minghao Zhong: None; Tong Sun: None; Pei Hui: None; Peter Humphrey: None

Background: Seminomas are the most common testicular germ cell tumors (TGCT) in young adult males. Based on clinical, morphological and immunophenotypic features, it has been postulated that seminomas arise from germ cells. To address this, we evaluated zygosity of seminomas by short tandem repeat (STR) testing.

Design: We collected 20 consecutive seminoma cases from young adults with available tissue. Paired tissue samples of cancerous and normal tissue were subjected to macro-dissection to isolate well-defined tumor and normal tissue for DNA extraction. The gDNA were summited for multiplex PCR amplification targeting 15 STR loci with amplicon sizes ranging from 100 to 350 base pairs. The assay tests 13 loci of the Combined DNA Index System (CODIS) plus 2 additional loci, D2S1338 and D19S433. We also reviewed slides for germ cell neoplasia in situ (GCNIS) and rete testis involvement.

Results: For all tested seminomas, all informative STR loci demonstrated a diploid pattern which is identical to the paired normal tissue. In addition, several abnormal alleles and imbalanced alleles were found in some loci from seminoma. A total of 12 cases had GCNIS and 5 cases had rete testis involvement.

Conclusions: In this study, we investigated genetic zygosity for seminomas by STR genotyping. Our results demonstrated that seminoma cells are diploid, suggesting that seminomas may not originate from germ cells which are haploid. The abnormal and imbalanced alleles are probably due to general cancer related phenomena, such as aneuploidy and loss of heterozygosity (LOH). In addition, we also hypothesize that GCNIS may not be a biological precursor of seminoma, but rather spread of seminoma cells into seminiferous tubules, just like rete testis in-situ involvement.

574 Genomic Classification of Clinically Advanced Prostate Cancer (CAPC) Based on Methylthioadenosine Phosphorylase (MTAP) Genomic Loss

David Kumpula[1], Oleksandr Kravtsov[1], Vamsi Parimi[2], Richard Huang[3], Natalie Danziger[4], Jeffrey Ross[1]
[1]SUNY Upstate Medical University, Syracuse, NY, [2]Foundation Medicine, Inc., RTP, NC, [3]Foundation Medicine, Inc., Cary, NC, [4]Foundation Medicine, Inc., Cambridge, MA

Disclosures: David Kumpula: None; Oleksandr Kravtsov: None; Vamsi Parimi: *Employee*, Foundation Medicine Inc.; Richard Huang: *Employee*, Foundation Medicine; *Employee*, Roche; Natalie Danziger: *Employee*, Foundation Medicine Inc.; *Stock Ownership*, F. Hoffman La Roche Ltd.; Jeffrey Ross: *Employee*, Foundation Medicine; *Employee*, Foundation Medicine

Background: CAPC has a poor prognosis and treatment options are limited. MTAP is often co-deleted with the tumor suppressor gene *CDKN2A*, and its loss is an important target for synthetic lethality. We used comprehensive genomic profiling (CGP) to compare the genomic alterations (GA) in CAPC with intact *MTAP* to CAPC with MTAP loss.

Design: 8,436 cases of CAPC underwent hybrid-capture based CGP to evaluate all classes of GA. Tumor mutational burden (TMB) was determined on up to 1.1 Mbp of sequenced DNA and microsatellite instability (MSI) was determined on 114 loci. PD-L1 tumor cell expression was assessed by IHC (Dako 22C3).

Results: 110 (1.3%) of CAPC featured loss of *MTAP* which was accompanied by *CDKN2A* loss in 99.1% and *CDKN2B* loss in 93.6% which were significantly higher than that seen in the *MTAP* intact mCRPC. When *CDKN2A/B* GA are not included the GA/tumor in both groups were similar. For currently untargetable GA, when compared with *MTAP* intact CAPC cases, *MTAP* loss CAPC featured significantly lower frequencies of *CDK12*, and *RB1* GA and a higher frequency of *TP53* GA. For GA associated with potential PARPi efficacy, *MTAP* loss mCRPC featured significantly lower total GA in *BRCA2* (including *BRACA2* loss), and *RAD21*. For other potentially targetable GA, *MTAP* loss CAPC featured significantly higher *PTEN* GA than *MTAP* intact CAPC. Kinase target GA were low and not different in both groups. *AR* GA predominantly associated with androgen ablation treatments were significantly higher in *MTAP* intact cases. *TMPRSS2:ERG* fusion and *SPOP* mutation frequencies were similar in both groups. For immune-oncology (IO) biomarkers, there were no significant differences between the 2 groups except for a significantly higher mean TMB in the *MTAP* loss CAPC cases.

	CAPC *MTAP* Intact	**CAPC *MTAP* Loss**	**P Value**
Number of Cases	8,326	110	
Median age (range) years	68 (38-89+)	68 (39-89+)	
Mean age	68.6	67.6	NS
GA/tumor	3.82	7.03	
Important CAPC GA			
TMPRSS2:ERG Fusion	31.7%	27.3%	NS
AR	14.3% (9.3% amp)	6.4%	=.02
CDK12	5.9%	0.9%	=.02
RB1	5.4%	0.9%	=.03
SPOP	8.7%	4.5%	NS
Other Currently Untargetable GA			
CDKN2A	1.3%	99.1%	<.0001
CDKN2B	0.3%	93.6%	<.0001
TP53	40.4%	50.0%	=.05
CDK6	1.3%	2.7%	NS
MSH6	1.4%	0%	NS
APC	8.6%	10.0%	NS
GA Associated with PARP Inhibitor Efficacy			
BRCA1	1.1% (0.1% loss)	3.6% (0.9% loss)	=.04
BRCA2	8.9% (2.7% loss)	2.7% (0.9% loss)	=.02
ATM	5.7%	2.7%	NS
RAD21	10.6%	4.5%	=.04
Other Currently Targetable GA			
PTEN	30.5%	48.2%	=.0002
ERBB2	0.7%	0%	NS
BRAF	3.5%	0.9%	NS
PIK3CA	6.3%	8.2%	NS
IO Biomarkers			
STK11	0.3%	1.8%	NS
KEAP1	0.2%	0.9%	NS
MDM2	0.8%	1.8%	NS
CD274 Amp	0.2%	1.8%	NS
MSI-High	2.8%	0.9%	NS

Median TMB	2.5	1.3	
Mean TMB	2.6	3.8	=.0002
TMB ≥10 mut/Mb	5.8%	3.6%	NS
TMB ≥20 mut/Mb	4.0%	0.9%	NS
PD-L1 Low Positive (TPS 1-49%)	11.4% (2,526 cases)	15.0% (40 cases)	NS
PD-L1 High Positive (TPS ≥50%)	1.0%	2.5%	NS

TPS - Tumor Proportion Score

*when *CDKN2A/B* GA are excluded

Conclusions: A small number of cases of CAPC have *MTAP* loss (1.3%). *MTAP* loss is associated with a higher mean TMB, and has a significantly different GA profile, indicating a potential benefit for directed therapy of CAPC based on *MTAP* status. Of particular interest, CAPC with *MTAP* loss has lower frequencies of GA in *AR*, *CDK12* and *RB1*, and higher frequencies of GA in *CDKN2A*, *CDKN2B*, *TP53*. Additionally, those with *MTAP* loss have lower frequencies of GA associated with PARPi efficacy (in *BRCA2* and *RAD21*) These findings suggest that CGP in CAPC can lead to targeted therapies and synthetic lethality treatments based on *MTAP* status, improving patient outcomes.

575 Implications of Correlation Between PBRM1 and PD-L1 Expression in Renal Cell Carcinoma, Clear Cell Type

Jieun Lee[1], Gheeyoung Choe[1], Kyu Sang Lee[1]
[1]*Seoul National University Bundang Hospital, Seongnamsi, South Korea*

Disclosures: Jieun Lee: None; Gheeyoung Choe: None; Kyu Sang Lee: None

Background: The most common altered gene found in clear cell renal cell carcinoma (ccRCC) is the von Hippel-Lindau (VHL). After VHL, Polybromo-1 (PBRM1) is the second most frequently altered in ccRCC. Interestingly, PBRM1 alteration is reported as a significant barrier to immune checkpoint blockade response including anti-PD-L1 target therapy. However, the correlation between PBRM1 and PD-L1 expression in ccRCC remains unclear.

Design: Here, we analyzed the loss of PBRM1 (A301-591A; dilution: 1:250, Bethyl Laboratories, Montgomery, TX) expression and PD-L1 (22C3; pharmDx assay, Agilent, Santa Clara, CA) expression in a retrospective cohort of 526 surgically resected ccRCC in a single institute.

Results: Based on a cut-off of the combined positive score (CPS) ≥1%, positive staining for PD-L1 was found in 139 (26.4%) cases. Loss of PBRM1 expression was observed in 205 (39.0%) cases. PD-L1 expression was positively associated with loss of PBRM1 expression ($P < 0.001$) in ccRCC. Notably, among the ccRCC cases which expressed the PD-L1, loss of PBRM1 was identified in more than 50% of cases. In addition, loss of PBRM1 expression showed correlations with aggressive clinicopathological features including higher ISUP/WHO grade, high pT stage, angiolymphatic invasion, venous invasion, and tumor necrosis ($P <0.05$). Kaplan–Meier analysis indicated that loss of PBRM1 expression and PD-L1 expression was positively correlated with tumor recurrence ($P < 0.001$ and $P = 0.003$, respectively).

Conclusions: In ccRCC, previous clinical trials reported that there is no significant correlation between PD-L1 expression and anti-PD-L1 therapeutic effect. Our study showed that the loss of PBRM1 is significantly correlated with PD-L1 expression in ccRCC. This result can suggest that the PD-L1 blockade may not be effective even though the PD-L1 was expressed in ccRCC due to the interference of PBRM1 alteration.

576 Spectrum of Clinicopathologic Findings in Primary and Post-Chemotherapy Retroperitoneal Lymph Node Dissection for Testicular Germ Cell Tumors- A Single Institute Experience

Maria Sarah Lenon[1], Zhengshan Chen[2], Shivani Kandukuri[3], Andy Sherrod[4], Guang-Qian Xiao[4], Mahul Amin[5], Manju Aron[4]
[1]University of Southern California, LA, CA, [2]University of California, Los Angeles, Los Angeles, CA, [3]University of Southern California, Keck School of Medicine of USC, Los Angeles, CA, [4]Keck School of Medicine of USC, Los Angeles, CA, [5]The University of Tennessee Health Science Center, Memphis, TN

Disclosures: Maria Sarah Lenon: None; Zhengshan Chen: None; Shivani Kandukuri: None; Andy Sherrod: None; Guang-Qian Xiao: None; Mahul Amin: *Advisory Board Member*, Ibex; *Consultant*, Google/Verily; *Advisory Board Member*, Precipio, Cell Max; Manju Aron: None

Background: The indications for primary retroperitoneal lymph node dissection (p-RPLND) and post-chemotherapy retroperitoneal lymph node dissection (pc-RPLND) are often dependent on the histology and stage of the testicular germ cell tumor (t-GCT). Optimal pathological evaluation of these specimens has significant therapeutic and prognostic implications both in the primary and post chemotherapy setting. This study highlights the clinical and pathological features in a contemporary cohort from a tertiary referral center.

Design: RPLND specimens for t-GCT were retrieved from the pathology database (2013-2020) after institutional board review. Relevant clinical data including follow up information and pertinent histologic findings were documented and statistical analysis performed.

Results: 24 (24%) p-RPLND and 78 (76%) pc-RPLND were identified. Stage III-IV t-GCT patients more commonly underwent pc-RPLND than p-RPLND (p=0.017). There was also a significant difference in the tumor histology in the orchiectomy and RPLND specimens in both the groups. Seminoma was an exceedingly rare t-GCT (9%) in patients who underwent pc-RPLND, while it was the second most common (38%) t-GCT in p-RPLND patients. Teratoma (41%) and absence of tumor (31%) were the predominant findings in pc-RPLND specimens, while MGCT (46%) and seminoma (29%) were most frequent in p-RPLND. Somatic malignancy was also more common in pc-RPLND, with primitive neuroectodermal tumor (PNET) being the commonest (5/7; 71%). There was no statistical difference between the two groups in the lymph node stage and status of extranodal extension. Discordance between the diagnosis on orchiectomy and RPLND was high in both groups (p-RPLND:75%; pc-RPLND:85%). Salvage therapy was given in 31 patients (p-RPLND:12; pc-RPLND:19). On follow up 92% of p-RPLND and 88% of pc-RPLND had no evidence of disease, while 1 case of p-RPLND (MGCT) and 4 cases of pc-RPLND(1:MGCT and 3: teratomas, with extensive visceral metastasis of MGCT) died of disease.

Summary of Clinical and Pathological Findings on RPLND specimens

	p-RPLND: 24 (24%)	pC-RPLND: 78 (76%)	P value
Age in years: median (range)	37 (21- 66)	34 (21-77)	
Follow-up in months: median (range)	21 (2 -143)	28 (1-56)	
Status on last follow-up: (%) NED AWD DOD	22 (92) 1 (4) 1 (4)	69 (88) 5 (5) 4 (4)	
Salvage therapy (%) Mixed GCT Somatic Malignant Transformation	4 / 11 (36) 0 / 1 (0)	11 / 12 (92) 1 / 7 (14)	
Total number of lymph nodes dissected: median (range)	40 (17- 58)	25 (1- 72)	
Number of positive lymph nodes: median (range)	2 (1-9)	1 (1-30)	
Size of largest positive lymph node/lymph nodal mass: median (range)	2.6 (1.3- 7.5)	5.4 (1- 22)	
RP lymph node density (%): median (range) Calculated as no. of (positive LN / Total no. of LN dissected) * 100	7 (2 to 35)	10 (2 to 94)	
Extra nodal extension: (%) Present Absent	7 / 24 (29%) 17 / 24 (71%)	10 / 22 (45%) 12 / 22 (55%)	0.3608
Nodal Stage (%) pN0 pN1 pN2 pN3	5 (21%) 5 (21%) 12 (50%) 2 (8%)	25 (32%) 13 (17%) 19 (24%) 21 (27%)	0.0515
TNM stage of orchiectomy (%) 0 I	0 5 (21%) 18 (75%)	7 (9%) 12 (15%) 31 (40%)	0.0017 0-II VS III-IV

II III A & B III-C / IV	0 1 (4%)	14 (18%) 14 (18%)	
Pathologic diagnosis on radical orchiectomy (%) No Tumor Seminoma Teratoma Mixed GCT Somatic malignancy	0 (0%) 9 (38%) 2 (8%) 12 (50%) 1 (4%)	13(16%) 5 (6%) 7 (9%) 52 (67%) 1 (1%)	0.005244
Pathologic diagnosis on RPLND (%) No Tumor Seminoma Teratoma Mixed GCT Somatic malignancy	4 (17%) 7 (29%) 1 (4%) 11 (46%) 1 (4%)	24 (31%) 3 (4%) 32 (41%) 12 (15%) 7 (9%)	< 0.00001
Concordance of orchiectomy and RPLND diagnoses (%) Concordant Discordant	5 / 20 (25%) 15 / 20 (75%)	8 / 54 (15%) 46 / 54 (85%)	0.3194

NED: No evidence of disease; AWD: Alive with disease; DOD: Dead of disease. Chi-square test performed for statistical analysis

Figure 1 - 576

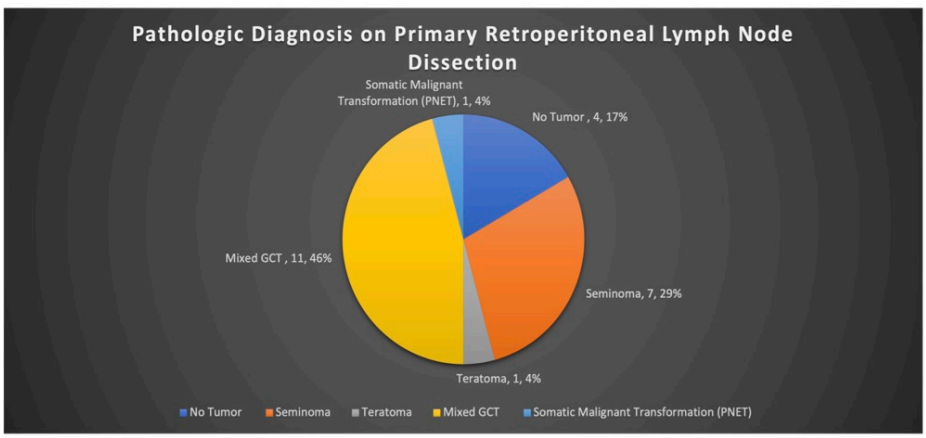

Figure 2 – 576

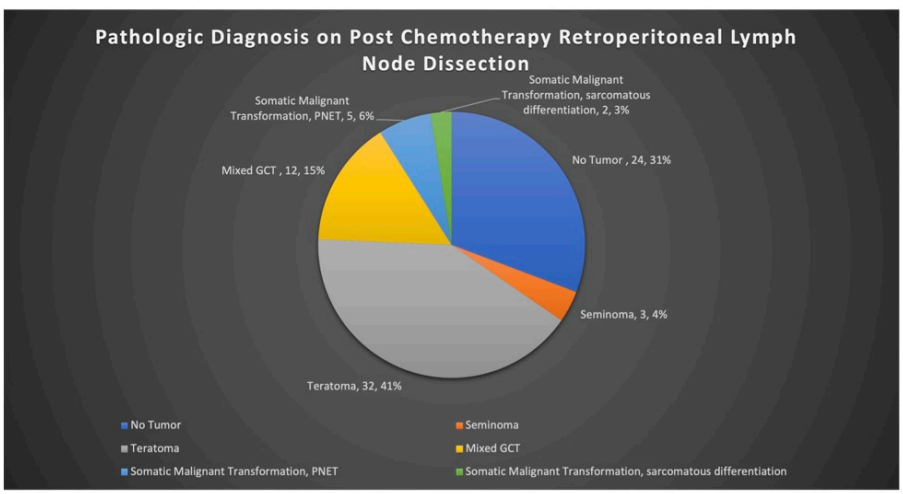

Conclusions: p-RPLND in our center is performed in a select group of patients with lower stage t-GCT. Teratoma, as previously reported, is the most common finding in pc-RPLND, and is rare in the setting of p-RPLND. Somatic malignancy is rare with PNET being the commonest . Discordance between t-GCT and RPLND specimens is high, underscoring the importance of RPLND in these cases . Despite the presence of MGCT in these specimens most patients do extremely well with salvage therapy, except those with widespread metastasis.

577 3D Light-Sheet Microscopy and Microdissection of Primary Prostate Cancer Reveals Important Latent Sub-clonal Mutations

Luisa Lerma[1], Colin Pritchard[1], Eric Konnick[1], Michael Haffner[2], Michael Schweizer[3], Hongyi Huang[4], Adam Glaser[1], Lawrence True[5], Jonathan Liu[1], Nicholas Reder[1]
[1]University of Washington, Seattle, WA, [2]Fred Hutchinson Cancer Research Center, Seattle, WA, [3]University of Washington School of Medicine, WA, [4]University of Washington - Pathology, Seattle, WA, [5]University of Washington Medical Center, Seattle, WA

Disclosures: Luisa Lerma: None; Colin Pritchard: None; Eric Konnick: *Speaker*, Roche; *Speaker*, Clinical Care Options; Michael Haffner: None; Michael Schweizer: *Grant or Research Support*, Lightspeed Microscopy, Inc; *Consultant*, AstraZeneca; *Consultant*, PharmaIn; *Consultant*, Resverlogix; *Grant or Research Support*, Zenith Epigenetics, Bristol Myers Squibb, Merck, Immunomedics, Janssen, AstraZeneca, Pfizer, Madison Vaccines, Hoffman-La Roche, Tmunity, Elevate Bio; Hongyi Huang: None; Adam Glaser: *Stock Ownership*, Lightspeed Bio; Lawrence True: *Stock Ownership*, LightSpeed Microscopy, Inc.; Jonathan Liu: *Stock Ownership*, Lightspeed Microscopy Inc.; Nicholas Reder: *Employee*, Lightspeed Microscopy, Inc.; *Employee*, Lightspeed Microscopy, Inc.

Background: Intratumoral molecular heterogeneity is a well described phenomenon in primary prostate cancer. Increased genomic heterogeneity is associated with more aggressive clinical behavior, including recurrence and metastasis. However, current methods to characterize heterogeneity suffer from tradeoffs between generating high quality morphologic information, correlating morphology with molecular alterations, and labor/workflow considerations. We describe the development of a suite of technologies to image prostate samples in 3D with high resolution while preserving nucleic acids for DNA sequencing, and then performing 3D microdissection of regions of interest (ROIs) for enhanced sequence performance.

Design: Fresh prostate samples (~2x2x0.4cm) were obtained from radical prostatectomy specimens (N=9) and bisected each sample to create 2 mirror image samples. One half was sent for traditional formalin fixation and paraffin embedding (FFPE). The other half was preserved in an ethanol-based fixative, imaged using 3D light-sheet fluorescence microscopy (LSFM), and image-guided microdissection was performed on ROIs with distinct morphologies. Microdissected ROIs measured 0.5x0.5x0.2cm. FFPE samples and 3D microdissected samples were sent for DNA extraction and sequencing using an NGS gene panel platform.

Results: 3D microdissected samples had 2.3 x read depth compared to FFPE samples. The most compelling sample in our cohort contained three morphologically distinct ROIs. ROI1 was 3D microdissected to include only large cribriform architecture (Grade Group 4). Biallelic loss of APC (VAF=0.3) and three other molecular alterations occurred exclusively in ROI1. Three independent focal copy losses, including POLE, were found exclusively in ROI2, a region of GG3. ROI3 (GG1) contained neither an APC nor a POLE mutation. All 3 mutations present in the FFPE sample with VAF>0.3 were also present in at least 2 ROIs.

Conclusions: This study demonstrates the potential for 3D microdissection to detect morphologically distinct subclones. For example, we identified a POLE subclonal mutation in a GG3 area and an APC subclonal mutation in a GG4 area, both of which were not detectable on the FFPE sample. While the implications of this study are limited due to small sample size, we are currently expanding our patient cohort to assess the rate of latent sub-clonal mutations detected by 3D LSFM imaging with microdissection.

578 Clinical Significance and Potential Signal Pathway of Up-Regulated Pituitary Tumor-Transforming Gene 1 (PTTG1) in Metastatic Prostate Cancer Based on Bioinformatic Methods

Jing-Xiao Li[1], Gang Chen[1], Juan He[1], Rong-Quan He[1], Deng Tang[1], Yi-Wu Dang[1], Zhi-Guang Huang[1]
[1]*The First Affiliated Hospital of Guangxi Medical University, Nanning, China*

Disclosures: Jing-Xiao Li: None; Gang Chen: None; Juan He: None; Rong-Quan He: None; Deng Tang: None; Yi-Wu Dang: None; Zhi-Guang Huang: None

Background: Prostate cancer (PCa) ranks the second most common mortality among cancers in males. Many patients lacked subjective symptoms and delayed diagnosis and treatment, which leads to occurrence of metastatic PCa (MPCa). The present study aims to explore the expression and clinical significance of pituitary tumor-transforming gene 1 (PTTG1) in PCa and MPCa.

Design: A total of 19 PCa and 10 MPCa public datasets were collected and performed to analyze the expression level and discrimination of PTTG1. Differential co-expressed genes (DCEGs) were screened from MPCa series and applied for enrichment analysis. The hubgenes were also screened, and then we explored the correlations between hubgenes and PTTG1.

Results: The analysis results indicated PTTG1 was significantly upregulated in PCa (SMD=0.55, 95%CI:0.29, 0.83) and MPCa (SMD=2.28, 95%CI: 1.38, 3.19). Additionally, PTTG1 showed a moderate potential to discriminate PCa from normal cells (AUC=0.75, 95%CI: 0.71, 0.79), and it also showed a high potential to discriminate MPCa from LPCa cells (AUC=0.97, 95%CI: 0.95, 0.98) (Table 1 and Figure 1). A total of 314 genes were identified as PTTG1 DCEGs in MPCa. Among the screened DCEGs, CCNA2, CCNB1 and CDK1 were identified as hubgenes of PTTG1, which were proved having positive correlations with PTTG1 (Figure 2A). Most of clinical parameters did not show correlation with expression of PTTG1, but we found PTTG1 expression was associated with M-stage and recurrence based on data from The Cancer Genome Atlas (TCGA) database, this also suggested that the differential expression of PTTG1 was related to the metastasis of PCa. Gene Ontology (GO) analysis indicated that PTTG1 DCEGs significantly enriched in cell division, nucleoplasm and protein binding. Moreover, Kyoto Encyclopedia of Genes and Genomes (KEGG) analysis showed DCEGs of PTTG1 mainly enriched in Cell cycle (Figure 2B).

Table 1. The means and standard deviations of PTTG1 expression values in localized prostate cancer (LPCa) and metastatic prostate cancer (MPCa) based on 10 studies. PTTG1, Pituitary tumor-transforming gene 1; N, numbers; M, means; SD, standard deviations.

Study	Country	Year	Sample	MPCa			LPCa		
			type	N	M	SD	N	M	SD
GSE3325	USA	2005	tissue	4	11.805	1.797	5	8.945	0.177
GSE32269	USA	2011	tissue	29	6.613	1.247	22	4.879	1.257
GSE77930	USA	2016	tissue	149	3.446	0.848	22	0.791	1.079
GSE6919	USA	2007	tissue	25	8.010	0.557	66	6.511	0.548
GSE116918	UK	2018	tissue	22	0.172	0.306	225	0.148	0.121
GSE68882	USA	2015	tissue	9	7.848	0.263	23	7.579	0.265
GSE55935	Norway	2014	tissue	8	9.371	1.339	38	6.281	0.902
GSE27616	USA	2011	tissue	4	13.937	1.367	5	-3.681	0.543
GSE35988	USA	2012	tissue	32	14.108	1.411	59	13.309	1.353
TCGA	NA	NA	tissue	21	2.506	0.890	478	1.733	0.722

Figure 1 - 578

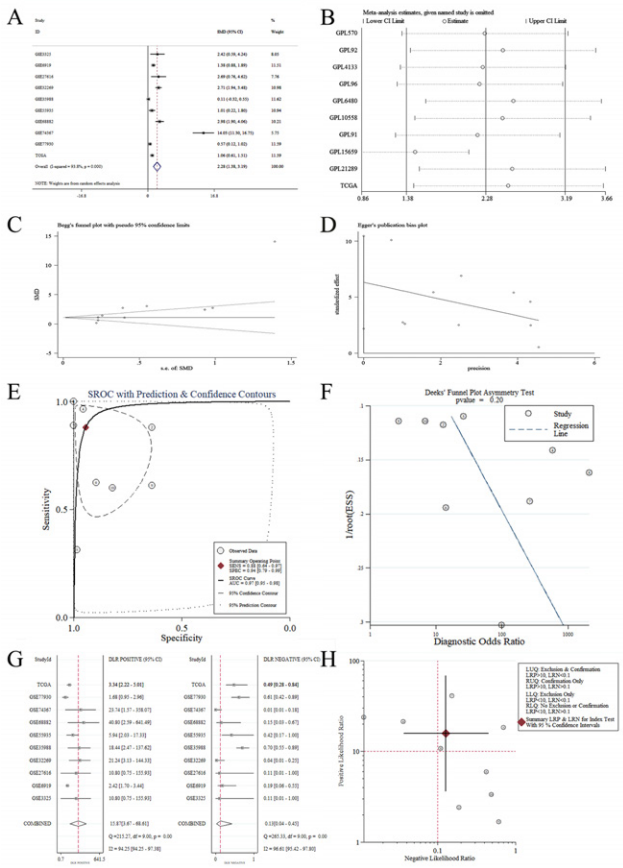

Figure 2 - 578

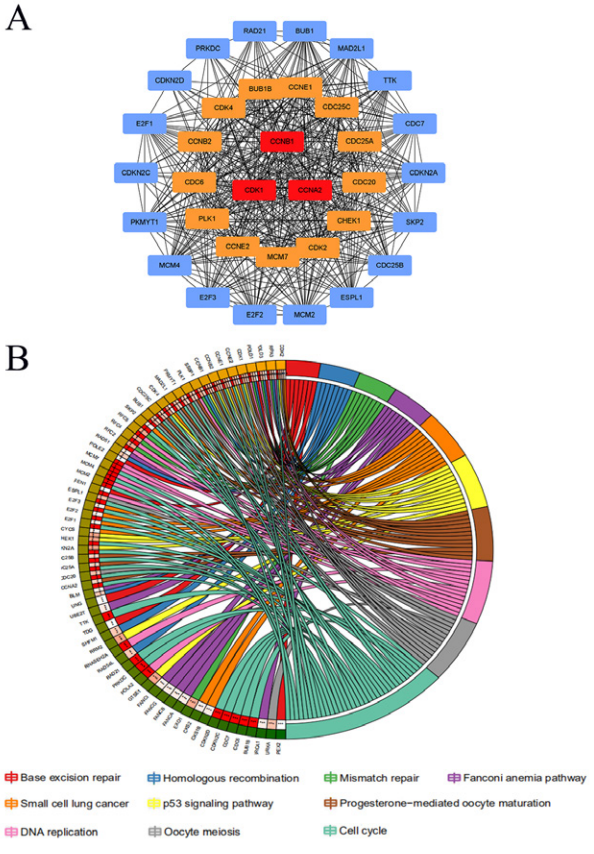

Conclusions: PTTG1 was upregulated in PCa and MPCa, and probably could be applied to discriminate MPCa from LPCa cells.

579 Using Prostate Epithelial to Stroma Ratio to Assess the Residual Cancer Burden/Extent of Treatment Response and Its Correlation with Clinical Outcome

Hui-Hua Li[1], Steve Cho[1], Shane Wells[1], Christos Kyriakopoulos[1], David Jarrard[2], Alejandro Roldán-Alzate[2], Joshua Lang[1], Wei Huang[2]

[1]University of Wisconsin School of Medicine and Public Health, Madison, WI, [2]University of Wisconsin, Madison, WI

Disclosures: Hui-Hua Li: None; Steve Cho: None; Shane Wells: None; Christos Kyriakopoulos: *Advisory Board Member*, Exelixis, AVEO, Sanofi-Aventis, EMD Serono, Janssen; *Primary Investigator*, Sanofi-Aventis, Gilead, Incyte; David Jarrard: None; Alejandro Roldán-Alzate: None; Joshua Lang: None; Wei Huang: None

Background: Neoadjuvant chemotherapy (NC) is commonly used for locally advanced PCa. However, currently there is no reliable and practical method to assess the extent of treatment response (ETR) for PCa histologically largely due to the lack of knowledge of baseline PCa burden (BCB). As an epithelial tumor, the treatment response of PCa to NC is primarily reflected in epithelial change (shrinking or vanishing) whereas the prostate stroma remains relatively stable. In this study, we proposed that the epithelial to stroma ratio (E/S) can be used as a surrogate to assess BCB, residual cancer burden (RCB) and the ETR.

Design: A clinical cohort of patient (n=16) with PCa underwent NC followed by radical prostatectomy (RP) were included in this study. The H&E slides from patients' biopsy (Bx) at PCa diagnosis and RP post NC were scanned with Aperio AT2 (Leica, IL) at 40x to create whole slide imaging (WSI). 5-10 representative PCa images (0.8 mm^2 each, an Aperio 10x field) from each patient's Bx and RP were selected. Epithelial and stromal segmentation and measurement were performed using inForm 1.4.0 software. E/S ratios (BCB and RCB) were then calculated. The pretreatment E/S ratio (BCB) from the Bx was adjusted (aBCB) using the slope of the regression line (0.82) derived from paired Bx and RP samples without any treatment to reflect the sampling difference from RP

samples. For each patient, RCB was also adjusted (aRCB) with the formula aRCB = RCB ÷ aBCB. The ETR was calculated with the formula ETR (%) = 100 x (1 - aRCB). Correlation between patients' aRCB and clinical outcomes was analyzed.

Results: We found that the patients with recurrent disease had significant greater aRCB (2 folds, $p<0.05$) compared to the patients without recurrent disease. Similarly, the patients with metastatic disease on PET scan had significantly greater aRCB (2.6 folds, $p<0.05$) compared to the patients without evidence of metastasis on PET scan.

Conclusions: E/S ratio can be used as a reliable surrogate for the accurate assessment of RCB and ETR for clinical trials and clinical management of patients.

580 Expression Profile and Clinical Significance of Immune Checkpoint Proteins B7-H4 and HHLA2 in Prostatic Adenocarcinoma

Xiaoyan Liao[1], Hiroshi Miyamoto[1], Dongwei Zhang[1]
[1]*University of Rochester Medical Center, Rochester, NY*

Disclosures: Xiaoyan Liao: None; Hiroshi Miyamoto: None; Dongwei Zhang: None

Background: Although immune checkpoint inhibitors such as anti-PD-1/PD-L1 have proven efficacy in many human cancers, patients with advanced prostate cancer often have a poor response to PD-1/PD-L1 blockade. B7-H4 and HHLA2 are two newly discovered members of the B7 immune checkpoint family and considered potential new therapeutic targets. We aimed to investigate the expression profile of B7-H4 and HHLA2 in prostate cancer and its clinical impact.

Design: Immunohistochemical stains for B7-H4, HHLA2, and CD8 were performed on a set of tissue microarray consisting of 141 radical prostatectomy (RP) specimens. Positive B7-H4 or HHLA2 expression was defined as cytoplasmic staining in >10% tumor cells. The cell density of $CD8^+$ intratumoral lymphocytes was determined quantitatively. Biochemical recurrence (BCR) was defined as a single prostate specific antigen (PSA) level of ≥0.2 ng/ml post RP.

Results: Positive HHLA2 was detected in 109 (77.3%) cases, among which 60 (42.6%) showed low expression and 49 (34.8%) showed high expression. Compared to the high frequency of HHLA2 expression, positive B7-H4 was only detected in 14 (10.0%) cases, among which 2 (14%) showed high expression, and 11 (79%) also had positive HHLA2 expression. B7-H4 positive tumors had slightly higher $CD8^+$ density (86 vs. 78 per mm^2) although the difference did not reach statistical significance. The expression of HHLA2 and B7-H4 did not correlate significantly with patient's age at RP, preoperative PSA level, tumor grade, or pT/pN stage category (Table 1). Kaplan–Meier analysis revealed that patients with B7-H4-positive tumor had a significantly lower risk of BCR than those with B7-H4-negative tumor (P=0.03). There was no significant association between HHLA2 expression and BCR.

Table 1. Association between clinicopathological features with B7H4 expression in prostatic adenocarcinoma

Clinicopathologic features		Total No. (%)	B7H4 expression		P **value**
			Positive	Negative	
Total case		141	14 (10%)	127 (90%)	
Age (years)	<60	68 (%)	5 (4%)	63 (45%)	NS
	≥60	73 (%)	9 (6%)	64 (45%)	
Grade group (GG)	GG1	46 (33%)	5 (4%)	41 (29%)	NS
	GG2	64 (45%)	8(19%)	56 (40%)	
	GG3	13 (9%)	1 (7%)	12 (9%)	
	GG4	12 (8%)	0	12(9%)	
	GG5	6 (4%)	0	6 (4%)	
T stage	T2	106 (75%)	11 (8%)	95 (67%)	NS
	T2+	2 (1%)	0	2 (1%)	
	T3a	24 (17%)	2 (1%)	22 (16%)	
	T3b	9 (6%)	1 (0.7%)	8 (6%)	
Biochemical recurrence (BCR)	PSA<0.2	122 (87%)	14 (10%)	108 (77%)	NS
	PSA≥0.2	19 (13%)	0	19 (13%)	
Outcome	Died of disease	8 (6%)	1 (0.7%)	7 (5%)	NS
	Alive or died of other causes	133 (94%)	13 (9.2%)	120 (85%)	

Conclusions: HHLA2 was commonly expressed in prostatic adenocarcinoma, whereas B7-H4 was less frequently expressed. Nonetheless, B7-H4 expression correlated with lower risk of BCR along with higher density of $CD8^+$ T cells, suggesting that activating B7-H4 may serve as a potential new strategy of immunotherapy in patients with prostatic adenocarcinoma.

581 The Impact of Routine Frozen Section Analysis during Nephroureterectomy or Segmental Ureterectomy for Urothelial Carcinoma on Final Surgical Margin Status and Long-Term Oncologic Outcome

Wilrama Lima[1], Ying Wang[1], Hiroshi Miyamoto[1]
[1]*University of Rochester Medical Center, Rochester, NY*

Disclosures: Wilrama Lima: None; Ying Wang: None; Hiroshi Miyamoto: None

Background: Intraoperative frozen section analysis (FSA) generally provides critical information which enables immediate decision making for optimal patient care. However, the utility of FSA at the surgical margins (SMs) in patients with upper urinary tract cancer has not been established. We herein assess the clinical significance of routine FSA of the SMs during nephroureterectomy (NU) or segmental ureterectomy (SU).

Design: A retrospective review of our Surgical Pathology database identified consecutive patients undergoing NU (n=268) or SU (n=47) for urothelial carcinoma (UC) from 2004-2019. FSA was correlated with the diagnosis of frozen section control (FSC), the status of final SM, and patient outcome.

Results: During NU FSA of the SM was performed in 20 (8%) patients and was significantly more often requested in cases with ureteral tumor [15/110 (14%); *P*=0.002], particularly that at the lower ureter [5/28 (18%); *P*=0.008], than in those with renal pelvis/calyx tumor [5/158 (3%)]. Final positive SMs at distal ureter/bladder cuff were slightly (*P*=0.242) more often seen in non-FSA cases (8%) than in FSA cases (0%). During SU FSA was performed in 40 (85%) cases, including 22 (47%) at either proximal or distal SM (SU-FSA1) and 18 (38%) at both SMs (SU-FSA2). Final positive SMs were significantly more often seen in non-FSA patients (43%) than in all FSA cases (8%; *P*=0.035) or SU-FSA2 cases (0%; *P*=0.015). In the entire cohort, FSAs were reported as positive or high-grade carcinoma (n=7), atypical or dysplasia (n=13), and negative (n=40), and all these diagnoses were confirmed accurate on the FSCs, except 2 cases with revisions from negative or atypical to atypical or carcinoma, respectively. Meanwhile, 15 (75%) of 20 cases with initial positive/atypical FSA achieved negative conversion by excision of additional tissue. Kaplan-Meier analysis revealed that FSA did not considerably reduce the risk of tumor recurrence in the bladder (*P*=0.122/NU, *P*=0.678/SU), disease progression (*P*=0.555/SU), or cancer-specific mortality (*P*=0.701/SU). Nonetheless, NU FSA was strongly associated with reduced progression-free (*P*=0.002) and cancer-specific (*P*=0.018) survival rates, compared with non-FSA, implying a selection bias (*e.g.* FSA for clinically more aggressive tumors).

	NU-FSA(-) (n=248)	NU-FSA(+) (n=20)	P	SU-FSA(-) (n=7)	SU-FSA1 (n=22)	SU-FSA2 (n=18)	P[a]
Age (mean, yr)	70.6	67.4	0.293	74.4	74.0	72.0	0.800
Sex			0.813				0.396
Male	149 (60%)	13 (65%)		3 (43%)	16 (73%)	11 (61%)	
Female	99 (40%)	7 (35%)		4 (57%)	6 (27%)	7 (39%)	
Laterality			0.819				0.701
Right	116 (47%)	10 (50%)		4 (57%)	9 (41%)	10 (56%)	
Left	132 (53%)	10 (50%)		3 (43%)	13 (59%)	8 (44%)	
UC histology			0.709				1.000
Conventional	221 (89%)	17 (85%)		7 (100%)	22 (100%)	16 (89%)	
Variant	27 (11%)	3 (15%)		0 (0%)	0 (0%)	2 (11%)	
Tumor grade			0.587				0.655
Low	52 (21%)	3 (15%)		1 (14%)	5 (23%)	7 (39%)	
High	196 (79%)	17 (85%)		6 (86%)	17 (77%)	11 (61%)	
pT			0.246				0.731
a / is	90 (36%)	4 (20%)		5 (71%)	10 (45%)	12 (67%)	
1	38 (15%)	5 (25%)		1 (14%)	3 (14%)	2 (11%)	
2-4	120 (48%)	11 (55%)		1 (14%)	9 (41%)	4 (22%)	
pN			0.156[b]				1.000[b]
0	120 (48%)	9 (45%)		2 (29%)	10 (45%)	9 (50%)	
1-2	27 (11%)	5 (25%)		0 (0%)	2 (9%)	0 (0%)	
X	101 (41%)	6 (30%)		5 (71%)	10 (45%)	9 (50%)	
SM (at ureter)			0.242				0.035
Negative	227 (92%)	20 (100%)		4 (57%)	19 (86%)	18 (100%)	

Positive	21 (8%)	0 (0%)		3 (43%)	3 (14%)	0 (0%)	
SM (elsewhere)			1.000				1.000
Negative	239 (96%)	19 (95%)		7 (100%)	22 (100%)	40 (100%)	
Positive	9 (4%)	1 (5%)		0 (0%)	0 (0%)	0 (0%)	
[a] SU-FSA(-) vs. SU-FSA(+); [b] pN0 vs. pN1-2							

Conclusions: Performing FSA during SU significantly reduced the risk of positive SMs yet did not considerably improve oncologic outcomes. In NU cases, final positive SM was relatively uncommon, and no significant clinical benefit of FSA was observed.

582 Histopathological and Genomic Features of PD-L1-Positive Prostate Carcinoma

Douglas Lin[1], Huihui Ye[2], Vamsi Parimi[3], Mirna Lechpammer[1], Douglas Mata[1], Brennan Decker[1], Matthew Hiemenz[1], Julia Elvin[1], Jeffrey Ross[4], Richard Huang[5]
[1]Foundation Medicine, Inc., Cambridge, MA, [2]University of California, Los Angeles, Los Angeles, CA, [3]Foundation Medicine, Inc., RTP, NC, [4]SUNY Upstate Medical University, Syracuse, NY, [5]Foundation Medicine, Inc., Cary, NC

Disclosures: Douglas Lin: *Employee*, Foundation Medicine, Inc.; *Stock Ownership*, Roche; Huihui Ye: None; Vamsi Parimi: *Employee*, Foundation Medicine Inc.; Mirna Lechpammer: *Employee*, Foundation Medicine, Inc; Douglas Mata: *Employee*, Foundation Medicine, Inc.; *Speaker*, Astellas Pharma, Inc.; Brennan Decker: *Employee*, Foundation Medicine; *Stock Ownership*, Roche; Matthew Hiemenz: *Employee*, Foundation Medicine / Roche; Julia Elvin: *Employee*, Foundation Medicine; *Stock Ownership*, Hoffmann-La Roche; Jeffrey Ross: *Employee*, Foundation Medicine; Richard Huang: *Employee*, Foundation Medicine; *Employee*, Roche

Background: Immunotherapy may have a role in the treatment of a subset of prostate carcinomas (PC). However, in the KEYNOTE-199 study, which investigated the efficacy and safety of pembrolizumab in metastatic castration-resistant PC, the objective response rates were 5% and 3% for PD-L1^{positive} and PD-L1^{negative} PC, respectively, as assessed by a combined positive score (CPS) ≥1. Therefore, higher thresholds or specific parameters are needed to unravel the predictive potential of PD-L1 positivity in PC. The aim of this study was to determine the histopathological and genomic characteristics of PD-L1^{positive} PC.

Design: 2,162 acinar-type, 100 neuroendocrine, 23 ductal-type, 3 carcinosarcomas and 3 squamous cell carcinomas of prostatic origin, tested with both comprehensive genomic profiling and PD-L1 immunohistochemistry (Dako 22C3, tumor proportion score, TPS), were analyzed with regards to PD-L1 tumor cell positivity (defined as TPS of ≥1%), microsatellite instability (MSI), tumor mutational burden (TMB) and genomic alterations. 100 consecutive acinar PCs, originally scored with TPS, were re-scored using CPS.

Results: Tumor cell-specific PD-L1 positivity was significantly enriched in prostate neuroendocrine and squamous cell carcinomas compared with acinar-type or ductal-type carcinomas (24%, 67%, 10.2% and 0%, respectively). PD-L1^{positive} PC had significantly higher frequencies of MSI-High, TMB-High and genomic alterations involving *RB1*, *MSH2*, *CD274* (encodes for PD-L1), *CDKN2A* and *CDK12* compared with PD-L1^{negative}. In contrast, PD-L1^{positive} PC had lower frequencies of *TMPRSS2* fusions and no differences in *TP53*, *AR*, *PTEN, MYC, PIK3CA, CTNNB1,* or *BRCA1/2* alterations compared with PD-L1^{negative}. PD-L1 expression in PC occurred more frequently in metastatic sites compared with primary site (13.1% vs. 8.7%, p=0.0009). Rescoring 100 consecutive prostate acinar carcinomas revealed that 59% of acinar-type carcinomas had immune cell staining (CPS of at least 1) even in the absence of tumor cell staining (TPS=0).

Conclusions: Tumor cell specific PD-L1 positivity in PC co-occurs more frequently with biomarkers associated with immunogenicity and is enriched in metastases with parameters associated with prior treatment such as neuroendocrine or squamous cell differentiation and *RB1* mutations. TPS is a significantly more stringent PD-L1 scoring method in PC compared with CPS. Further studies predicting immunotherapy response in PD-L1^{positive} PC with these features are warranted.

583 High Molecular Weight Cytokeratin-Expressing Prostate Cancer: Clinicopathologic Features and a Potential Mechanism of Hormonal Therapy Resistance

Emily Lo[1], Brian Ma[2], Cleandrea Williams[3], Jiajie Lu[4], Guang-Qian Xiao[5]

[1]University of Southern California, LAC+USC Medical Center, Los Angeles, CA, [2]LAC+USC Medical Center, [3]University of Southern California, Keck School of Medicine of USC, LAC+USC Medical Center, Los Angeles, CA, [4]LAC+USC Medical Center/Keck Medicine of USC, CA, [5]Keck School of Medicine of USC, Los Angeles, CA

Disclosures: Emily Lo: None; Brian Ma: None; Cleandrea Williams: None; Jiajie Lu: None; Guang-Qian Xiao: None

Background: High molecular weight cytokeratin (HMWCK) is used as a marker in the diagnosis of prostatic carcinoma (PC), often as part of the triple antibody PIN cocktail to confirm the absence of basal cells. With the exception of frank squamous carcinoma, expression of HMWCK in classic PC has not been studied so far. This study aimed to investigate the clinicopathologic features of the HMWCK- expressing PC.

Design: A total of 401 cases with PIN cocktail immunostain (HMWCK (34BE12), p63 and AMACR) between 2016-2021 were reviewed, including 115 biopsies, 63 prostatectomies and 222 cases from 5 TMAs mounted with PC from prostatectomies. Of the 401 cases, 39 were post-radiotherapy and 56 post-androgen deprivation therapy (ADT) PCs. The remaining 306 were treatment-naïve PCs. Some of these cases were also stained with AR and NKX3.1. PC was diagnosed based on the morphology and supported by the absence of p63-stained basal cells. The percentage of HMWCK$^+$ PC cells in its home tumor nodule was assessed. The intensity of AR, NKX3.1, p504s IHC was evaluated in the HMWCK$^+$ PC. The Gleason scores and specific morphologic patterns associated with HMWCK$^+$ PC were recorded. Clinicopathologic features, including treatment status and pathologic staging were gathered.

Results: Among the 401 PC cases, 26 (6.5%) was identified with HMWCK$^+$ PC cells, 20 from prostatectomies and 6 from biopsies. The amount of HMWCK$^+$ PC was ≤50% in majority (89%) of the cases (Fig.1). 22/26 (85%) were treatment-naïve, 4/26 (15%) post-treatment. Among the 22 treatment-naïve HMWCK$^+$ PCs with gradable pattern, 21/22 (96%) exhibited Gleason pattern (GP) 4/5, and were especially associated with cribriform pattern and comedonecrosis. The expression of AR, NKX3.1 and AMACR was all diminished or lost in the HMWCK$^+$ PC cells. Vast majority (95%) presented with high tumor stage (≥pT3). See Table 1.

% of HMWCK$^+$ PC cells in index tumor	Age	Morphologic patterns					Treatment			Diminished to loss of other biomarkers' expression			Home/index tumor grade group (G)	pTN (for prostatectomies)
		Gleason pattern 3	Gleason pattern 4/5			IDC	None	ADT	RT	AR	NKX3.1	AMACR		
			Crib	Non-Crib	Comedo-necrosis									
1%-10% (n=10)	69±8	1/10 (10%)	7/10 (70%)	7/10 (70%)	4/10 (40%)	4/10 (40%)	10/10 (100%)	0/0 (0%)	0/0 (0%)	2/2 (100%)	3/3 (100%)	9/9 (100%)	1 IDC only (10%) 1 G3 (10%) 4 G4 (40%) 4 G5 (40%)	5 pT3N0 (5/8=63%) 3 pT3N1 (3/8=37%)
11-50% (n=13)	69±11	0/13 (0%)	11/13 (85%)	8/13 (62%)	10/13 (77%)	6/13 (46%)	10/13 (77%)	2/13 (15%)	1/13 (8%)	7/7 (100%)	6/6 (100%)	13/13 (100%)	4 G4 (31%) 9 G5 (69%)	1 pT2N0 (1/10=10%) 2 pT3N0 (2/10=20%) 6 pT3N1 (6/10=60%) 1 pT4N1 (1/10=10%)
>50% (n=3)	67±6	0/3 (0%)	1/3 (33%)	0/3 (0%)	1/3 (33%)	1/3 (33%)	2/3 (67%)	0/3 (0%)	1/3 (33%)	2/2 (100%)	1/1 (100%)	2/2 (100%)	2 G4 (67%)	1 pT3N0 (1/1=100%)
Total (n=26)		1 (4%)	19 (73%)	15 (58%)	15 (58%)	11 (42%)	22/26 (85%)	2/26 (8%)	2/26 (8%)	11/11 (100%)	10/10 (100%)	24/24 (100%)		

*HMWCK: High molecular weight cytokeratin; ADT: androgen deprivation therapy; RT: radiotherapy; PC: prostatic carcinoma; IDC: intraductal carcinoma; Crib: cribriform; AR: Androgen receptor.

Figure 1 - 583

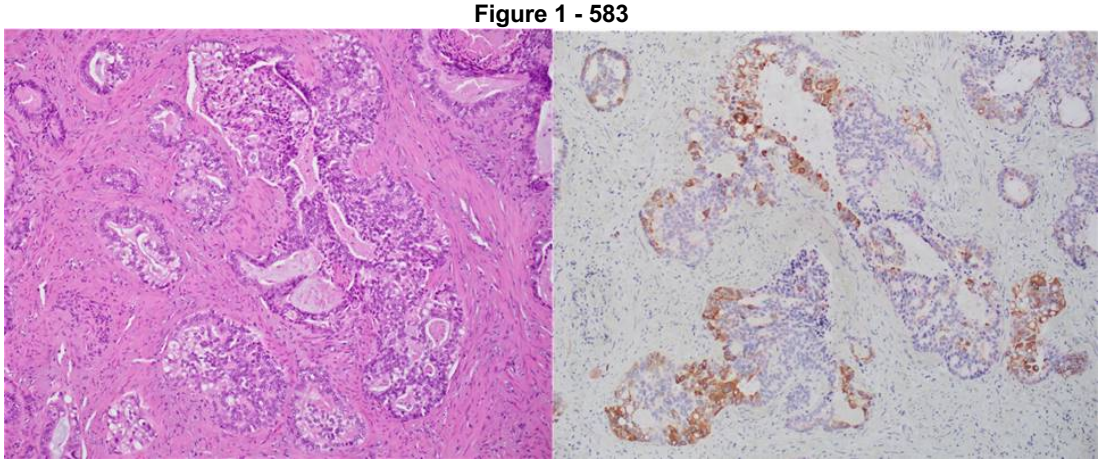

Conclusions: The study demonstrated that 1) HMWCK$^+$ PC was uncommon and often focally present in its home tumor; 2) Vast majority were associated with high Gleason scores/unfavorable patterns and tumor stage; 3) There was no significant association with prior treatment or age; 4) All displayed diminished or loss of AR and NKX3.1, which indicated a less dependence on androgen for growth. The results support the expression of HMWCK as a useful surrogate biomarker for PC aggressiveness as well as androgen independence. Identification of such PC subgroup has significant implications in decision-making in the combat against this common and often deadly disease.

584 Evaluation of programmed death-ligand1(PD-L1) expression in a contemporary cohort of penile squamous cell carcinomas (PC) and its correlation with clinicopathologic and survival parameters: A study of 134 patients

Anandi Lobo[1], Ankit Tiwari[2], Sourav Mishra[3], Shilpy Jha[3], Shivani Sharma[4], Niharika Pattnaik[3], Nakul Sampat[3], Ekta Jain[4], Romila Tiwari[3], Manas Baisakh[5], Mallika Dixit[6], Sudhasmita Rauta[7], Deepika Jain[6], Gauri Munjal[6], Dinesh Pradhan[8], Anil Parwani[9], Sambit Mohanty[3]

[1]Kapoor Centre of Urology and Pathology, Raipur, India, [2]NISER, [3]Advanced Medical and Research Institute, Bhubaneswar, India, [4]Core Diagnostics, Gurgaon, India, [5]Apollo Hospitals, Bhubaneswar, India, [6]Core Diagnostics, Gurugram, India, [7]Prolife Diagnostics, Bhubaneswar, BHUBANESWAR, India, [8]The University of Texas MD Anderson Cancer Center, TX, [9]The Ohio State University, Columbus, OH

Disclosures: Anandi Lobo: None; Ankit Tiwari: None; Sourav Mishra: None; Shilpy Jha: None; Shivani Sharma: None; Niharika Pattnaik: None; Nakul Sampat: None; Ekta Jain: None; Romila Tiwari: None; Manas Baisakh: None; Mallika Dixit: None; Sudhasmita Rauta: None; Deepika Jain: None; Gauri Munjal: None; Dinesh Pradhan: None; Anil Parwani: None; Sambit Mohanty: None

Background: PCs are rare malignancies and the prognosis with metastatic disease remains dismal, therefore novel immunotherapeutic modalities are an unmet need for this neoplasm. This emphasizes the evaluation of immune checkpoint molecules such as PD-L1 in PC. Herein, we sought to analyze the PD-L1 expression and its correlation with various clinicopathologic parameters in a contemporary cohort of 134 PC patients.

Design: A cohort of 134 PC patients was studied for PD-L1 immunohistochemistry (IHC) using the rabbit monoclonal antibody E1L3N (Cell signalling) on an autostainer. The PD-L1 expression was evaluated using combined proportion score (CPS) with a cut-off of ≥1% to define positivity. CPS includes the number of positive tumor cells, lymphocytes and macrophages divided by the total number of viable tumor cells multiplied by 100. The results were correlated with various clinicopathologic parameters. For statistical comparison, Pearson's chi-square test and log-rank analysis was performed.

Results: Overall,77(57%) had positive PD-L1 expression (low positive [0-19%]=62%; high positive [≥20%]=38%). Significantly high PD-L1 expression was observed in high grade tumors (p=0.006). PD-L1 positive tumors had a 3.61 times higher chances of being node positive compared to PD-L1 negative tumors (p=0.0009). PD-L1 high positive tumors had a 5 times higher chances of being p16 negative than PD-L1 low positive tumors (p=0.004). PD-L1 expression did not correlate with patient's age, histologic

subtype, p53 IHC and adjuvant therapy (Fig 1). PD-L1 positive tumors had a lower overall (OS) and cancer specific (CSS) survival as compared to PD-L1 negative tumors (Fig 2).

Figure 1 - 584

Figure 1A

Characteristics	PD-L1 Positive	PD-L1 Negative	p	OR
Median Age at Time of Surgery (range in years)	64 (41-80)	65 (49-80)		
Tumor grade				
I and II	42	43	0.013	5.02
III	35	14		
Histopathologic type				
Others	55	20	0.42	1.64
Warty and/or basaloid	37	22		
Lymph node involvement				
Positive	36	11	0.0009	3.67
Negative	41	46		
Adjuvant therapy				
Yes	32	20	0.45	1.32
No	45	37		
p53 IHC				
Positive	43	30	0.71	1.14
Negative	34	27		
p16 IHC				
p16 positive	32	32		
p16 negative	45	25	0.095	0.58

Figure 1B

Characteristics	PD-L1 Low Positive (0-19%)	PD-L1 High positive (Greater or equal to 20)	p	OR
Median Age at Time of Surgery (range in years)	64 (41-80)	63 (49-74)		
Tumor Grade/Differentiation				
I and II	32	10	0.006	1.72
III	16	19		
Histopathologic Type				
Others	24	5	0.087	2.63
Warty and/or basaloid	31	17		
Lymph node involvement				
Positive	20	16	0.25	1.72
Negative	28	13		
Adjuvant Therapy				
Yes	19	13	0.65	1.24
No	29	16		
P53 IHC				
Positive	24	19	0.18	1.9
Negative	24	10		
p16 IHC				
p16 positive	26	6	0.004	0.22
p16 negative	22	23		

Figure 2 – 584

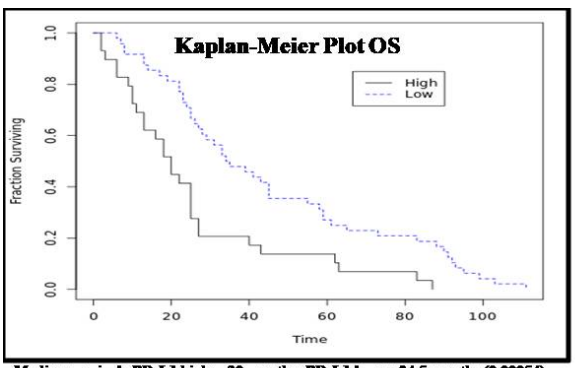

Median survival: PD-L1 high = 20 months; PD-L1 low = 34.5 months (0.00054)

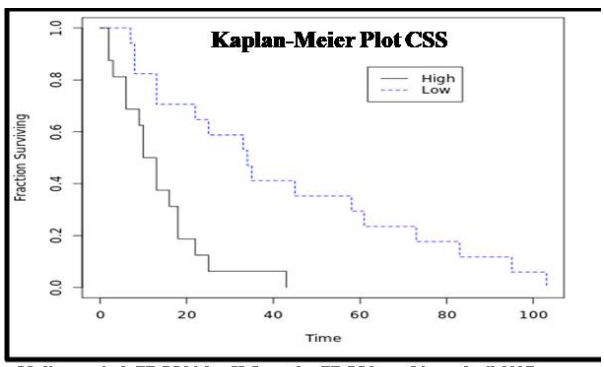

Median survival: PD-L1 high = 11.5 months; PD-L1 low = 34 months (0.0005)

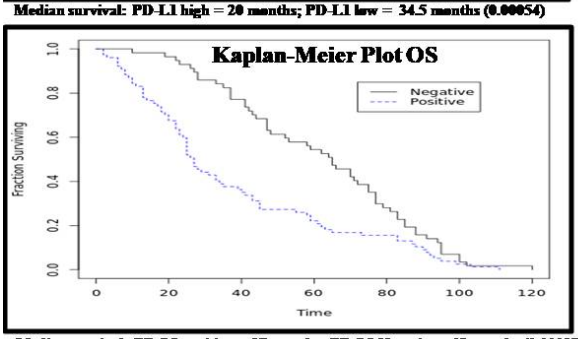

Median survival: PD-L1 positive = 27 months; PD-L1 Negative= 65 months (0.00037)

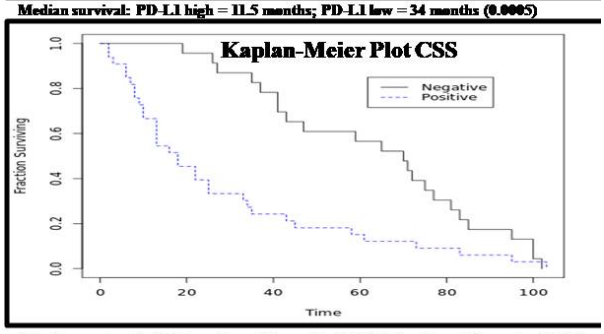

Median survival: PD-L1 positive = 18 months; PD-L1 Negative = 70 months (0.001)

Conclusions: 1. This is the largest study so far to assess the expression of PD-L1 in a clinically well annotated cohort of PC. 2. PD-L1 expression is associated with high grade and metastatic (nodal metastasis) tumors. 3. PD-L1 positivity including higher expression portends lower OS and CSS. 4. This data provide a rational for further investigating PD-L1-based immunotherapeutics in patients with PC.

585 Testicular germ cell tumor with neuroglial differentiation and its association with primitive neuroectodermal tumor

Brian Ma[1], Kyle Hurth[2], Emily Lo[3], Manju Aron[2], Andy Sherrod[2], Guang-Qian Xiao[2]
[1]LAC+USC Medical Center, [2]Keck School of Medicine of USC, Los Angeles, CA, [3]University of Southern California, LAC+USC Medical Center, Los Angeles, CA

Disclosures: Brian Ma: None; Kyle Hurth: None; Emily Lo: None; Manju Aron: None; Andy Sherrod: None; Guang-Qian Xiao: None

Background: Germ cell tumor (GCT) with neuroglial overgrowth/differentiation is rare and only occasional case reports/series have been published and the clinicopathology of this type of tumor is still evolving. In addition, only one case report has shown neuroglial (NG) and primitive neuroectodermal tumor (PNET) coexisting in the same tumor and the association between NG and PNET is yet unknown. In this study, we presented and investigated the clinicopathology of 14 metastatic GCTs with NG and or PNET along with the corresponding primary GCTs.

Design: The testicular GCT cases accessioned between 2016 and 2021 were reviewed. 14 cases were identified to have either NG or PNET or both in the metastasis and/or testis sites. The NG and PNET overgrowth was diagnosed based on both morphology and IHC (GFAP, synaptophysin, CD99, CD57, CD56, PLZF, and other GCT markers) and was defined by ≥5mm (1 low power field). Clinicopathological data were gathered.

Results: Patient age ranged from 22 to 65 (33.8 ± 13.7). 5 of the 14 primaries and all the 14 metastases contained either or both NG/PNET. When present, the % NG ranged 10-100% and PNET 5-100%. All the 5 primaries with PNET/NG were associated with teratoma, and 11 of the 14 (79%) metastases with NG/PNET were associated with teratoma. The 3 of 14 metastases not associated with teratoma were likely metastasis from NG/PNET of the primary GCT. 2/14 (14%) metastases had no prior chemotherapy, and the rest (86%) occurred after treatment. Coexisting NG and PNET in the same tumor was seen in 7/14 (50%) cases. 4/14 (29%) NG were not associated with a history of PNET. 2 primary GCT with PNET only showed NG in the metastasis. 2/9 (22%) PNET were not associated with NG history in either the primary or metastasis. Limited follow-up showed no death.

Table 1: Primary and metastatic testicular Germ Cell Tumor with neuroglial and/or primitive neuroectodermal tumor overgrowth

Age/ years	Primary GCT in testis	Metastatic GCT with neuroglial and or PNET element					Follow up data
		Post-Chemo	Metastatic site and tumor size	Neuroglial element	PNET	Non-NG/PNET GCT elements	
29	Teratoma, EC, YST, PNET, Anaplastic astrocytoma (12cm)	Yes	Retroperitoneal 11 cm	80% (anaplastic astrocytoma)	20%	No	1 yr, then lost to F/U
24	Teratoma, glioma with astrocytic features (8.5 cm)	Yes	Retroperitoneal 10 cm	100% (glioma with astrocytic features)	0	No	Lost to F/U
40	Seminoma, YST (4.2 cm)	Yes	Retroperitoneal 4 cm	0	15%	YST, teratoma	Lost to F/U
25	EC, teratoma, seminoma (3.5 cm)	Yes	Para-aortic 7 cm	90% (glioma)	5%	Teratoma	1 yr (alive)
33	Teratoma	Yes	Retroperitoneal 17 cm	20% (Glioneuronal)	0	Teratoma	4 yrs (alive)
24	EC, YST, seminoma (3.6 cm)	Yes	Precaval 7 cm	30% (glioneuronal)	10%	Teratoma, YST	4 yrs (alive)
25	EC, YST (2.4 cm)	Yes	Inter-aortocaval 2 cm Mediastinal 4 cm	10%, 5% (ganglioneuroma)	0	Teratoma	4 yrs (alive)
20	Teratoma, YST, choriocarcinoma (7 cm)	No	Inter-aortic 2 cm	10% (glioma)	10%	Teratoma, YST, EC	2 yrs (alive),
65	YST, teratoma, PNET and glial element (11 cm)	No	Mid-spermatic cord metastasis 1 cm	0	100%	No	Lost to F/U
22	Teratoma, YST, PNET (6 cm)	Yes	Retroperitoneal 13 cm	15% (glioneuronal)	5%	Teratoma	1 yr, then lost to F/U
57	Teratoma, YST, PNET (12 cm)	Yes	Retroperitoneal 11 cm	80% (glioneuronal)	0	Teratoma	2 yrs (alive)
45	Teratoma, YST	Yes	Retroperitoneal 3 cm	90% (glioma)	0	Teratoma	Lost to F/U
37	Teratoma, YST (10 cm)	yes	Retroperitoneal 11 cm	0	80%	Teratoma	1 yr (alive)
27	Teratoma, EC, YST and choriocarcinoma (6 cm)	Yes	Retroperitoneal 16 cm	50% (glioneuronal)	0	teratoma	4 yrs (alive)

GCT: Germ cell tumor; EC: Embryonal Carcinoma; YST: Yolk sac tumor, NG: neuroglial element; PNET: primitive neuroectodermal tumor, Yr: Year; F/u: Follow up

Conclusions: The study demonstrated that GCT with NG and/or PNET were uncommon and most often associated with teratoma. Both NG and PNET can occur in primary tumors and, more frequently in post-chemotherapy metastasis, especially for NG. We also

showed that it was not uncommon to see NG coexist with PNET in the same tumor or in cases with a history of PNET. The frequent association of NG with PNET may infer a derivation of NG from PNET differentiation and, in the presence of NG, more extensive sampling may be needed to exclude PNET. The findings help us in better understanding the clinicopathology as well as the histogenesis of this unusual tumor. Further studies with large cohorts and long-term follow-up are warranted.

586 Integrated Clinico-Pathological and Proteogenomic Characterization of Clear Cell Renal Cell Carcinoma by the Clinical Proteomic Tumor Analysis Consortium (CPTAC)

Rahul Mannan[1], Yize Li[2], Siqi Chen[2], Lijun Chen[3], Yuping Zhang[4], Yige Wu[2], Noshad Hosseini[5], Felipe da Veiga Leprevost[5], Saravana Dhanasekaran[5], Christopher Ricketts[6], Michael Schnaubelt[3], Chelsea Newton[7], Rita Jui-Hsien Lu[2], Fengyun Su[5], Xuhong Cao[5], Iga Kołodziejczak[8], Chandan Kumar-Sinha[5], Gilbert Omenn[5], Qing Kay Li[9], Eunkyung An[10], Mathangi Thiagarajan[11], Tara Hiltke[12], Ana Robles[10], Henry Rodriguez[12], Mehdi Mesri[10], Daniel Chan[3], Scott Jewell[7], Galen Hostetter[7], Arul Chinnaiyan[5], Maciej Wiznerowicz[13], Alexey Nesvizhskii[5], Hui Zhang[14], Li Ding[15], Rohit Mehra[5]
[1]Michigan Medicine, University of Michigan, Ann Arbor, MI, [2]Washington University in St. Louis, St. Louis, MO, [3]Johns Hopkins Medicine, Baltimore, MD, [4]Michigan Center for Translational Pathology, Ann Arbor, MI, [5]University of Michigan, Ann Arbor, MI, [6]Center for Cancer Research, National Cancer Institute, MD, [7]Van Andel Institute, Grand Rapids, MI, [8]Poznan, Poland, [9]Johns Hopkins Hospital, Baltimore, MD, [10]National Cancer Institute, Bethesda, MD, [11]Frederick National Laboratory for Cancer Research, Frederick, MD, [12]National Cancer Institute, National Institutes of Health, Bethesda, MD, [13]Poznan University of Medical Sciences, Poznan, Poland, [14]Johns Hopkins University, Baltimore, MD, [15]Washington University in St. Louis, St. Louis, MD

Disclosures: Rahul Mannan: None; Yize Li: None; Siqi Chen: None; Lijun Chen: None; Yuping Zhang: None; Yige Wu: None; Noshad Hosseini: None; Felipe da Veiga Leprevost: None; Saravana Dhanasekaran: None; Christopher Ricketts: None; Michael Schnaubelt: None; Chelsea Newton: None; Rita Jui-Hsien Lu: None; Fengyun Su: None; Xuhong Cao: None; Iga Kołodziejczak: *Employee*, International Institute for Molecular Oncology; Chandan Kumar-Sinha: None; Gilbert Omenn: None; Qing Kay Li: None; Eunkyung An: None; Mathangi Thiagarajan: None; Tara Hiltke: None; Ana Robles: None; Henry Rodriguez: None; Mehdi Mesri: None; Daniel Chan: None; Scott Jewell: None; Galen Hostetter: None; Arul Chinnaiyan: None; Maciej Wiznerowicz: None; Alexey Nesvizhskii: None; Hui Zhang: None; Li Ding: None; Rohit Mehra: None

Background: The Clinical Proteomic Tumor Analysis Consortium (CPTAC) initially set out to characterize 103 treatment-naïve clear cell renal cell carcinoma (CCRCC) patient specimens. The present study increases the cohort size (110 more) thereby rendering higher statistical power for proteogenomic analysis of different molecular subtypes. Further, this is the first study to carry out integrative analyses with extensive histopathological annotations to glean a more comprehensive understanding of CCRCC disease biology.

Design: A sample cohort comprised of 213 patient CCRCC surgical specimens with matched normal tissues, having detailed clinical data. A comprehensive schematic histopathology evaluation recorded 21 histopathological parameters defining low- and high-grade features, spatial architecture, and tumor microenvironment. Extensive proteogenomic characterization was carried out using whole-exome sequencing, whole-genome sequencing (WGS), RNA sequencing, DNA methylation, and proteomic profiling using mass spectrometry-based TMT and DIA methodologies to estimate total protein and phosphoprotein. The molecular data and histopathological annotations were used in integrative analysis to understand molecular mechanisms that drive CCRCC.

Results: Based on a thorough histopathological evaluation, high-grade and low-grade feature counts were tabulated, and these annotations were employed in proteogenomic association studies. First, integrated copy number analysis using both WGS/ WES identified a distinct subset of samples (10-15%) with a higher copy number burden. Structural variants analysis helped characterize the genomic breakpoint of various chromosomal re-arrangements including chromosomes 3-5, 3-2, 3-8 among others. Proteogenomic effects of the most frequent copy number variation (CNV dosage analysis) observed in CCRCC, showed an association between various molecular concepts and CNV aberrations. A subset of samples was also examined for intra-tumor proteogenomic heterogeneity. Finally, we characterized the proteogenomic events associated with select recurrent molecular aberrations.

Conclusions: Herein, we describe the initial findings from the ongoing CPTAC study where we performed a comprehensive proteogenomic and histopathological characterization of CCRCC. The high-quality molecular data generated here will also serve as an invaluable public resource for future studies and to generate experimental hypotheses with the aim of developing targeted therapies.

587 Integrated Protein and mRNA Biomarker Assessment in a Rapid Autopsy Series of Castrate Resistant Metastatic Prostate Cancer

Rahul Mannan[1], Xiaoming (Mindy) Wang[2], Anya Chinnaiyan[2], Jean Tien[3], Sanjana Eyunni[2], Arul Chinnaiyan[2], Pushpinder S. Bawa[1], Seema Chugh[2], Allecia Wilson[2], Jeffrey Jentzen[2], Joshi Alumkal[2], Megan Caram[4], Ajjai Alva[3], Ulka Vaishampayan[2], Daniel Spratt[5], Sylvia Zelenka-Wang[6], Lisa McMurry[6], Fengyun Su[2], Javed Siddiqui[2], Xuhong Cao[2], Todd Morgan[2], Chandan Kumar-Sinha[2], Saravana Dhanasekaran[2], Arul Chinnaiyan[2], Zachery Reichert[2], Rohit Mehra[2]
[1]Michigan Medicine, University of Michigan, Ann Arbor, MI, [2]University of Michigan, Ann Arbor, MI, [3]University of Michigan, [4]Michigan Medicine, University of Michigan, [5]UH Cleveland Medical Center, Cleveland, OH, [6]Michigan Center for Translational Pathology, Ann Arbor, MI

Disclosures: Rahul Mannan: None; Xiaoming (Mindy) Wang: None; Anya Chinnaiyan: None; Jean Tien: None; Sanjana Eyunni: None; Arul Chinnaiyan: None; Pushpinder S. Bawa: None; Seema Chugh: None; Allecia Wilson: None; Jeffrey Jentzen: None; Joshi Alumkal: None; Megan Caram: None; Ajjai Alva: None; Ulka Vaishampayan: None; Daniel Spratt: None; Sylvia Zelenka-Wang: None; Lisa McMurry: None; Fengyun Su: None; Javed Siddiqui: None; Xuhong Cao: None; Todd Morgan: None; Chandan Kumar-Sinha: None; Saravana Dhanasekaran: None; Arul Chinnaiyan: None; Zachery Reichert: None; Rohit Mehra: None

Background: A subset of patients with prostate cancer eventually develop castrate resistant prostate cancer (CRPC). Here, we aimed to perform a comprehensive biomarker assessment utilizing immunohistochemistry (IHC) and RNA in situ hybridization (RNA-ISH) on diverse sites in patients with CRPC for commonly used diagnostic, tumor lineage, transdifferentiation, clinical outcomes, and prostate cancer-specific death biomarkers.

Design: We generated a cohort of 241 tissues (120 non-osseous and 57 osseous metastatic samples) from 12 patients of CRPC enrolled in our in-house warm autopsy program and 27 samples from 9 patients with clinically localized prostate cancer. For each patient, multiple tumor sites and per site 2-3 different topographical areas were included to interrogate biomarker heterogeneity from a functional perspective utilizing 18 IHC markers (PSA, NKX3-1, AR, p63, GATA3, SYP, CgA, RB1, cyclin D1, Ki-67, ERG, p53, PTEN, CDK12, EZH2, and PD-L1) and 5 RNA-ISH markers (*SChLAP1*, *EZH2*, *ADRB2*, *PTEN,* and *ERG*) for gene expression.

Results: While neuroendocrinal (NE) markers, SYP and CgA were expressed in 32.8% and 19.7% of samples; loss of RB1 and cyclin D1 (indicating defective Rb pathway activity) with overexpression of *ADRB2* and Ki-67 (further indicative of NE transdifferentiation) was seen in 9.7%, 16.5%, 44.6%, and 23.1% samples. p53 mutational dysregulation (missense and null type) and nuclear beta-catenin (Wnt pathway activation) was seen in 57.0%, 5.4%, and 13.6% samples. Biomarkers with established poor clinical outcome annotations, loss of PTEN, *SChLAP-1*, and epigenetic metastasis driver EZH2 protein and mRNA transcript were noted in 51.7%, 34.2%, 45.9%, and 36.8% of samples. Therapeutically significant biomarkers PD-L1 and CDK12 loss were seen in 13.9% and 48.6% of samples. A biomarker heat map constructed demonstrates tumor heterogeneity. Interestingly, there was a statistically significant difference between gene expression scores of *EZH2, PTEN, and ADRB2* when comparing osseous and non-osseous metastases.

Figure 1 - 587

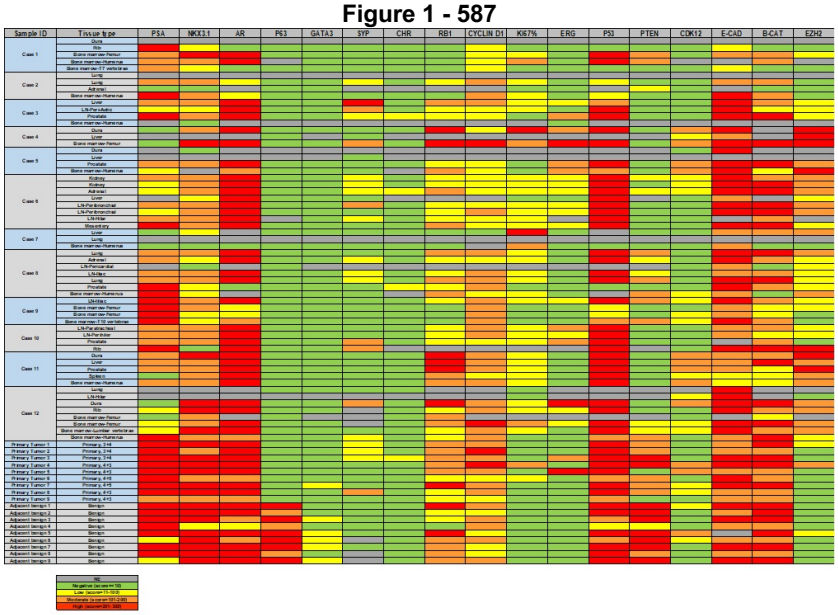

Conclusions: Loss of RB1 and cyclin D1 with overexpression of *ADRB2* showed good performance to detect early NE transdifferentiation. Our study also validated through the novel RNA-ISH technology, genes associated with aggressiveness and metastasis- *SChLAP1*, *EZH2*, *ADRB2*, and *PTEN*. Clinical therapeutics targeting biomarkers (like PD-L1, EZH2, CDK12 amongst others) need to reconcile such expression heterogeneity towards determining clinical efficacy and drug resistance mechanisms.

588 ABCC2 Prominent Brush Border Expression (>50%) in Papillary Renal Cell Carcinoma Identifies a Subgroup with Poor Outcome

Mehdi Masoomian[1], Kiril Trpkov[2], Catherine Streutker[3], Corwyn Rowsell[4], Vidya Beharry[4], Rola Saleeb[5]
[1]University of Toronto, Toronto, Canada, [2]University of Calgary, Calgary, Canada, [3]Unity Health Toronto, Toronto, Canada, [4]St. Michael's Hospital, Toronto, Canada, [5]St. Michael's Hospital/University of Toronto, Toronto, Canada

Disclosures: Mehdi Masoomian: None; Kiril Trpkov: None; Catherine Streutker: None; Corwyn Rowsell: None; Vidya Beharry: None; Rola Saleeb: None

Background: Classic papillary renal cell carcinoma (PRCC) subtyping classification (type 1 vs type 2) is currently not favoured and WHO/ISUP nucleolar grade is now used as prognostic parameter in PRCC. Previous publications have assessed the prognostic significance of the renal transporter ABCC2 in stratifying PRCC. ABCC2 was shown to be highly expressed in high grade PRCC, on both mRNA and protein level and significant survival differences were found between the PRCC with vs without ABCC2 expression. The expression of ABCC2 as a prognostic marker is not currently validated. The possible significance of specific patterns of ABCC2 expression has not been previously assessed in PRCC

Design: We evaluated a confirmed PRCC nephrectomy cohort (n=120), fully annotated with clinicopathological data including: age, gender, laterality, tumour size, nucleolar grade, pathological stage, disease recurrence, metastasis, and survival status. Outliers RCCs were excluded by appropriate work up. TMAs were constructed for 80 cases (3 cores per sample), while remaining cases were assessed as whole slides. ABCC2 immunohistochemistry (IHC) was optimized and validated. ABCC2 demonstrated two patterns by IHC: 1.) cytoplasmic, and 2.) brush border (BB) expression. All cases were assessed for ABCC2 as: a) negative, b) cytoplasmic, c) cytoplasmic and BB <50%, and d) cytoplasmic and BB >50%. Statistical analysis was performed using GraphPad Prism and SPSS.

Results: Univariate analysis of progression free survival (PFS) showed significant differences between the ABCC2 groups (p=0.0015). The PFS between all 3 ABCC2 positive groups and the ABCC2 negative group was also significantly different (p=0.0458). Specifically, the PRCC group >50% BB (n= 14) had a significantly worse PFS than the ABCC2 negative (n= 43)(p=0.0005), cytoplasmic (n= 26)(p=0.042), and <50% BB (n= 37) (p=0.039) groups. In comparison, the WHO/ISUP nucleolar grade failed to show significance on univariate PFS analysis (p=0.459). The subgroup with >50% BB expression also maintained its significance on multivariate Cox regression PFS analysis, adjusting for grade and age (p=0.013). The >50% BB subgroup was notably associated with high clinical stage 3 (13%) and 4 (20%) disease

Figure 1 - 588

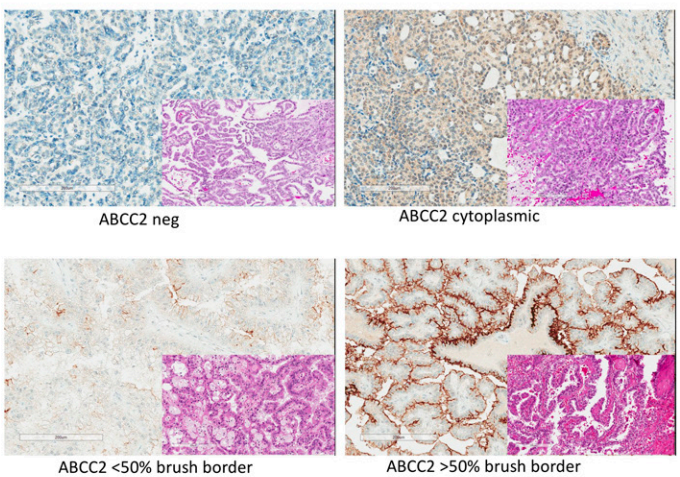

Figure 2 – 588

Figure 2: Univariate progression free survival analysis of ABCC2 expression groups (negative, cytoplasmic, brush border <50%, brush border >50%)

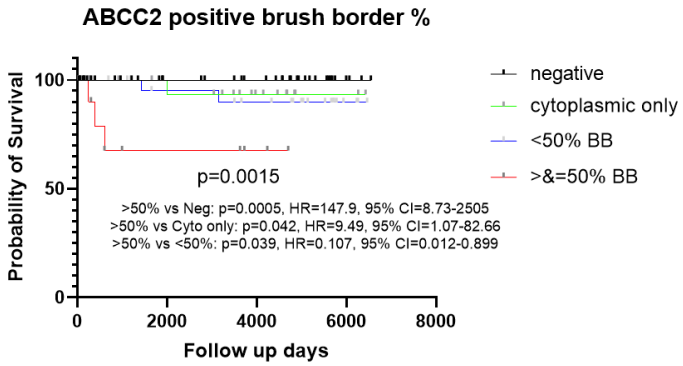

Conclusions: ABCC2 expression showed prognostic significance in PRCC. In particular, a prominent ABCC2 BB expression (>50%) identified a PRCC subset associated with poor prognostic parameters and significantly worse PFS. This finding highlights the additional clinical value of ABCC2 assessment for the prognostic stratification of PRCC.

589 Comparison of Sarcomatoid Urothelial Carcinoma and Conventional Urothelial Carcinoma Within Same Tumors Using Digital Spatial Profiling Technology

Andres Matoso[1], Sonia Kamanda[2], David Corney[3]
[1]Johns Hopkins Medical Institutions, Baltimore, MD, [2]James Buchanan Brady Urological Institutions, Johns Hopkins Hospital, Johns Hopkins Medical Institutions, Baltimore, MD, [3]GENEWIZ, South Plainfield, NJ

Disclosures: Andres Matoso: None; Sonia Kamanda: None; David Corney: *Employee*, GENEWIZ

Background: Sarcomatoid urothelial carcinoma is a histologic variant that is considered more aggressive than conventional urothelial carcinoma and is known to contain a rich immune microenvironment. The differences between the tumor microenvironment in sarcomatoid and conventional urothelial carcinoma in the same patient/specimen has not been studied and could bear implications to response to immune check point inhibitors.

Design: Tissue microarrays were constructed using FFPE specimens from 8 patients with mixed urothelial carcinoma and sarcomatoid carcinoma. Paired conventional urothelial carcinoma and sarcomatoid carcinoma were analysed using Nanostring Digital Spatial Profiling Analysis using the Cancer Transcriptome Atlas assay that includes ~1,800 mRNA targets. Cores with regions of interest (ROI) were selected in real-time based on histology, panCK and CD45 stains as epithelioid/urothelial carcinoma (n=26), sarcomatoid (n=18), and mixed (n=15). Data QC was performed to identify ROIs with low coverage, low number of cells, etc. Of 59 ROIs, 54 passed QC. A Linear Mixed Model with Benjamini-Hochberg correction for multiple hypothesis testing was applied to the ROIs to identify differentially expressed genes. Pathway analysis was performed on the differentially expressed genes.

Results: Differentially genes were identified between sarc, mixed and epithelial ROIs and pathway enrichment analysis reveals enrichment of ECM-related pathways within sarc ROIs. Spatial deconvolution of the gene expression data revealed that macrophages and fibroblasts were preferentially expressed in the sarcomatoid and mixed areas. Other immune cells that were highly present but without significant difference between sarcomatoid, epithelioid or mixed areas include neutrophils, T-CD4 memory cells, T-CD4 naive cells, T-CD8 memory cells, and B naive cells. There was no significant difference in expression of PD-L1, or CTLA-4 among groups.

Conclusions: Digital spatial profiling allows for discriminatory assessment of gene expression in areas of tumors with different morphology. In this study, we used this technology to compare the tumor immune microenvironment in the sarcomatoid and epithelioid areas of specimens from the same patients. The identification of macrophages as being the main cell type differentially

expressed in the sarcomatoid areas could have implications in the overall understanding of the tumor microenvironment specific to sarcomatoid variant as well as to bear implications for immunotherapy.

590 Molecular and Immunophenotypic Correlates of Metastatic Epithelioid Angiomyolipoma Include Alterations of TP53, RB1 and ATRX

Michael McCarthy[1], Rafael Jimenez[1], Loren Herrera Hernandez[1], Christine Lohse[2], R. Houston Thompson[2], Stephen Boorjian[1], Bradley Leibovich[2], John Cheville[1], Sounak Gupta[1]
[1]Mayo Clinic, Rochester, MN, [2]Mayo Clinic

Disclosures: Michael McCarthy: None; Rafael Jimenez: *Consultant*, Histowiz, Inc; Loren Herrera Hernandez: None; Christine Lohse: None; R. Houston Thompson: None; Stephen Boorjian: *Consultant*, Ferring, FerGene, ArTara; Bradley Leibovich: None; John Cheville: None; Sounak Gupta: None

Background: Renal tumors with somatic or germline alterations of *TSC1/ TSC2* genes include angiomyolipoma (AML). A subset of epithelioid AML (eAML; a morphologic variant of AML) have metastatic potential.

Design: The discovery cohort comprised comprehensive molecular profiling data for 25 AML from 21 patients, including 5 patients with metastatic, presumably eAML (American Association for Cancer Research GENIE registry, accessed and visualized using cBioPortal). The validation cohort comprised 12 consecutively diagnosed cases of eAML from our institutional registry and 1 case received in consultation. This included eAML in 3 patients with tuberous sclerosis complex (TSC) and metastatic eAML in 3 patients, 2 of whom had TSC. Immunohistochemistry (IHC) was performed for all 13 cases for PAX8, cathepsin K, ATRX, P53, and RB.

Results: Recurrent molecular alterations were seen for *TSC2* (18/21, 86%), *TP53* (3/21, 14%), *ATRX* (2/21, 10%), *MYCN* (2/21, 10%), and *RAD50* (2/21, 10%). Metastatic eAML were enriched for alterations of *TP53* (3/5), *ATRX* (2/5), and *RB1* (1/5), and combined alterations of at least 1 of these 3 genes was seen in 4/5 metastatic eAML. The validation cohort included 7 women and 6 men with a median age at nephrectomy of 49 years, a median tumor size of 8.3 cm (n=12), and a median duration of follow up of 11 years (n=12); 2 patients died of unknown causes within 1 year of nephrectomy. Notable co-morbidities/molecular alterations included colorectal adenocarcinoma in 2 patients, 1 patient each with an oncocytic adrenocortical neoplasm, *BRCA1* alteration, and neurofibromatosis type2, respectively. IHC in this cohort confirmed a PAX8-/cathepsin K+ immunophenotype and revealed retained ATRX expression for all cases (13/13), loss of RB expression and a mutant pattern of P53 expression (loss) in 2/13 patients, both with metastatic eAML. Equivocal and wild-type pattern of P53 expression was noted in 3/10 and 7/10 patients with non-metastatic disease, respectively.

Conclusions: Our results suggest that patients with non-metastatic AML lack alterations of *TP53*, *ATRX* and *RB1* (0/16 patients, 0%) and that these alterations are enriched in patients with metastatic eAML (4/5 patients). Within our validation cohort, 3/13 (23%) patients with eAML developed metastatic disease, with at least 2/3 patients showing a mutant pattern of P53 expression (loss) and absence of RB. These findings, if confirmed on molecular profiling and validated in larger datasets, have the potential to predict metastatic behavior in eAML.

591 The Spectrum of Biopsy Site Histologic Change in the Radical Prostatectomy Specimen

Jonathan Melamed[1], Joyce Ren[2], Fang-Ming Deng[3], Deepthi Hoskoppal[4], Hongying Huang[2], Derek Jones[5]
[1]New York University, New York, NY, [2]NYU Langone Health, New York, NY, [3]New York University Medical Center, New York, NY, [4]New York University Langone Medical Center, New York, NY, [5]NYU Langone Medical Center, New York, NY

Disclosures: Jonathan Melamed: None; Joyce Ren: None; Fang-Ming Deng: None; Deepthi Hoskoppal: None; Hongying Huang: None; Derek Jones: None

Background: Biopsy of the prostate is a frequent diagnostic procedure with some patients subject to repeated procedures as part of active surveillance and targeted biopsy protocols. Significant pathologic changes such as needle biopsy tumor tracking have been previously reported, occurring in 2% of radical prostatectomy cases. While some reports illustrate cases with biopsy change, the spectrum, incidence and distribution of morphologic alterations induced by biopsy have not been systematically evaluated.

Design: We evaluated 40 radical prostatectomy cases performed at our institution over a 4 month period. The distribution of cancer was previously mapped using topographic maps. We reviewed cases specifically for reparative changes that resulted from prior biopsy. The features evaluated included 1) Hemosiderin deposition in peripheral tissue as evidence of prior hemorrhage 2) Fibrosis – based on increased fibroblast cellularity in capsule fibroadipose tissue 3) Traumatic neuroma based on small neural twig proliferation 4) Needle track based on stellate scars in prostate 5) Dislocation of epithelium or corpora amylacea outside of prostate. These findings were identified as to type of reparative change, location in prostate (delineated on maps) and whether the change could impact stage assignment.

Results: In 33 cases (82.5%) biopsy related change was seen - in an average of 3 sections per case (7% of sections; range 1-6 sections). The changes were in the posterior portions of the prostate (94%) and in the apex (6%), with nearly half of the case showing bilateral distribution. The most frequent change was hemosiderin deposition (77%), which occurred in combination with neuromatous hyperplasia/ traumatic neuroma (57%) and fibroplasia (32%) and as isolated finding (19%). Dislocation of corpora amylacea and needle track were less common (38% and 22% of cases) findings.

Conclusions: The majority of radical prostatectomy cases (82.5%) show histologic evidence of reparative change, secondary to prior biopsy. These changes occur in few sections (7%) and are often subtle findings seen focally in the section. The changes most often seen are a combination of hemosiderin deposition, neuromatous hyperplasia and fibrosis. These findings are important to recognize as provide evidence of prior biopsy. Based on this study, these changes are unlikely to impact pathologic staging.

592 Prognostic Impact of Periostin Expression in Stroma Surrounding Upper Urinary Tract Urothelial Carcinoma

Kosuke Miyai[1], Kazuki Kawamura[2], Keiichi Ito[2], Hitoshi Tsuda[2]
[1]National Defense Medical College, Japan, [2]National Defense Medical College, Tokorozawa, Japan

Disclosures: Kosuke Miyai: None; Kazuki Kawamura: None; Keiichi Ito: None; Hitoshi Tsuda: None

Background: Periostin, an extracellular matrix protein observed in several normal tissues, is involved in regulating intercellular adhesion and maintenance of mechanical stress. Periostin overexpression has been found in various human cancer cells and intervening stroma, such as breast, colon, and ovarian cancers, which is usually related to tumor progression and patients' poor outcomes. With regards to urothelial carcinoma, only a few reports have investigated epithelial (i.e. cancer cells) periostin expression of urinary bladder cancer, and its role is still inconclusive. In addition, there has been no report investigating the periostin expression of cancer cells and surrounding stroma in upper urinary tract urothelial carcinomas (UUTUCs).

Design: We evaluated 126 consecutive patients with newly diagnosed invasive UUTUCs (69 with renal pelvic cancers and 57 with ureteral cancers) treated with nephroureterectomy or partial ureterectomy between 1999 and 2018 in our hospital. Samples were analyzed for overexpression of periostin by immunohistochemistry. Intensities of immunoreactivity and the fraction of positive cancer cell and stroma (i.e. epithelial and stromal expression, respectively) were classified into each 4 categories (intensity, 0 to 3; fraction, 0–25% = 1, 26–50% = 2, 51–75% = 3, and >75% = 4). The overall score was determined by multiplication of both scores and overall scores greater than 4 were considered periostin overexpression.

Results: Among the 126 UUTUCs, 55 (44%; 27 renal pelvic and 28 ureteral cancers) showed stromal overexpression of periostin. No case was considered epithelial periostin overexpression. Stromal overexpression of periostin was related to non-papillary gross finding, higher pathological T stage, lymphovascular invasion, concomitant carcinoma in situ and variant histology, high tumor budding, lymph node metastasis, and positive surgical margin. The multivariate Cox analysis revealed that stomal periostin overexpression was an independent predictor for overall survival (P = 0.00072, hazard ratio = 3.62) and lymphovascular invasion and stromal periostin overexpression tumor were independent predictors for cancer-specific survival (P = 0.032 and 0.020, hazard ratio = 2.61 and 3.07, respectively).

Conclusions: Stromal overexpression of periostin is related to several adverse clinicopathological factors, and is suggested to be useful as a novel predictive prognostic factor of patients with invasive UUTUCs.

593 Molecular Characterization of Clear Cell Adenocarcinoma of the Urinary Bladder

Sambit Mohanty[1], Anandi Lobo[2], Mahmut Akgul[3], Shilpy Jha[1], Niharika Pattnaik[1], Bindu Challa[4], Manas Baisakh[5], Shivani Sharma[6], Ruhani Sardana[7], Aditi Aggarwal[6], Nada Shaker[8], Seema Kaushal[9], Nakul Sampat[1], Anil Parwani[8], Sean Williamson[10]

[1]Advanced Medical and Research Institute, Bhubaneswar, India, [2]Kapoor Centre of Urology and Pathology, Raipur, India, [3]Albany Medical Center, Albany, NY, [4]The Ohio State University Wexner Medical Center, Columbus, OH, [5]Apollo Hospitals, Bhubaneswar, India, [6]Core Diagnostics, Gurgaon, India, [7]Advanced Medical Research Institute and Hospital, Bhubaneswar, India, [8]The Ohio State University, Columbus, OH, [9]All India Institute of Medical Sciences, New Delhi, India, [10]Cleveland Clinic, Cleveland, OH

Disclosures: Sambit Mohanty: None; Anandi Lobo: None; Mahmut Akgul: None; Shilpy Jha: None; Niharika Pattnaik: None; Bindu Challa: None; Manas Baisakh: None; Shivani Sharma: None; Ruhani Sardana: None; Aditi Aggarwal: None; Nada Shaker: None; Seema Kaushal: None; Nakul Sampat: None; Anil Parwani: None; Sean Williamson: None

Background: Clear cell adenocarcinoma (CCA) of the urothelial tract is a rare genitourinary malignancy, occurring predominantly in the urethra and bladder. Several theories have been proposed regarding the pathogenesis of CCA. However, the molecular landscape has not been adequately explored due to limited number of cases studied. To address this, we sought to molecularly categorise these tumors, with the aim to provide insights into the possible pathogenesis and potential targeted therapy for CCA of the urinary tract.

Design: Formalin fixed paraffin embedded tumor tissue blocks of the selected tumor specimens were used for molecular evaluation using targeted next generation sequencing based panel to detect small nucleotide variants/substitutions, small indels (insertions and/or deletions) and copy number variations in 324 cancer-associated genes. The panels also detects selected gene rearrangements as well as genomic signatures including microsatellite instability and tumor mutational burden. The panel was based on Illumina® Hi Seq 4000 platform.

Results: The results are illustrated in table 1 and figures 1 and 2. Among the various clinicopathologic parameters in this cohort of 19 patients, the tumor size ranged from 1.7-9cm (mean=4.6 cm), no associated urothelial carcinoma or variant histology were observed, and all of them underwent resection with either neo-adjuvant or adjuvant therapy; radiation therapy was given in 4 patients. The follow-up duration ranged from 3-31 months (mean=14 months) in 12 patients. Eight had died of disease and 4 were alive. All the deceased and 2 surviving patients harboured PI3KCA mutations which was the most common abnormality. Most (74%) had *PI3KCA* gain-of-function mutation, followed by *KRAS* , *ERBB2, SMAD4, RB1,TP53, MET* and *APC.*

Age/Gender	Gene Symbol (Somatic)	Transcript ID	Variant annotation (p.)	Variant annotation (c.DNA)	Allelic frequency	Pathogenic Role
75/M	*PIK3CA*	NM_006218.4	p.Glu545Lys	c.1633G>A	17.5%	Pathogenic
20/F	*PIK3CA*	NM_006218.4	p.Glu545Lys	c.1633G>A	23.7%	Pathogenic
69/M	*ERBB2*	NM_001005862.3	p.Ser457Leu	c.1370C>T	27.6%	VUS
	RB1 deletion	NM_000321.3	p.Arg661Trp	c.1981C>T	63%	Pathogenic
23/F	*PIK3CA*	NM_006218.4	p.Glu545Lys	c.1633G>A	33.8%	Pathogenic
	TP53	NM_001126114.3	p.Arg273Cys	c.817C>T	19.2%	Pathogenic/Likely Pathogenic
47/M	*PIK3CA*	NM_006218.4	p.Glu545Lys	c.1633G>A	21%	Pathogenic
	SMAD4	NM_005359.6	p.Ser144Ter	c.431C>G	66%	Pathogenic
65/M	TSC1	NM_000368.4	p.Glu876Ter	c.2626G>T	25%	Pathogenic
	MET	NM_000245.4	p.Thr992Ile	c.2975C>T	44.2%	VUS
71/F	*PIK3CA*	NM_006218.4	p.Glu545Lys	c.1633G>A	30.6%	Pathogenic
48M	*SMAD4*	NM_005359.6	p.Ser144Ter	c.431C>G	52%	Pathogenic
73/M	*ERBB2*	NM_001005862.3	p.Ser457Leu	c.1370C>T	18.4%	VUS
	RB1 deletion	NM_000321.3	p.Arg661Trp	c.1981C>T	70.3%	Pathogenic
39/F	*PIK3CA*	NM_006218.4	p.Glu545Lys	c.1633G>A	20.8%	Pathogenic
68/M	*KRAS*	NM_033360.4	p.Gly12Asp	c.35G>A	35%	Pathogenic
	PIK3CA	NM_006218.4	p.Glu545Lys	c.1633G>A	33.9%	Pathogenic
50/F	*PIK3CA*	NM_006218.4	p.Glu545Lys	c.1633G>A	16%	Pathogenic
	ERBB2	NM_001005862.3	p.Ser457Leu	c.1370C>T	20%	VUS
	TSC1	NM_000368.4	p.Glu876Ter	c.2626G>T	23.1%	Pathogenic
61/M	*PIK3CA*	NM_006218.4	p.Glu545Lys	c.1633G>A	31.8%	Pathogenic
	KRAS	NM_033360.4	p.Gly12Asp	c.35G>A	19%	Pathogenic
49F	*PIK3CA*	NM_006218.4	p.Glu545Lys	c.1633G>A	35%	Pathogenic
	APC	NM_000038.6	p.Ser127Gly	c.379A>G	82%	VUS
62/M	*PIK3CA*	NM_006218.4	p.Glu545Lys	c.1633G>A	20.7%	Pathogenic

	SMAD4	NM_005359.6	p.Ser144Ter	c.431C>G	54.2%	Pathogenic
43/F	*PIK3CA*	NM_006218.4	p.Glu545Lys	c.1633G>A	44%	Pathogenic
	KRAS	NM_033360.4	p.Gly12Asp	c.35G>A	39.7%	Pathogenic
59/F	*PIK3CA*	NM_006218.4	p.Glu545Lys	c.1633G>A	23%	Pathogenic
	RB1 deletion	NM_000321.3	p.Arg661Trp	c.1981C>T	70.5%	Pathogenic
	KRAS	NM_033360.4	p.Gly12Asp	c.35G>A	35.1%	Pathogenic
41/M	*SMAD4*	NM_005359.6	p.Ser144Ter	c.431C>G	69%	Pathogenic
63/M	*PIK3CA*	NM_006218.4	p.Glu545Lys	c.1633G>A	39.5%	Pathogenic
	ERBB2	NM_001005862.3	p.Ser457Leu	c.1370C>T	8.4%	VUS
	KRAS	NM_033360.4	p.Gly12Asp	c.35G>A	28%	Pathogenic

VUS: Variant of uncertain significance

Figure 1 - 593

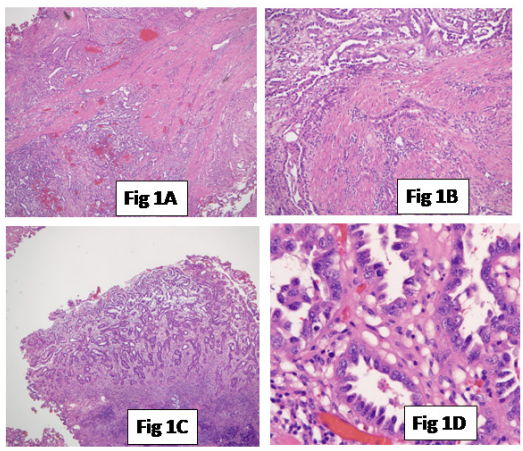

Fig 1(A-D):A (H&E,100X) Infiltrative CCAC; B(H&E,200X)Muscle invasion; C(H&E,100X) Mucosal involvement; D(H&E,400X) Tubulocystic pattern

Figure 2 – 593

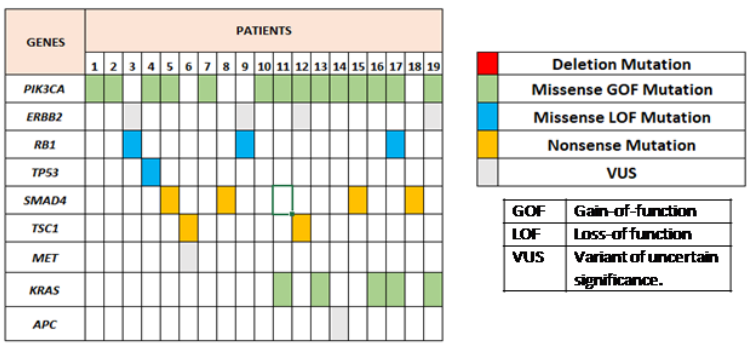

Fig 2: Molecular profiles of clear cell adenocarcinoma of urinary bladder

Conclusions: Based on the largest series of CCAC of the bladder to date, we identified a distinct oncogenic pathway involving the *PI3K/AKT/mTOR* pathway activation demonstrated by *PIK3CA* (74%) and *KRAS* (26%) gain-of-function mutations. Also, it involves loss-of-function mutations of tumor suppressor genes (*TP53, SMAD4, RB1, and APC*) and amplification of proto-ocogenes (*ERBB2 and MET*). These results may provide possible therapeutic targets for this aggressive urothelial malignancy.

594 The Current State of Emerging Renal Oncocytic Neoplasms: A Survey of Urologic Pathologists

Sambit Mohanty[1], Anandi Lobo[2], Anil Parwani[3], Amit Adhya[4], Ankur Sangoi[5], Bijal Kulkarni[6], Brett Delahunt[7], Christopher Przybycin[8], Claudia Manini[9], Daniel Luthringer[10], Deepika Sirohi[11], Divya Midha[12], Ekta Jain[13], Fiona Maclean[14], Giovanna Giannico[15], Gladell Paner[16], Guido Martignoni[17], Hikmat Al-Ahmadie[18], Holger Moch[19], Jesse McKenney[8], Jonathan Epstein[20], Jose Lopez[21], Kiril Trpkov[22], Liang Cheng[23], Lisa Browning[24], Mahmut Akgul[25], Mahul Amin[26], Manas Baisakh[27], Manju Aron[28], Maria Picken[29], Maria Tretiakova[30], Michelle Hirsch[31], Ming Zhou[32], Naoto Kuroda[33], Niharika Pattnaik[1], Nilesh Gupta[34], Ondrej Hes[35], Priya Rao[36], Rajal Shah[37], Rohit Mehra[38], Samson Fine[18], Sangeeta Desai[39], Sankalp Sancheti[40], Santosh Menon[41], Sara Wobker[42], Satish Tickoo[18], Seema Kaushal[43], Shilpy Jha[1], Shivani Kandukuri[44], Shivani Sharma[13], Steven Smith[45], Suvradeep Mitra[46], Victor Reuter[18], B Vishal Rao[47], Ying-Bei Chen[18], Sean Williamson[8]
[1]Advanced Medical and Research Institute, Bhubaneswar, India, [2]Kapoor Centre of Urology and Pathology, Raipur, India, [3]The Ohio State University, Columbus, OH, [4]All India Institute of Medical Sciences, Bhubaneswar, India, [5]El Camino Hospital, Mountain View, CA, [6]Kokilaben Ambani hospital, Nagpur, India, [7]Wellington School/Medicine, New Zealand, [8]Cleveland Clinic, Cleveland, OH, [9]University of Turin, Turin, Italy, [10]Cedars-Sinai Medical Center, West Hollywood, CA, [11]University of Utah / ARUP, Salt Lake City, UT, [12]Tata Medical Center, Kolkata, India, [13]Core Diagnostics, Gurgaon, India, [14]Douglass Hanly Moir Pathology, Melbourne, Australia, [15]Vanderbilt University Medical Center, Nashville, TN, [16]University of Chicago, Chicago, IL, [17]University of Verona, Ospedale Pederzoli, Peschiera del Garda, Italy, [18]Memorial Sloan Kettering Cancer Center, New York, NY, [19]University Hospital Zurich, Zürich, Switzerland, [20]Johns Hopkins Medical Institutions, Baltimore, MD, [21]Cruces University Hospital, Barakaldo, Spain, [22]University of Calgary, Calgary, Canada, [23]Indiana University, Indianapolis, IN, [24]Oxford University Hospitals NHS Foundation Trust, Oxford, United Kingdom, [25]Albany Medical Center, Albany, NY, [26]The University of Tennessee Health Science Center, Memphis, TN, [27]Apollo Hospitals, Bhubaneswar, India, [28]Keck School of Medicine of USC, Los Angeles, CA, [29]Loyola University Medical Center, Maywood, IL, [30]University of Washington, Seattle, WA, [31]Brigham and Women's Hospital, Boston, MA, [32]Tufts University School of Medicine, Boston, MA, [33]Kinrou Hospital, Kochi City, Japan, [34]Henry Ford Health System, Detroit, MI, [35]Biopticka laborator s.r.o., Plzen, Czech Republic, [36]The University of Texas MD Anderson Cancer Center, Houston, TX, [37]UTSouthwestern Medical Center, Dallas, TX, [38]University of Michigan, Ann Arbor, MI, [39]Tata Memorial Centre, Mumbai, India, [40]Homi Bhabha Cancer Hospital, Chandigarh, India, [41]Tata Memorial Hospital, Mumbai, India, [42]The University of North Carolina at Chapel Hill, Chapel Hill, NC, [43]All India Institute of Medical Sciences, New Delhi, India, [44]University of Southern California, Keck School of Medicine of USC, Los Angeles, CA, [45]VCU School of Medicine, Richmond, VA, [46]Postgraduate Institute of Medical Education and Research, [47]Basavatarakam Indo-American Cancer Hospital and Research Institute, West Bengal, India

Disclosures: Sambit Mohanty: None; Anandi Lobo: None; Anil Parwani: None; Amit Adhya: None; Ankur Sangoi: None; Bijal Kulkarni: None; Brett Delahunt: None; Christopher Przybycin: None; Claudia Manini: None; Daniel Luthringer: None; Deepika Sirohi: None; Divya Midha: None; Ekta Jain: None; Fiona Maclean: None; Giovanna Giannico: None; Gladell Paner: None; Guido Martignoni: None; Hikmat Al-Ahmadie: *Consultant*, AstraZeneca, Janssen Biotech, Paige.ai; Holger Moch: None; Jesse McKenney: None; Jonathan Epstein: None; Jose Lopez: None; Kiril Trpkov: None; Liang Cheng: None; Lisa Browning: None; Mahmut Akgul: None; Mahul Amin: *Advisory Board Member*, Ibex; *Consultant*, Google/Verily; *Advisory Board Member*, Precipio, Cell Max; Manas Baisakh: None; Manju Aron: None; Maria Picken: None; Maria Tretiakova: None; Michelle Hirsch: *Consultant*, Janssen Pharmaceuticals; Ming Zhou: None; Naoto Kuroda: None; Niharika Pattnaik: None; Nilesh Gupta: None; Ondrej Hes: None; Priya Rao: None; Rajal Shah: None; Rohit Mehra: None; Samson Fine: None; Sangeeta Desai: None; Sankalp Sancheti: None; Santosh Menon: None; Sara Wobker: None; Satish Tickoo: None; Seema Kaushal: None; Shilpy Jha: None; Shivani Kandukuri: None; Shivani Sharma: None; Steven Smith: *Consultant*, Elsevier/Amirsys Publishing; Suvradeep Mitra: None; Victor Reuter: None; B Vishal Rao: None; Ying-Bei Chen: None; Sean Williamson: None

Background: Oncocytic renal neoplasms are diagnostically challenging but usually nonaggressive. Several newer entities have been recently described, including eosinophilic solid and cystic renal cell carcinoma (ESC RCC), low-grade oncocytic tumor (LOT), eosinophilic vacuolated tumor (EVT), and papillary renal neoplasm with reverse polarity (PRNRP), the acceptance and clinical significance of which are still emerging.

Design: A survey instrument was shared among 65 urologic pathologists using SurveyMonkey.com (SurveyMonkey, Santa Clara, CA, USA). De-identified and anonymized respondent data were analyzed.

Results: Sixty participants completed the survey and contributed to the study. Participants were from Asia (n=21; 35%); North America (n=31; 52%); Europe (n=6; 10%), and Australia (n=2; 3%). Practice experience was <10 years (27%), 10-20 years (44%), or >20 years (29%). Half encounter oncocytic renal neoplasms that are difficult to classify at least monthly. Most (70%) indicated that there is enough evidence to consider ESC as a distinct entity now, whereas there was less certainty for LOT (27%), EVT (29%), and PRNRP (37%). However, >50% reported that eventually (if not already) these would likely be regarded as distinct entities. Most (60%) would not render an outright diagnosis of oncocytoma in a needle core biopsy and would provide a comment

rather than erring toward one diagnosis. There was a dichotomy in the routine use of immunohistochemistry (IHC) in the evaluation of oncocytoma (yes=52%; no=48%). Most used IHC markers included keratin 7 and 20, KIT, AMACR, PAX8, CA9, melan A, SDHB, and FH. When prompted with a scenario of a tumor with ESC-like features but papillary growth noted, there was a mixture of response between interpreting as ESC (48%) vs unclassified RCC (35%). Genetic techniques used included *TSC1/TSC2/MTOR* (67%) or *TFE3* (74%); however, the majority reported using these very rarely. Only 40% have encountered low-grade oncocytic renal neoplasms that are deficient for fumarate hydratase.

Conclusions: ESC is the most strongly accepted as a distinct entity (70%), although most (>50%) felt that LOT, EVT, and PRNRP would likely be distinct entities eventually (if not already). Genetic techniques are currently being used rarely, but most used markers include the TSC/MTOR pathway and translocations.

595 Uropathologists' Perspectives on Utilization of Key Morphologic and Molecular Parameters in Urothelial, Renal, and Prostatic Cancers Based on Clinical Practice Guidelines

Sambit Mohanty[1], Gladell Paner[2], Anandi Lobo[3], Anil Parwani[4], Ankur Sangoi[5], Brett Delahunt[6], Claudia Manini[7], Daniel Luthringer[8], Deepika Sirohi[9], Divya Midha[10], Fiona Maclean[11], Giovanna Giannico[12], Guido Martignoni[13], Hikmat Al-Ahmadie[14], Holger Moch[15], Jatin Gandhi[16], John Srigley[17], Jonathan Epstein[18], Jose Lopez[19], Kiril Trpkov[20], Liang Cheng[21], Lisa Browning[22], Mahmut Akgul[23], Manju Aron[24], Maria Picken[25], Maria Tretiakova[16], Michelle Hirsch[26], Murali Varma[27], Naoto Kuroda[28], Nilesh Gupta[29], Pheroze Tamboli[30], Priya Rao[30], Rohit Mehra[31], Sangeeta Desai[32], Santosh Menon[33], Sean Williamson[34], Seema Kaushal[35], Shilpy Jha[1], Shivani Kandukuri[36], B Vishal Rao[37], Mahul Amin[38]
[1]Advanced Medical and Research Institute, Bhubaneswar, India, [2]University of Chicago, Chicago, IL, [3]Kapoor Centre of Urology and Pathology, Raipur, India, [4]The Ohio State University, Columbus, OH, [5]El Camino Hospital, Mountain View, CA, [6]Wellington School/Medicine, New Zealand, [7]University of Turin, Turin, Italy, [8]Cedars-Sinai Medical Center, West Hollywood, CA, [9]University of Utah / ARUP, Salt Lake City, UT, [10]Tata Medical Center, Kolkata, India, [11]Douglass Hanly Moir Pathology, Melbourne, Australia, [12]Vanderbilt University Medical Center, Nashville, TN, [13]University of Verona, Ospedale Pederzoli, Peschiera del Garda, Italy, [14]Memorial Sloan Kettering Cancer Center, New York, NY, [15]University Hospital Zurich, Zürich, Switzerland, [16]University of Washington, Seattle, WA, [17]Trillium Health Partners, Credit Valley Hospital, Montréal, Canada, [18]Johns Hopkins Medical Institutions, Baltimore, MD, [19]Cruces University Hospital, Barakaldo, Spain, [20]University of Calgary, Calgary, Canada, [21]Indiana University, Indianapolis, IN, [22]Oxford University Hospitals NHS Foundation Trust, Oxford, United Kingdom, [23]Albany Medical Center, Albany, NY, [24]Keck School of Medicine of USC, Los Angeles, CA, [25]Loyola University Medical Center, Maywood, IL, [26]Brigham and Women's Hospital, Boston, MA, [27]University Hospital of Wales, Essex, United Kingdom, [28]Kinrou Hospital, Kochi City, Japan, [29]Henry Ford Health System, Detroit, MI, [30]The University of Texas MD Anderson Cancer Center, Houston, TX, [31]University of Michigan, Ann Arbor, MI, [32]Tata Memorial Centre, Mumbai, India, [33]Tata Memorial Hospital, Mumbai, India, [34]Cleveland Clinic, Cleveland, OH, [35]All India Institute of Medical Sciences, New Delhi, India, [36]University of Southern California, Keck School of Medicine of USC, Los Angeles, CA, [37]Basavatarakam Indo-American Cancer Hospital and Research Institute, West Bengal, India, [38]The University of Tennessee Health Science Center, Memphis, TN

Disclosures: Sambit Mohanty: None; Gladell Paner: None; Anandi Lobo: None; Anil Parwani: None; Ankur Sangoi: None; Brett Delahunt: None; Claudia Manini: None; Daniel Luthringer: None; Deepika Sirohi: None; Divya Midha: None; Fiona Maclean: None; Giovanna Giannico: None; Guido Martignoni: None; Hikmat Al-Ahmadie: *Consultant*, AstraZeneca; *Consultant*, Janssen Biotech; *Consultant*, Paige.ai; Holger Moch: None; Jatin Gandhi: None; John Srigley: None; Jonathan Epstein: None; Jose Lopez: None; Kiril Trpkov: None; Liang Cheng: None; Lisa Browning: None; Mahmut Akgul: None; Manju Aron: None; Maria Picken: None; Maria Tretiakova: None; Michelle Hirsch: *Consultant*, Janssen Pharmaceuticals; Murali Varma: None; Naoto Kuroda: None; Nilesh Gupta: None; Pheroze Tamboli: None; Priya Rao: None; Rohit Mehra: None; Sangeeta Desai: None; Santosh Menon: None; Sean Williamson: None; Seema Kaushal: None; Shilpy Jha: None; Shivani Kandukuri: None; B Vishal Rao: None; Mahul Amin: *Advisory Board Member*, Ibex; *Consultant*, Google/Verily; *Advisory Board Member*, Precipio, Cell Max

Background: There are clinical guidelines (EAU, AUA, NCCN, CAP, GUPS and ISUP) incorporating histopathologic and molecular parameters in urothelial (UC), prostate (PC) and renal (RCC) cancers; however, their awareness, reporting trend and resource utilization practice patterns among pathologists is not known. This prompted us for a multi-institutional international survey to assess utilization and reporting trends and practices among uropathologists.

Design: A survey instrument was shared among 65 uropathologists using SurveyMonkey software and the de-identified and anonymized respondent data were analysed.

Results: 41 participants completed the survey. Only 26% would do genomic testing by Decipher GS assay in RP for PC. 75% agreed that presence of a primary pattern 4/5 in PC is an independent predictor of poor outcome. There is a dichotomy in risk

stratifying PC based on GP, GG, cores involved and Tcategory. Majority (88%) were aware of criteria for positive surgical margin associated with unfavorable outcome. 71% would consider HRR assay in an IDCP and 67% have a fairly good idea on the mutual exclusiveness of DNA repair mutation and small cell histology. 88% of pathologists acknowledged the variables involved in defining renal sinus involvement and would quantify percent of sarcomatoid change. 88% would re-examine specimen in >7 cm RCC. 67% considered nodal involvement as the most significant pathologic parameters in a cystectomy specimen and 56% would consider prostatic urethral invasion as the highest risk for cystectomy in T1 bladder cancer. They are equally divided in their opinion on considering dysplasia in the surveillance protocol and in their opinion on cystectomy when concomitant non-invasive high grade-papillary UC and CIS are present. 77% considered plasmacytoid UC requires aggressive management even at T1 stage.58% emphasized that UC with glandular differentiation should be differentiated from a pure adenocarcinoma. Majority (83%) agreed on the indications for MSI assay in the upper tract UC for Lynch syndrome.

Conclusions: In spite of well promulgated international guidelines, there are still differing views on implementation in clinical practice and in risk stratification of PC, renal sinus involvement and urothelial dysplasia. Molecular testing is still at an evolving stage and is primarily driven by clinicians despite of dedicated uropathology services, and requires more genotype-phenotype correlation studies.

596 Renal Cell Carcinoma in African-American Patients with End Stage Renal Disease

Aysha Mubeen[1], Sofia Canete-Portillo[2], Soroush Rais-Bahrami[2], Cristina Magi-Galluzzi[2]
[1]Brigham and Women's Hospital, Boston, MA, [2]The University of Alabama at Birmingham, Birmingham, AL

Disclosures: Aysha Mubeen: None; Sofia Canete-Portillo: None; Soroush Rais-Bahrami: None; Cristina Magi-Galluzzi: None

Background: Patients with end stage renal disease (ESRD) have increased risk of developing renal cell carcinoma (RCC). Acquired cystic disease (ACD) resulting from chronic dialysis also predisposes ESRD patients to cancer. ACD-associated RCC (ACD-RCC) is specific to ESRD patients on long-term dialysis. Other common histologic subtypes of RCC in ESRD patients are clear cell papillary renal cell carcinoma (CCPRCC), papillary RCC (PRCC) and clear cell renal cell carcinoma (CCRCC).

Design: We aimed to assess the incidence and clinicopathologic features of RCC in ESRD patients at our institution, with a particular focus on African-American patients. Clinicopathologic data from all nephrectomies performed from 2010-2020 in ESRD patients with a cancer diagnosis was retrospectively reviewed.

Results: Of the 1098 patients diagnosed with RCC at our institution from 2010 to 2020, 57 (5.2%) were ESRD patients. Fifty-two (91%) ESRD patients with RCC were African-Americans; thirty-nine (68%) were males; median age was 61 years (range: 39-78). Sixty-six RCC were identified: 29 (44%) CCPRCC, 20 (30%) ACD-RCC, 11 (17%) PRCC, and 6 (9%) CCRCC. Tumors' mean size was 3.2 cm (range: 0.1-9.5). Most ACD-RCC, CCPRCC and PRCC were pathologic (p) stage T1; 3 (60%) CCRCC were pT3 (Table 1). Angiomyolipoma (n=1) and papillary adenoma (n=1) were observed in two patients. Mean follow-up was 17 months (range: 1-73). Most patients (82%) were alive with no evidence of disease at follow-up. One African-American patient with CCRCC developed distant metastasis and died of disease.

	ACD-RCC	CCPRCC	PRCC	CCRCC
# Patients	17	25	10	5
Mean age, years	55	64	60	66
Males (%)	12 (70%)	14 (56%)	9 (90%)	4 (80%)
African-Americans Whites Hispanic Unknown	16 1 0 0	22 1 1 1	10 0 0 0	4 1 0 0
# Tumors (%)	20 (30%) (3 bilateral)	29 (44%) (4 multifocal)	11 (17%) (1 bilateral)	6 (9%) (1 bilateral)
Tumor mean size, cm	2.3	2.2	2.3	6.0
Tumor pathologic stage: pT1 pT2 pT3 n/a (biopsy followed by cryoablation)	15 (88%) 1 (6%) 0 1	21 (84%) 0 1 3	9 (90%) 0 1 (10%) 0	1 (20%) 1 (20%) 3 (60%) 0

Conclusions: The incidence of RCC in ESRD in our population was 5.2%. CCPRCC (44%) and ACD-RCC (30%) were the most common RCC subtypes in our predominantly African-American ESRD patient population. Most tumors were low stage (pT1/pT2) and indolent. One of the 5 patients with CCRCC died of disease.

597 Single Region Sampling Does Not Capture the Intra-Tumoral Immune Heterogeneity of Sarcomatoid Renal Cell Carcinoma

Varsha Nair[1], Xiangjun Tian[1], Cameron Noorbakhsh[1], Yong Lee[2], Michael Hwang[3], Jing Wang[1], Zixing Wang[1], Ken Chen[1], Jose Karam[1], Kasthuri Kannan[1], Krishna Bhat[1], Kanishka Sircar[1]
[1]The University of Texas MD Anderson Cancer Center, Houston, TX, [2]HTG Molecular Diagnostics, Inc., Tucson, AZ, [3]Indiana University Health, Indianapolis, IN

Disclosures: Varsha Nair: None; Xiangjun Tian: None; Cameron Noorbakhsh: None; Yong Lee: None; Michael Hwang: None; Jing Wang: None; Zixing Wang: None; Ken Chen: None; Jose Karam: *Consultant*, Merck, Pfizer, Johnson and Johnson; *Grant or Research Support*, Mirati, Merck, Elypta, Roche/Genentech; *Stock Ownership*, MedTek, RomTech; Kasthuri Kannan: None; Krishna Bhat: None; Kanishka Sircar: None

Background: Sarcomatoid renal cell carcinoma (sRCC), consisting of an epithelioid (E-) and a sarcomatous (S-) component, has recently shown promising response to immune checkpoint inhibitor (ICI) therapy. The S- component has shown a more pronounced immune adaptive phenotype (PD1/PDL1+) based on prior immunohistochemical studies, suggesting intra-tumoral heterogeneity (ITH). Given this regional variation, our aim was to more comprehensively study the ITH of the immune landscape of sRCC.

Design: We studied two cohorts of patients who had surgically resected advanced sRCC of clear cell subtype, without neoadjuvant therapy and where the E- and S- components were macrodissected prior to gene expression profiling. The first cohort consisted of 66 FFPE samples (31 E- and 35 S-) from 34 patients interrogated by the Precision Immuno-Oncology Panel (HTG EdgeSeq) which assays the RNA expression of 1392 immune related genes. The second cohort consisted of 35 frozen samples (15 E- and 10 S-) from 15 patients assayed by genome wide RNA-seq (Illumina HiSeq 2000). Differential gene expression analysis was conducted, including deconvolution of RNA-seq data using MCP-counter for the FFPE cohort and CIBERSORT for the frozen cohort.

Results: 546 genes showed significant differential expression between E- and S- among the FFPE cohort. 231 out of these 546 genes were also differentially expressed in the frozen cohort. These genes included CD274/PDL1, CD276, CD44, TGFB1, DUSP4, spanning multiple cell types and processes as shown in Table 1.
Interestingly, there was no significant difference in the relative abundance of immune cell types between the E- and S- components of sRCC according to MCP-counter analysis of 8 immune cell types on the FFPE cohort and CIBERSORT analysis of 22 immune cell types on the frozen cohort (Figure 1).

Table 1: Differential gene expression in S vs E components of sRCC

Gene	Type	log2 FC S v E (FFPE)	p value FFPE	log2 FC S v E (Frozen)	p value Frozen
LRBA	CD4 T HELPER	-0.54053545	0.00000007	-0.58883529	0.01439351
CD274 (PDL1)	CO INHIBITOR	0.98199310	0.00000149	1.12446242	0.01751260
CD44	IMMUNE CHECKPOINTS	0.79023615	0.00025736	1.64450907	0.00002293
CD276	IMMUNE CHECKPOINTS	0.44698768	0.00004070	0.93481816	0.00282102
FN1	MACROPHAGE MARKERS	1.57096834	0.00000001	1.91205039	0.00000498
MARCO	MACROPHAGE MARKERS	1.35173784	0.00003490	2.62609661	0.00004850
TGFB1	MDSC	0.60251806	0.00006150	2.14376470	0.00000706
ALOX15B	NEUTROPHIL MARKERS	-0.82992096	0.00121631	-2.15846970	0.00030517
DUSP4	NK CELLS	0.37345754	0.04680516	1.27541251	0.00928569
BIRC5	TH2 RESPONSE	1.49760616	0.00000000	2.61486750	0.00000003

Figure 1 - 597

Figure 1. Proportion of immune cells is similar between E (red) and S (blue) components of sarcomatoid RCC

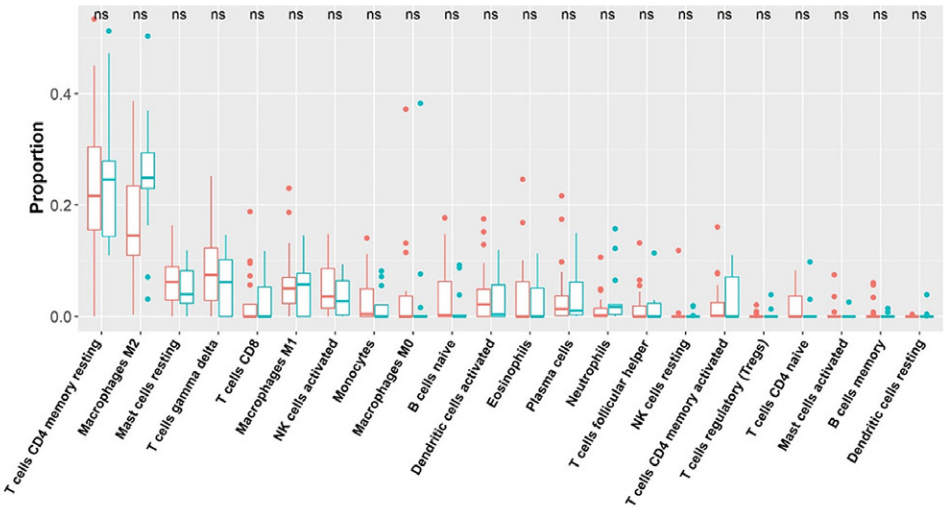

Conclusions: Our data suggest that single region sampling may not capture the intra-tumoral immune heterogeneity of sRCC. Further, it appears that the S- component is more immunosuppressive despite similar proportions of immune cell types between E- and S- components of sRCC.

598 Amyloid is Underdiagnosed in Prostate Specimens and May Be Clinically Significant

Jane Nguyen[1], Mohamed Alhamar[2], Sean Williamson[1]
[1]Cleveland Clinic, Cleveland, OH, [2]Memorial Sloan Kettering Cancer Center, New York, NY

Disclosures: Jane Nguyen: None; Mohamed Alhamar: None; Sean Williamson: None

Background: Amyloid in the seminal vesicles (SV) or ejaculatory ducts (ED) of prostatic specimens is not unusual and typically thought to be of little clinical significance. However, amyloid deposits in the prostate other than in the SV or ED are rare and may indicate systemic disease.

Design: We queried the pathology database at two academic institutions for prostate specimens which showed amyloid, confirmed by Congo red stain. Amyloid in the SV or ED was excluded. When possible, mass spectrometry analysis was performed for amyloid subtype. We reviewed the patients' electronic medical records for prior or subsequent diagnosis of systemic amyloidosis and clinical course.

Results: Prostatic amyloidosis was identified in 32 patients from 2009-2021. Median age at time of diagnosis was 75 years (range 60-84). Most (n=24) were prostate biopsies, whereas 5 were prostatectomies, 2 were transurethral resections, and 1 was a cystoprostatectomy. Almost all (29 of 32) were new diagnoses of amyloidosis, 2 patients had known cardiac ATTR amyloidosis and 1 had nerve ATTR amyloidosis with carpel tunnel syndrome (CTS). From one institution, 13/14 were diagnosed by a single pathologist. The distribution of amyloid was as follows: 23 perivascular, 4 perivascular and stromal, and 5 stromal. Of the 32 patients, 21 patients had available clinical follow-up. Half (n=16) had prostatic adenocarcinoma (PCa), whereas amyloid was found with only benign tissue in the other half. Subtyping revealed ATTR in 10 patients, 5 of which had cardiac involvement. Of these, 2 received cardiac transplantation. Monoclonal gammopathy of uncertain significance was found in 2 patients. One had an IgG lambda plasma cell neoplasm at bone marrow examination, 2 had non-Hodgkin lymphoma, and 1 patient was found to have AL amyloid. Overall, 31% (10/32) had a clinically significant diagnosis. Of the 32 patients, 3 were deceased (1 found to have systemic amyloidosis at autopsy, 2 due to malignancy other than PCa), and 29 were alive at most recent follow up. Four had a clinical history of CTS.

Conclusions: Amyloidosis in prostatic tissues is likely underdiagnosed and was more common in biopsy tissue, possibly due to the tendency to evaluate these specimens at higher magnification. Identification of amyloid in non-SV or ED tissues may be an

impactful diagnosis, as shown by a subset of patients who were subsequently confirmed to have hematologic neoplasms, cardiac amyloidosis, and either death or heart transplantation.

599 Clear Cell Renal Cell Carcinoma with Syncytial-type Multinucleated Giant Tumor Cells and Emperipolesis: A Review of 125 cases of Clear Cell Renal Cell Carcinomas

Luiz Nova-Camacho[1], Ander Ezkurra-Altuna[2], Carlos Barbarin[2], Nerea Segues[2], Angel Panizo[3]
[1]Hospital Universitaio Donostia - Osakidetza, Donostia-San Sebastian, Spain, [2]Hospital Universitaio Donostia - Osakidetza, San Sebastian-Donostia, Spain, [3]Complejo Hospitalario de Navarra, Pamplona, Spain

Disclosures: Luiz Nova-Camacho: None; Ander Ezkurra-Altuna: None; Carlos Barbarin: None; Nerea Segues: None; Angel Panizo: None

Background: Clear cell renal cell carcinoma (CCRCC) typically demonstrates characteristic histologic features that facilitate its recognition morphologically. The presence of syncytial-type multinucleated giant tumor cells and emperipolesis in CCRCC is extremely rare with only 31 cases published to date.

Design: We carried out a retrospective study of CCRCC from the files of our hospital over a period of 10 years (2010-2020). We re-examined 125 cases of CCRCC (G3-G4 ISUP grade) searching for a syncytial-type multinucleated giant tumor cells component with/without emperipolesis. Clinical data were review and microscopic examination of files slides was supplemented with immunohistochemistry (Cytokeratin AE1/AE3, EMA, CD10, carbonic anhydrase IX, vimentin, CD68, β-human chorionic gonadotropin, TFE3, cathepsin K, Cytokeratin 7, Cytokeratin 20, HMB45, C-KIT) analysis using paraffin-embedded tissue.

Results: We found fourteen cases of CCRCC that exhibited these components. The mean age of the patients was 66.8 years, with no sex differences. Tumor size ranged from 3.8 to 12 cm. Four patients had recurrence/metastasis. Two patients died because of the disease, one is alive with the disease, and eight are alive with no evidence of the disease; three cases have no data available. Microscopically all tumors had at least a component of low-grade CCRCC. The component of syncytial-type multinucleated giant tumor cells showed eosinophilic voluminous cytoplasm and numerous nuclei. The percentage of this component varied between 2 – 20%. Other findings included emperipolesis (85.71%), necrosis (71.43%), and hyaline globule (71.43%). Three (21.43%) cases showed a sarcomatoid component and four (28.57%) cases had rhabdoid differentiation. Eight (57.14%) cases were stage pT3, four (28.57%) cases were pT1, one case (7.14%) was pT2, and one (7.14%) case was pT4. Immunohistochemical (IHC) staining typically revealed that most of these cells were positive for cytokeratin AE1/AE3, EMA, CD10, carbonic anhydrase IX, and vimentin; and negative for CD68, β human chorionic gonadotropin, TFE3, cathepsin K, Cytokeratin 7, Cytokeratin 20, HMB45 and C-KIT.

Conclusions: The presence of a syncytial-type multinucleated giant tumor cell component in clear cell renal cell carcinomas is associated with aggressive behavior. The IHC study is a helpful tool to confirm an epithelial linage similar to usual CCRCC, and facilitates discrimination from trophoblastic or histiocytic differentiation, epithelioid angiomyolipoma, and other tumors.

600 Clinical, Pathological, and Molecular Features of Papillary Renal Cell Neoplasm with Reverse Polarity: A Review of 196 Papillary Renal Cell Carcinomas

Luiz Nova-Camacho[1], Maialen Arruti[2], Juan Garces[2], Katti Perez de Heredia[2], Nerea Segues[2], Angel Panizo[3]
[1]Hospital Universitaio Donostia - Osakidetza, Donostia-San Sebastian, Spain, [2]Hospital Universitaio Donostia - Osakidetza, San Sebastian-Donostia, Spain, [3]Complejo Hospitalario de Navarra, Pamplona, Spain

Disclosures: Luiz Nova-Camacho: None; Maialen Arruti: None; Juan Garces: None; Katti Perez de Heredia: None; Nerea Segues: None; Angel Panizo: None

Background: Papillary renal cell neoplasm with reverse polarity (PRNRP) is a recently described entity of renal tumor that differs clinically, morphologically, and molecularly from papillary renal cell carcinoma (PRCC). To date about 100 cases of PRNRP have been reported.

Design: We carried out a retrospective study of PRCC type 1 and 2 from the files of our hospital over a period of 20 years (2000-2020). From 196 re-examined nephrectomy specimens of PRCC, we selected those that exhibited a tumor morphology consistent with papillary renal cell neoplasm with reverse polarity (prominent thin papillary architecture, oncocytic cytoplasm, and apically localized nuclei). Clinical and pathological data were review in detail, and the expression of CK7, EMA, PAX-8, CD10, AMACR,

vimentin, L1CAM, and GATA-3 by immunohistochemistry (IHC) were evaluated using paraffin-embedded tissue. A search for KRAS gene mutation was performed using the Idylla KRAS mutation test (Biocartis, Mechelen, Belgium), a CE-IVD labelled, fully automated, real-time PCR-based molecular diagnostics system that allows characterization of predefined hot-spot mutations in exons 2, 3, and 4 of KRAS.

Results: We found seven cases consistent with papillary renal cell neoplasm with reverse polarity. The median age of the patients was 64.2 years, six patients were males, and one was female. Two patients had end-stage renal disease. No recurrence, metastasis, or tumor-related death occurred in a mean follow-up period of 72.1 months (range 12-144 months). Tumor size ranged from 1.5 to 3.7 cm. All cases of PRNRP were pT1. Six cases showed cystic changes, and one had solid areas. No foamy cells, clear cells change, or psammoma bodies were seen (Fig. 1A-1D). The IHC analysis revealed diffuse positive staining of CK7, EMA, PAX8, nuclear GATA3 (Fig. 1E) and membranous L1CAM (Fig. 1F); and weak or negative staining of CD10, AMACR and vimentin. KRAS gene mutation was detected in five (71.4%) cases. These KRAS mutation types were G12V (2 cases), G12D (1 case), G12S (1 case), and Q61K (1 case).

Figure 1 - 600

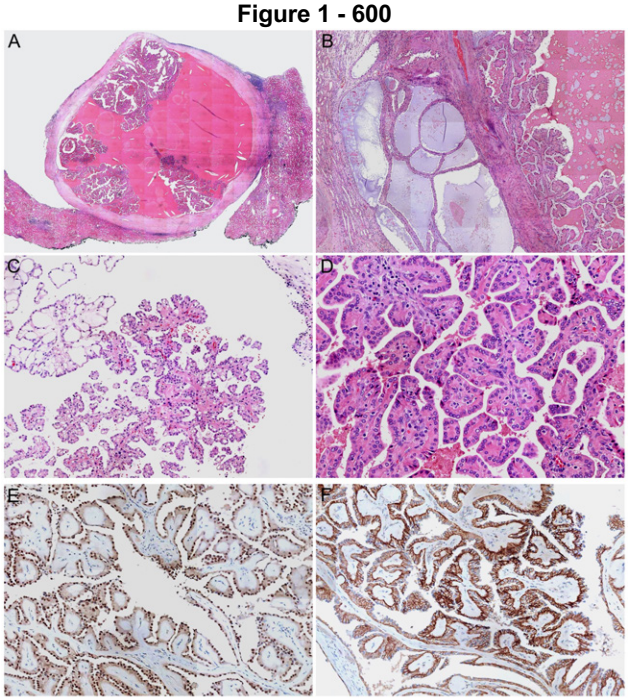

Conclusions: Papillary renal cell neoplasm with reverse polarity represents 3.57% of PRCC in our study. PRNRP is a distinct and rare entity with characteristic morphological features and frequent mutation in KRAS genes. The positivity of GATA3 and L1CAM support that this tumor arises from the distal renal ducts. Our findings support that PRNRP has an indolent clinical behavior according to the data published to date.

601 The Clinical Significance of Either Extraprostatic Extension or Microscopic Bladder Neck Invasion Alone vs. Both in Men with pT3a Prostate Cancer Undergoing Radical Prostatectomy

Numbereye Numbere[1], Yuki Teramoto[1], Ying Wang[1], Hiroshi Miyamoto[1]
[1]University of Rochester Medical Center, Rochester, NY

Disclosures: Numbereye Numbere: None; Yuki Teramoto: None; Ying Wang: None; Hiroshi Miyamoto: None

Background: The presence of extraprostatic extension (EPE) or microscopic bladder neck invasion (mBNI) is classified as pT3a in the current staging system for prostate cancer. However, pT3a disease does not uniformly indicate a poor prognosis, and further risk stratification is required. We herein compare radical prostatectomy (RP) findings and long-term oncologic outcomes in patients with pT3a prostate cancer exhibiting either EPE or mBNI vs. both.

Design: We assessed consecutive patients who had undergone RP from 2009-2013. Within our Surgical Pathology database, we identified a total of 483 men with pT3a disease without neoadjuvant therapy.

Results: The patient cohort consists of 4 groups: G1) focal EPE (F-EPE) only (n=99; 20%); G2) nonfocal/established EPE (E-EPE) only (n=331; 69%); G3) mBNI only (n=17; 4%); and G4) both EPE and mBNI (n=36; 8%). Compared with G1, G2 showed significantly higher tumor grade and significantly larger tumor volume. Similarly, G4 had significantly higher incidence of positive margins and adjuvant therapy immediately after RP, as well as significantly larger tumor volume, compared with G2 or G1-G3. In addition, preoperative prostate-specific antigen (PSA) level was significantly higher in G2 (vs. G1) or G4 (vs. G2 or G1-G3). Kaplan-Meier analysis revealed significantly higher risks of disease progression following RP in E-EPE only patients (vs. F-EPE only, *P*=0.003) or EPE/mBNI patients (vs. E-EPE only, *P*=0.006; or mBNI only, *P*=0.007). There were no significant differences in progression-free survival (PFS) between F-EPE and mBNI (*P*=0.789) as well as between E-EPE and mBNI (*P*=0.092). Overall, patients with both EPE and mBNI had a significantly higher risk of progression than those with either EPE or mBNI (*P*<0.001). These significant differences in PFS were also seen in subgroups of patients, such as those with (n=65; *P*=0.016) or without (n=418; *P*=0.006) adjuvant therapy and those with pN0 disease (n=388; *P*<0.001). In multivariate analysis with Cox model in the entire cohort, EPE/mBNI (vs. EPE or mBNI only) showed significance for progression (HR 1.965, 95%CI 1.166-3.311, *P*=0.011).

	G1: F-EPE(+) mBNI(-) (n=99)	G2: E-EPE(+) mBNI(-) (n=331)	G3: EPE(-) mBNI(+) (n=17)	G4: EPE(+) mBNI(+) (n=36)	P (G1 vs G2)	P (G2 vs G4)	P (G1-3 vs G4)
Age (mean, year)	63.5	63.2	61.5	61.8	0.690	0.261	0.254
PSA (mean, ng/mL)	6.3	8.3	7.2	15.2	<0.001	0.011	0.007
Grade Group					<0.001[a]	0.382[a]	0.862[a]
1	3 (3%)	0 (0%)	0 (0%)	0 (0%)			
2	68 (69%)	165 (50%)	15 (88%)	21 (58%)			
3	19 (19%)	105 (32%)	2 (12%)	10 (28%)			
4	5 (5%)	31 (9%)	0 (0%)	1 (3%)			
5	4 (4%)	30 (9%)	0 (0%)	4 (11%)			
pN					0.113[b]	0.350[b]	0.189[b]
0	79 (80%)	272 (82%)	10 (59%)	27 (75%)			
1	3 (3%)	29 (9%)	1 (6%)	5 (14%)			
X	17 (17%)	30 (9%)	6 (35%)	4 (11%)			
Lymphovascular invasion					0.059	1.000	1.000
Absent	94 (95%)	291 (88%)	17 (100%)	32 (89%)			
Present	5 (5%)	40 (12%)	0 (0%)	4 (11%)			
Surgical margin					0.250	<0.001	<0.001
Negative	84 (85%)	263 (79%)	8 (47%)	10 (28%)			
Positive	15 (15%)	68 (21%)	9 (53%)	26 (72%)			
Tumor volume (mean, cc)	7.2	9.4	5.6	14.2	<0.001	0.009	0.003
Adjuvant therapy					0.166	0.033	0.014
Not performed	91 (92%)	285 (86%)	16 (94%)	26 (72%)			
Performed	8 (8%)	46 (14%)	1 (6%)	10 (28%)			
[a] GG1-2 vs. GG3-5; [b] pN0 vs. pN1							

Figure 1 - 601

Figure 1. Progression-free survival in all patients.

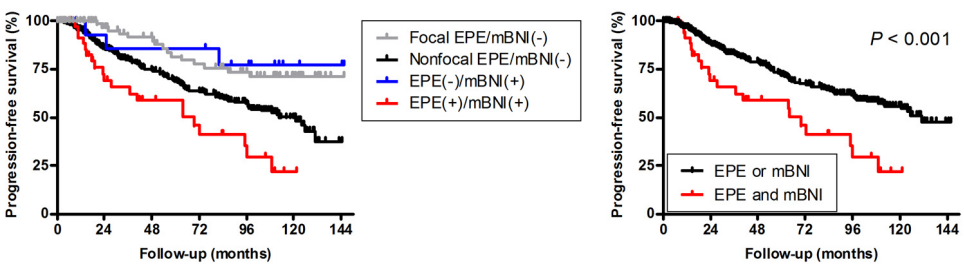

Figure 2 – 601

Figure 2. Progression-free survival in subgroups of patients.

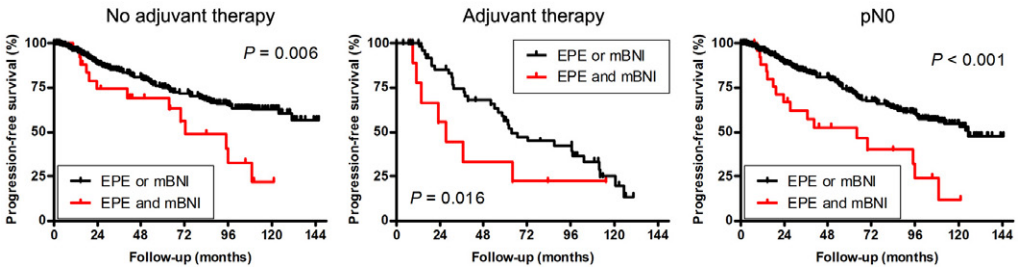

Conclusions: We confirmed the prognostic value of F-EPE vs. E-EPE in pT3a prostate cancer. More strikingly, the presence of both EPE and BNI, as an independent predictor, was found to be associated with worse patient outcome, compared with EPE or mBNI alone. These findings support the importance of specifying the presence or absence of F-EPE/E-EPE, as well as mBNI, on RP showing pT3a disease.

602 The Clinical Significance of pT3a Lesions as Well as Unilateral vs. Bilateral Invasion into the Seminal Vesicle in Men with pT3b Prostate Cancer Undergoing Radical Prostatectomy: A Proposal for a New pT3b Subclassification

Numbereye Numbere[1], Yuki Teramoto[1], Ying Wang[1], Hiroshi Miyamoto[1]
[1]University of Rochester Medical Center, Rochester, NY

Disclosures: Numbereye Numbere: None; Yuki Teramoto: None; Ying Wang: None; Hiroshi Miyamoto: None

Background: Seminal vesicle invasion (SVI) by prostate cancer has been considered as a key prognosticator. However, pT3b disease does not uniformly indicate poor outcomes, and further risk stratification is required. The present study aims to determine the clinical impact of pT3a lesions [*i.e.* extraprostatic extension (EPE), microscopic bladder neck invasion (mBNI)], as well as unilateral (Uni) vs. bilateral (Bil) SVI, in patients with pT3b prostate cancer.

Design: We assessed consecutive patients who had undergone radical prostatectomy (RP) from 2009-2018. Within our Surgical Pathology database, we identified a total of 248 men with pT3b disease without undergoing neoadjuvant therapy prior to RP.

Results: Of possible combinations of the presence or absence of EPE (focal/nonfocal), mBNI, and Uni-SVI/Bil-SVI (see Figure 1), we eventually divided our patient cohort into 4 groups: G1) Uni/Bil-SVI & EPE(-)/mBNI(-) (n=28; 11%); G2) Uni-SVI & either EPE or mBNI (n=103; 42%); G3) Bil-SVI & either EPE or mBNI (n=70; 28%); and G4) Uni/Bil-SVI & EPE(+)/mBNI(+) (n=47; 19%). When RP findings (*e.g.* tumor grade, LVI, surgical margin status, estimated tumor volume, lymph node metastasis) were compared, significant differences between G2 and G3 were observed. In addition, G4 showed higher levels of PSA, a higher rate of positive margins, and larger tumor volume, compared with G3. Kaplan-Meier analysis revealed that the prognosis was worse in the following order: G1, G2, G3, and G4; and that the differences in progression-free survival (PFS) between any two groups were statistically significant. Significant differences in PFS were also seen in subgroups of patients, such as those without (n=139; G1 vs. G2) or with (n=109; G2 vs. G3) adjuvant therapy immediately after RP and those with pN0 (n=153; G1 vs. G2, G2 vs. G3) or pN1 (n=93; G3 vs. G4) disease. In multivariate analysis with Cox model in the entire cohort (G1 as a reference), G2 (HR=9.089, *P*=0.031), G3 (HR=16.39, *P*=0.007), and G4 (HR=27.56, *P*=0.002) showed significance for progression. Moreover, when G3 and G4 are combined (*i.e.* G1 vs. G2 vs. G3/G4), differences in RP findings and PFS rates were more significant.

	G1: Uni/Bil-SVI EPE(-)/mBNI(-) (n=28)	G2: Uni-SVI EPE or mBNI (n=103)	G3: Bil-SVI EPE or mBNI (n=70)	G4: Uni/Bil-SVI EPE & mBNI (n=47)	P (G1 vs G2)	P (G2 vs G3)	P (G3 vs G4)
Age (mean, year)	66.2	64.5	63.8	63.4	0.224	0.485	0.791
PSA (mean, ng/mL)	9.2	10.0	10.8	26.8	0.561	0.589	0.034
Grade Group					0.821[a]	0.007[a]	0.570[a]
2	7 (25%)	20 (19%)	7 (10%)	4 (9%)			
3	13 (46%)	50 (49%)	26 (37%)	15 (32%)			
4	2 (7%)	5 (5%)	6 (9%)	4 (9%)			
5	6 (21%)	28 (27%)	31 (44%)	24 (51%)			
pN					0.479[b]	0.037[b]	0.706[b]
0	22 (79%)	71 (69%)	37 (53%)	23 (49%)			
1	6 (21%)	31 (30%)	32 (46%)	24 (51%)			
X	0 (0%)	1 (1%)	1 (1%)	0 (0%)			
LVI					0.159	0.009	0.568
Absent	26 (93%)	83 (81%)	43 (61%)	26 (55%)			
Present	2 (7%)	20 (19%)	27 (39%)	21 (45%)			
Surgical margin					0.593	0.023	<0.001
Negative	24 (86%)	82 (80%)	44 (63%)	6 (13%)			
Positive	4 (14%)	21 (20%)	26 (37%)	41 (87%)			
Tumor volume (mean, cc)	10.1	13.1	20.1	34.3	0.088	<0.001	<0.001
Adjuvant therapy					0.666	0.209	0.135
Not performed	19 (68%)	65 (63%)	37 (53%)	18 (38%)			
Performed	9 (32%)	38 (37%)	33 (47%)	29 (62%)			
PSA, prostate-specific antigen; LVI, lymphovascular invasion							
[a] GG2-3 vs. GG4-5; [b] pN0 vs. pN1							

Figure 1 - 602

Figure 1

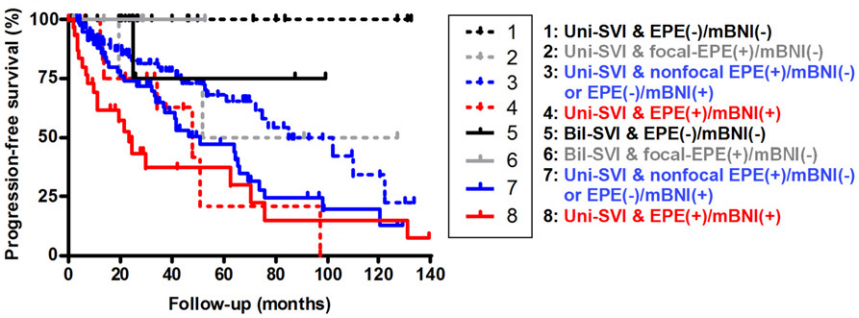

Figure 2 – 602

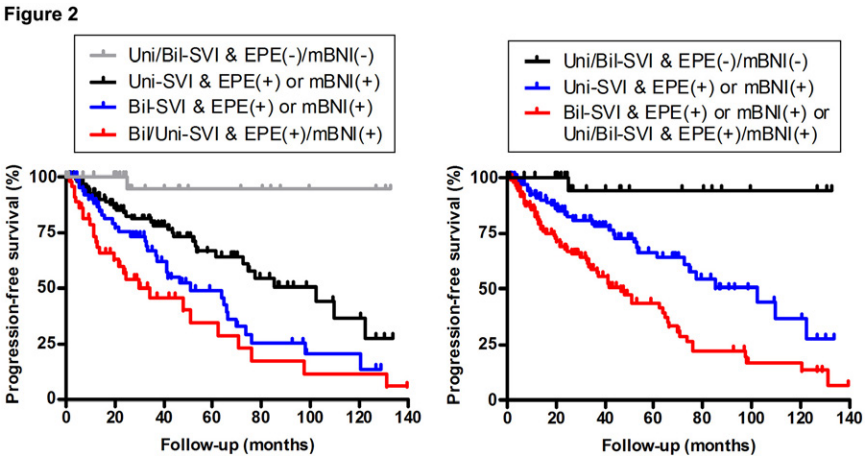

Conclusions: We believe these data provide a logical rationale for a novel subclassification, pT3b1 (G1), pT3b2 (G2), and pT3b3 (G3/G4) [or pT3b3 (G3)/pT3b4 (G4)], which more accurately stratifies the prognosis of pT3b prostate cancer. Further studies in larger patient cohorts, ideally prospectively designed, are warranted to validate our results.

603 Diagnostic Utility Focusing on Clear and Eosinophilic Cytoplasmic Features of Clear Cell Renal Cell Carcinoma

Chisato Ohe[1], Takashi Yoshida[2], Mahul Amin[3], Naho Atsumi[2], Yoshiki Yasukochi[2], Junichi Ikeda[2], Koichiro Higasa[2], Koji Tsuta[2]

[1]Kansai Medical University, Osaka, Japan, [2]Kansai Medical University, Hirakata, Japan, [3]The University of Tennessee Health Science Center, Memphis, TN

Disclosures: Chisato Ohe: *Speaker*, AstraZeneca; *Grant or Research Support*, Chugai Pharmaceutical; *Speaker*, Janssen Pharmaceutical; *Speaker*, Merck Biopharma; Takashi Yoshida: None; Mahul Amin: *Advisory Board Member*, Ibex; *Consultant*, Google/Verily; *Advisory Board Member*, Precipio, Cell Max; Naho Atsumi: None; Yoshiki Yasukochi: None; Junichi Ikeda: *Speaker*, Janssen Pharmaceutical; *Speaker*, Astellas Pharma; Koichiro Higasa: None; Koji Tsuta: *Speaker*, MSD, Roche, Novartis, Janssen Pharmaceutical K.K; *Grant or Research Support*, Ono Pharmaceutical Co., Ltd; *Speaker*, AstraZeneca

Background: Clear cell renal cell carcinoma (ccRCC) displays heterogeneous histological features. We have recently shown that histological phenotypes based on cytoplasmic features, such as clear, mixed, and eosinophilic correlate with survival outcomes and the response to angiogenesis and checkpoint blockade in ccRCC patients. The present study aimed to ascertain whether a deep learning approach can be applied in the recognition of histological phenotypes and to validate the utility of histological phenotypes using The Cancer Genome Atlas (TCGA) cohort.

Design: Histological phenotypes, such as clear, mixed, and eosinophilic, were determined using H&E-stained slides at the highest-grade area. A total of 99 tumor-rich areas, corresponding to the region of each histological phenotype, were sampled, and the correlation between human and computer analyses was examined. Moreover, 162 ccRCC cases available from the TCGA cohort were validated for the association of histological phenotypes with gene expression signatures and prognoses.

Results: Artificial intelligence (AI) scores significantly correlated with clear, mixed, and eosinophilic histological phenotypes assessed by a pathologist ($p<0.001$). Regarding the histological phenotypes, 72 (44%) patients with the clear type, 76 (47%) with the mixed type, and 14 (9%) with the eosinophilic type were observed. In the gene expression analysis using the RNA sequencing data of the TCGA cohort, angiogenesis gene signature scores were significantly higher in the clear type than in the mixed and eosinophilic types ($p=0.003$), whereas immune checkpoint gene signature scores were significantly lower in the clear type than in the mixed and eosinophilic types ($p=0.014$). Kaplan-Meier survival curve stratified histological subtypes of ccRCC by the patient outcome in the TCGA cohort.

Figure 1 - 603

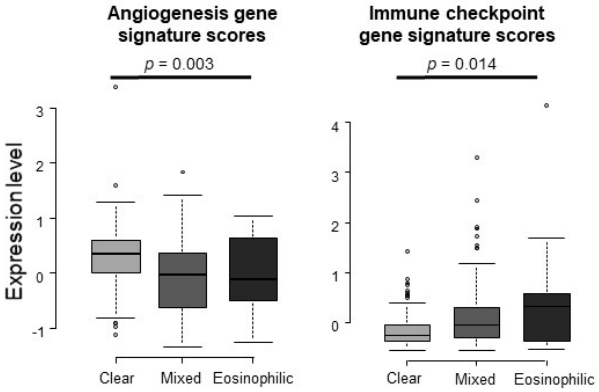

Figure 2 - 603

Figure 2: Kaplan-Meier curve of overall survival (TCGA cohort)

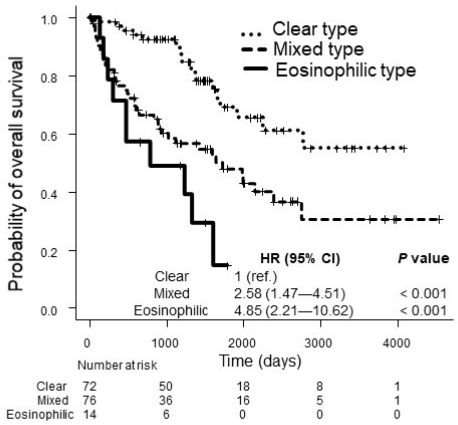

Conclusions: We successfully applied a deep learning approach to assess the histological phenotypes of ccRCC and shown an association of the histological phenotypes with gene expression signatures and prognoses. Methodology assessing cytoplasmic features of ccRCC based on highest grade is simple and can be incorporated in AI algorithms to evaluate angiogenesis and cancer immunity, as well as the oncological outcome.

604 Do African American (AA) have more Aggressive Prostate Cancer (PCa) Diagnosed by Multiparametric Magnet Resonance Imaging (mpMRI) Combined with Fusion Biopsy: Our Institutional Experience in a Racially Mixed Population

Oluwayomi Oyedeji[1], Daniel Schultz[1], Nilesh Gupta[1], Oudai Hassan[1]
[1]Henry Ford Health System, Detroit, MI

Disclosures: Oluwayomi Oyedeji: None; Daniel Schultz: None; Nilesh Gupta: None; Oudai Hassan: None

Background: Multiparametric magnet resonance imaging (mpMRI) combined with fusion biopsy is a novel approach with the goal of increased accuracy of detection of clinically significant prostate cancer (PCa). The aim of this study is to compare the findings of mpMRI between African Americans (AA) and European Americans (EA) in our institution.

Design: All patients who underwent fusion biopsy at our institution between 2015-2021 are included. Pathological findings including tumor grade and tumor size in the lesion of interest (LOI) were collected from our pathology archives. Clinical information including age, mpMRI findings and PSA density were collected from medical records. Statistical analysis was performed using chi square test and T-test.

Results: 390 patients were included in our cohort. 279 (71.6%) EA, 82 (21%) AA and 29 (7.4%) were labeled as other races. Median age was 67 (43, 89), median PSA level was 5.8 ng/ml (0.2, 61), median PSA density was 0.12 (0.03, 1.46). Median number of total combined cores was 16 (9, 58). Median number of LOIs biopsied was 1 (1,5). Median number of cores per LOI was 4 (1, 13). Median largest tumor focus in LOI was 6 mm (0.2, 37). There was no significant association between race and the highest Gleason score (GS) or largest tumor focus in the LOI. There was also no significant association between race and PSA density. (table 1)

Highest Gleason score at LOI							
Study groups	No tumor(%)	(3=3) (%)	(3+4) (%)	(4+3) (%)	(4+4) (%)	Any 5 (5)	P-value
EA	101 (36.2)	39 (13.89)	82 (29.39)	36 (12.9)	8 (2.87)	13 (4.66)	0.15
AA	28 (34.15)	11 (13.41)	19 (23.17)	11 (13.41)	8 (9.76)	5 (6.1)	
Largest tumor size at LOI							
Study groups	Less than 1 mm(%)		1-5 mm (%)	6-10 mm (%)	More than 10 mm (%)		P-value
EA	18 (10.06)		59 (32.96)	73 (40.78)	29 (16.2)		0.4
AA	8 (14.8)		19 (35.2)	18 (33.33)	9 (16.7)		

Conclusions: The majority of men who had mpMRI had PCa in their LOIs with 182 (50.4%) showing clinically significant PCa (GS 7 or higher) in their LOIs. Race was not an independent predictor of GS or size in LOI. African American do not have more aggressive prostate cancer diagnosed by mpMRI.

605 Multinucleated Tumor Cells In Clear Cell Renal Cell Carcinoma Are Present In All Nuclear Grades

Richard Pacheco[1], Arkar Htoo[1], Tipu Nazeer[2], Andrea Lightle[1], Mahmut Akgul[1]
[1]Albany Medical Center, Albany, NY, [2]Albany Medical College, Albany, NY

Disclosures: Richard Pacheco: None; Arkar Htoo: None; Tipu Nazeer: None; Andrea Lightle: None; Mahmut Akgul: None

Background: Multinucleated tumor cells (MTCs) are occasionally present in clear cell renal cell carcinoma CCRCC with otherwise lower International Society of Urologic Pathology (ISUP) nuclear grade (1-3, Figure 1) and how they impact the prediction of the tumor behavior or patient outcome is unclear.

Design: Patients whom underwent nephrectomy (partial or total) in years between 2010-2018 with the diagnosis of CCRCC were included to the study. Patient's age at the time of diagnosis, gender, and tumor size were recorded. Hematoxylin-eosin slides of the specimens were reviewed (MA) and pathological stage (TNM, American Joint Committee on Cancer) and ISUP nuclear grade were determined. Multinucleation was used to detect MTC rather than as a grading feature. Comparison between CCRCC with and without MTCs was performed using Student's t-test and the Mann-Whitney U test when indicated. Comparisons for categorical variables were performed using the Chi-square test and Fisher's exact test when indicated. Spearman's rank correlation coefficients (r_s) were computed to assess the relationship between multinucleation and several covariates. A *p*-value <0.05 was considered statistically significant.

Results: Table 1 summarizes all findings. A total of 220 patients (Male/Female=145/75) with resected CCRCC (73 partial, 127 total) were identified, with median age of 62 (range 29-90 years). Median tumor size was 4.1 cm (range 0.8-21 cm). The most common pathological tumor stage was pT1a (n=92, 42%), and 154 (70%) of the cases tumor was confined to kidney (

The number of tumors with ISUP nuclear grade 1, 2, 3 and 4 were 21 (10%), 101 (46%), 80 (36%), and 18 (8%), respectively. MTCs were present in 86 (39%) of CCRCC, and ISUP nuclear grade 1, 2, 3, and 4 CCRCC had 2 (%), 35, 34, and 15 CCRCC with MTCs. There was a significant association with CCRCC with MTCs and higher ISUP nuclear grade (p<0.001) as well as the tumor size (p<0.001). Among ISUP nuclear grade 1-3, MTCs were associated with advanced stage (≥pT3a or N1 or M1) in only ISUP nuclear grade 3 CCRCC (<0.007). In CCRCC with ISUP nuclear grade 1 and 2, MTC was not significantly associated with adverse stage (1, p=0.095;2, p=0.196)

TABLE 1	**CCRCC without MTCs**		**CCRCC with MTCs**		**P value**
ISUP Nuclear Grade	N (%)		N(%)		
1	19 (90)		2 (10)		**<0.001**
2	66 (65)		35 (35)		
3	46 (57)		34 (43)		
4	3 (17)		15 (83)		
ISUP Nuclear Grade	Organ confined	Advanced disease	Organ confined	Advanced disease	
1	19 (100)	0	1 (50)	1 (50)	0.095
2	51 (77)	15 (23)	27 (77)	23 (23)	0.196
3	37 (80)	9 (20)	17 (50)	17 (50)	**0.007**
pTNM Stage (AJCC 8th Ed)					

Organ confined	108 (81)	48 (56)	**<0.001**
Advanced	26 (19)	38 (44)	
Size (cm)			
Mean (median, range)	4.2 (3.5, 0.8-14.7)	6.8 (5.5, 1.6-21.0)	**<0.001**
AJCC, American Joint Committee on Cancer; CCRCC, clear cell renal cell carcinoma; ISUP, International Society of Urologic Pathology; MTCs, multinucleated tumor cells; Organ Confined (			

Figure 1 - 605

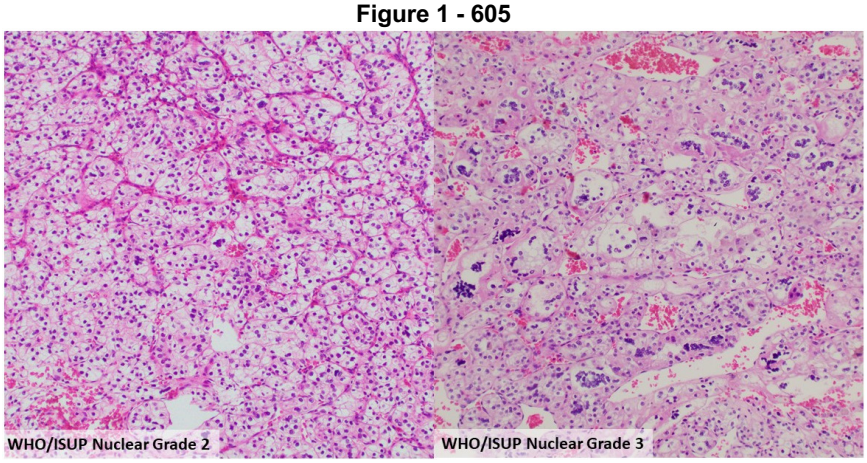

Conclusions: MTCs can be seen in all ISUP nuclear grades in CCRCC and may not be associated with higher tumor stage in ISUP nuclear grade 1 and 2 tumors. Studies with larger cohorts are required to determine whether MTCs in lower ISUP nuclear grade CCRCC are innately present or an indication of adverse features.

606 Comparative Genomics Study of 7,739 Clinically Advanced Urothelial Cancers Reveals Unique Genomic Profile of Aggressive Neuroendocrine Carcinoma of the Bladder (NEBC)

Vamsi Parimi[1], Natalie Danziger[2], Ryon Graf[1], Douglas Lin[2], Naomi Lynn Ferguson[3], Karthikeyan Murugesan[2], Brennan Decker[2], Douglas Mata[2], Ethan Sokol[2], Matthew Hiemenz[2], Shakti Ramkissoon[4], Mia Levy[5], Julia Elvin[2], Richard Huang[6], Jeffrey Ross[7]

[1]Foundation Medicine, Inc., RTP, NC, [2]Foundation Medicine, Inc., Cambridge, MA, [3]Foundation Medicine, Inc., NC, [4]Foundation Medicine, Inc., Morrisville, NC, [5]Foundation Medicine, Inc., Boston, MA, [6]Foundation Medicine, Inc., Cary, NC, [7]SUNY Upstate Medical University, Syracuse, NY

Disclosures: Vamsi Parimi: *Employee*, Foundation Medicine Inc.; Natalie Danziger: *Employee*, Foundation Medicine Inc.; *Stock Ownership*, F. Hoffman La Roche Ltd.; Ryon Graf: None; Douglas Lin: *Employee*, Foundation Medicine, Inc.; *Stock Ownership*, Roche; Naomi Lynn Ferguson: *Employee*, Foundation Medicine; *Stock Ownership*, Foundation Medicine; Karthikeyan Murugesan: *Employee*, Foundation Medicine; *Stock Ownership*, Roche Holdings AG; Brennan Decker: *Employee*, Foundation Medicine; *Stock Ownership*, Roche; Douglas Mata: *Employee*, Foundation Medicine, Inc.; *Speaker*, Astellas Pharma, Inc.; Ethan Sokol: *Employee*, Foundation Medicine; *Stock Ownership*, Roche; Matthew Hiemenz: *Employee*, Foundation Medicine / Roche; *Employee*, Foundation Medicine / Roche; Shakti Ramkissoon: None; Mia Levy: None; Julia Elvin: *Employee*, Foundation Medicine; *Stock Ownership*, Hoffmann-La Roche; Richard Huang: *Employee*, Foundation Medicine; *Employee*, Roche; Jeffrey Ross: *Employee*, Foundation Medicine

Background: Small-cell urothelial carcinoma, which constitutes most NEBC, is a rare morphologic variant of bladder associated with unique histology and an aggressive clinical course. Current NCCN guidelines recommend neoadjuvant platinum/etoposide ± immune checkpoint inhibitors followed by radical cystectomy/radiotherapy for NEBC, which differs from the recommended treatment for conventional urothelial bladder carcinoma (UBC). We performed comprehensive genomic profiling (CGP) on a series of clinically advanced NEBC and compared the landscape of genomic alterations (GAs) to that identified in a series of 7,739 UBC.

Design: All 245 cases (small-cell NEC=234, and large-cell NEC=11) underwent tissue-based hybrid capture CGP. Tumor mutational burden (TMB) was determined on up to 1.1 Mb of sequenced DNA, and microsatellite instability (MSI) was determined on 95 loci. PD-L1 positivity was determined by DAKO 22C3 pharmDx IHC using a combined positive score (CPS) ≥10 cut-off. The diagnosis of NEBC was confirmed by central pathology review and neuroendocrine IHC marker status.
Pathogenic *RB1* and *TP53* inactivation included nonsense, deletions, splice-site, and frameshift alterations.

Results: Dual *RB1/TP53* inactivation was more frequent in the NEBC cohort, and *CDKN2A/B* deletions were rare (p<0.0001 for both). A similar pattern was seen for pathogenic mutations involving either *RB1* or *TP53* alone (p<0.0001 for both) (Table 1). PD-L1 positivity (53%) and *FGFR1/2/3* variants (17%) were more common among UBC vs. NEBC (p<0.0001). NEBC and UBC had similar frequencies of high TMB, with 34% of cases featuring TMB ≥10 Mut/Mb. Potentially "targetable" GAs, including those in *FGFR3*, *ERBB2*, *TSC1*, and *MTAP*, were more frequent among UBC compared to NEBC (p<0.0001). *MYCL1*, *PTEN, RICTOR, FGF10,* and *MCL1* GAs were significantly higher in the NEBC tumors, whereas *KDM6A*, *CCND1*, *FGF19/4/3*, and *MDM2* GAs were found at a higher frequency among UBC (Figure 1).

Figure 1 - 606

Table 1.	UBC	NEBC	p value
Number of Cases	7739	245	
Median age in years (range)	70 [62-70]	69 [62-76]	0.21
Males/Females	5667/2072 (73%/27%)	196/49 (80%/20%)	0.019
Ancestry: European/Non-European	6524/1215 (84%/16%)	201/44 (82%/18%)	0.33
PDL1+	1342 (n=2538) (53%)	11 (n=47) (23%)	<0.0001
TMB, median, mut/Mb [IQR]	6.3 [3.8-12.2]	7.0 [3.6-11.3]	0.76
TMB>10	2596 (34%)	84 (34%)	0.84
MSI-H	62 (1%)	1 (<1%)	1
APOBEC	2320 (30%)	73 (30%)	1
Gene Alterations			
FGFR1/2/3, SV or fusion (no amps)	1325 (17%)	2 (1%)	<0.0001
SV	1026	1	
Fusion	220	1	
Multiple	78	0	
RB1 alteration	1603 (21%)	191 (78%)	<0.0001
RB1 loss	1323 (17%)	162 (66%)	<0.0001
nonsense*	569 (43%)	67 (41%)	0.74
frameshift*	399 (30%)	44 (27%)	0.47
splice site*	60 (4.5%)	6 (3.7%)	0.84
deletion*	210 (16%)	35 (21%)	0.07
multiple*	85 (6.4%)	10 (6.2%)	1.00
TP53 alteration	4765 (62%)	225 (92%)	<0.0001
TP53 loss	1538 (20%)	77 (31%)	<0.0001
nonsense*	854 (56%)	35 (45%)	0.10
frameshift*	492 (32%)	26 (34%)	0.80
splice site*	47 (3.1%)	6 (7.8%)	0.04
deletion*	88 (5.7%)	6 (7.8%)	0.45
multiple*	56 (3.6%)	4 (5.2%)	0.53
Dual *TP53* loss/*RB1* loss	357 (5%)	58 (24%)	<0.0001

*reported as % of cases with gene loss

Figure 2 – 606

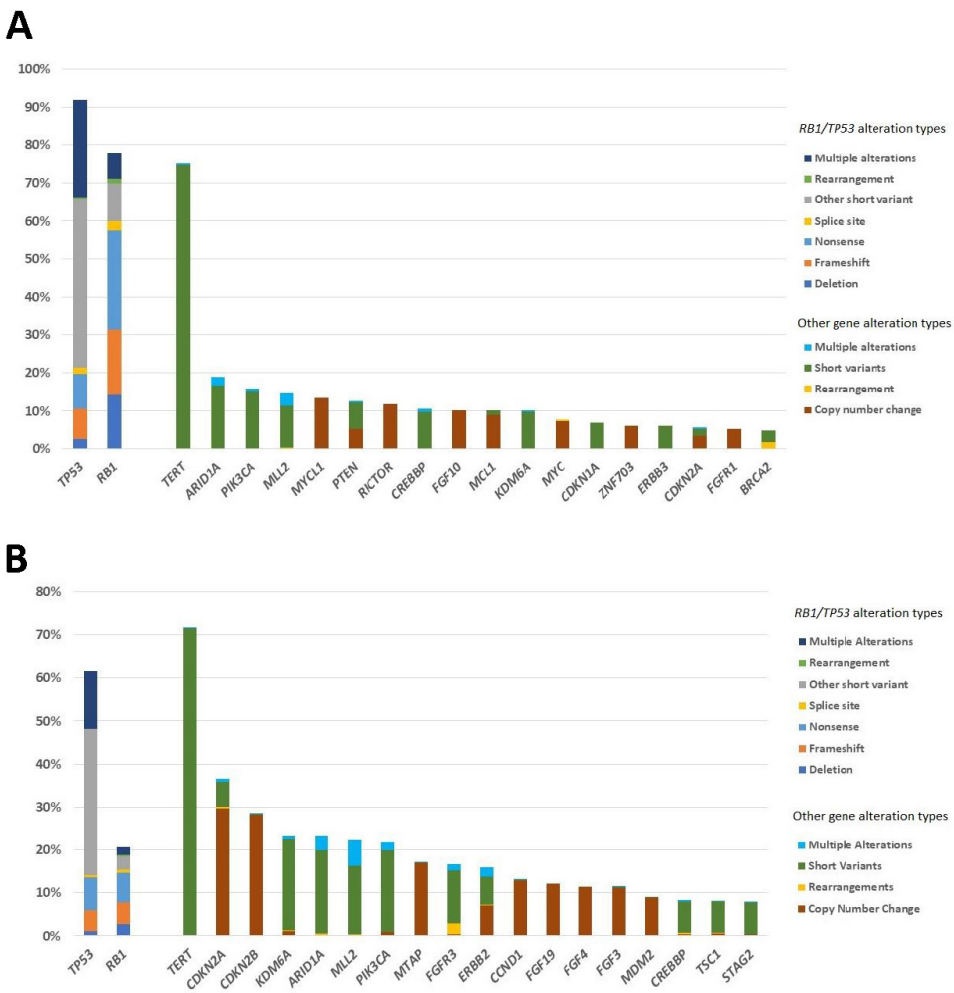

Figure 1. A. Longtail showing the landscape of gene alterations in the 20 most frequently mutated genes in the neuroendocrine bladder carcinoma cohort. **B.** Longtail showing the landscape of gene alterations in the 20 most frequently mutated genes in the urothelial bladder carcinoma cohort.

Conclusions: When compared with UBC, NEBC exhibits unique histology and a characteristic GA profile. NEBC is characterized by higher dual *RB1* and *TP53* GAs and lower potentially "targetable" therapy options. The double-hit *RB1/TP53* inactivation may be a genomic biomarker for neuroendocrine differentiation and the clinical aggressiveness of NEBC. Further studies are needed to determine whether *RB1/TP53* co-mutation is an independent prognostic biomarker in UBC and whether this finding can be leveraged to improve diagnostic interpretation in liquid biopsy.

607 Kidney Tumor Classifier Using Whole Genome Methylation Array

Kyung Park[1], Jonathan Serrano[2], Fei Chen[1], Ivy Tran[3], Varshini Vasudevaraja[4], Deepthi Hoskoppal[5], Fang-Ming Deng[4], Matija Snuderl[2]

[1]NYU Langone Health, New York, NY, [2]New York University, New York, NY, [3]New York University Langone Health, NY, NY, [4]New York University Medical Center, New York, NY, [5]New York University Langone Medical Center, New York, NY

Disclosures: Kyung Park: None; Jonathan Serrano: None; Fei Chen: None; Ivy Tran: None; Varshini Vasudevaraja: None; Deepthi Hoskoppal: None; Fang-Ming Deng: None; Matija Snuderl: None

Background: More than 15 distinct subtypes of renal cell carcinomas (RCCs) are recognized and the number is increasing. Histologic evaluation is the most important and effective tool to classify RCCs; however, overlapping morphologic and

immunohistochemical profiles are often encountered. In this pilot study, we attempt to investigate the methylation patterns in multiple RCC subtypes and test if differential patterns can be correlated with histologic diagnoses.

Design: Sixty-four renal tumors were collected; 13 clear cell, 14 papillary, 9 chromophobe, 8 clear cell papillary, 9 oncocytoma, and 11 oncocytic neoplasms. Tumor FFPE DNA was profiled using the Illumina MethylationEPIC array. Methylation data was analyzed with the R Bioconductor package minfi. Subsequent filtering was performed using a p-value cutoff = 0.01 and a minimum mean difference of the Beta-value of 0.1. Clustering was performed using tSNE analysis.

Results: Unsupervised clustering clearly distinguishes between tumors believed to be derived from proximal tubule (clear cell and papillary) and those from more distal origin (oncocytoma and chromophobe) (Figure 1). Oncocytoma and chromophobe RCCs are located in close proximity illustrating their close relationship and will require more samples for differentiation. Heatmap of top 100 probes highlights differential methylation between clear cell/papillary and oncocytoma/chromophobe (Figure 2). Pathway analysis shows enrichment for Rap1 signaling pathway in RCCs.

Figure 1 - 607

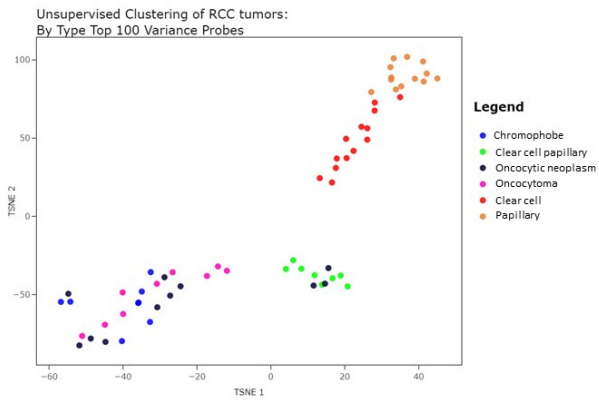

Figure 2 – 607

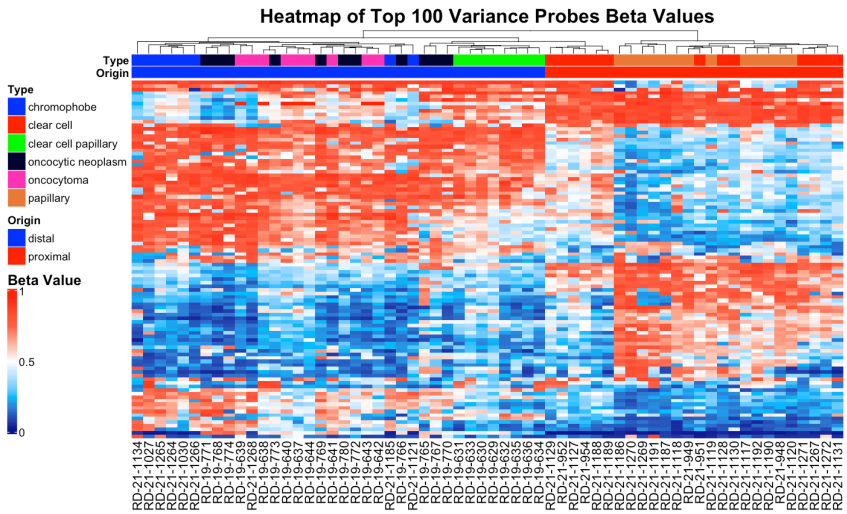

Conclusions: This preliminary cohort of RCCs demonstrate that methylation can be used as a diagnostic classifier. A more refined classifier system will help diagnostically challenging cases requiring FISH/IHC or unclassified category of RCCs.

608 Methylation Profiling of Papillary Renal Neoplasm with Reverse Polarity

Kyung Park[1], Jonathan Serrano[2], Ivy Tran[3], Xiaojun Feng[1], Fei Chen[1], Varshini Vasudevaraja[4], Leili Mirsadraei[5], Matija Snuderl[2], Fang-Ming Deng[4]

[1]NYU Langone Health, New York, NY, [2]New York University, New York, NY, [3]New York University Langone Health, NY, NY, [4]New York University Medical Center, New York, NY, [5]NYU Langone Health/NYU Winthrop Hospital, Mineola, NY

Disclosures: Kyung Park: None; Jonathan Serrano: None; Ivy Tran: None; Xiaojun Feng: None; Fei Chen: None; Varshini Vasudevaraja: None; Leili Mirsadraei: None; Matija Snuderl: None; Fang-Ming Deng: None

Background: Papillary renal neoplasm with reverse polarity (PRNRP), previously called oncocytic papillary renal cell carcinoma (RCC), has been recently proposed as a distinct subtype of renal cell neoplasm. PRNRP is characterized by its morphologic features and recurrent KRAS mutations. In this study, we attempt to characterize PRNRP using DNA sequencing and methylation array.

Design: Eight PRNRPs and one papillary adenoma with classic PRNRP features (both morphology and immunoprofile) are collected. Five samples were sequenced using NYU Langone Genome PACT, a FDA cleared next generation sequencing platform. Four samples were sequenced using Oncomine Focus Assay (Thermo Fisher Scientific). Tumor FFPE DNA from all 9 samples was profiled using the Illumina MethylationEPIC array. Methytaion data was analyzed with the R Bioconductor package minfi. Clustering was performed using tSNE analysis. Methylation clustering pattern was compared with other common renal cell neoplasms (including clear cell RCC, papillary RCC, clear cell papillary RCC, chromophobe RCC, and oncocytoma). Copy numbers were analyzed using conumee package.

Results: Targeted DNA sequencing confirmed that all samples harbored KRAS mutations: 5 G12V and 3 G12D in PRNRPs. The papillary adenoma with PRNRP morphology measuring 0.3 cm had G12V mutation. Unsupervised clustering demonstrated that PRNRPs formed a tight group on tSNE and were distant from papillary RCCs while close to clear cell papillary RCCs (Figure 1). Heatmap of top 100 probes also showed that PRNRPs were a distinct subtype (Figure 2). No significant copy number alterations were detected in PRNRPs.

Figure 1 - 608

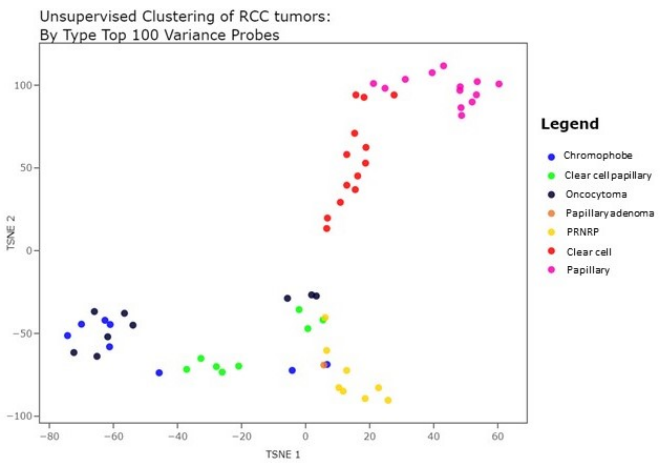

Figure 2 – 608

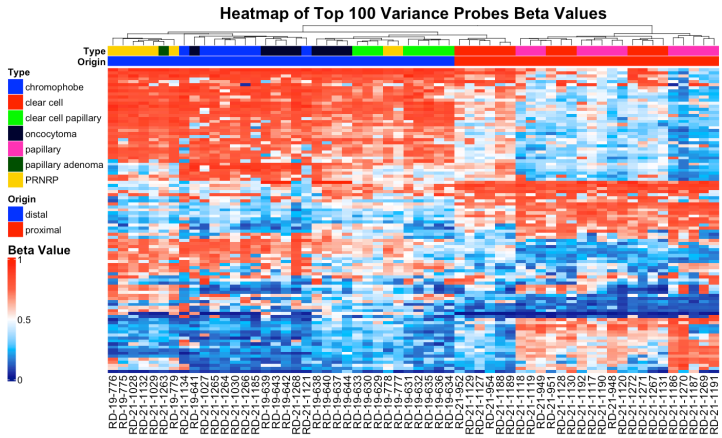

Conclusions: Molecularly, PRNRP is a unique renal cell neoplasm defined by KRAS mutations and methylation patterns. KRAS mutation is an early event in this tumor type as illustrated by the small papillary adenoma. Methylation studies suggest that PRNRP is different from papillary RCC and may arise from the distal renal tubular epithelium.

609 Systematic Screening of Upper Tract Lynch Syndrome-Related Urothelial Carcinoma: Analysis of 162 Patients from a Single European Institution

Kristyna Pivovarcikova[1], Tomas Pitra[2], Karolina Buchova[2], Reza Alaghehbandan[3], Petr Steiner[4], Ivan Subrt[2], Michal Michal[1], Ondrej Hes[1]

[1]Biopticka laborator s.r.o., Plzen, Czech Republic, [2]Charles University Hospital Plzen, Plzen, Czech Republic, [3]Royal Columbian Hospital, University of British Columbia, Vancouver, Canada, [4]Biopticka laborator s.r.o., Znojmo, Czech Republic

Disclosures: Kristyna Pivovarcikova: None; Tomas Pitra: None; Karolina Buchova: None; Reza Alaghehbandan: None; Petr Steiner: None; Ivan Subrt: None; Michal: None; Ondrej Hes: None

Background: Upper tract urothelial carcinomas (UTUC) associated with Lynch syndrome (LS) are well- documented. The current guidelines of urologic societies usually recommend to screen patients for LS up to 65 years of age. In this study, we examined patients with UTUC for potential association with LS at Charles University Faculty of Medicine in Pilsen, Czech Republic.

Design: A total of 162 patients with UTUC were screened by immunohistochemistry for mismatch repair proteins (MMRp) - MSH6, MSH2, PMS2, MLH1. Patients with loss of MLH1 and PMS2 staining were further tested for *MLH1* promoter methylation status. Patient with loss of MSH6 and MSH2 expression as well as patients with loss of MLH1 and PMS2 without MLH1 promoter methylation were referred to genetic counselling and germ line mutations testing. Personal history of patients with established LS were also analyzed (i.e, other neoplasms) (Fig 1).

Results: Patients included 102 males and 60 females, with age range 32-89 (mean 69.1, median 71 years). Loss of one or more MMRp was identified in 12 of 162 patients, of whom 5 were confirmed LS (3%). Patients with LS were 3 females and 2 males, with age range 46-75 (mean 66.2, median 71 years). The male patients in this cohort were 71 and 73 years, while the females were 66, 75 and 46 years. Tumors were located in ureter in 3 cases and in the renal pelvis in 2 cases. All LS-related UTUC showed low pathologic stage (4x pT1, and 1x pTa). 3 of 5 patients had low-grade UTUC (grade 2 WHO 1973), and the remaining 2 cases were high-grade (grade 2 and 3 WHO 1973). In 3 patients with LS, other malignancy was documented in anamnesis (colorectal adenocarcinoma, follicular lymphoma, and endometrial adenocarcinoma).

Figure 1 - 609

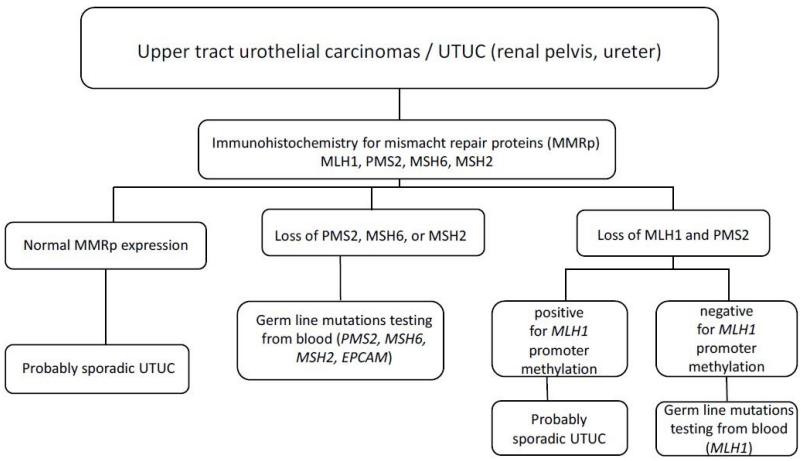

Conclusions: UTUC is a common malignancy in LS and can be the first clinical manifestation in such setting, as is in our study (2/5 patients had no previous malignancy history). Mean age of patients with LS-related UTUC in our study (66,2 years; 3/5 patients older than 70 years) raises the need to revisit the current guidelines on age cutoff (<65 years) in screening hereditary UTUC.

610 PROGNOSIS Factors of Papillary Renal Cell Carcinoma: a Comprehensive Clinicopathological and Genetic Study of a Monocentric Cohort Including Metastatic Cases

Fanny Reinhart[1], Marc-Olivier Timsit[2], Léa Collignon[2], Chloe Broudin[3], Anne-Paule Gimenez-Roqueplo[2], Arnaud Mejean[4], Nelly Burnichon[2], Virginie Verkarre[2]
[1]Hôpital Européen Georges Pompidou, APHP, Paris, France, [2]APHP.5 Hôpital Européen Georges Pompidou; INSERM UMR970, Paris Descartes University, Paris, France, [3]HEGP, Chatillon, France, [4]APHP.5 Hôpital Européen Georges Pompidou; Paris Descartes University, Paris, France

Disclosures: Fanny Reinhart: None; Marc-Olivier Timsit: None; Léa Collignon: None; Chloe Broudin: None; Anne-Paule Gimenez-Roqueplo: None; Arnaud Mejean: None; Nelly Burnichon: None; Virginie Verkarre: None

Background: *Papillary renal cell carcinoma (PRCC) accounts for 15% of renal cell carcinoma. Metastatic cases occurring in 6-10% are a major concern for patient care. To optimize follow up and treatment of PRCC, further identification of prognosis factors and druggable pathways is required.*

Design: We performed a comprehensive clinicopathological and genetic analysis of a large monocentric retrospective cohort of primary PRCC patients who have benefited from a nephrectomy at Georges Pompidou European hospital from 2010 to 2020. After reviewing slides, immunohistochemistry was performed using TMA from FFPE samples with 14 antibodies targeting FH, SMARCB1, SMARCA4, TFE3, MET, BAP1, PBRM1, 4-EBP1-P, S6K-P, PDL1, CD3, CD8, CD163 and CD20. Somatic genetic analysis was performed on primary PRCC of metastatic patients by NGS using an in-house panel (Twist Bioscience®) including 29 genes involved in renal tumorigenesis.

Results: Our cohort included 242 patients/316 PRCC (SR: 4.9/1; mean age: 61.2 (24 to 87)) treated by partial or total nephrectomy (67%/33%). After a mean follow-up of 37.4 month (1 to 133), 10.3% (25/242) of patients carrying 32 PRCC developed metastases either synchronous (n=11) or metachronous (n=14) at mean interval of 11.8 months (3 to 35). Stage pT3-4, pN1, grade 4, sarcomatoid/rhabdoid tumors and extended necrosis were significantly higher in the metastatic group compared with the non-metastatic group (Table). In the metastatic group, the immune microenvironment was statistically enriched in lymphocytic infiltrate and tertiary lymphoid structures and exhibited a weak infiltrate of foamy macrophages. Expression of PDL1 on tumoral cells (TC) were higher. Metastatic tumors showed more loss of P16 without loss or overexpression of other markers. On 24 primary PRCC metastatic (1 type 1, 7 type 2, 2 mixed, 12 unclassified and 1 biphasic), we identified pathogenic or likely pathogenic somatic variants in 58% (14/24) of tumors (multiple variants in 8 cases) involving *SMARCB1* and *NF2* in 16% each (n=4), *MET*, *BAP1* and *VHL* in 12.5% each (n=3), *SETD2* and *PBRM1* in 8.3% each (n=2) and *FH*, *KDM6A*, *TP53*, *TSC1* and *TSC2* in 4.2% (n=1).

	M+ P=25/T=32	M- P=217/T=284	p
Age	63,5 (24-87)	60,9 (51-86)	
Type of variant			
Type 1 PRCC	5 (15.6%)	114 (40.1%)	0.0066
Type 2 PRCC	8 (25%)	50 (17.6%)	0.3348
Mixed PRCC	2 (6.3%)	26 (9.2%)	0.7526
Biphasic alveolo squamoid PRCC	5 (15.6%)	31 (10,9%)	0.3868
Oncocytic PRCC	0	19 (6.7%)	0.2362
Unclassifiable PRCC	12 (37.5%)	44 (15.5%)	0.0054
Stage at diagnosis			
pT1	10 (31.2%)	236 (83,1%)	**<0.0001**
pT2	3 (9.4%)	20 (7%)	0.7158
pT3	16 (50%)	28 (9.9%)	**<0.0001**
pT4	3 (9.4%)	0	**<0.0010**
Statut pN1	9 (37.5%)	0	**<0.0001**
WHO/ISUP Grade			
1-2	5 (15.6%)	133 (46.8%)	0.0006
3	13 (40.6%)	132 (46.5%)	0.5783
4	14 (43.8%)	19 (6.7%)	**<0.0001**
Sarcomatoid component	11 (34.4%)	15 (5.3%)	**<0.0001**
% Sarcomatoid	31.8% (10.90%)	13% (5-30%)	
Rhabdoid component	4 (12.5%)	2 (0.7%)	**<0.0011**
Tumor necrosis			
0	5 (15.6%)	148 (52.2%)	**<0.0001**
<50%	9 (28.1%)	89 (31.3%)	<0.8411
³ 50%	18 (56.3%)	47(16.5%)	**0.0001**
Intratumoral immune infiltrate			
Lymphocytes absence 0	3 (9.4%)	47 (16.5%)	0.4425
Lymphocytes intensity 1	19 (59.4%)	217 (76.5%)	0.0515
Lymphocytes intensity 2	10 (3.2%)	20 (7%)	**0.0002**
Foamy macrophages 0	17 (53,1%)	51 (18%)	**0.0001**
Foamy macrophages intensity 1/2	14 (43,8%)	186 (65.5%)	0.0200
Foamy macrophages intensity 3	1 (3,2%)	47 (16.5%)	0.0641
Macrophages	10 (31.2%)	56 (19.7%)	0.1660
Neutrophils	4 (12.5%)	27 (9.5%)	0.5357
Tertiary lymphoid structure	7 (21.9%)	13 (4.6%)	**0.0017**
Immunohistochemistry :			
P16	19/31 (61,3%)	212/257 (82.5%)	**0.0002**
PDL-1 TC/ IC			
% of + PDL-1 TC	11/30 (36.7%)	36/244 (14.8%)	**0.0001**
Number of + PDL-1 TC /mm2	77.1	31.9	
% of + PDL-1 IC	10/27 (37%)	57/226 (25,2%)	0.0566
Number of + PDL-1 IC/mm^2	5,4	2,4	

Conclusions: Our study has highlighted new predictive parameters of metastatic evolution in PRCC in addition to stage and grade such as the immune microenvironment and loss of P16 expression. It also suggests that *SMARCB1* and *NF2* tumor mutations could be associated with metastatic disease and subsequently used as targets for therapy.

611 Global Grade on MRI-targeted Prostate Biopsies Correlates Better than Highest Grade to Radical Prostatectomy Specimens

Joyce Ren[1], Jonathan Melamed[2], Fang-Ming Deng[3]
[1]NYU Langone Health, New York, NY, [2]New York University, New York, NY, [3]New York University Medical Center, New York, NY

Disclosures: Joyce Ren: None; Jonathan Melamed: None; Fang-Ming Deng: None

Background: Magnetic resonance imaging (MRI) targeted prostate biopsy has become an increasingly common method of diagnosing prostate cancer. Previous study from our institution demonstrates the biopsy global Gleason grade (gGG) and highest Gleason grade (hGG) show substantial concordance with the radical prostatectomy Gleason grade (RPGG) while the discordance predominantly comprise of upgrading in gGG and downgrading in hGG. We performed a larger cohort focused analysis on the agreement of gGG and hGG to the RPGG when they differ.

Design: A retrospective review of radical prostatectomy specimens between 10/2016 and 12/2020 from our institution with prior MRI-targeted biopsies was conducted. A gGG (aggregate GG of all positive cores) and a hGG (highest GG in any core) was assigned to each MRI-targeted lesion. Only cases with different gGG versus hGG were selected for further analysis. The concordance of gGG and hGG with RPGG was evaluated using kappa coefficient analyses. The power of pre-biopsy PSA and PI-RADS scores to predict upgrading based on gGG was also analyzed.

Results: Of the 489 radical prostatectomy specimens with prior MRI-targeted biopsies, 82 cases (17%) differed in gGG versus hGG. Using the gGG, 33 cases (40%), 46 cases (56%), and 3 cases (4%) were upgraded, unchanged, and downgraded at radical prostatectomy, respectively (Kappa = 0.302, weighted Kappa = 0.334). Based on the hGG, 9 cases (11%), 24 cases (29%), and 49 cases (60%) were upgraded, unchanged, and downgraded at radical prostatectomy, respectively (Kappa = 0.040, weighted Kappa = 0.198) (Figure 1). When stratified by RPGG, gGG shows the best concordance in RPGG2 and RPGG3 lesions. The hGG resulted in substantial downgrading at RPGG4 or less and upgrading at RPGG5 (Figure 2). No significant difference in the mean PSA [H(2) = 5.89, p = 0.053] or PI-RADS score [H(2) = 4.48, p = 0.107] was found among the cases upgraded, unchanged, and downgraded based on the gGG. Neither the pre-biopsy PSA (OR = 1.92, 95% CI = 0.65-5.64, p = 0.117) nor the PI-RADS score (OR = 0.899, 95% CI = 0.31-2.607, p = 0.423) was predictive of upgrading based on gGG.

Table 1. Clinical Characteristics of MRI-targeted Prostate Biopsy Lesions (n = 82)

		Mean	SD	Range
Age (yrs.)		64.50	3.85	43-80
PSA (ng/mL)		9.34	9.32	1.8-74.24
PI-RADS		3.93	0.82	1-5
No. total cores		4.25	1.55	1-9
No. positive cores		4.04	1.48	1-9
		Number	Percentage (%)	
RPGG	1	0	0	
	2	27	32.9	
	3	35	42.7	
	4	10	12.2	
	5	10	12.2	

Figure 1 - 611

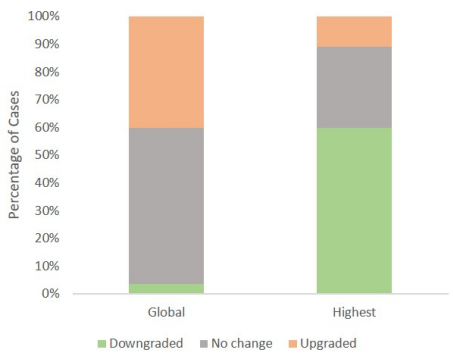

Figure 1. Concordance of Global Gleason Grade (gGG) and Highest Gleason Grade (hGG) with radical prostatectomy Gleason Grade in MRI-targeted lesions with different gGG and hGG.

Figure 2 - 611

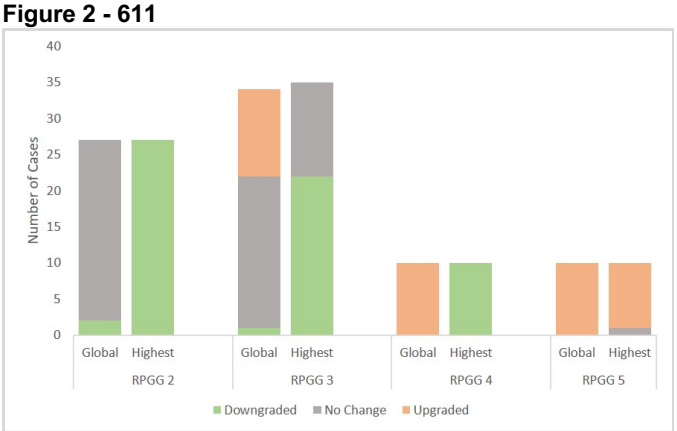

Figure 2. Concordance of Global Gleason Grade (gGG) and Highest Gleason Grade (hGG) with radical prostatectomy Gleason Grade stratified by RGPP.

Conclusions: When the gGG and hGG differ, the gGG correlates better with the RPGG than the hGG in the majority of cases for RPGG2 and RPGG3 lesions (46 cases, 74%). It results in upgrading in high grade lesions (GG4 and GG5) with potentially minimal impact on clinical management. Further studies are needed to substantiate a standard GG reporting method for MRI-targeted prostate biopsies.

612 Neuropilin-2 Expression as a Potential Marker to Predict Androgen Deprivation Therapy Outcome in Regional Node Positive Prostatic Adenocarcinoma

Pranav Renavikar[1], Sanika Bodas[1], Samikshan Dutta[1], Kaustubh Datta[1], Subodh Lele[1]
[1]University of Nebraska Medical Center, Omaha, NE

Disclosures: Pranav Renavikar: None; Sanika Bodas: None; Samikshan Dutta: None; Kaustubh Datta: None; Subodh Lele: None

Background: Regionally advanced prostate cancer (pN1) is managed with radical prostatectomy, radiation and androgen deprivation therapy (ADT). Despite the multiple modalities, biochemical recurrence is seen in some patients. Limited studies have addressed molecular or immunohistochemical markers that predict therapy resistance. NRP2 (neuropilin-2) is a transmembrane non-tyrosine kinase protein that serves as a co-receptor for plexins in neuronal cells and VEGFR in endothelial cells. Prior studies from our group have shown that NRP2 is frequently expressed in high grade prostate cancers, protects tumor cells from oxidative/therapy-induced stress, and correlates to poor survival. Additionally, we have shown that in certain high-grade tumors, NRP2 can translocate to the nuclear membrane to form a transcriptional complex with androgen receptors. Thus, we hypothesized that NRP2 expression and site of localization in tumor cells may determine treatment resistance to androgen deprivation in pN1 prostate cancer.

Design: 500 radical prostatectomies from our institutional database were screened. 6% patients had regional node positive disease (pN1). We included cases with any T stage and Gleason grade. All the cases had been signed out by one pathologist. Tumor tissues were stained for NRP2 (HPA039980, Sigma-Aldrich, USA) and follow up information was obtained to determine clinical course.

Results: Of the pN1 cases, 45% had Gleason score of 7, 40% had Gleason score of 9, and 15% did not have follow-up information. All Gleason score 7 cases were negative for NRP2. Of the Gleason score 9 cases, 50% were NRP2 cytoplasmic+, 8% were NRP2 nuclear+ and 42% were NRP2(-). Further, the 8% of Gleason score 9 cases (NRP2 nuclear+) had recurrent metastatic disease post radical prostatectomy with ADT resistance. The remaining 92% cases showed either complete remission with radical prostatectomy and pelvic dissection or were responsive to ADT post recurrence.

Conclusions: Our study demonstrates that NRP2 stains a subset of high-grade node positive prostate cancers. ADT responsive patients were either negative or showed cytoplasmic staining for NRP2. Importantly, nuclear staining corresponded to ADT resistance, directly indicating that translocation of NRP2 to the nuclear membrane may mediate the resistance. Further exploration of molecular differences in NRP2(+) and (-) tumors may help to mechanistically dissect the resistance pathways. Thus, NRP2 may be a valuable marker to predict outcome of ADT in pN1 prostate cancers.

613 Clinical Significance of Focal High-Grade Component in an otherwise Noninvasive Low-Grade Papillary Urothelial Carcinoma

Kasturi Saikia[1], Ejas Palathingal Bava[1], Shereen Zia[1], Shannon Rodgers[2], Siya Gupta[2], Daniel Schultz[1], Nilesh Gupta[1], Oudai Hassan[1]
[1]Henry Ford Health System, Detroit, MI, [2]Henry Ford Hospital, Detroit, MI

Disclosures: Kasturi Saikia: None; Ejas Palathingal Bava: None; Shereen Zia: None; Shannon Rodgers: None; Siya Gupta: None; Daniel Schultz: None; Nilesh Gupta: None; Oudai Hassan: None

Background: Introduction: The clinical significance of focal high-grade component in an otherwise noninvasive low grade papillary urothelial carcinoma (LGTCC) is not well understood. We looked at follow-up findings in patients diagnosed with focal noninvasive high-grade papillary urothelial carcinoma (fHG).

Design: All consecutive cases with the diagnosis of fHG in a transurethral resection of a bladder tumor (TURBT) performed at our institution between 2010-2018 were included. All cases with a previous diagnosis of noninvasive high-grade papillary urothelial carcinoma (HGTCC) or invasive urothelial carcinoma (INTCC) were excluded. All slides were reviewed by two pathologists (OH and KS) including one urologic pathologist (OH). Selected cases were reviewed by a second urologic pathologist (NSG). We divided the cohort based on the percentage of high-grade component (HG) into (5% or less HG, 10% or less HG, 15% or less HG). Anything with more than 15% HG was considered as HGTCC. Follow-up data was collected from our medical records. Statistical analysis was performed using the Chi square test.

Results: 56 patients were included. Median age was 70 (39-96). 44 patients were male and 12 were female. Follow-up period ranged between 2 and 84 months with a range between 1 and 7 follow-ups. 8 patients (14.3%) had no follow-up in our system and were excluded. Of the remaining 48 patient's follow-up showed INTCC in 2 (4.2%) patients, HGTCC in 23 (47.9%) patients, LGTCC in 8 (16.7%) patients, atypical cells in urine cytology in 5 (10.4%) patients and follow-up was negative in the remaining 10 (20.8%) patients. There was no statistically significant relationship between the percentage of HG and follow-up. (table 1)

Study groups	5% HG or less (%)	More than 5% HG (%)	10% HG or less (%)	More than 10% HG (%)	15% HG or less (%)	More than 15% HG (%)
INTCC or HGTCC ON FOLLOW UP	6 (12.5)	19 (39.6)	11 (23)	14 (29)	14 (29.1)	11 (23)
LGTCC/Atypical urine cells or negative follow up	5 (10.4)	18 (37.5)	12 (25)	11 (23)	15 (31.2)	8 (16.7)
P-value	0.85		0.57		0.5	

Conclusions: Previous studies have shown that the rate of progression of LGTCC into HGTCC or INTCC range between 4-10%. In our cohort of noninvasive papillary urothelial carcinoma with focal high-grade component, 52.1% of patients showed progression into INTCC or HGTCC. The percentage of HG was not related to progression rate. These findings suggest that noninvasive papillary urothelial carcinoma with focal high-grade component and noninvasive low-grade papillary urothelial carcinoma have different clinical course and noninvasive papillary urothelial carcinoma with focal high-grade component should be managed as noninvasive high-grade papillary urothelial carcinoma regardless of the percentage of HG.

614 Significant Geographic Variation in the Prevalence of HPV16 in Penile intraepithelial Neoplasia (PeIN). A Study of 172 International Cases from 4 Regions

Diego F Sanchez[1], Laia Alemany[2], Omar Clavero[3], María José Fernandez-Nestosa[4], Sofia Canete-Portillo[5], Silvia de Sanjosé[2], Nubia Munoz[6], Francesc Xavier Bosch[7], Wim Quint[8], Nuria Guimerà[9], Carlos Prieto Granada[5], Maria Del Carmen Rodriguez Pena[10], Jennifer Gordetsky[11], Melissa Hogan[11], Michael Orejudos[12], Jonathan Epstein[13], Tarik Gheit[14], Michael Herfs, Massimo Tommasino[14], Giovanna Giannico[11], Antonio Cubilla[1]

[1]Instituto de Patologia e Investigacion, Asuncion, Paraguay, [2]Institut Catala d'Oncologia, [3]Institut Catala d'Oncologia, Barcelona, Spain, [4]Universidad Nacional de Asunción, San Lorenzo, Paraguay, [5]The University of Alabama at Birmingham, Birmingham, AL, [6]National Cancer Institute of Colombia, [7]Catalan Institute of Oncology (ICO), [8]DDL Diagnostic Laboratory, [9]DDL Diagnostic Laboratory, Rijswijk, Netherlands, [10]Clinical Center, National Institutes of Health, Bethesda, MD, [11]Vanderbilt University Medical Center, Nashville, TN, [12]The Johns Hopkins Medical Institutions, [13]Johns Hopkins Medical Institutions, Baltimore, MD, [14]International Agency for Research on Cancer, France

Disclosures: Diego F Sanchez: None; Laia Alemany: None; Omar Clavero: None; María José Fernandez-Nestosa: None; Sofia Canete-Portillo: None; Silvia de Sanjosé: None; Nubia Munoz: None; Francesc Xavier Bosch: None; Wim Quint: None; Nuria Guimerà: None; Carlos Prieto Granada: None; Maria Del Carmen Rodriguez Pena: None; Jennifer Gordetsky: *Consultant*, Jansen; Melissa Hogan: None; Michael Orejudos: None; Jonathan Epstein: None; Tarik Gheit: None; Michael Herfs: None; Massimo Tommasino: None; Giovanna Giannico: None; Antonio Cubilla: None

Background: There is geographic variation in the prevalence of invasive penile carcinomas. The data on geographic distribution of penile precancerous lesions is limited. The majority of penile intraepithelial neoplasias (PeIN) are HPV-related, with a heterogeneous array of genotypes. Our aim was to compare the geographic distribution of PeIN HPV genotypes

Design: Geographical regions evaluated were Asia-Oceania, Europe, USA, and Latin America with 10, 52, 31 and 79 lesions, respectively. Only HPV-positive basaloid, warty-basaloid (WB) or warty PeINs were included. HPV-negative cases including differentiated PeIN or others were excluded (WHO 2016). HPV genotypes were determined by either whole tissue section PCR (99 lesions) or laser capture microdissection PCR (73 lesions), performed in 4 different laboratories. Statistical significance was evaluated using the Fisher's Exact Test with simulated p-value

Results: Overall, 16 HPV genotypes were detected **(Table)**. HPV16 was the most frequent genotype, prevailing in Asia-Oceania, USA and Europe and was less frequent in Latin America. HPV16 was found in solitary or coexisting with other genotypes in 87, 85, 80 and 48% of cases from USA, Europe, Asia-Oceania, and Latin America respectively, p-value = 5e-07 (Fig. 1, Multiple_HPV16 indicates positivity of HPV16 genotype along other HPV genotypes in the same lesion. Multiple_non_HPV16 is used to denote positivity for more than one HPV genotype and no HPV16 detection). Considering the nonavalent HPV vaccine genotypes, coverage would occur in 100, 90, 83 and 63% of lesions of Asia Oceania, Europe, USA, and Latin America, respectively (p-value = 0.0019) (**Fig. 2)**

Genotype	Total (%)	Asia Oceania (%)	Europe (%)	USA (%)	Latin America (%)
HPV11	3 (2)	0	0	0	3 (4)
HPV16	101 (59)	8 (80)	38 (73)	18 (58)	37 (47)
HPV18	6 (4)	0	0	2 (6)	4 (5)
HPV30	4 (2)	0	0	0	4 (5)
HPV31	1 (0.5)	0	1 (2)	0	0
HPV33	6 (4)	1 (10)	2 (4)	0	3 (4)
HPV35	2 (1)	0	0	0	2 (3)
HPV39	3 (2)	0	0	0	3 (4)
HPV44	1 (0.5)	0	0	0	1 (1)
HPV52	2 (1)	0	0	0	2 (3)
HPV56	11 (6)	0	0	0	11 (14)
HPV58	3 (2)	1 (10)	1 (2)	0	1 (1)
HPV61	1 (0.5)	0	0	0	1 (1)
HPV66	1 (0.5)	0	0	0	1 (1)
HPV73	1 (0.5)	0	0	0	1 (1)
HPV84	1 (0.5)	0	0	0	1 (1)
HPV87	1 (0.5)	0	0	0	1 (1)
Undetermined	2 (1)	0	2 (4)	0	0
Multiple_HPV16	16 (9)	0	6 (11)	9 (29)	1 (1)
Multiple_non_HPV16	6 (3)	0	2 (4)	2 (7)	2 (3)

Multiple_HPV16 indicates positivity of HPV16 genotype along other HPV genotypes in the same lesion. Multiple_non_HPV16 is used to denote positivity for more than one HPV genotype and no HPV16 detection.

Figure 1 - 614

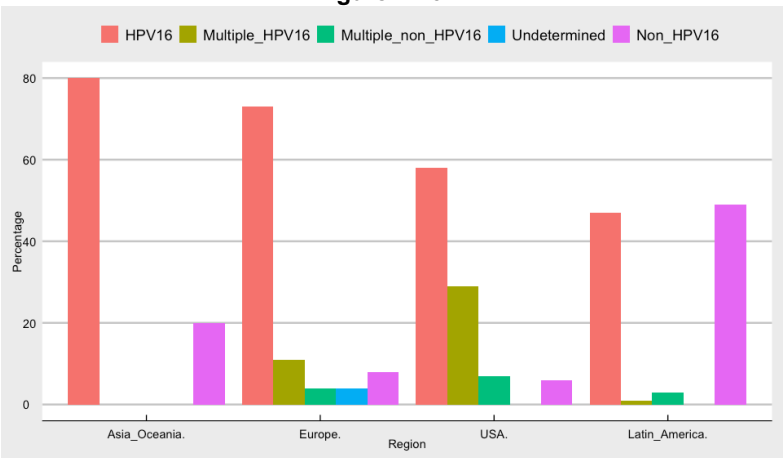

Figure 2 – 614

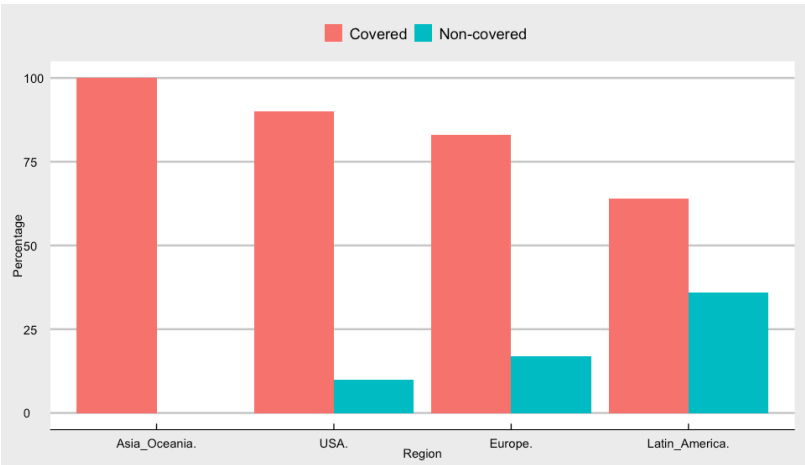

Conclusions: There were significant geographic differences in the distribution of HPV16. This genotype was more prevalent in all regions but Latin America. Variegated, non-HPV16 genotypes, were more prevalent in the latter. These differences may affect coverage of current vaccination programs. Non coverage would occur in 0, 10, 17, and 36% of cases in Asia-Oceania, USA, Europe, and Latin America, respectively. Further research with a more uniform methodology for HPV detection is needed for analyzing these trends

615 TNM Model in Penile Cancer: Stage-by-Stage Critical Revision and Proposal for Changes

Diego F Sanchez[1], Sofia Canete-Portillo[2], María José Fernandez-Nestosa[3], Ingrid Rodríguez Servín[4], Antonio Cubilla[1]
[1]Instituto de Patologia e Investigacion, Asuncion, Paraguay, [2]The University of Alabama at Birmingham, Birmingham, AL, [3]Universidad Nacional de Asunción, San Lorenzo, Paraguay, [4]Universidad Nacional de Asuncion, Asunción, Paraguay

Disclosures: Diego F Sanchez: None; Sofia Canete-Portillo: None; María José Fernandez-Nestosa: None; Ingrid Rodríguez Servín: None; Antonio Cubilla: None

Background: We recently analyzed and explained changes proposed in the 8th Edition of TNM staging for penile cancer. There was considerable improvement comparing with previous models. However, we identified problematic issues which need to be addressed in future manuals

Design: We identified stage-by-stage problems and proposed diverse approaches looking for solutions

Results: Problems identified and recommendation in different stages are shown in the table. Other factors identified are: A) the designation of invasion of preputial LP and dartos as the same stage is not based on evidence and it is contrary to our experience where LP invasion is not associated with tumor spread. B) There is emerging evidence that size may be an important prognostic factor, especially after exclusion of low-grade verruciform tumors from the analysis and it is not considered in the present staging model. C) Depth or tumor thickness may be more important than anatomical levels and it is not considered in the current model. D) There are insufficient studies to stage tumors exclusive of foreskin, coronal sulcus and shaft, comprising about a third of penile cancers, which is an important omission. E) The model does not consider tumor type as an automatic prognostic predictor (verrucous and pseudohypoerplastic carcinomas do not metastasize independently of depth of invasion). F) Detection of HPV, known to be associated with a better prognosis, is not considered in the current model

Stage/factor	Problem identified	Recommendation/solution proposal
pTis vs. pTa	Limits between in situ and noninvasive lesions are not well determined	Eliminate pTa
pT1 vs. pT2	There are not sharp boundaries between LP and CS.	Perform special stain for elastic fibers (orcein) (typical in CS; LP lacks organized elastic fibers) to identify precisely anatomical level involved.
pT2 vs. pT3	There are no studies evaluating outcome in tumors with only TA invasion.	Perform stain for elastic fiber (evident in CS but not in CC) for correct classification.
	The controversy of urethral invasion	Design and develop a study to evaluate outcome according to site of urethral invasion (proximal, medial distal).

LP: Lamina propria, CS: Corpus spongiosum, CC: Corpora cavernosa, TA: Tunica albuginea

Conclusions: We identified issues in every stage. Retrospectively generated data produce weak evidence. We suggest to prospectively design a staging model based on: complete sectioning of the surgical specimen; localizing the anatomical site of origin; gross and photographic evidence for tumor size and precise level of invasion; tumor thickness and depth of invasion for comparing with anatomical level of invasion identifying best predictor by anatomic site; evaluating the role of vascular and PNI according to anatomical levels; studying the histology of the anatomical levels at these sites using histochemistry or immunohistochemistry to delineate boundaries; evaluating significance of TA invasion and urethral invasion by site of tumor invasion; correct pathological classification of tumor types and tumor grading; use of p16 in known HPV-related tumors as well as in poorly differentiated carcinomas; at least 3-year follow up. We propose a critical evaluation and change of current staging model, according to the explained issues

616 Clear Cell Renal Cell Carcinoma with Psammomatous Calcifications: A Rare Occurrence Mimicking Translocation Carcinoma

Ankur Sangoi[1], Khaleel Al-Obaidy[2], Liang Cheng[3], Chia-Sui (Sunny) Kao[4], Emily Chan[5], Sudha Sadasivan[6], Isabel Alvarado-Cabrero[7], Lakshmi Kunju[8], Jasreman Dhillon[9], Maria Tretiakova[10], Steven Smith[11], Ondrej Hes[12], Sean Williamson[13]

[1]El Camino Hospital, Mountain View, CA, [2]Cleveland Clinic Foundation, Cleveland, OH, [3]Indiana University, Indianapolis, IN, [4]Stanford Medicine/Stanford University, Stanford, CA, [5]University of California, San Francisco, San Francisco, CA, [6]Henry Ford Health System, Detroit, MI, [7]Mexican Oncology Hospital SXXI, IMSS, Mexico City, Mexico, [8]University of Michigan, Ann Arbor, MI, [9]H. Lee Moffitt Cancer Center & Research Institute, Tampa, FL, [10]University of Washington, Seattle, WA, [11]VCU School of Medicine, Richmond, VA, [12]Biopticka laborator s.r.o., Plzen, Czech Republic, [13]Cleveland Clinic, Cleveland, OH

Disclosures: Ankur Sangoi: None; Khaleel Al-Obaidy: None; Liang Cheng: None; Chia-Sui (Sunny) Kao: None; Emily Chan: None; Sudha Sadasivan: None; Isabel Alvarado-Cabrero: None; Lakshmi Kunju: None; Jasreman Dhillon: None; Maria Tretiakova: None; Steven Smith: None; Ondrej Hes: None; Sean Williamson: None

Background: A renal neoplasm with clear cells and psammoma-like calcifications would often raise suspicion for MITF family translocation renal cell carcinoma (RCC). However, we have rarely encountered tumors that otherwise appear consistent with clear cell RCC, despite focal psammoma-like or punctate calcifications.

Design: We queried the archives of multiple institutions for tumors diagnosed as clear cell RCC with any psammoma-like or punctate calcification noted (excluding dystrophic calcification in fibrous stroma, Gamna-Gandy-like structures, or metaplastic bone formation). We studied these neoplasms with immunohistochemistry and fluorescence in situ hybridization (FISH).

Results: Twenty-one tumors were identified in 12 men and 9 women, age 45 to 85 (median 59). Tumor size was 2.3 to 14.0 cm (median 6.75). Nucleolar grade was 3 (n=14), 2 (n=4), or 4 (n=3). Calcifications were psammoma-like in 15 (Figure), punctate (not lamellated) and psammoma-like in 4, psammoma-like and ring-shaped in 1, and punctate in 1. Two also had calcification within necrosis. In addition to clear cell morphology, tumors contained eosinophilic cells (n=12), syncytial giant cells (n=4), rhabdoid features (n=2), branched glandular structures (n=1), early spindle cell change (n=1), and poorly differentiated morphology (n=1). Labeling for carbonic anhydrase 9 (CA9) was usually 80-100% of the tumor cells (n=17/21). Tumors with less than 100% CA9 labeling all contained eosinophilic cells and had a minimum of 50% labeling. Keratin 7 was either negative or labeled rare cells (n=20/20). Melan-A, HMB45, and cathepsin K were negative. Alpha-methylacyl-CoA racemase (AMACR) labeling ranged from 20-100% of tumor cells in 18/19 tumors, with intensity varying from weak to strong. CD10 typically labeled 75-100% of cells (n=15/18), or rarely 5-40% of cells (n=3/18). FISH was negative for *TFE3* (n=19) or *TFEB* rearrangement (n=12). Chromosome 3p25 loss was identified in 7/19 (37%). One of 19 had trisomy of chromosomes 7/17, but otherwise appeared a typical clear cell RCC with diffuse CA9 labeling.

Figure 1 - 616

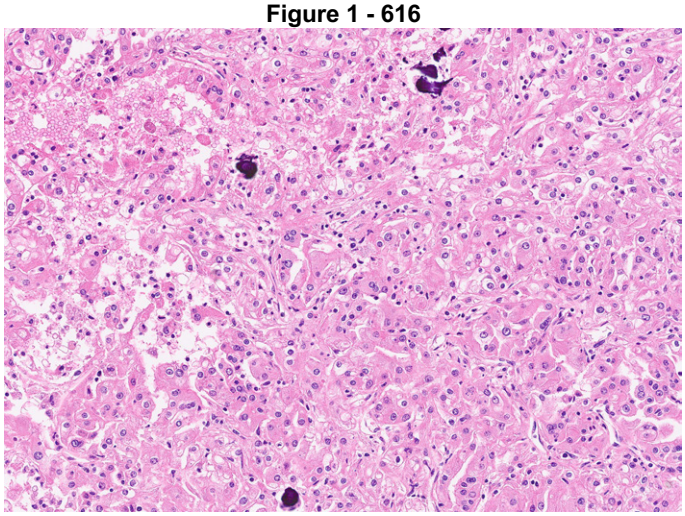

Conclusions: We conclude that rare true clear cell RCCs with punctate calcifications do occur, as evidenced by diffuse CA9 labeling, negative markers of translocation carcinoma, a substantial rate of chromosome 3p loss, and lack of *TFE3/TFEB* rearrangements.

617 Granulomas Associated with Renal Neoplasms: A Multi-Institutional Clinicopathologic Study of 92 Cases

Ankur Sangoi[1], Fiona Maclean[2], Reba Daniel[3], Priti Lal[3], Sofia Canete-Portillo[4], Cristina Magi-Galluzzi[4], Kristine Cornejo[5], Katrina Collins[6], Michael Hwang[7], Sambit Mohanty[8], Sara Falzarano[9], Michael Feely[10], Melad Dababneh[11], Lara Harik[11], Maria Tretiakova[12], Mahmut Akgul[13], Emily Chan[14], Varsha Manucha[15], Farshid Siadat[16], Kanika Arora[17], Guliz Barkan[18], Liang Cheng[19], Michelle Hirsch[20], Li Lei[21], Matthew Wasco[22], Sean Williamson[23], Andres Acosta[24]

[1]El Camino Hospital, Mountain View, CA, [2]Douglass Hanly Moir Pathology, Melbourne, Australia, [3]University of Pennsylvania, Philadelphia, PA, [4]The University of Alabama at Birmingham, Birmingham, AL, [5]Massachusetts General Hospital, Boston, MA, [6]Indiana University School of Medicine, Indianapolis, IN, [7]Indiana University Health, Indianapolis, IN, [8]Advanced Medical and Research Institute, Bhubaneswar, India, [9]University of Florida College of Medicine, Gainesville, FL, [10]University of Florida, Gainesville, FL, [11]Emory University School of Medicine, Atlanta, GA, [12]University of Washington, Seattle, WA, [13]Albany Medical Center, Albany, NY, [14]University of California, San Francisco, San Francisco, CA, [15]University of Mississippi Medical Center, Jackson, MS, [16]University of Calgary, Calgary, Canada, [17]Henry Ford Health System, Detroit, MI, [18]Loyola University Healthcare System, Maywood, IL, [19]Indiana University, Indianapolis, IN, [20]Brigham and Women's Hospital, Boston, MA, [21]UC Davis Health, CA, [22]St. Joseph Mercy Hospital, Ann Arbor, MI, [23]Cleveland Clinic, Cleveland, OH, [24]Brigham and Women's Hospital, Harvard Medical School, Boston, MA

Disclosures: Ankur Sangoi: None; Fiona Maclean: None; Reba Daniel: None; Priti Lal: None; Sofia Canete-Portillo: None; Cristina Magi-Galluzzi: None; Kristine Cornejo: None; Katrina Collins: None; Michael Hwang: None; Sambit Mohanty: None; Sara Falzarano: None; Michael Feely: None; Melad Dababneh: None; Lara Harik: None; Maria Tretiakova: None; Mahmut Akgul: None; Emily Chan: None; Varsha Manucha: None; Farshid Siadat: None; Kanika Arora: None; Guliz Barkan: None; Liang Cheng: None; Michelle Hirsch: *Consultant*, Janssen Pharmaceuticals; Li Lei: None; Matthew Wasco: *Stock Ownership*, Warde Medical Laboratory; Sean Williamson: None; Andres Acosta: None

Background: Formal depiction of granulomatous inflammation in association with renal neoplasms have mostly consisted of case reports and small series. Herein, we investigate the clinicopathologic features and potential significance of granulomas associated with renal tumors from a large multi-institutional cohort.

Design: Database search was undertaken from 19 different institutions for cases of renal neoplasms containing either peritumoral or intratumoral granulomas from nephrectomy specimens. Cases were entirely reviewed with detailed clinicopathologic features recorded including follow-up investigation of sarcoidosis.

Results: 92 study cases were collected, including 52 partial nephrectomies and 40 radical nephrectomies, of equal laterality distribution. Patient ages ranged from 27-85 years (average 59.9 years; male= 62%). Renal neoplasms were composed of clear cell renal cell carcinoma (RCC; 85%), papillary RCC (9%), chromophobe RCC (2%), clear cell papillary RCC (2%), mixed epithelial stromal tumor (1%), and oncocytoma (1%). RCC nuclear grades included grade 2 (52%), grade 3 (35%), grade 1 (7%), and grade 4 (6%). Most RCC cases were pathologic stage pT1a (50%) followed pT1b (22%), pT3a (22%), and pT2 (6%). Granulomas were peritumoral in 40% of cases, intratumoral in 17% of cases, and both in 43% cases. Total granuloma count per case ranged from 1 to 286 (median 15) with size of largest granuloma ranging from 0.15mm to 15mm (mean 1.9mm). Necrotizing granulomas were seen in 12% of cases. Histochemical stains for organisms were performed on 47% of cases (all negative). 16 cases (17%) had a prior biopsy/procedure performed, and 4 patients had neoadjuvant immunotherapy or chemotherapy. A total of 10 patients (11%) had a confirmed diagnosis of sarcoidosis, including 4 in whom sarcoidosis was diagnosed after nephrectomy. One patient presented with concurrent lung nodules at the time of nephrectomy (thought to be metastatic RCC), with histologic documentation of nephrectomy granulomas leading to timely clinical diagnosis of sarcoid.

Figure 1 - 617

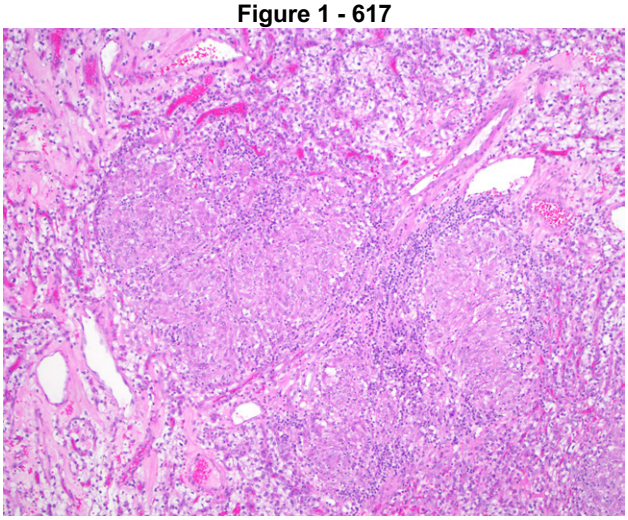

Conclusions: Based on this largest case series to date, peritumoral/intratumoral granulomas associated with renal neoplasms may be more common than initially perceived, and can be seen in both benign and malignant tumors. The extent of granulomatous inflammation can vary widely and may or may not have necrosis, with possible etiology from prior procedure. Although a clinical association with sarcoidosis is infrequent, it can still occur and warrants reporting.

618 p53 Null Phenotype is a "Positive Result" in Urothelial Carcinoma in Situ: A Clinicopathologic and Molecular Study of 25 Cases

Ankur Sangoi[1], Emily Chan[2], Eman Abdulfatah[3], Bradley Stohr[2], Jane Nguyen[4], Kiril Trpkov[5], Farshid Siadat[5], Michelle Hirsch[6], Sara Falzarano[7], Aaron Udager[8], Lakshmi Kunju[9]

[1]El Camino Hospital, Mountain View, CA, [2]University of California, San Francisco, San Francisco, CA, [3]Michigan Medicine, University of Michigan, Ann Arbor, MI, [4]Cleveland Clinic, Cleveland, OH, [5]University of Calgary, Calgary, Canada, [6]Brigham and Women's Hospital, Boston, MA, [7]University of Florida College of Medicine, Gainesville, FL, [8]University of Michigan Medical School, Ann Arbor, MI, [9]University of Michigan, Ann Arbor, MI

Disclosures: Ankur Sangoi: None; Emily Chan: None; Eman Abdulfatah: None; Bradley Stohr: None; Jane Nguyen: None; Kiril Trpkov: None; Farshid Siadat: None; Michelle Hirsch: *Consultant*, Janssen Pharmaceuticals; Sara Falzarano: None; Aaron Udager: None; Lakshmi Kunju: None

Background: The concept of a "p53 null phenotype" (complete loss of staining) is well-recognized in the gynecopathology literature, with an understanding that this staining pattern represents a *TP53* mutation. However, in the genitourinary literature, a p53 null phenotype has only been addressed regarding prognosis for invasive urothelial carcinoma, and not as a diagnostic biomarker for urothelial carcinoma in situ (CIS).

Design: Archives of multiple institutions were queried for cases of CIS showing a p53 null staining pattern. Confirmatory diagnoses of urothelial CIS were made on hematoxylin and eosin (H&E) stained sections. Clinicopathologic features and morphologic patterns of CIS were noted for all cases. One representative tissue block per case was selected for next-generation DNA sequencing (NGS).

Results: 25 cases of CIS showing a p53 null staining pattern (i.e., complete absence of p53 reactivity in neoplastic cells in the setting of positive internal control) were retrieved from 22 patients (16 males and 6 females, age range 52-85 years; average 69.6 years), with most cases (n=20) showing large cell pleomorphic morphology. 21 cases passed quality control for NGS. All 21 cases (100%) showed at least 1 *TP53* mutation (majority nonsense or frameshift mutations), including 3 cases with 2 mutations and 3 cases with 3 mutations. 3 patients with multiple available samples harbored 1 or more shared *TP53* mutations at 2 different time points, indicating clonality of the temporally distinct lesions. Additionally, 2 patients had an additional unique *TP53* mutation at a later time point, suggesting intratumoral heterogeneity and/or temporal clonal evolution.

Figure 1 - 618

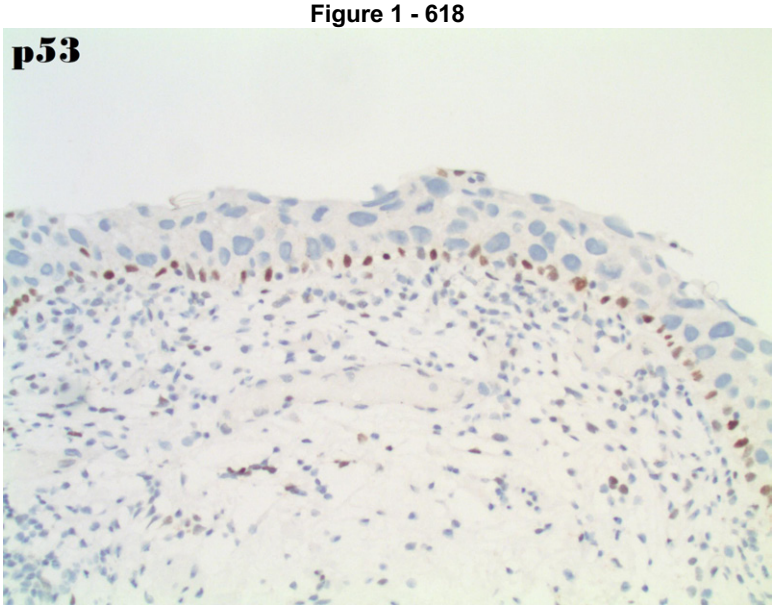

Conclusions: While urothelial carcinoma in situ remains an H&E diagnosis in most cases, a p53 immunostain may be useful in a subset of challenging cases. This study demonstrates that a p53 null phenotype represents an aberrant result in urothelial CIS with supportive molecular analysis showing a previously unknown level of complexity for *TP53* mutations among these noninvasive lesions. Hence, adequate recognition of the p53 null phenotype as a "biologically supportive result", similar to strong and diffuse staining with p53, is important, and may warrant a formal consensus statement for recommended p53 reporting (i.e., “wild type” versus “aberrant or mutant”).

619 Predictors of Progression in Lamina Propria Invasive Urothelial Carcinomas on Biopsy and Transurethral Resection Specimens

Judy Sarungbam[1], Bin Xu[1], Hikmat Al-Ahmadie[1], Nicole Benfante[1], Anuradha Gopalan[1], Ying-Bei Chen[1], Samson Fine[1], S. Joseph Sirintrapun[1], Satish Tickoo[1], Victor Reuter[1]
[1]Memorial Sloan Kettering Cancer Center, New York, NY

Disclosures: Judy Sarungbam: None; Bin Xu: None; Hikmat Al-Ahmadie: None; Nicole Benfante: None; Anuradha Gopalan: None; Ying-Bei Chen: None; Samson Fine: None; S. Joseph Sirintrapun: None; Satish Tickoo: None; Victor Reuter: None

Background: Bladder cancers have been broadly grouped into muscle-invasive(MIBC) and non muscle-invasive carcinoma(NMIBC), however not all NMIBC have similar prognosis. Various studies have reported the importance of defining the depth of invasion in lamina propria invasive urothelial carcinoma (LPI-UC). However, there is no consensus as to the method to be used for substaging. We aimed to determine the pathologic factors associated with a progression in patient with LPI-UC.

Design: All patients with a first time diagnosis of LPI-UC between 2008 and 2014, with at least 12 months follow-up, were identified. Patients with prior LPI or deeper invasive UC, cystectomy ≤ 3 months from diagnosis and upper tract urothelial carcinomas were excluded. Detailed histopathological analysis was performed for multiple histological parameters. Clinical details were collected from a prospectively maintained bladder cancer database. Progression was defined as a patient developing MIBC or nodal/distant metastasis. Log rank test to evaluate progression free survival (PFS) was performed.

Results: A total of 113 cases fulfilling the above criteria were included in the study. Median age of patients was 68.8.years (46.2 – 94.9), median follow-up of 64 months (12-138), with male: female ratio of 3.9:1. Muscularis mucosae (MM), thick walled vasculature (TWV) and muscularis propria were identified in 86 (76%), 99 (87.6%) and 76 (67.3%) cases, respectively. Depth of invasion, in mm and in relation to MM/TWV, could not be determined in 14 (12.0%) and 10 (8.8%) cases, respectively. Seven (6.2%) patients progressed. Results of statistical analysis are tabulated (Table 1). While using receiver operating curve (ROC), an ideal cut-off could not be determined for aggregate length of invasive carcinoma and percent of invasive component in the tumor. However, by Cox-regression method, both of these factors showed significant association with PFS. Using ROC, a cut-off of 1.5 mm for largest focus of invasion, showed significant association with PFS (p=0.039).

Table 1. Morphologic features and their association with PFS

Morphologic features (n =113)		Frequency (%)	PFS*, p value
Grade	Low grade	7 (6.2)	0.486
	High Grade	106 (93.8)	
Type of lesion	Papillary	83 (73.5)	0.579
	Flat	23 (20.5)	
	Papillary and flat	7 (6.2)	
Depth in relation to muscularis mucosae/thick walled vasculature (MM/TWV)	Superficial to MM/TWV	74 (65.5)	0.006
	At the level of MM/TWV	13 (11.5)	
	Deep to MM/TWV	16 (14.2)	
Location of invasion in papillary carcinoma (n=90)	Limited to stalk	26 (23)	0.140
	Beyond stalk	64 (56.6)	
Foci of invasion	Single	42 (37.2)	0.295
	Multiple	71 (62.8)	
Variant histology/divergent differentiation	Absent	102 (90.3)	0.078
	Present	11 (9.7)	
Desmoplasia	Absent	73 (64.6)	0.046
	Present	40 (35.4)	
Lymphovascular invasion	Absent	109 (96.5)	0.624
	Present	4 (3.5)	
Measured parameters (n=113)	Median	Range	PFS*, p value
Number of foci of invasion	2	1 - 20	0.770
Largest focus of invasion (mm)	0.70	0.02 – 11.40	0.001
Aggregate linear length of the invasive carcinoma (mm)	1.50	0.02 - 86	0.001
Percent of invasive component in the tumor (%)	2.00	0.05 - 100	0.005
Depth in mm	0.36	0.05 - 6.00	0.390

*PFS = progression free survival

Conclusions: 1. Grade of the tumor is not predictive of progression in lamina propria invasive urothelial carcinoma in this cohort. 2. Depth in relation to muscularis mucosae/thick walled vasculature (when measurable), size of largest focus of invasion, aggregate linear length of invasive carcinoma, percent of invasive component and presence of desmoplasia are significant predictors of PFS. 3. An area of invasion of 1.5 mm or more was predictive of adverse PFS.

620 Utility of A Novel Biomarker Beta-tubulin III (TUB3) in Renal Neoplasms

Swati Satturwar[1], Dimitrios Korentzelos[2], Susana Jorge[3], Gabriela Quiroga-Garza[2], Sheldon Bastacky[2], Hugo Santos[4], Jose-Luis Capelo-Martínez[5], Rajiv Dhir[6]

[1]The Ohio State University Wexner Medical Center/James Cancer Hospital, Columbus, OH, [2]University of Pittsburgh Medical Center, Pittsburgh, PA, [3]LAQV-REQUIMTE, Lisbon, Portugal, [4]LAQV-REQUIMTE, Caparica, Portugal, [5]Caparica, Portugal, [6]UPMC Shadyside Hospital, Pittsburgh, PA

Disclosures: Swati Satturwar: *Grant or Research Support*, University Pittsburgh Medical Center Developmental Laboratory; *Grant or Research Support*, University Pittsburgh Medical Center Developmental Laboratory; Dimitrios Korentzelos: None; Susana Jorge: None; Gabriela Quiroga-Garza: None; Sheldon Bastacky: None; Hugo Santos: None; Jose-Luis Capelo-Martínez: None; Rajiv Dhir: None

Background: Renal carcinomas diagnosed at higher stage carry dismal prognosis. Beta-tubulin III (TUB3), is a novel biomarker that was identified by our group using cancer proteomics. Initial tissue-micro array based results showed that TUB3 was expressed mostly in papillary renal cell carcinomas (pRCCs). PMID: 34482820 This study was undertaken to evaluate TUB3 immunohistochemistry (IHC) in different renal neoplasms using whole slide sections and to explore association with histologic grade in pRCCs.

Design: A cohort of 84 cases, comprising of 21 each cases of clear cell (ccRCC), pRCC, chromophobe RCC (chRCC) and renal oncocytoma (RO) was used. Clinical and histopathologic data was collected. IHC was performed using same mouse monoclonal antibody (clone 2G10, Abcam) for TUB3 protein. Membranous and/or cytoplasmic staining of any intensity was considered as positive and scored as (0=Negative; 1:1-10%; 2: >10-50%; 3: >50%) and percent positivity was recorded. Whether TUB3 expression in pRCCs is associated with increasing WHO histologic grade was explored.

Results: Figures 1 and 2 summarizes IHC results. Although there was variation in staining intensity and % positivity for TUB3, majority of the pRCCs were positive for TUB3 whereas ccRCC, chRCC and ROs were mostly negative. With a cut-off of 2 or above score and >10% cells positivity; TUB3 has a sensitivity of 80.9% and a specificity of 95.2% to distinguish pRCC from other renal neoplasms. There was no significant association between TUB3 expression by pRCCs with histologic grade (p= 0.6559).

Figure 1 - 620

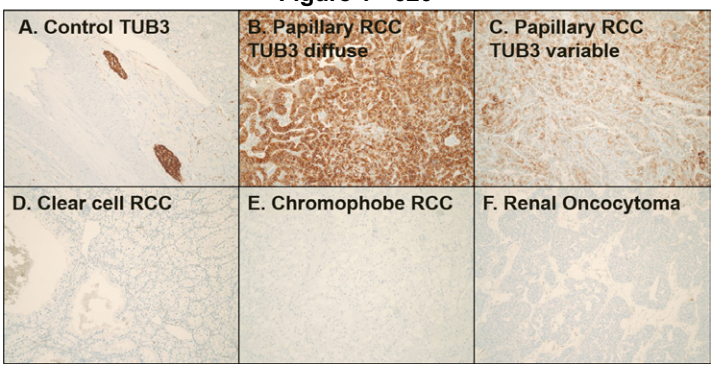

Figure 2 – 620

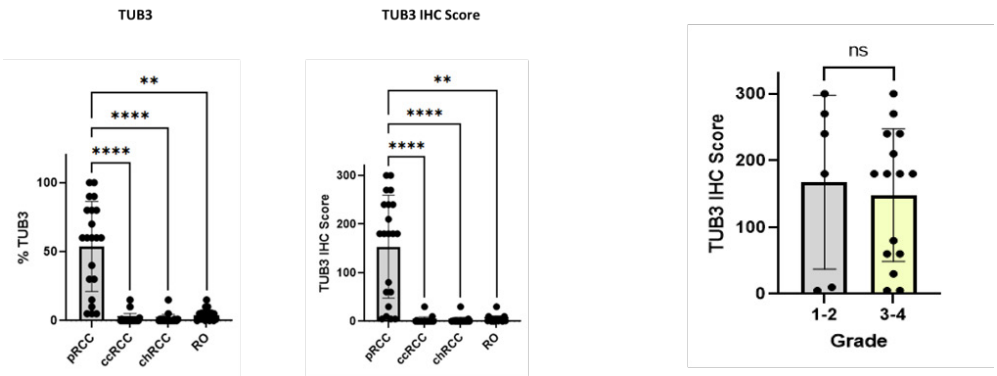

Conclusions: Our whole slide section based data suggests that TUB3 may emerge as a specific marker for pRCC that represent a different subtype at proteomic level. In this limited sample study there was no association between TUB3 expression by pRCCs and histologic grade. Prognostic significance of TUB3 expression remains to be explored.

621 A Contemporary Clinicopathologic Analysis of Primary Sarcomas of the Perinephric Soft Tissue and Hilar Vessels including a Subset Secondarily Involving the Kidney

Ashley Scheiderer[1], Armita Bahrami[1], Adeboye Osunkoya[2]
[1]Emory University School of Medicine, Atlanta, GA, [2]Emory University, Atlanta, GA

Disclosures: Ashley Scheiderer: None; Armita Bahrami: None; Adeboye Osunkoya: None

Background: A variety of primary malignant mesenchymal neoplasms can arise from the perinephric soft tissue and hilar vessels and potentially involve the kidney, mimicking primary renal tumors. Only few case series and case reports have specifically analyzed the clinicopathologic features of these tumors.

Design: A search was made for patients that underwent radical nephrectomy for perinephric and hilar vessel sarcomas at a major academic institution from 2010 to 2021. Clinicopathologic parameters and follow-up data were obtained.

Results: Twenty-seven cases were identified. Mean patient age was 59 years (range: 25-83 years), with 16 (59%) females and 11 (41%) males. There was a slight right-side predominance of 14 (52%) cases. Tumors arose from the perinephric/retroperitoneal region in 21 (78%) cases and the renal vein/inferior vena cava in 6 (22%) cases. The mean tumor size was 20.8 cm (range: 0.05-36.5 cm). Among the perinephric/retroperitoneal sarcomas, 14/21 (67%) were dedifferentiated liposarcoma, 4/21 (19%) were well-

differentiated liposarcoma, 2/21 (9%) were leiomyosarcoma, and 1/21 (5%) was round cell sarcoma. There were 4 grade 1 (19%; all well-differentiated liposarcoma), 9 grade 2 (43%), and 8 grade 3 (38%) tumors. All 6 sarcomas arising from the renal vein/inferior vena cava were identified as leiomyosarcoma: grade 2 in 1 (17%), grade 3 in 4 (67%), and ungraded (due to neoadjuvant therapy effect) in 1 (17%) case. Four of the 27 (15%) total cases involved adjacent organs, such as kidney and adrenal gland. All 4 cases were grade 3 sarcomas. Follow-up data revealed 8/27 (30%) patients developed local recurrence and/or metastasis. The mean time for recurrence was 22 months (range: 7-48 months). Two cases progressed with distant metastasis, both of which were grade 3 leiomyosarcoma, had metastasized to the lungs, and had appeared 11 months after the initial diagnosis.

Conclusions: Primary sarcomas of the perinephric soft tissue and hilar vessels are typically large masses of adipocytic or smooth muscle cell origin. Direct invasion by a perinephric sarcoma into the kidney, which can mimic a renal primary with extrarenal extension, occurs seldom and is usually associated with grade 3 malignancies. Our data suggest that while local recurrence is prevalent with most subtypes of perinephric sarcomas, high-grade leiomyosarcoma has a distinct proclivity for distant metastasis, with the lungs being the most common site.

622 A Modified Histopathological Staging System of Penile Cancer: Comparison with 8th AJCC Staging System and Correlation with Outcome Variables

Ashish Shah[1], Santosh Menon[1], Akash Sali[2], Ganesh Bakshi[1], Gagan Prakash[1], Mahendra Pal[1], Vedang Murthy[1], Amit Joshi[1], Sangeeta Desai[3]

[1]Tata Memorial Hospital, Mumbai, India, [2]Homi Bhabha Cancer Hospital, Sangrur, India, [3]Tata Memorial Centre, Mumbai, India

Disclosures: Ashish Shah: None; Santosh Menon: None; Akash Sali: None; Ganesh Bakshi: None; Gagan Prakash: None; Mahendra Pal: None; Vedang Murthy: None; Amit Joshi: None; Sangeeta Desai: None

Background: Penile squamous cell carcinoma (PSCC) staging is based on American Joint Committee on Cancer Staging System, 8th edition (AJCC-8E) which categorizes corpus spongiosum (CS) versus corpora cavernosa (CC) as pT2 and pT3 respectively. However, several studies have not been able to validate these changes of AJCC-8E. In the current study, we compare the AJCC-8E pT2 & pT3 stages with a modified histopathological staging system (MHSS) incorporating histopathological parameters.

Design: In this retrospective study, H&E slides of PSCC from 2013 to 2017 that had undergone primary surgical treatment were retrieved and reviewed. pT2 and pT3 tumor stages were constructed according to AJCC-8E (as described above) and MHSS. According to MHSS, tumors invading CS/CC without lymphovascular invasion (LVI) and perineural invasion (PNI) and that were not grade-3, were categorized as pT2; while those invading CS/CC either with LVI and/or PNI or were grade-3 were labeled pT3. Both the staging systems were compared & correlated with respect to nodal metastasis & disease-free survival (DFS). Survival curves were calculated using Kaplan-Meier analysis (log rank test).

Results: The study included 105 cases. pT1 and pT4 tumors were 14 and 5 cases respectively. pT2 and pT3 tumors were noted in a total of 86 cases with distribution according to AJCC-8E & MHSS as depicted in Table 1. For further analysis, only pT2 and pT3 cases were considered. Lymph nodal dissection was performed in 67 cases (78%, n=67/86). MHSS (p<0.001) correlated with the nodal metastasis, however, AJCC-8E (p=0.667) failed to. Follow-up was available in 73 patients (84.9%) with a median follow-up of 15 months (range 1-86 months). Recurrence on follow-up was noted in 25 cases (34.2%). Only MHSS (p=0.001) and not AJCC-8E (p=0.244) correlated statistically with the DFS (Figure 1).

Table 1: Cross-tabulation of pT2 & pT3 stages of AJCC-8E & MHSS against nodal metastasis

Staging systems	Nodal metastasis			
	Absent	Present	Total (N=67)	p-value
1. AJCC-8E				0.667
a. pT2	23 (47.9%)	25 (52.1%)	48	
b. pT3	08 (42.1%)	11 (57.9%)	19	
2. MHSS				<0.001
a. pT2	17 (80.9%)	04 (19.1%)	21	
b. pT3	14 (30.4%)	32 (69.6%)	46	

Figure 1 - 622

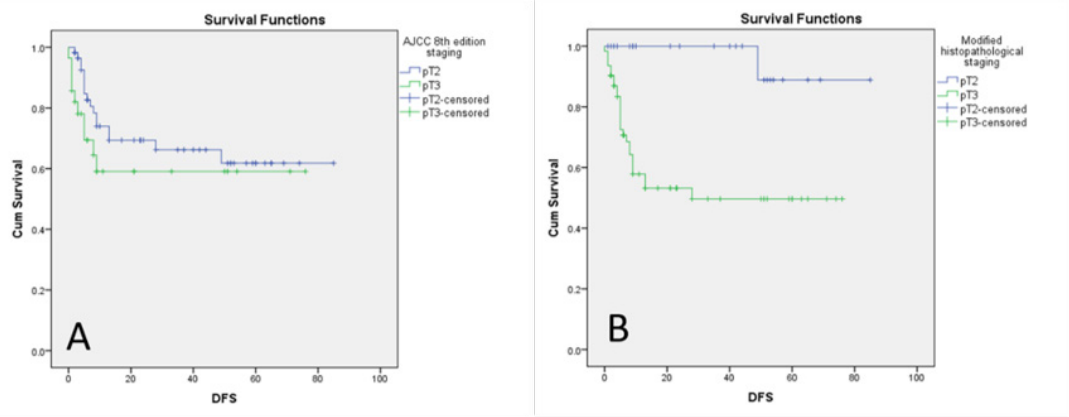

Figure 1: Kaplan Meier plots of DFS for pT2/pT3 stages for PSCC. A) 8th AJCC Staging (p=0.244); B) MHSS (p=0.001)

Conclusions: We conclude that the pT2 and pT3 stages constructed as per MHSS are a better predictor of nodal metastasis and DFS than AJCC-8E. This finding may have significant management implications. Further prospective validation studies may improve the staging system in penile cancer.

623 Gene Mutations in Urothelial Carcinoma of the Upper Urinary Tract

Ahmed Shehabeldin[1], Charles Guo[2], Kingsley Ebare[2], Bogdan Czerniak[2], Patrick Hensley[2]
[1]The University of Texas MD Anderson Cancer Center, TX, [2]The University of Texas MD Anderson Cancer Center, Houston, TX

Disclosures: Ahmed Shehabeldin: None; Charles Guo: None; Kingsley Ebare: None; Bogdan Czerniak: None; Patrick Hensley: None

Background: Despite the histologic similarities, urothelial carcinomas (UC) of the upper urinary tract (UUT) may be genetically different from those of the urinary bladder. Recent studies have revealed distinct genomic alterations in bladder UC that may aid personalized treatment strategies. Herein we analyzed the gene mutational profile of UUTUC in correlation with the clinical and pathological features.

Design: We searched our pathology files from 2014-2016 and identified 15 patients with UUTUC who underwent Next-Generation-Sequencing (NGS) on formalin-fixed paraffin-embedded tissue specimens. Pathologic features were reviewed, and clinicopathologic parameters were collected from patient records.

Results: The patient cohort included 9 males and 6 females. The patients' mean age was 66 years (range, 41-82 years). NGS tests were performed on 12 primary lesions from the renal pelvis (4), ureter (2), and multifocal tumors involving the pelvis and the ureter (6) and 3 metastatic lesions (inguinal lymph node, colon, and liver). Most tumors were high-grade UC (11), and 4 showed variant features, including micropapillary (2), sarcomatoid (1), and neuroendocrine differentiation (1). Somatic mutations were identified in 14 cases. Mutations were detected in 41 different genes, and the most common mutations included TP53 (7), KIT (5), PIK3CA (4), FGFR3 (3), APC (3), and CSMD3 (3). All patients died of disease at a mean survival time of 37 months (range, 6-107 months). The mean survival time for patients with variant histology was 20 months. The mean survival time for patients with TP53, KIT, PIK3CA, FGFR3, APC, and CSMD3 gene mutations were 37, 38, 15, 30, 43, and 32 months, respectively.

Conclusions: The majority of UUTUCs show mutations in several oncogenes and tumor suppressor genes, which may contribute to the oncogenesis of this rare disease. The presence of variant histology in UUTUC is associated with a shorter survival time. Our preliminary results suggest that PIK3CA mutation may be associated with poor outcomes in UUTUC, and FGFR3 may be associated with favorable outcomes. However, the results need to be validated in independent studies.

624 20 Core Template Prostate Biopsy Approach: Are More Cores the Better? A Unique Pathology Perspective from a Single Institution with Follow Up

Yuan Shui[1], Benjamin Ristau[2], Ryan Daigle[2], Christian Schaufler[2], Harold Yamase[2], Mingfu Yu[2], Peter Albertsen[2], Gahie Nam[3]

[1]University of Connecticut, CT, [2]UCONN Health, Farmington, CT, [3]University of Connecticut, Farmington, CT

Disclosures: Yuan Shui: None; Benjamin Ristau: None; Ryan Daigle: None; Christian Schaufler: None; Harold Yamase: None; Mingfu Yu: None; Peter Albertsen: None; Gahie Nam: None

Background: Transrectal (TR) prostate biopsy for the diagnosis of prostate cancer has remained largely unchanged since it was introduced in the 1980s. Recently, however, transperineal (TP) biopsy has been increasingly utilized. TP biopsy has been reported to have the similar diagnostic accuracy and a lower risk of sepsis and rectal bleeding compared to the TR approach. We investigated differences in cancer detection and subsequent prostatectomy rates using 20 core TP versus 12 core TR biopsy template.

Design: We present a single institution, retrospective review of 20 TP cores (2017-2019) and 12 TR cores (2019-2021) in 344 men who were biopsy naïve, had elevated PSA with prior negative biopsy and on active surveillance. Prebiopsy clinical characteristics and pathologic biopsy results, including detection of PCa, detection of csPCA (grade group, GG ≥ 2), high grade PCa (GG ≥ 4), atypical small acinar proliferation (ASAP) rate and follow-up biopsy rate. Subsequent prostatectomy rate, final grade group and stage were collected retrospectively from review of patient records.

Results: There was no difference in age, BMI, and PSA between 20 TP (Group 1) vs 12 TR (Group 2) (table 1). Detection of any cancer (76.7% vs 56.7%, p=0) was higher in Group 1 relative to Group 2. ASAP rate was lower at 3/180 in Group 1 vs 14/164 in Group 2 (p=0.007). Subsequent additional biopsy rate was higher in Group 2 (27/164 vs 8/180, p=0.001). There were no statistical differences between the two group in csPCa detection (90/180 vs 63/164), GG ≥ 4 (40/180 vs 25/164) and subsequent prostatectomy rate (47/180 vs 41/164). Both groups had similar overall GG on resection: GG1 (1/47 vs 1/41), GG2 (24/47 vs 19/41), GG3 (8/47 vs 10/41), GG4 (5/47 vs 4/41) and GG5 (9/47 vs 7/41). There were no differences in pathologic stage between the groups T2 (26/47 vs 21/41), T3a (9/47 vs 9/4), T3b (12/47 vs 9/4) and T4 (0/47 vs 1/4).

	TP 20 cores, Group 1 (n=180)	TR 12 cores, Group 2 (n=164)	P value
Age (Mean±SE)	65.19± 0.54	64.05± 0.64	0.23
BMI ((Mean±SE))	28.99± 0.35	28.28± 0.38	0.17
PSA (Mean±SE), ng/ml	13.34± 1.4	18.89± 4.9	0.083
Cancer detect on Biopsy	138	93	0
≥GG2 group	90	63	0.691
≥GG4 group	40	25	0.727
Subsequent additional biopsy	8	27	0.001
Atypical small acinar proliferation (ASAP)/ Atypical glands suspicious for cancer (ATYP)	3	14	0.007
Received Prostatectomy	47	41	1.0
final GG group1	1	1	0.908
final GG group 2	24	19	0.573
final GG group 3	8	10	0.36
final GG group 4	5	4	0.922
final GG group 5	9	7	0.843
Final GG group Upgrade from Biopsy	28	26	0.603
T2	26	21	0.891
T3a	9	9	0.656
T3b	12	9	0.792
T4	0	1	0.28

Conclusions: 20 sector TP biopsy approach may be more informative in management decision making process in recommending prostatectomy (given higher PCa detection, lower ASAP and lower subsequent biopsy rate) than the traditional 12 sector TR approach. However, since up to 9 prostate cores are billable (professional charge) per Medicare and every specimen part may be associated with significant cost (in labor, reagent, processing) and delay within the Pathology department, cost effectiveness of routine submission of increased biopsy cores should be further investigated.

625 Clinicopathologic and Molecular Spectrum of Testicular Sex-Cord Stromal Tumors Not Amenable to Specific Histopathologic Subclassification

Stephanie Siegmund[1], Harrison Tsai[1], Christopher Fletcher[1], Kristine Cornejo[2], Muhammad Idrees[3], Khaleel Al-Obaidy[4], Katrina Collins[3], Jennifer Gordetsky[5], Sara Wobker[6], Michelle Hirsch[1], Cristina Magi-Galluzzi[7], Sofia Canete-Portillo[7], Lynette Sholl[8], Andres Acosta[9]

[1]Brigham and Women's Hospital, Boston, MA, [2]Massachusetts General Hospital, Boston, MA, [3]Indiana University School of Medicine, Indianapolis, IN, [4]Cleveland Clinic Foundation, Cleveland, OH, [5]Vanderbilt University Medical Center, Nashville, TN, [6]The University of North Carolina at Chapel Hill, Chapel Hill, NC, [7]The University of Alabama at Birmingham, Birmingham, AL, [8]Harvard Medical School, Boston, MA, [9]Brigham and Women's Hospital, Harvard Medical School, Boston, MA

Disclosures: Stephanie Siegmund: None; Harrison Tsai: None; Christopher Fletcher: None; Kristine Cornejo: None; Muhammad Idrees: None; Khaleel Al-Obaidy: None; Katrina Collins: None; Jennifer Gordetsky: *Consultant*, Jansen; Sara Wobker: None; Michelle Hirsch: *Consultant*, Janssen Pharmaceuticals; Cristina Magi-Galluzzi: None; Sofia Canete-Portillo: None; Lynette Sholl: *Consultant*, Genentech; *Grant or Research Support*, Genentech; *Consultant*, Lilly; Andres Acosta: None

Background: Testicular neoplasms of sex-cord or stromal derivation that cannot be definitively classified into a specific tumor subtype are designated "unclassified sex-cord stromal tumors" (USCSTs). Given the rarity of USCSTs, their clinicopathologic and molecular features remain largely unexplored.

Design: This study evaluated a multi-institutional series of testicular USCSTs to better define the spectrum of tumors comprised in this diagnostic category. Eighteen USCSTs from 17 patients diagnosed between 1996 and 2021 were evaluated by review of histology slides, review of clinicopathologic data, and by massively parallel DNA sequencing.

Results: The age at diagnosis ranged from 5-72 years (median 52 yrs). Tumor size ranged from 1.1 to 9.1 cm (median 2.5 cm). Microscopically, USCSTs demonstrated spindle cells (7/18), epithelioid cells (8/18) or a mixture thereof (3/18). Architectural patterns included solid sheets, nests, trabeculae, microcysts, and fascicles, with multiple patterns seen in most cases. Mitoses ranged from <1 to 169/10 HPF (median 3/10 HPF). Histopathologic features suggestive of malignancy (size >5 cm, invasive growth, necrosis, prominent mitotic activity) were seen in 5 cases. DNA sequencing was successful in 14/18 tumors. Overall, these tumors had a low mutational burden. Relevant pathogenic alterations included single nucleotide variants and small indels in *CTNNB1* (4/14), *APC* (1/14 with loss of heterozygosity [LOH]), and *TP53* (1/14 with LOH), a rearrangement in *BRCA2* (1/14 with LOH), and homozygous deletions in *RB* (2/14). Recurrent broad copy number changes (present in >25% of cases) included chromosome-wide gains of chromosomes 3, 6, 7, 8, 9, 12, 14, 15 and 20. Importantly, none of the cases with *CTNNB1* mutations had morphologic features of Sertoli cell tumor, and no cases harbored mutations characteristic of other specific SCST subtypes (e.g., *FH*, *PRKAR1A*, *DICER1*, *FOXL2*). Clinical follow-up data were available for 9 patients (range 2 mo-25 yrs). Six patients were alive with no evidence of disease after surgery. Of the remaining three patients, two were alive with disease 5 and 9 months after surgery, and one was dead of disease 6 months after surgery.

Figure 1 - 625

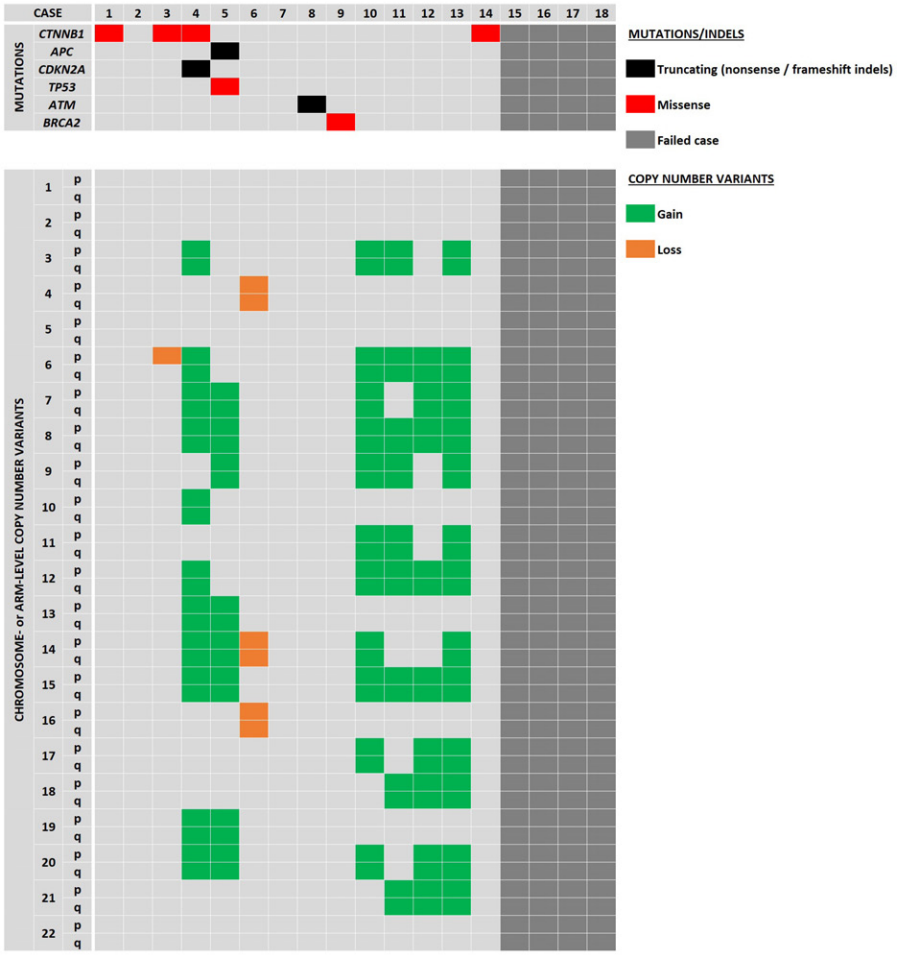

Conclusions: The results of this study demonstrate that USCSTs comprise tumors with variable clinicopathologic features and molecular alterations, including a significant proportion (5/14; 36%) driven by mutations of WNT pathway genes (*CTNNB1*, *APC*). Analysis of additional cases is on-going.

626 Concordance of mTOR Mutation and the Diagnosis of a Low Grade Renal Oncocytic Tumor (LOT)

Stephanie Siegmund[1], Khaleel Al-Obaidy[2], Andres Acosta[3], Mahmut Akgul[4], Muhammad Idrees[5], Harrison Tsai[1], Michelle Hirsch[1]

[1]Brigham and Women's Hospital, Boston, MA, [2]Cleveland Clinic Foundation, Cleveland, OH, [3]Brigham and Women's Hospital, Harvard Medical School, Boston, MA, [4]Albany Medical Center, Albany, NY, [5]Indiana University School of Medicine, Indianapolis, IN

Disclosures: Stephanie Siegmund: None; Khaleel Al-Obaidy: None; Andres Acosta: None; Mahmut Akgul: None; Muhammad Idrees: None; Harrison Tsai: None; Michelle Hirsch: *Consultant*, Janssen Pharmaceuticals

Background: The differential diagnosis for oncocytic renal tumors spans the spectrum from benign entities to indolent behavior to more aggressive renal cell carcinomas (RCC). Recent work has characterized a provisional renal oncocytic neoplasm (RON), low-grade oncocytic tumor (LOT), which demonstrates intermediate morphologic features between oncocytoma and chromophobe RCC in that the tumors demonstrate solid to nested architecture, edematous stroma, round low-grade nuclei and occasional perinuclear halos, as well as a distinctive immunohistochemical profile (diffusely positive for CK7, negative for CKIT). Notably, two recent studies have identified molecular alterations in mTOR pathway genes in 80-100% of LOTs. Given the diagnostic overlap among eosinophilic tumors, we looked for concordance/discordance of mTOR mutations in LOTs and other RONs

Design: We evaluated 30 low-grade RONs, where LOT was in the differential diagnosis. Histologic review of all cases included H&E morphology and immunohistochemistry for CK7 and CKIT (0, negative; 1+, up to 10%; 2+, 10-75%, 3+, > 75%). Tumors were classified as "Determinate" (ie, LOT) for cases with solid, nested or vaguely tubular growth and 3+ CK7 staining and negative CKIT. Tumors were classified as "Indeterminate" if the morphology and/or immunostains did not fully support a definitive LOT diagnosis. Molecular analysis was then conducted, blind to the diagnoses, via massively parallel DNA sequencing, to evaluate single nucleotide variants, structural variants, and copy number analysis in all cases.

Results: Classification revealed 15 tumors within the Determinate (LOT) category and 15 tumors in the Indeterminate category. Molecular analysis identified mTOR pathway mutations (including *mTOR*, *TSC1/2*, *RHEB*) in 80% (12/15) of the LOTs, compared with only 7% (1/15) in the Indeterminate group of tumors. Of the 3 LOTs without mTOR pathway mutations, one tumor exhibited widespread copy number gains including chromosomes 7 and 17. Among the Indeterminate tumors with an mTOR mutation, one was a low grade RON that extended into the renal vein. Additional notable alterations in the Indeterminate group included pathogenic mutations in *FLCN*, *TCEB1*, and *SDHA*.

Conclusions: Overall, mTOR mutations were highly concordant with RONs that met full criteria for LOTs, but were not entirely specific. Diffuse CK7 expression and an absence of CKIT must be interpreted in the setting of appropriate morphologic features as they too are not entirely specific.

627 Clinicopathologic Findings in Patients with MRI-Guided Ablation Therapy for Prostate Cancer Including a Subset of Patients with Subsequent Radical Prostatectomy.

Jason Singh[1], Sherif Nour[2], Adeboye Osunkoya[2]
[1]Emory University Hospital, GA, [2]Emory University, Atlanta, GA

Disclosures: Jason Singh: None; Sherif Nour: None; Adeboye Osunkoya: None

Background: MRI-Guided ablation therapy for prostate cancer (PCa) is a form of focal targeted therapy. This therapeutic approach provides an alternative to active surveillance in select patients or other more invasive conventional procedures in patients who need active management. The clinicopathologic findings in the pre and post MRI-guided ablation setting has not been well characterized in the Pathology literature.

Design: A search was performed for cases of PCa with MRI-guided ablation therapy at our Institution. Multiple parameters were obtained including the interval between initial PCa diagnosis and MRI-guided ablation, histopathologic findings, number of ablations per PCa Grade group, and PSA levels (pre and post procedure). A subset of patients who also underwent follow-up/repeat MRI-guided ablation therapy and/or salvage radical prostatectomy were also included in the study.

Results: Forty two patients were included in the study. The mean patient age was 71 years (range: 55 to 80 years). The mean age of those who received ablations was highest for patients with PCa Grade group 4 (76 years) and lowest for patients with PCa Grade group 1 (68 years). The mean interval between initial biopsy and MRI-guided ablation for the entire cohort was 6 months (range: 1 to 40 months). The number of ablations per each Grade group category was 18 (PCa, Grade group 1), 29 (PCa, Grade group 2), 6 (PCa, Grade group 3), 5 (PCa, Grade group 4). From pre-ablation levels, post-ablation PSA levels all showed a significant decrease with PCa Grade group 4 patients having the highest pre and post PSA levels. Eight of 42 (20%) patients had a subsequent follow-up/repeat MRI-guided ablation procedure. Three patients underwent subsequent salvage radical prostatectomies. Their residual tumors in the prostatectomy specimens ranged from PCa Grade group 2 to PCa Grade group 3, with tertiary Gleason grade 5. None of the radical prostatectomy cases had lymph node metastases or seminal vesicle invasion, however, 2/3 had extraprostatic extension.

Conclusions: This is the largest study to date specifically analyzing the clinicopathologic findings of pre and post MRI-guided ablation therapy. The procedure was successful in the majority of patients in our cohort, including associated significant decreases in PSA levels between pre and post ablation. MRI-guided ablation therapy is a viable alternative therapeutic strategy for PCa in carefully selected patients.

628 Automated Nuclear Size, Shape, and Mitotic Index Measurements that Objectively Distinguish Low-Grade from High-Grade Non-Invasive Papillary Urothelial Carcinoma

Ava Slotman[1], Minqi Xu[2], Dan Winkowski[3], Celine Hardy[1], Lina Chen[1], Regan Baird[4], Chelsea Jackson[5], Robert Gooding[6], David Berman[1]

[1]Queen's University, Kingston, Canada, [2]Kingston General Hospital, Queen's University, Kingston, Canada, [3]Visiopharm A/S, Denmark, [4]Visiopharm A/S, Westminster, CO, [5]Queen's University, Kingston Health Sciences Centre, Kingston, Canada, [6]Queen's University

Disclosures: Ava Slotman: None; Minqi Xu: None; Dan Winkowski: *Employee*, Visiopharm; Celine Hardy: None; Lina Chen: None; Regan Baird: *Employee*, Visiopharm; Chelsea Jackson: None; Robert Gooding: None; David Berman: None

Background: Grade drives important treatment and management decisions in early bladder cancer. However, grading, as currently performed by pathologists, is subjective and suffers from poor inter- and intra-observer reliability. Nuclear size and shape have been shown to differ between bladder cancer grades, but past studies were limited in size and scope. Powerful image analysis tools can now be brought to the pathologist's desktop, enabling rapid and reliable measurement of histopathologic features. Here we use computational pathology to select morphometric features and build models that objectively distinguish between bladder cancer grades.

Design: We used tissue-microarray images from a large non-invasive papillary urothelial carcinoma (NIPUC) cohort of 514 low-grade (LG) cores and 125 high-grade (HG) cores. All cores underwent ISUP/WHO2004 consensus grading. We deployed artificial intelligence (AI) based image analysis software to segment tissue regions and measure nuclear features in NIPUC images (Figure 1). Data on nuclear size, shape, and mitotic index, was obtained for over 3.5 million tumour nuclei.

Results: Nuclear size, and more dramatically the variation in size were highly associated with grade (Figure 2). Surprisingly, nuclear shape metrics showed only weak association with grade and nuclear intensity (hyperchromasia) and its variance showed little relation to grade. A univariate model using the standard deviation (SD) in nuclear area across low- and high-grade cores produced an area under the receiver operator curve (AUC) for grade of 0.88 with 81% balanced accuracy. Linear and logistic regression models constructed using additional geometric features obtained AUCs of 0.91. With 1000x cross-fold validation these multivariate models differentiated between LG and HG cores with 84% balanced accuracy. When mitotic index was added, AUCs for models increased to 0.93 and cross-validated accuracy to 86%.

Figure 1 - 628

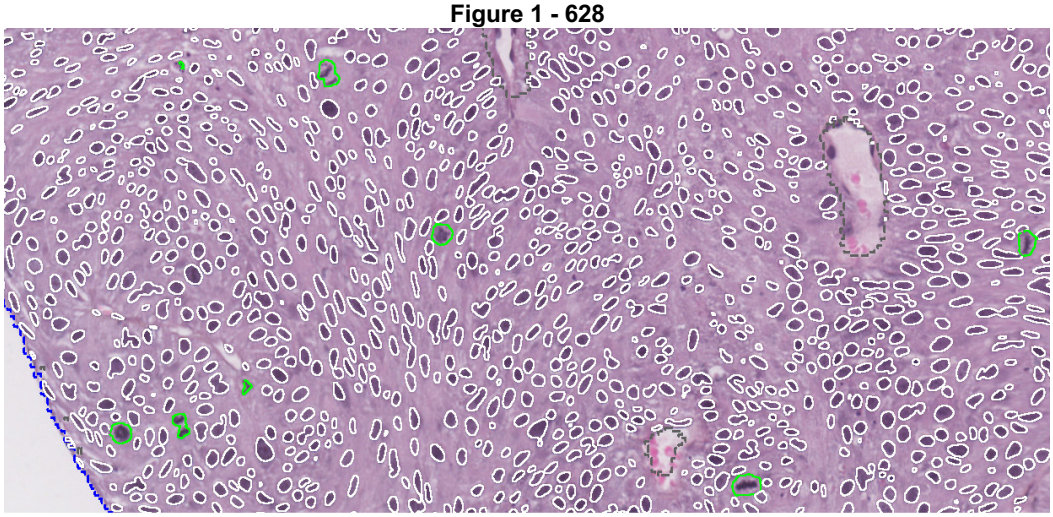

Figure 1. Automated artificial intelligence-based software accurately segmented tissue regions, individual nuclei, and mitotic figures. Blue dashed lines indicate the tissue-slide boundary. Grey dashed lines surround non-tumour/stromal regions of tissue. White circles outline the perimeter of tumour nuclei and green circles outline mitotic figures.

Figure 2 – 628

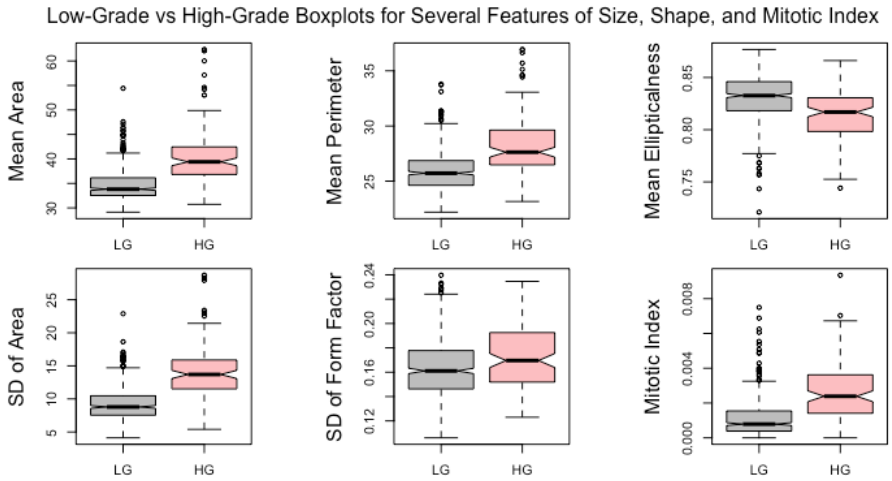

Figure 2. Boxplots demonstrating the difference between low-grade (LG) and high-grade (HG) values for 6 features. Coloured boxes indicate the interquartile range for each grade, bold horizontal lines indicate the median, and notches demonstrate 95% confidence intervals around the median.The whiskers are the lines on either side of each box and extend to the upper and lower extremes of the data. Circles indicate possible outliers. SD = Standard deviation

Conclusions: These results indicate that nuclear morphometry and automated mitotic figure counts can be used to objectively and accurately differentiate between LG and HG NIPUC. Variation in nuclear area was the best univariate discriminator however the addition of shape-related variables and mitotic activity in regression models significantly increased accuracy. Future efforts will explore more complex combinatorial models, externally validate them, and tune them to clinical endpoints. Upon validation, the resulting classifiers should improve diagnosis and patient care.

629 Clinical and Gene Expression Analysis of Patients with Non-Invasive Papillary Urothelial Carcinoma Demonstrating Progression to Muscle-invasive or Metastatic Disease

Priti Soin[1], Jeffrey Putt[1], Alireza Aminsharifi[1], Jay Raman[1], David DeGraff[1], Joshua Warrick[2]
[1]Penn State Health Milton S. Hershey Medical Center, Hershey, PA, [2]Penn State College of Medicine, Hershey, PA

Disclosures: Priti Soin: None; Jeffrey Putt: None; Alireza Aminsharifi: None; Jay Raman: None; David DeGraff: *Grant or Research Support*, Bristol Myers Squibb; *Grant or Research Support*, Bristol Myers Squibb; Joshua Warrick: None

Background: Noninvasive papillary urothelial carcinoma (NIPUC) accounts for 70% of new bladder cancer diagnoses. It recurs commonly, and a small subset of cases progress to advanced-stage disease. At present, it is difficult to predict which subset of NIPUC patients will experience disease progression.

Design: We constructed a detailed disease chronology for 102 patients initially diagnosed with NIPUC, including all recurrences and treatments, as well as stage progression (defined as progression to muscle-invasive bladder cancer or metastasis). RNA sequencing on NIPUC from patients experiencing progression was performed, including the initial and recurrent tumors (n=4 patients; 3-5 tumors each).

Results: Of the 102 patients, seven experienced stage progression. Among progressors, median time to progression was 98 months, and median number of recurrences was five, including the progression event. Among the 95 patients who did not experience progression, median follow up time was 67 month, and median number of recurrences was two. Risk of progression was greater in patients who experienced a recurrence as lamina propria-invasive cancer (p=0.006, Fisher's exact test, 57% vs. 11%, progressors versus non-progressors). There was no difference between progressors and non-progressors in tumor grade at initial diagnosis (p=0.5, Fisher's exact test), recurrence as high-grade NIPUC (p=0.2, Fisher's exact test), or rate of BCG treatment in patients with high-risk disease (p=0.6, Fisher's exact test). RNA sequencing revealed recurrent tumors tended to be similar to one another within a patient. For example, in 75% of progressors tested, late cell cycle activity differed by less than 20% among all tumors (activity defined using ssGSEA applied to late cell cycle genes, range defined as max minus min expression for all tumors, log2 transformed RPKM). In the fourth patient, there was a single outlier, and the remaining tumors were within 20% of each other.

Subtyping in the UROMOL schema showed all were either Class 1 or Class 3, both low-risk classes [Lindskrog, Nat Commun, 2021]. In two patients, all tumors were Class 3.

Conclusions: Patients with an initial diagnosis of NIPUC have higher risk of progression with recurrence as lamina propria-invasive carcinoma, emphasizing that progression of NIPUC is best predicted using the patient's disease course. Within a single patient, recurrent tumors tend to have similar cell cycle activity and expression type.

630 Molecular Characterization of Carcinomas Arising in the Urinary Bladder Following Augmentation Cystoplasty: A Multi-Institutional Study

Bradley Stohr[1], Emily Chan[1], Joshua Anderson[2], Andres Matoso[3], Belkiss Murati Amador[4], Liang Cheng[5], Adeboye Osunkoya[6]

[1]University of California, San Francisco, San Francisco, CA, [2]Western Washington Pathology, Tacoma, WA, [3]Johns Hopkins Medical Institutions, Baltimore, MD, [4]Johns Hopkins University School of Medicine, Baltimore, MD, [5]Indiana University, Indianapolis, IN, [6]Emory University, Atlanta, GA

Disclosures: Bradley Stohr: None; Emily Chan: None; Joshua Anderson: None; Andres Matoso: None; Belkiss Murati Amador: None; Liang Cheng: None; Adeboye Osunkoya: None

Background: Development of malignancy is a rare complication following augmentation cystoplasty. The majority of tumors observed in this setting are adenocarcinomas, and the molecular signatures of these tumors have not been well-characterized in the literature. Here, we describe targeted DNA sequencing results for a multi-institutional cohort of carcinomas that developed in the urinary bladder following augmentation cystoplasty.

Design: Carcinomas arising in the urinary bladder of patients with history of augmentation cystoplasty were obtained from 4 major academic institutions, with cases originally diagnosed as urothelial carcinoma excluded from the study. The cases were analyzed using a clinically validated targeted DNA sequencing panel that includes 529 cancer-related genes and genome-wide copy number alterations.

Results: Across the ten analyzed cases, the most frequently altered genes included *TP53*, *KRAS*, and *MYC*, and the vast majority of cases demonstrated mutational profiles consistent with gastrointestinal adenocarcinomas. One of the cases demonstrated an *EML4-ALK* fusion together with an *MSH3* frameshift mutation and hypermutated phenotype, a mutational profile characteristic of a rare but aggressive subtype of colorectal adenocarcinoma that may benefit from targeted ALK inhibition therapy. Importantly, six other tumors in the cohort also had potentially targetable molecular alterations, involving *ATM* (2 cases*), BRCA1* (2 cases), *EGFR* (1 case), and *ERBB2* (1 case). Of note, one case with morphologic features of large cell undifferentiated carcinoma demonstrated a mutational profile most consistent with urothelial and not gastrointestinal origin (with mutations in *KMT2C, KMT2D, STAG2*, and the *TERT* promoter, among others).

Figure 1 - 630

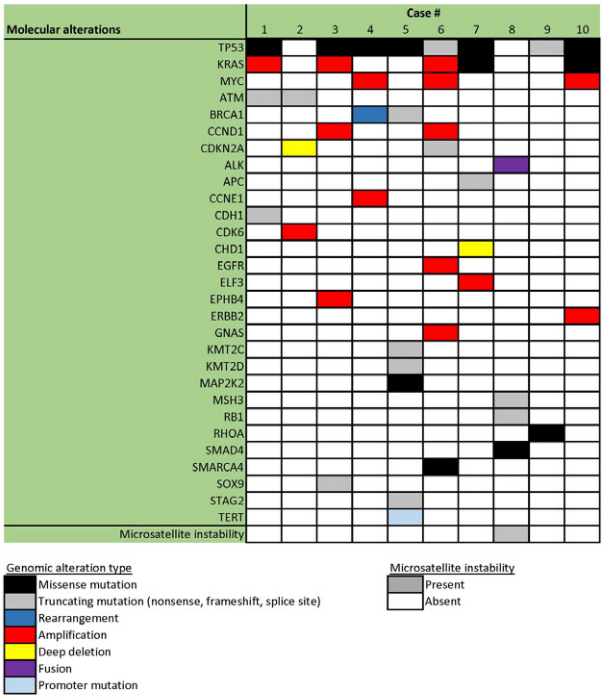

Conclusions: To our knowledge, this study represents the most comprehensive molecular characterization to date of carcinomas arising in the urinary bladder following augmentation cystoplasty. Despite the unique environment of the augmented tissue, the resulting tumors demonstrate a spectrum of driver mutations similar to that of primary gastrointestinal adenocarcinomas. In addition, molecular alterations potentially amenable to targeted therapy were identified in the majority of cases, which is a novel and critical finding in view of the aggressive nature of these tumors.

631 Pathologic Findings and Clinical Outcomes in Patients who Required Neoadjuvant Chemotherapy Prior to Orchiectomy for Testicular Germ Cell Tumors

Jeffrey Stump[1], Rumeal Whaley[2], Liang Cheng[3], Andres Acosta[4], Jennifer Gordetsky[1]
[1]Vanderbilt University Medical Center, Nashville, TN, [2]Indiana University School of Medicine, Indianapolis, IN, [3]Indiana University, Indianapolis, IN, [4]Brigham and Women's Hospital, Harvard Medical School, Boston, MA

Disclosures: Jeffrey Stump: None; Rumeal Whaley: None; Liang Cheng: None; Andres Acosta: None; Jennifer Gordetsky: *Consultant*, Jansen

Background: Current treatment for metastatic testicular germ cell tumor (GCT) includes orchiectomy with adjuvant chemotherapy. A subset of patients with testicular GCT present with significant metastatic disease, precluding orchiectomy. These patients receive neoadjuvant chemotherapy to reduce disease burden prior to orchiectomy. The pathologic findings and clinical outcomes in these patients are not well known. We investigated the pathologic findings and clinical outcomes in patients who underwent neoadjuvant chemotherapy prior to orchiectomy for testicular GCT.

Design: Surgical pathology databases were queried for post-treatment orchiectomy cases across 3 institutions. Clinicopathologic data were obtained. Complete testicular response to chemotherapy was defined as ypT0.

Results: We identified 34 patients with an age range of 15-59 years. Orchiectomy findings included teratoma (n=21), no residual tumor (n=7), mixed GCTs (n=3), seminoma (n=1), yolk sac tumor (YST) (n=1), and GCNIS (n=1). Cancer specific death occurred in 3/34 (9%) patients with mean time to death of 13 months. 14/34 (41%) patients had disease progression after initial chemotherapy. 8/34 (24%) patients had salvage chemotherapy, of which 2/8 (25%) died. Retroperitoneal lymph nodes were the most common site of metastases, followed by lung and mediastinum. Overall, the most common type of tumor found in metastases was teratoma (29%) and YST (26%). Choriocarcinoma was the most common metastasis in those requiring salvage chemotherapy. 21/34 (62%)

of patients had testes with only residual teratoma, of which 8 had disease progression and 2 died. In metastases of these patients, non-teratoma components were found in 13 patients. 6/34 (17.6%) patients had residual testicular non-teratoma/mixed GCT, of which 5 had disease progression and 1 died. In metastases, choriocarcinoma and teratoma were the most common in those with residual testicular non-teratoma/mixed GCT. Of the 7 patients with no residual testicular disease, 1 had disease progression and there were no cancer specific deaths. Seminoma was the most common metastasis in this group.

Clinicopathologic Results

	Residual Teratoma Only	Residual Non-Teratoma/Mixed Germ Cell Tumor	ypT0
Number of cases	21/34 (62%)	6/34 (17.6%)	7/34 (20.5%)
Deaths	2/21 (9.5%)	1/6 (16.6%)	0
Mean time to death (months)	14	11	N/A
Recurrence	8/21 (38%)	5/6 (83%)	1/7 (14.2%)
Most common metastasis	YST (6/21, 29%)	Choriocarcinoma and teratoma (2/6 each, 33%)	Seminoma (3/7, 43%)
Salvage Chemotherapy	4/21 (19%)	3/6 (50%)	1/7 (14%)

Conclusions: Patients requiring neoadjuvant chemotherapy for testicular GCT prior to orchiectomy have overall high disease progression but high survival. Most testes had only residual teratoma or no residual disease, suggesting good response in the testes to chemotherapy for GCT. Post-chemotherapy testes with no residual disease or only residual teratoma may be a good prognostic marker in these patients.

632 Clinicopathologic Features of Scrotal Leiomyosarcoma

Anne Taylor[1], Shawn Dason[1], Debra Zynger[2]
[1]The Ohio State University Medical Center, Columbus, OH, [2]The Ohio State University Wexner Medical Center, Columbus, OH

Disclosures: Anne Taylor: None; Shawn Dason: None; Debra Zynger: None

Background: Scrotal leiomyosarcoma arises from the subcutaneous smooth muscle layer and is an exceptionally rare disease process with only 6 patients in the largest reported case series. The rarity creates uncertainties regarding diagnosis, surgical management, and clinical outcomes. Our purpose was to describe our institutional experience with scrotal leiomyosarcoma.

Design: A retrospective institutional search was performed to identify scrotal leiomyosarcoma diagnosed from 2010-2019. Slides were reviewed and immunohistochemistry was performed for Ki67 and desmin. Mitotic activity, nuclear atypia, and strong desmin expression were required for inclusion. Clinicopathologic data for the cohort was obtained.

Results: Nine patients with scrotal leiomyosarcoma were identified. The mean age at diagnosis was 50 years (range 29-68 years). Most (n=7) presented with a scrotal mass, of which 5 were enlarging and 1 was painful. Clinical differential diagnosis was a nonneoplastic cyst for 8 patients. Mean tumor size was 1.7 cm (range 0.4-3.7 cm). Margins were positive in 3 cases and close in 1 case (mean distance to margin 0.3 cm) yielding 4 re-excisions (3 wide local excisions and 1 Mohs micrographic surgery). Mean mitotic rate was 2.4 per 10 high power field (HPF) (range 1-11 HPF) with mean Ki67 of 5% (range 1-15%). None demonstrated lymphovascular invasion, perineural invasion, or necrosis. Eight of the tumors were grade 1, while 1 was grade 2 (due to mitotic activity). Median follow-up was 84 months (range 18-116 months). Four patients had disease specific follow-up (3 with serial imaging and 1 with annual skin examinations). The single patient with a grade 2 tumor, which was also unusual in that it was suspected to be a neoplasm, was the largest tumor, and had highest mitotic rate, is undergoing the most rigorous surveillance regimen including re-staging scans every 3-6 months for the first two years, and less frequently thereafter. The remaining 5 patients have not had disease specific surveillance. None of the 9 patients have shown evidence of recurrence.

Conclusions: Scrotal leiomyosarcoma is a rare tumor with a deceptive presentation and heterogeneous management. With complete surgical resection, scrotal leiomyosarcoma has an excellent prognosis and rigorous follow-up or adjuvant treatment are not likely to be necessary. Cases with unusual clinical or pathologic findings, such as large tumor size or high mitotic rate, may merit more intensive disease specific surveillance.

633 Quantification of Perineural Invasion by Prostate Cancer on Needle Core Biopsy: Implication for Risk Stratification

Yuki Teramoto[1], Ying Wang[1], Hiroshi Miyamoto[1]
[1]*University of Rochester Medical Center, Rochester, NY*

Disclosures: Yuki Teramoto: None; Ying Wang: None; Hiroshi Miyamoto: None

Background: The presence of perineural invasion (PNI) by prostate cancer on biopsy (Bx) has been considered as a key prognosticator. However, it remains unclear how the number of actual PNI foci in Bx specimen has an impact on patient outcomes. In the present study, we quantified PNIs with the aim of creating a simple and useful index for the prognostic prediction.

Design: We assessed consecutive patients with PNI on standard sextant Bx (typically 2 cores/site) followed by radical prostatectomy (RP) both performed at our institution from 2009-2016. We identified 262 cases from our Surgical Pathology database while excluded 10 cases (*i.e.* H&E-stained slides unavailable, no PNI during slide review). Data for PNI and tumor length on targeted Bx were not used for analysis.

Results: Only 1 PNI in the entire specimen was present in 152 (60.3%) cases, while 2 [53 (21.0%)], 3 [19 (7.5%)], 4 [12 (4.8%), and 5-10 [16 (6.3%)] PNIs were found in other cases. Compared with cases exhibiting a single PNI, multiple PNIs were significantly associated with higher preoperative prostate-specific antigen (PSA), higher Grade Group on Bx or RP, higher pT/pN category, positive surgical margin, and larger estimated tumor volume. When total tumor length on each Bx was considered, significant differences in Grade Group on RP and pN status between cases with ≤1 vs. >1 PNI per 10-mm tumor were observed. Kaplan-Meier analysis revealed a significantly higher risk of progression in patients with multiple PNIs (vs. a single PNI per Bx; Figure 1) as well as those with >1 PNI per 10-mm tumor (vs. ≤1 PNI; Figure 2). Significant differences in progression-free survival (PFS) between ≤1 vs. >1 PNI/10-mm tumor were also seen in subgroups, including those with ≤10-mm tumor (P=0.021), >10/≤20-mm tumor (P<0.001), and >20-mm tumor (P=0.005), and those showing PNI only at 1 sextant site (P=0.029). Additionally, when the cohort was divided into 3 groups (*i.e.* 1 vs. 2 vs. 3-10 PNI/case, ≤1 vs. >1/≤2 vs. >2 PNI/10-mm tumor), significant differences in PFS were still seen. In multivariate analysis, both multiple PNI foci/case (HR=4.533, 95%CI=2.544-8.074, P<0.001) and >1 PNI/10-mm tumor (HR=2.863, 95%CI=1.687-4.861, P<0.001) showed significance for progression.

	Single PNI/case	Multiple PNIs/case	p value	≤1 PNI/10-mm tumor	>1 PNI/10-mm tumor	p value
n	152	100		170	82	
Age (mean, year)	62.4	63.7	0.134	62.8	63.1	0.794
PSA (median, ng/mL)	6.14	7.36	0.027	6.35	6.44	0.405
Bx tumor length (median, mm)	16	29	<0.001	25	9	<0.001
Grade Group (Bx)			<0.001			0.272
1	22 (14.5%)	3 (3.0%)		12 (7.1%)	13 (15.9%)	
2	77 (50.7%)	27 (27.0%)		72 (42.4%)	32 (39.0%)	
3	31 (20.4%)	33 (33.0%)		45 (26.5%)	19 (23.2%)	
4	17 (11.2%)	26 (26.0%)		31 (18.2%)	12 (14.6%)	
5	5 (3.3%)	11 (11.0%)		10 (5.9%)	6 (7.3%)	
Grade Group (RP)			<0.001			0.009
1	10 (6.6%)	1 (1.0%)		3 (1.8%)	8 (9.8%)	
2	89 (58.6%)	29 (29.0%)		81 (47.6%)	37 (45.1%)	
3	37 (24.3%)	42 (42.0%)		60 (35.3%)	19 (23.2%)	
4	7 (4.6%)	10 (10.0%)		8 (4.7%)	9 (11.0%)	
5	9 (5.9%)	18 (18.0%)		18 (10.6%)	9 (11.0%)	
pT			<0.001			0.255
2	71 (46.7%)	14 (14.0%)		56 (32.9%)	29 (35.4%)	
3a	67 (44.1%)	54 (54.0%)		87 (51.2%)	34 (41.5%)	
3b	14 (9.2%)	32 (32.0%)		27 (15.9%)	19 (23.2%)	
pN			<0.001			0.014
0	135 (88.8%)	76 (76.0%)		148 (87.1%)	63 (76.8%)	
1	7 (4.6%)	23 (23.0%)		19 (11.2%)	11 (13.4%)	
X	10 (6.6%)	1 (1.0%)		3 (1.8%)	8 (9.8%)	
Surgical margin			0.004			0.741
Negative	130 (85.5%)	70 (70.0%)		136 (80.0%)	64 (78.0%)	
Positive	22 (14.5%)	30 (30.0%)		34 (20.0%)	18 (22.0%)	
Tumor volume (median, cc)	6.50	11.25	<0.001	8.50	7.60	0.567

Figure 1 - 633

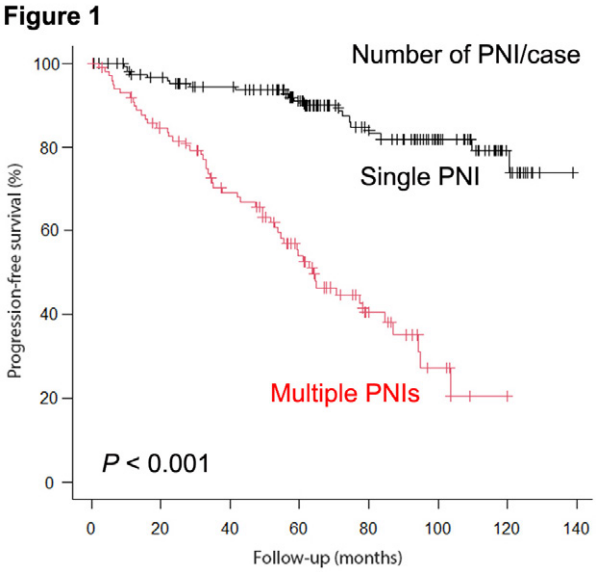

Figure 2 - 633

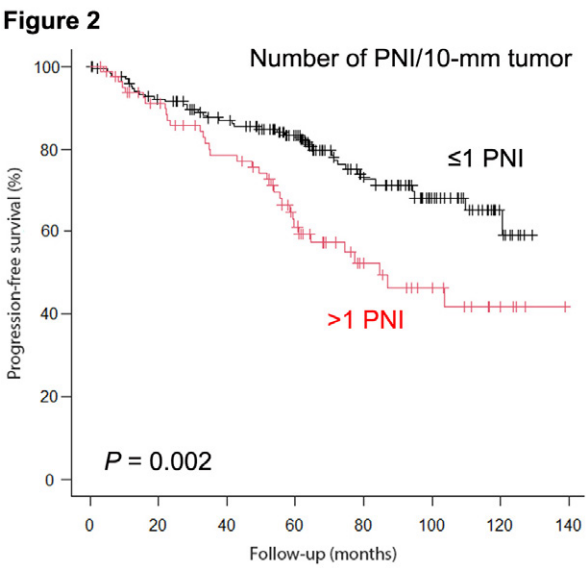

Conclusions: Multiple PNIs and >1 PNI per 10-mm tumor on each Bx were found to be associated with poor prognosis, as independent predictors, in men with prostate cancer undergoing RP. Remarkably, the prognostic impact of the latter remained significant in all subgroups of patients examined.

634 The Clinical Significance of Perineural Invasion by Prostate Cancer Detected on Needle Core Biopsy: Unilateral vs. Bilateral Involvement

Yuki Teramoto[1], Numbereye Numbere[1], Ying Wang[1], Hiroshi Miyamoto[1]
[1]University of Rochester Medical Center, Rochester, NY

Disclosures: Yuki Teramoto: None; Numbereye Numbere: None; Ying Wang: None; Hiroshi Miyamoto: None

Background: The presence of perineural invasion (PNI) by prostate cancer, particularly in biopsy (Bx) specimen, has been implicated with adverse pathologic features, including extraprostatic extension, and resultant poor patient outcomes. However, the impact of PNI laterality (*i.e.* right or left vs. both sides) on Bx remains poorly understood. We herein compare radical prostatectomy (RP) findings and long-term oncologic outcomes in prostate cancer patients with PNI in 2 Bx sites.

Design: We assessed consecutive patients who had undergone standard sextant prostate Bx (*i.e.* 6 sites: right apex, right mid, right base, left apex, left mid, left base) followed by RP from 2009-2016. A total of 155 men in our Surgical Pathology database met the inclusion criteria for PNI detected in 2 of 6 Bx sites. Cases with PNI on targeted Bx were excluded.

Results: PNI occurred unilaterally in 128 (83%) cases and bilaterally in 27 (17%) cases. Bilateral PNI was associated with significantly higher numbers of cancer-positive sites, compared with unilateral PNI. Similarly, PNI was identified at spatially contiguous (*e.g.* right apex/right mid, right apex/left apex) or separate (*e.g.* right apex/right base, right apex/left mid) lesion(s) in 103 (66%) or 52 (34%) cases, respectively. Positive surgical margin in RP specimens was significantly more often seen in separate PNI cases than in contiguous PNI cases. There were no significant differences in other clinicopathologic features between unilateral vs. bilateral PNI cohorts or contiguous vs. separate PNI cohorts. Kaplan-Meier analysis revealed a significantly higher risk of disease progression after RP in patients with bilateral PNI on Bx, compared to those with unilateral PNI. However, there was no significant difference in progression-free survival between patients with contiguous vs. separate PNIs. Interestingly, separate PNI was associated with a significantly higher risk of progression in a subgroup of patients showing bilateral PNI, but not unilateral PNI. In multivariate analysis with Cox model in the entire cohort, bilateral (vs. unilateral) PNI showed significance for progression (HR=2.517, 95%CI=1.204-5.263, *P*=0.014).

	Unilateral (n=128)	Bilateral (n=27)	P	Contiguous (n=103)	Separate (n=52)	P
Age (mean, year)	62.3	61.1	0.454	62.5	61.4	0.401
PSA (mean, ng/mL)	8.3	7.8	0.644	8.0	8.7	0.570
Bx cancer-positive sites			0.002[a]			0.811[a]
2	10 (8%)	3 (11%)		10 (10%)	3 (6%)	
3	54 (42%)	2 (7%)		38 (37%)	18 (35%)	
4	29 (23%)	6 (22%)		22 (21%)	13 (25%)	
5	15 (12%)	11 (41%)		17 (17%)	9 (17%)	
6	20 (16%)	5 (19%)		16 (16%)	9 (17%)	
Bx Grade Group (highest)			0.819[b]			0.881[b]
1	17 (13%)	2 (7%)		14 (14%)	5 (10%)	
2	46 (36%)	10 (37%)		37 (36%)	19 (37%)	
3	30 (23%)	6 (22%)		24 (23%)	12 (23%)	
4	22 (17%)	5 (19%)		16 (16%)	11 (21%)	
5	13 (10%)	4 (15%)		12 (12%)	5 (10%)	
RP Grade Group			0.848[b]			0.763[b]
1	3 (2%)	0 (0%)		1 (1%)	2 (4%)	
2	64 (50%)	16 (59%)		56 (54%)	24 (46%)	
3	36 (28%)	6 (22%)		26 (25%)	16 (31%)	
4	7 (5%)	0 (0%)		6 (6%)	1 (2%)	
5	18 (14%)	5 (19%)		14 (14%)	9 (17%)	
pT			0.476[c]			0.451[c]
2	33 (26%)	9 (33%)		30 (29%)	12 (23%)	
3a	71 (55%)	11 (41%)		55 (53%)	27 (52%)	
3b	24 (19%)	7 (26%)		18 (17%)	13 (25%)	
pN			0.799[d]			0.536[d]
0	94 (73%)	21 (78%)		77 (75%)	38 (73%)	
1	28 (22%)	5 (19%)		20 (19%)	13 (25%)	
X	6 (5%)	1 (4%)		6 (6%)	1 (2%)	
Surgical margin			1.000			0.048
Negative	97 (76%)	20 (74%)		83 (81%)	34 (65%)	
Positive	31 (24%)	7 (26%)		20 (19%)	18 (35%)	
Tumor volume (mean, cc)	11.4	14.3	0.329	10.8	14.1	0.106

[a] 2 vs. 3 vs. 4 vs. 5-6; [b] 1-2 vs. 3 vs. 4-5; [c] 2 vs. 3; [d] 0 vs. 1

Figure 1 - 634

Figure 1. Progression-free survival in all patients.

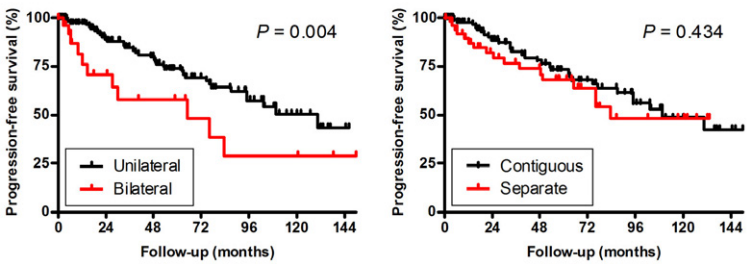

Figure 2 – 634

Figure 2. Progression-free survival in subgroups of patients.

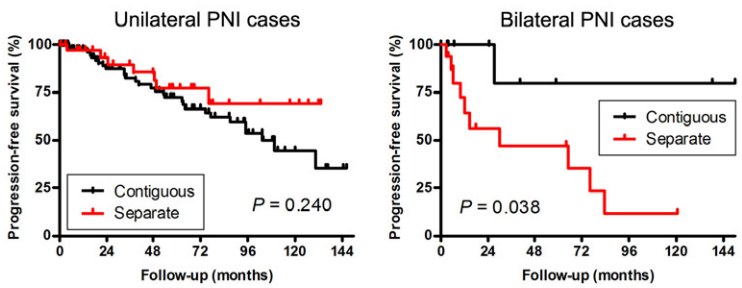

Conclusions: In Bx specimens exhibiting PNI in 2 of sextant sites, bilateral PNI was found to be associated with poorer prognosis as an independent predictor, but not worse histopathologic features in RP specimens, compared with unilateral PNI. Further studies in larger patient cohorts are required to assess the impact of PNI locations on prostate Bx.

635 Penile Squamous Cell Carcinomas: Association with Human Papillomavirus, p53 Immunohistochemical Status and Clinic-Pathological Features

Isabel Trias[1], Natalia Rakislova[1], Jose Guerrero Pineda[2], Marta del Pino[1], Rafael Parra-Medina[3], Luis Veloza Cabrera[4], Lorena Marimon[5], Juan Manuel Corral[6], Tarek Ajami[6], Oscar Reig[6], Maria Ribal[6], María Teresa Rodrigo[1], Laurina Chulo[7], Jaume Ordi[8], Inmaculada Ribera[1]

[1]Hospital Clinic, Barcelona, Spain, [2]Hospital Clinic, University of Barcelona, Barcelona, Spain, [3]Fundacion Universitaria de Ciencias de la Salud, Bogotá, Colombia, [4]CHUV and University of Lausanne, Lausanne, Switzerland, [5]Institute for Global Health (ISGloblal), Spain, [6]Hospital Clínic de Barcelona, Barcelona, Spain, [7]Hospital Central de Maputo, maputo, Mozambique, [8]University of Barcelona, Barcelona, Spain

Disclosures: Isabel Trias: None; Natalia Rakislova: None; Jose Guerrero Pineda: None; Marta del Pino: None; Rafael Parra-Medina: None; Luis Veloza Cabrera: None; Lorena Marimon: None; Juan Manuel Corral: None; Tarek Ajami: None; Oscar Reig: None; Maria Ribal: None; María Teresa Rodrigo: None; Laurina Chulo: None; Jaume Ordi: None; Inmaculada Ribera: None

Background: *Two different pathways have been described for penile squamous cell carcinomas (PSCC), one associated with human papillomavirus (HPV), and the other independent of HPV infection. We aimed to evaluate the morphological, immunohistochemical and clinic-pathological characteristics of HPV-associated and HPV-independent PSCC from Spain, a western country with a low prevalence of HPV infection.*

Design: We included 53 PSCC diagnosed in the period comprised between 2000 and 2021. In all tumors a thorough histological revision, HPV DNA detection using a PCR-based test (SPF10/DEIA/LiPA25), immunohistochemistry (IHC) for p16 and p53 were performed. All patients were followed up for a median period of 49 months (range 0.3-244). Diffuse p16 IHC staining and/or HPV DNA detected by PCR was considered as evidence of HPV infection. p53 staining was evaluated as normal (suggestive of wild-type protein, including scattered and mid-epithelial positivity) and abnormal patterns (suggestive of mutation, including basal, diffuse overexpression, cytoplasmic or null staining). Histological subtypes were grouped as probably HPV-associated and as probably HPV-independent, following WHO 2016 classification.

Results: Seventeen out of the 53 tumors (32%) were HPV-associated and 36 (68%) were HPV-independent. Histologically, 38 (71%) tumors were of histological types suggestive of being HPV-independent (30 usual type, 3 verrucous, 4 mixed and 1 cuniculatum), and 15 suggestive of HPV-associated (10 basaloid, 4 warty and 1 lymphoepithelioma). Twenty-six out of 53 had an abnormal pattern of p53 expression (49%). Abnormal patterns of p53 immunostaining were related with high clinical staging at diagnosis (stage 2 or more, p=0.03). Disease-free survival was strongly associated with staging (p<0.001). HPV-associated histological subtypes had better disease-free survival than those HPV-independent (p=0.019). Patients with HPV-independent tumors with normal p53 IHC expression were significantly older than those with abnormal p53 (75±13 vs. 65±13; p=0.023).

Conclusions: Most PSCC in our geographic area are HPV-independent. HPV-associated histological types had better disease-free survival than HPV-independent PSCC. Our study suggests that two different HPV-independent subgroups exist one with wild-type p53 IHC expression affecting older patients and a second one associated with mutated p53 arising in younger individuals.

636 Mismatch Repair (MMR) Deficiency in Early-Onset Prostatic Adenocarcinoma: A Clinicopathologic Study

Jonathan Tucci[1], Jennifer Gordetsky[1], Andries Zijlstra[2], Adel Eskaros[1], Daniel Barocas[3], Kristen R Scarpato[3], Sam Chang[1], Joseph Smith[1], David Penson[1], Giovanna Giannico[1]

[1]Vanderbilt University Medical Center, Nashville, TN, [2]Genentech, Inc., San Francisco, CA, [3]Vanderbilt University Medical Center

Disclosures: Jonathan Tucci: None; Jennifer Gordetsky: *Consultant*, Jansen; Andries Zijlstra: *Employee*, Genentech, Inc.; Adel Eskaros: None; Daniel Barocas: *Advisory Board Member*, Progenics; *Advisory Board Member*, ambu; Kristen R Scarpato: None; Sam Chang: *Consultant*, mIR, Merck, Urogen, Janssen, NantBiocel; Joseph Smith: None; David Penson: None; Giovanna Giannico: None

Background: Mismatch repair genes alterations have been demonstrated in a small subset of patients with aggressive, but targetable, prostate cancers. However, these alterations have yet to be described in early-onset prostatic adenocarcinoma. Here, we assessed the rates of MMR deficiency (dMMR) and compare the histologic features and clinical outcomes in cohorts of early-onset (yPCa) and non-early onset prostate cancer (vPCa).

Design: One-hundred eight cases of yPCa (≤45 years of age) and 115 vPCa cases (>45 years of age) were retrospectively identified between 2006-2020 and 2009-2014, respectively, and graded according to the 2014 modified Gleason system. Tissue microarrays containing 1-mm cores of cancer from the dominant nodule and normal tissue in duplicate were used to assess dMMR using antibodies for MLH1, PMS2 (Leica Biosystems), MSH2 (Dako) and MSH6 (Cell Marque Corporation). Statistical analysis was performed using STATA version 17.

Results: yPCa cases were more likely to be organ-confined (92.6% vs. 57.1%; p<0.001) and to have lower pre-operative prostate specific antigen level (6.31 vs. 9.70; p=0.005), mucinous morphology (20.4% vs. 3.5%; p<0.001), negative margins (17.6% vs. 41.1%; p<0.001), and lower rates of biochemical recurrence (BCR) (10.6% vs. 56.4%; p<0.001). Frequency of cribriform features (p=0.77) was similar between the two cohorts (Table 1). Despite yPCa having lower tumor stage and BCR rates, there was no difference in BCR-free survival between the two groups (log-rank, p=0.098; Figure 1). In yPCA, by univariate logistic regression, BCR was associated with grade (OR 6.24, p=0.001) and pathologic stage (OR 46.1, p<0.001) but not with cribriform morphology. In vPCa, by multivariate logistic regression, BCR was associated with cribriform morphology (OR 5.54, p=0.009) but not with grade or pathologic stage. One vPCa case demonstrated MSH2 and MSH6 loss but retained MLH1 and PMS2. yPCa cases were MMR proficient.

Table 1. Clinicopathologic characteristics of the early-onset and validation cohorts of prostatic adenocarcinoma.

Variable	Early-Onset (≤45 yrs)	Non-Early-Onset (>45 yrs)	P-value
N	108	112	—
Age (years), Mean (SD)	42.36 (2.1)	60.71 (6.5)	<0.001
Race, N (%)			0.044
White	81 (75.0)	94 (83.9)	
Black	27 (25.0)	16 (14.3)	
Other	0 (0.0)	2 (1.8)	
Pre-operative PSA (ng/ml), Mean(SD)	6.31 (5.8)	9.70 (10.9)	0.005
Grade Group, N (%)			0.027
1	45 (41.7)	35 (31.3)	
2	49 (45.4)	50 (44.6)	
3	13 (12.0)	16 (14.3)	
4	1 (0.9)	4 (3.6)	
5	0 (0.0)	7 (6.3)	
Cribriform Morphology, N (%)	34 (31.5)	33 (29.5)	0.77
Intraductal Carcinoma, N (%)	5 (4.6)	22 (19.6)	<0.001
Mucinous Morphology, N (%)			<0.001
Variant (>25%)	14 (13.0)	3 (2.7)	
Features (<25%)	8 (7.4)	1 (0.9)	
Absent	86 (79.6)	108 (96.4)	
Margin Positivity, N (%)	19 (17.6)	46 (41.1)	<0.001
AJCC 8th Edition Tumor Stage, N (%)			<0.001
2	100 (92.6)	64 (57.1)	
3a	5 (4.6)	21 (18.8)	
3b	2 (1.9)	27 (24.1)	
4	1 (0.9)	0 (0.0)	
Lymph Node Metastasis, N (%)			0.046
Present	2 (2.7)	8 (12.3)	
Absent	71 (97.3)	57 (87.7)	
Follow-up (months), Mean (SD)	44.7 (133.7)	61.2 (48.5)	0.23
BCR, N (%)	11 (10.6)	62 (56.4)	<0.001
Time to BCR (months), Mean (SD)	34.1 (42.3)	18.4 (22.9)	0.075

PSA, prostate specific antigen; AJCC, American Joint Committee on Cancer; BCR, Biochemical Recurrence

Figure 1 - 636

Figure 1. Kaplan-Meier curve of biochemical recurrence-free survival in early-onset (red) and non-early onset (blue) prostate cancer.

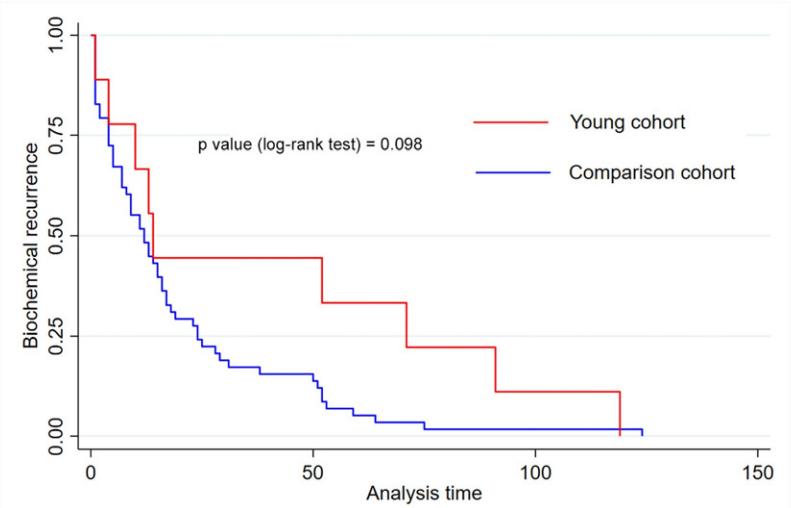

Conclusions: In summary, dMMR is unrelated to age of onset of PCa. yPCa is significantly associated with mucinous morphology.

637 Grading of Prostate Cancer in Africa Using Whole Slide Imaging: Interobserver Variation among Pathologists and Artificial Intelligence

Abraham van Wyk[1], Timothy Rebbeck[2], Brian Robinson[3], Olufemi Ogunbiyi[4], Olabode Oluwole[5], Lynnette Kyokunda[6], Cherif Dial[7], Afua Abrahams[8], Frederick Hobenu[9], Sun Woo Kim[10], Massimo Loda[3], Priti Lal[11]
[1]Stellenbosch University, Cape Town, South Africa, [2]Dana-Farber Cancer Institute, Harvard Cancer Center, Boston, MA, [3]Weill Cornell Medicine, New York, NY, [4]University of Ibadan/University College Hospital, Ibadan, Nigeria, [5]University of Abuja, Abuja, Nigeria, [6]Gaborone, Botswana, [7]Dakar, Senegal, [8]Korle-Bu Teaching Hospital, Accra, Ghana, [9]37 Military Hospital, Accra, Ghana, [10]Deep Bio Inc., Seoul, South Korea, [11]University of Pennsylvania, Philadelphia, PA

Disclosures: Abraham van Wyk: None; Timothy Rebbeck: None; Brian Robinson: None; Olufemi Ogunbiyi: None; Olabode Oluwole: None; Lynnette Kyokunda: None; Cherif Dial: None; Afua Abrahams: None; Frederick Hobenu: None; Sun Woo Kim: *Stock Ownership*, DeepBio; Massimo Loda: *Other*, Methylex; Priti Lal: None

Background: Histologic grading of prostate cancer is one of the strongest predictors of disease outcome and is the main stratification tool to decide on different treatment options. The notable interobserver variation among pathologists is its main weakness. In sub-Saharan Africa, prostate cancers are typically graded by general anatomic pathologists. This pool of pathologists is heterogeneous in terms of training, equipment, access to immunohistochemical stains and workload. In addition, previous interobserver studies were performed in non-African populations. The aims of this study were to assess the interobserver variability in prostate cancer grading between African general pathologists, between African pathologists and a US uropathologist and to assess agreement with an artificial intelligence (AI) tool.

Design: Participating African centers submitted tissue from 133 prostate cancer cases for whole slide scanning. For the 1st round evaluation, 34 whole slide images were randomly assigned to 8 African pathologists resulting in each digital slide being evaluated twice. A US genitourinary pathologist evaluated all 133 digital slides (central review). The slides were also graded using an AI tool. After a washout period of four months, a webinar on prostate cancer grading were attended by participating pathologists. Fifteen digital slides were randomly selected for a 2nd round evaluation and re-evaluated by African pathologists. Cohen's Kappa (κ) scores were calculated on the ISUP / WHO 2014 Grade Group grading.

Results: The virtual platform worked efficiently for all pathology groups in Africa. Poor tissue quality and artefacts were identified as possible sources of discordance. A κ of up to 0.57 was reached between central review and African pathologists in images assigned score 1 for quality. An overall κ was 0.43 for all comers. The interobserver concordance between the central uropathology review and participating centers was within the range published in the literature. AI could not reach a κ beyond 0.248 for all comers

and 0.22 for quality score 1 images. Interobserver variation between African pathologists and central review improved to κ = 0.67 after webinar-based training.

Table 1: Kappa scores between US genitourinary pathologist (central review), African general pathologists and AI according to tissue quality scores

Quality Score (1= best; 2=intermediate; 3=worst)		1	2	3	1+2	2+3	1+2+3
Evaluator 1	**Evaluator 2**	n=38	n=54	n=25	n=92	n=79	n=117
Central review	Artificial intelligence	0.222	0.231	0.333	0.227	0.260	0.248
Central review	Africa Set 1	0.474	0.370	0.478	0.413	0.403	0.426
Central review	Africa Set 2	0.568	0.352	0.417	0.440	0.372	0.435
Africa Set 1	Africa Set 2	0.487	0.330	0.364	0.418	0.368	0.407

Conclusions: 1) Whole slide scanned images are useful for international collaborative work. 2) The interobserver agreement between African pathologists and the US uropathologist was moderate to substantial and within the range of published literature. 3) Interobserver variation can be improved with online training.

638 Grading Intraductal Carcinoma in the Presence of Concurrent Prostatic Adenocarcinoma and its Impact on Grade Group Assignment

Karan Vats[1], Ingrid Tam[1], Nicholas Baniak[2]
[1]University of Saskatchewan, Saskatoon, Canada, [2]University of Saskatchewan, Saskatchewan Health Authority, Saskatoon, Canada

Disclosures: Karan Vats: None; Ingrid Tam: None; Nicholas Baniak: None

Background: The Gleason score/Grade Group (GS/GG) is an important parameter used in clinical decision-making. The two international societies for urologic pathology (Genitourinary Pathology Society and the International Society of Urologic Pathology) recently released consensus manuscripts for prostatic carcinoma. Many of the recommendations are in agreement, including not grading biopsies with pure intraductal carcinoma (IDC). However, there is disagreement regarding grading IDC in the presence of concurrent prostatic adenocarcinoma and the reports to date examining the influence of grading IDC have shown variable impacts on GS/GG re-assignment. The purpose of this study is to evaluate the effect of IDC grading on the overall GS/GG of prostate biopsies and radical prostatectomies.

Design: This study included 143 matched prostate biopsy and radical prostatectomy specimens that were collected between 2019 and 2021. All cases were graded by a genitourinary pathologist with and without grading IDC. Biopsy specimens were assessed for global GS/GG and highest GS/GG.

Results: Out of 143 prostate core biopsies, 41 (28.7%) had an invasive cribriform/IDC component. Grading IDC changed the global GS/GG in 4 cases (2.8%, P = 0.78). In 3/41 (7.3%), GG2 was upgraded to GG3 and in 1/41 (2.4%) GG3 was upgraded to GG5. The highest GS/GG changed in one case from GG3 to GG5 due to the presence of comedonecrosis. An invasive cribriform/IDC component was found in 94 (65.7%) of radical prostatectomy cases. Including IDC in the grade changed the GS/GG in 7/143 cases (4.9%, P = 0.02). In 1/94 (1.1%), GG2 was upgraded to GG3, 1/94 (1.1%) GG2 was upgraded to GG4, 4/94 (4.3%) GG3 was upgraded to GG5, and 1/94 (1.1%) GG4 was upgraded to GG5. Upgrading was due to comedonecrosis in 6/7 cases (one GG2 to GG4 (GS 3+5), four GG3 to GG5 and one GG4 to GG5).

Conclusions: The global and highest GS/GG is unchanged in the majority of cases if IDC is graded. However, incorporating IDC into the grade will change the management plan for some patients, more so after radical prostatectomy than biopsy. There is a need for consensus on grading IDC to provide patients with a consistent and effective management plan

639 INIFY Prostate* Predictions on Prostate Biopsies: Impact of Scanners, Preanalytical Factors and User Experience

Jennifer Vazzano[1], Kun Hu[2], Dorota Johansson[3], Kristian Euren[4], Lena Wilén[4], Ming Zhou[5], Anil Parwani[6]
[1]The Ohio State University Wexner Medical Center, Columbus, OH, [2]Tufts Medical Center, Boston, MA, [3]Stockholm, Sweden, [4]Contextvision AB, Stockholm, Sweden, [5]Tufts University School of Medicine, Boston, MA, [6]The Ohio State University, Columbus, OH

Disclosures: Jennifer Vazzano: None; Kun Hu: None; Dorota Johansson: *Consultant*, ContextVision; Kristian Euren: None; Lena Wilén: *Employee*, ContextVision AB; Ming Zhou: None; Anil Parwani: None

Background: Artificial intelligence (AI) algorithms can be used as a tool to augment diagnosis, grading and volume quantification of prostate cancer (PCa) in prostate biopsy (PBx). In this study we evaluated the impact of three common scanners and preanalytical factors (slide preparation) on the performance of an AI tool; INIFY Prostate. Two independent pathologists' evaluation of AI's performance reflected their user experience.

Design: 30 PBx slides from 30 unique cases were used: 15 (10 PCa and 5 benign) from each institution (TMC and OSU). The slides were scanned on Aperio, Hamamatsu and Philips scanners and whole slide images (WSI) produced. The algorithm (INIFY Prostate) was applied to predict suspicious PCa areas and tumor volume (% area of biopsy involved). Pathologists reviewed the algorithm's annotations to identify benign glands misclassified as PCa (false positive) and PCa glands misclassified as benign (false negative).

Results: INIFY identified all PCa slides as "suspicious". The % of suspicious PCa area calculated by the algorithm was similar for all 3 scanners and strongly correlated with the pathologist estimate of cancer length (Table). For WSIs with small cancer foci (≤1 mm), the algorithm identified all cancer glands (sensitivity 100%). The overall sensitivity and specificity was 99.4 and 97%. The AI worked equally well on images from 3 scanners and from 2 sites, with similar sensitivity and specificity. The pathologists identified WSIs where the AI found a small focus cancer (~0.1 mm of the core length) not easily seen in 2 of 3 cores (Fig 1). The few false negative PCa glands were small and close to the properly identified larger PCa (Fig 2). One pathologist judged all false positives as acceptable, while the other judged 25% as poor. Both agreed that the AI performance on finding PCa areas was good/acceptable in ~99% of images.

Table: Sensitivity and Specificity of INIFY for Identifying Cancer Areas in Prostate Biopsy

	Specificity (all images)	Sensitivity (cancer images)	Sensitivity Small focus cancer images (≤1mm)
Overall (mean for 3 scanners)	97.00%	99.40%	100%
	(±3.3%; n = 180)	(±2.5%, n = 120)	(± 0.0%, n = 30)
Aperio scanner	96.60%	98.90%	100%
	(±3.7%; n = 60)	(±3.8%; n = 60)	(± 0.0%; n = 10)
Hamamatsu scanner	96.60%	99.50%	100%
	(±3.6%; n = 60)	(±1.7%; n = 60)	(± 0.0%; n = 10)
Philips scanner	97.80%	99.60%	100%
	(±2.3%; n = 60)	(±1.1%; n = 60)	(± 0.0%; n = 10)
Boston site	95.50%	99.90%	100%
	(±3.6%; n = 90)	(±0.6%; n = 90)	(± 0.0%; n = 24)
Ohio site	98.50%	98.90%	100%
	(±1.7%; n = 90)	(±3.4%; n = 90)	(± 0.0%; n = 6)
Pathologist 1	98.50%	99.50%	100%
	(±3.0%; n = 90)	(±3.0%; n = 90)	(± 0.0%; n = 15)
Pathologist 2	97.90%	99.30%	100%
	(±2.9%; n = 90)	(±1.7%; n = 90)	(± 0.0%; n = 15)

Figure 1 - 639

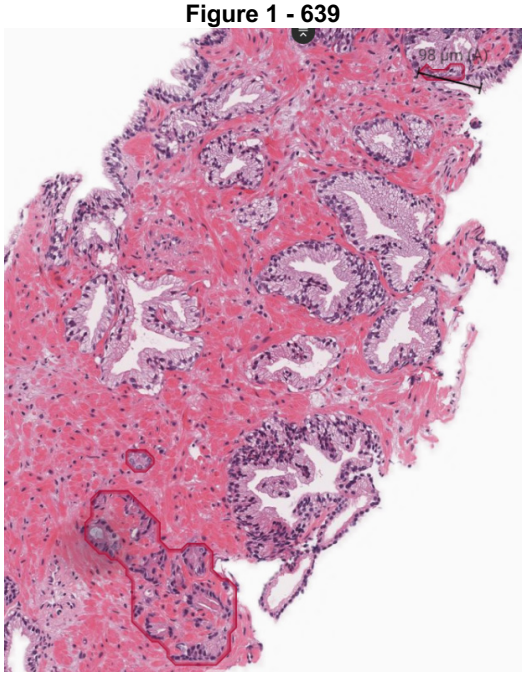

Figure 2 - 639

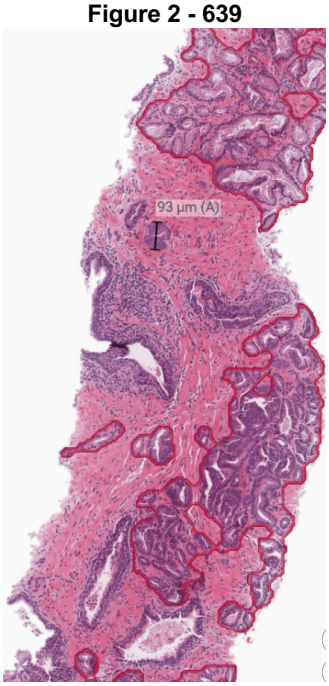

Conclusions: INIFY Prostate* predictions on WSIs scanned on 3 scanners from two different labs show excellent correlation in diagnostic accuracy and tumor volume estimation. INIFY identified all PCa slides. Sensitivity is 100% for small PCa (≤1 mm). Specificity is high and majority of false positives are minute foci of cancer mimickers easily confirmed by pathologists. No significant differences between scanners and labs have been identified. Such studies will be important as pathologists move forward with implementing AI algorithms to assist routine sign-out workflows.

640 Immunohistochemical and Next-Generation Sequencing (NGS) Characterization of 19 Cases of Adenosquamous Prostate Carcinoma (PCa) of the Prostate

Alejandra Villarroel[1], Tamara Lotan[2], Andres Matoso[1], Jonathan Epstein[1]
[1]Johns Hopkins Medical Institutions, Baltimore, MD, [2]Johns Hopkins University School of Medicine, Baltimore, MD

Disclosures: Alejandra Villarroel: None; Tamara Lotan: *Grant or Research Support*, Roche/Ventana; *Grant or Research Support*, DeepBio; *Grant or Research Support*, Myriad; Andres Matoso: None; Jonathan Epstein: None

Background: Adenosquamous PCa carcinoma is an exceedingly rare variant of prostate cancer, which is difficult to diagnose and has a very poor prognosis. There are few pathology-focused series or case reports of adenosquamous PCa. The only to look at NGS analyzed a few cases as part of a small NGS series of rare histological variants of PCa.

Design: In this series, 19 cases of adenosquamous PCa were selected, including 1 internal and 18 consults. In all cases, immunohistochemical study was performed for PTEN, ERG, AR, Rb and GATA3, and on selected cases, NGS.

Results: The mean age at diagnosis was 67 years (53 to 79 y). 7 men had a prior history of PCa, 5 of them treated by antiandrogen therapy and 1 radiotherapy. 11 cases were diagnosed on TURP, 5 on needle core biopsies, 2 on radical prostatectomies and 1 in an excision of a pelvic lymph node metastasis. The adenocarcinoma component was Group Grade 5 in 11 cases, Grade group 4 in 3 and not assessable in 5. In only 9/18 consult cases, adenosquamous PCa was noted in the differential diagnosis by the contributing pathologists. A small cell carcinoma component was observed in 1 case. The lymph node metastasis showed a sarcomatoid component. Homogeneous PTEN loss was observed in 10 cases, heterogeneous PTEN loss in 3 cases, intact PTEN in 4 cases and 2 non-interpretable results caused by a lack of internal control. ERG positivity was found in 8 cases (mostly focal expression). AR positivity was found in the adenocarcinoma component of 14 cases and only 1 case with focal expression on the squamous component. Rb loss was shown in 10 cases. The expression of GATA3 was mostly focal and only in 3 cases positivity was diffuse. Details of immunohistochemical results are showed in Figure 1 and Table 1. NGS was performed on 9 cases and the most common significant alterations were found in TP53 (4 cases) and PIK3CA (3 cases).

Table 1. Immunohistochemical features of PTEN, ERG, AR, Rb, GATA3, prostate markers, CK903 and p63.

Case Number	PTEN	ERG	AR		Rb	GATA3		Prostate markers*	CK903	p63
			(A)	(S)		(A)	(S)	(A)	(S)	(S)
1	NI	-	-	-	NI	-	-	+	+	+
2	Intact	+ Focal weak	90% ++/+++	-	Loss	-	-	+	+	NA
3	Loss	-	90% ++/+++	-	Retained	F +/++	F +/++	+	NA	Partial
4	Loss	-	-	-	Loss	-	-	NA	F	NA
5	Loss	-	5% +/++	-	Retained	-	F ++/+++	+	+	+
6	Het Loss	+ in (A)	90% ++/+++	-	Loss	F +/++	F +/++	+	NA	-
7	Loss	-	-	5% +/++	Retained	-	++/+++	+	F	F
8	Intact	-	30% ++/+++	-	Loss	40% ++/+++	++/+++	F	NA	F
9	Intact	-	-	-	Loss	-	++/+++	+	F	F
10	Loss	-	80% ++/+++	-	Loss	-	-	+	NA	NA
11 SCC	Loss	+ Partial	80% ++/+++	-	Loss	F +/++	F ++/+++	+	Partial	+
12	NI	NI	90% ++/+++	-	Retained	-	-	+	NA	+
13	Loss	+ Partial	90% ++/+++	-	Loss	-	F +	+	Partial	-
14	Loss	-	90% ++/+++	-	Retained	-	F +/++	NA	NA	NA
15 Sarc	Het Loss	+ Partial	80% ++/+++	-	Loss	F +	F ++/+++	+	NA	NA
16	Loss	+ Focal	80% +/++	NE	Retained	F +	NE	+	+	NA
17	Loss	+ Focal	-	-	Retained	-	F +	+	+	NA
18	Het Loss	+ Focal	90% ++/+++	-	Loss	F +/++	F +/++	+	NA	NA
19	Intact	-	80% ++/+++	-	Retained	-	F +/++	+	+	+

+ : Positive **-** : Negative
F: Focal staining (less than 5%) **SCC** – Associated small cell carcinoma component **Sarc** – Associated sarcomatoid component
* - Including NKX3.1, p501s, PSA or PSAP.
(A) - expression in adenocarcinoma component; **(S)** - expression in adenocarcinoma component
Het Loss- Heterogeneous PTEN loss; **Loss**- Homogeneous PTEN loss
NI- No interpretable, lack of internal control
NE- No evaluable, absence of squamous component on stains
NA – Not available

Figure 1 - 640

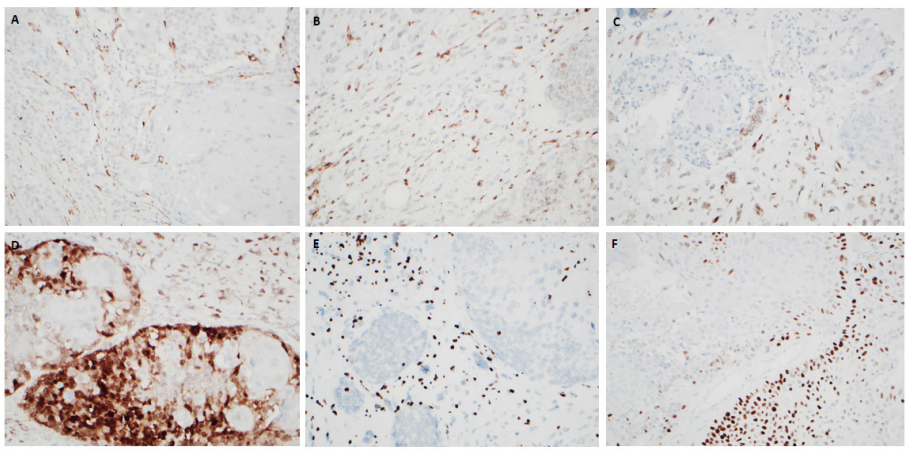

Figure 1. A. Homogeneous PTEN loss. Complete loss of PTEN expression (case 4, 20x). **B.** Heterogeneous PTEN loss. Partial positivity in the sarcomatoid and squamous areas (case 15, 20x). **C.** ERG partial positivity in both sarcomatoid and adenosquamous carcinoma (case 15, 20x). **D.** AR positivity in adenocarcinoma and sarcomatoid components. There is no expression in the squamous areas (case 15, 20x). **E.** Rb loss in the adenosquamous and sarcomatoid areas (case 15, 20x). **F.** GATA3 expression in the adenocarcinoma and squamous components (case 8, 20x).

Conclusions: This series represents the largest characterization of immunohistochemical and NGS findings in cases of adenosquamous PCa and sheds light on potential therapeutic targets. The presence of high molecular weight and GATA3 staining in some tumors can result in diagnostic confusion with invasive urothelial carcinoma with glandular differentiation. More cases are needed to support the NGS results, yet our results demonstrate findings commonly seen in aggressive tumors.

641 Morphologic and Molecular Profiling Decipher Intratumoral Heterogeneity in Clear Cell Renal Cell Carcinoma

Erica Vormittag-Nocito[1], Rahul Mannan[1], Xiaoming (Mindy) Wang[2], Anya Chinnaiyan[2], Yuping Zhang[3], Sylvia Zelenka-Wang[3], Xuhong Cao[2], Daniel Spratt[4], Khaled Hafez[2], Todd Morgan[2], Alon Weizer[2], Noah Brown[2], Eman Abdulfatah[1], Saravana Dhanasekaran[2], Arul Chinnaiyan[2], Rohit Mehra[2]
[1]Michigan Medicine, University of Michigan, Ann Arbor, MI, [2]University of Michigan, Ann Arbor, MI, [3]Michigan Center for Translational Pathology, Ann Arbor, MI, [4]UH Cleveland Medical Center, Cleveland, OH

Disclosures: Erica Vormittag-Nocito: None; Rahul Mannan: None; Xiaoming (Mindy) Wang: None; Anya Chinnaiyan: None; Yuping Zhang: None; Sylvia Zelenka-Wang: None; Xuhong Cao: None; Daniel Spratt: *Consultant*, Janssen; *Consultant*, Varian; Khaled Hafez: None; Todd Morgan: None; Alon Weizer: None; Noah Brown: None; Eman Abdulfatah: None; Saravana Dhanasekaran: None; Arul Chinnaiyan: None; Rohit Mehra: None

Background: Clear cell renal cell carcinoma (CCRCC) is the most common renal malignancy with high lethality. CCRCC is known to have chromosome 3p aberrancies with *VHL* loss, additional prognostic markers that have emerged include *BAP1*, *PBRM1*, and *SETD2*. Molecular heterogeneity, mostly on somatic mutational events reported in the literature, largely compares primary and metastatic disease. Here in, primary tumor analysis of morphologic and proteogenomic heterogeneity, that has not been fully investigated previously, will be evaluated.

Design: 77 nephrectomy cases from 2016-2021 were analyzed for morphologic architectural patterns and WHO/ISUP nucleolar grade frequencies. 10 high grade cases with 2 tissue blocks per case representing intratumoral heterogeneity were submitted for BAP1 and CAIX evaluation by IHC. 30 external cases where genomic aberration information was available were evaluated for both BAP1 and CAIX. 1 case with sufficient material for tissue microdissection was evaluated for mutational heterogeneity.

Results: 43 partial nephrectomy (PN) and 34 radical nephrectomy (RN) specimens were identified. PN were more likely to harbor lower WHO/ISUP grade CCRCC and less likely to show tumor nodularity and cytomorphologic heterogeneity. RN were more likely to demonstrate higher grade areas with a matched upscaling of tumor heterogeneity and morphologic complexity. Viable tumor cells within the 10 pilot cases showed staining with CAIX. Most low-grade areas showed retention of nuclear BAP1, some showing heterogenous staining. High-grade areas showed variable expression of BAP1 with only a minority of cases (2) showing retained BAP1 expression. Nodular loss of BAP1 was identified in the majority (8) cases, where most showed eosinophilic or rhabdoid features. The external cohort underwent similar analysis. The microdissected case showed *VHL* and *BAP1* mutation and loss of BAP1 staining in the rhabdoid area, while clear cell area showed *VHL* and *BCL7A* mutation and showed retention of CAIX and BAP1.

Conclusions: Intratumoral heterogeneity in CCRCC extends to architectural and cytomorphologic features and to protein-based biomarker expression with known roles in tumor biology (BAP1). Differential biomarker expression within CCRCC may influence prognosis and therapeutics. A larger cohort study with additional markers is underway to confirm our findings of varied expression in correlation to morphologic heterogeneity.

642 Expanded Clinicopathological and Molecular Characterization of Biphasic Hyalinizing Psammomatous Renal Cell Carcinoma (BHP RCC): Further Support for the Newly Proposed Entity

Xiaotong Wang[1], Qiuyuan Xia[2], Huiying He[3], Ming Zhao[4], Qiu Rao[5]
[1]Jinling Hospital, Nanjing University School of Medicine, Nanjing, China, [2]Jinling Hospital, Nanjing University School of Medicine, Shanghai, China, [3]Peking University, Beijing, China, [4]Zhejiang Provincial People's Hospital, People's Hospital of Hangzhou Medical College, Hangzhou, China, [5]Jinling Hospital, Nanjing, China

Disclosures: Xiaotong Wang: None; Qiuyuan Xia: None; Huiying He: None; Ming Zhao: None; Qiu Rao: None

Background: The classification of renal neoplasms continues to evolve with novel, emerging, and provisional entities being described constantly. BHP RCC associated with somatic *NF2* mutations is one such recently described renal entity, and considered a provisional category of RCC due to its limited data. Further studies of more cases are badly needed for more definitive classification.

Design: We identified three cases of BHP RCC, to further evaluate the clinicopathological and molecular features, and provide additional support for the newly proposed entity. Morphologic, immunohistochemical (IHC), and various molecular methodologies including NGS, FISH, and methylation-specific polymerase chain reaction were performed to investigate these tumors.

Results: There were 2 males and 1 female, 65, 56, 69 years old respectively. The neoplasms were unencapsulated, and all had a characteristic biphasic appearance of small cells clustering around basement membrane material within larger acini, forming pseudorosettes or a glomeruloid pattern. Hyalinized sclerotic stroma and psammoma bodies were at least focally present. 2 cases had areas of a less distinctive appearance, resembling CCRCC and MTSCC. The neoplasms did not have a distinctive IHC profile, though all labeled for Vimentin and CK7. Targeted DNA sequencing detected a somatic *NF2* mutation in one case, which was confirmed by Sanger sequencing. However, the other two cases lacked *NF2* mutations and instead showed *NF2* promoter methylation. Subsequent IHC assessment showed loss of expression of NF2 in all 3 cases, which evaluated NF2 status at the protein level. According to RNA sequencing-based clustering analysis, the 3 cases formed a distinct group with a shared specific transcriptional profile different from that of other common renal tumors. Clinically, one patient developed bone metastases and died of disease two years after diagnosis. The other two patients had no evidence of recurrence or metastases, at 4- and 5-years follow-up.

Figure 1 - 642

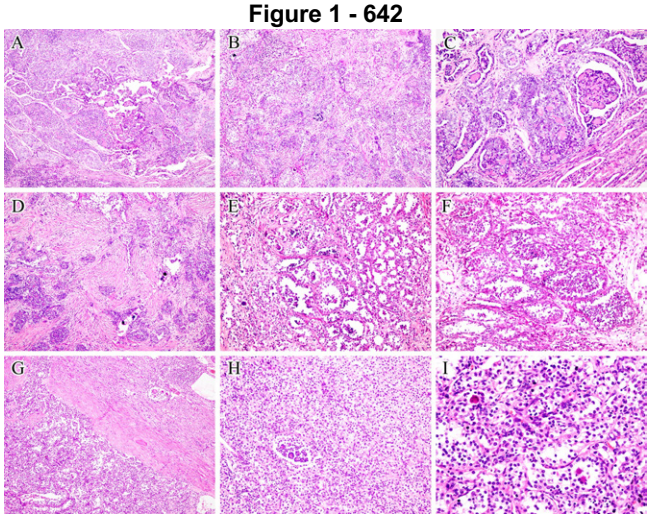

Figure 2 – 642

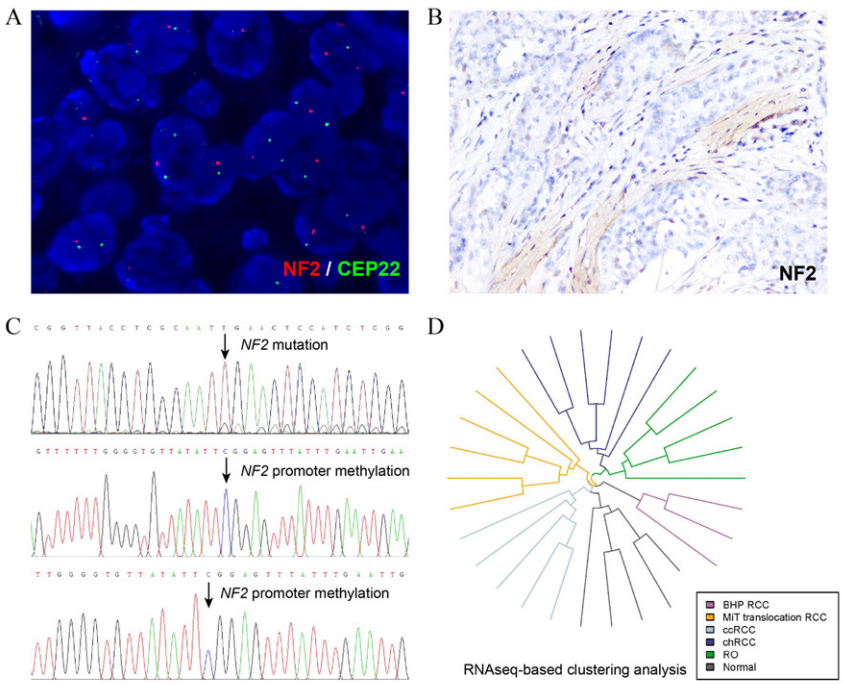

Conclusions: BHP RCC is a rare newly proposed renal entity, which demonstrates a characteristic biphasic morphology and mutations or promoter methylation of *NF2* gene. The precise nature of biologic behavior remains to be determined. Our study not only validates previously described clinicopathological features, but also expands the potentially genetic alterations and available clinical outcome data.

643 Second-generation Antiandrogens Treated (ADT) Metastatic Prostate Cancer: A rapid Autopsy Experience

Xiaoming (Mindy) Wang[1], Rahul Mannan[2], Anya Chinnaiyan[1], Joshi Alumkal[1], Daniel Spratt[3], Javed Siddiqui[1], Fengyun Su[1], Xuhong Cao[1], Chandan Kumar-Sinha[1], Vipulkumar Dadhania[2], Jeffrey Jentzen[1], Allecia Wilson[1], Saravana Dhanasekaran[1], Aaron Udager[4], Arul Chinnaiyan[1], Zachery Reichert[1], Rohit Mehra[1]
[1]University of Michigan, Ann Arbor, MI, [2]Michigan Medicine, University of Michigan, Ann Arbor, MI, [3]UH Cleveland Medical Center, Cleveland, OH, [4]University of Michigan Medical School, Ann Arbor, MI

Disclosures: Xiaoming (Mindy) Wang: None; Rahul Mannan: None; Anya Chinnaiyan: None; Joshi Alumkal: None; Daniel Spratt: *Consultant*, Janssen; *Consultant*, Varian; Javed Siddiqui: None; Fengyun Su: None; Xuhong Cao: None; Chandan Kumar-Sinha: None; Vipulkumar Dadhania: None; Jeffrey Jentzen: None; Allecia Wilson: None; Saravana Dhanasekaran: None; Aaron Udager: None; Arul Chinnaiyan: None; Zachery Reichert: None; Rohit Mehra: None

Background: Metastatic or recurrent prostate cancer is frequently treated with androgen deprivation therapy (ADT). The efficacy and potency of androgen pathway blockade has been improved by the development of second-generation ADTs (abiraterone, enzalutamide, etc.), which remain the standard of care for castration resistant prostate cancer (CRPC). Herein, we investigate morphological heterogeneity, neuroendocrine (NE) transdifferentiation, spatial and molecular genetic diversity in a cohort of 6 rapid autopsy patients with a lethal phenotype of metastatic CRPC (mCRPC) exposed to second-generations ADTs.

Design: Six recent patients with mCRPC enrolled in our in-house warm autopsy program were treated with multi-modality therapy including second-generation ADT. An extensive histopathological assessment was performed of diverse tumor sites from these patients to assess for spatial and morphological heterogeneity. Immunohistochemistry (IHC) was performed to assess inter-patient and intra-patient tumor heterogeneity with respect to for a diverse set of biomarkers. A subset of patients had correlative molecular data available (as performed during ante-mortem clinical management).

Results: The age range of the patients was 55 to 74 years. Osseous metastases (including femur, humerus and vertebra) were documented in all patients followed by liver and lung (5/6, 83.4% each). Morphological assessment revealed all cases exhibited evidence of conventional/acinar features in at least one of the metastatic sites included for pathological evaluation. Interestingly, features suggestive of NE transdifferentiation (small cell morphology, trabecular and organoid/nested pattern) was seen in 3/6 (50.0%) cases; 1/6 (16.7%) case also exhibited Paneth cell metaplasia. NE transdifferentiation was evidenced by differential intra-patient protein heterogeneity, including variable NKX3.1 PSA, AR, synaptophysin, chromogranin, Ki-67, RB1 and cyclin D1. Genomic interrogation of these patients identified varied mutational profiles such as BRCA2 deficiency, MSH2 mutation, AR amplification, ARID1A frameshift and MAP2K missense mutation in individual cases, amongst others.

Conclusions: Our interrogation of a cohort of rapid autopsy patients with mCRPC, status post second-generation ADT, demonstrated identifiable NE differentiation and tumor heterogeneity; diverse tumor sites within a single patient were found to have variable morphological and biomarker profiles.

644 A Transcriptional Network of Cell Cycle Dysregulation in Non-Invasive Papillary Urothelial Carcinoma

Joshua Warrick[1], Margaret Knowles[2], Carolyn Hurst[2], Lauren Shuman[3], Jay Raman[3], Vonn Walter[3], Jeffrey Putt[3], Lars Dyrskjøt[4], Mauro Castro[5], A. Gordon Robertson[6], David DeGraff[3]
[1]Penn State College of Medicine, Hershey, PA, [2]University of Leeds, Leeds, United Kingdom, [3]Penn State Health Milton S. Hershey Medical Center, Hershey, PA, [4]Aarhus University Hospital, Arhus, Denmark, [5]Universidade Federal do Paraná, Curitiba, Brazil, [6]BC Cancer, Vancouver, Canada

Disclosures: Joshua Warrick: None; Margaret Knowles: *Consultant*, Janssen; *Consultant*, LOXO Oncology; *Consultant*, QED; *Consultant*, QED; *Consultant*, QED; *Consultant*, Janssen; Carolyn Hurst: None; Lauren Shuman: None; Jay Raman: None; Vonn Walter: None; Jeffrey Putt: None; Lars Dyrskjøt: *Grant or Research Support*, AstraZeneca, Natera, C2i Genomics, Ferring, Photocure; *Speaker*, Roche; *Consultant*, Ferring; Mauro Castro: None; A. Gordon Robertson: None; David DeGraff: *Grant or Research Support*, Bristol Myers Squibb; *Grant or Research Support*, Bristol Myers Squibb

Background: Non-invasive papillary urothelial carcinoma (NIPUC) with cell cycle (CC) dysregulation has inferior recurrence and progression free survival. Human cancers display a restricted set of expression profiles, despite diverse mutational drivers. This has led to the hypothesis that select sets of transcription factors (TFs) act on similar target genes as an integrated network, buffering a tumor's transcriptional state.

Design: We set out to identify a transcriptional network of cell cycle dysregulation in NIPUC, utilizing RNA sequencing data from a Discovery Cohort (n=397; Lindskrog, Nat Commun, 2021) and a Validation Cohort (n=81, unpublished). The Discovery Cohort was used to identify TF targets using the ARACNe algorithm. The targets of each TF were termed its "TF regulon." We then identified TF regulons associated with CC-dysregulation using several statistical tests and orthogonal measures of CC-dysregulation, utilizing The Discovery and Validation Cohorts. Significant TF regulons were utilized for further analysis, which included assembly of a transcriptional network, pathway analysis, and comparison with muscle-invasive bladder cancer in the TCGA cohort and lamina propria-invasive cancer in a separate cohort (n=98, unpublished). TF activity was quantified using single sample Gene Set Enrichment Analysis (ssGSEA), applied to each TF regulon for each tumor.

Results: From a list of 1,639 curated TFs, activity of 121 TFs significantly associated with CC-dysregulation. Tumors with CC-dysregulation demonstrated greater activity of TFs with a known role in the cell cycle (E2F factors, MYB), ESR1, distal HOX factors, and TFs with a role in pluripotency (SOX2, SALL4). In contrast, tumors lacking CC-dysregulation demonstrated greater activity of PGR and multiple proximal HOX factors. In the assembled network, TF regulons with similar function had similar targets. Pathway analysis demonstrated strong associations between activity of TF regulons of CC-dysregulation and signatures of epithelial-mesenchymal-transition (EMT) and tumor pluripotency. Compared with NIPUC, both muscle-invasive and lamina propria-invasive cancers demonstrated substantially greater activity of TF regulons of CC-dysregulation.

Conclusions: Diverse TFs are active in NIPUC. A subset of these may prime NIPUC to evolve to an invasive phenotype by inducing expression of genes involved in EMT and pluripotency. This information may be useful in developing predictive biomarkers and developing targeted therapies.

645 Clinicopathologic and Immunohistochemical Analysis of 21 Sarcomatoid Chromophobe Renal Cell Carcinomas

Rumeal Whaley[1], Liang Cheng[2]
[1]Indiana University School of Medicine, Indianapolis, IN, [2]Indiana University, Indianapolis, IN

Disclosures: Rumeal Whaley: None; Liang Cheng: None

Background: Chromophobe renal cell carcinomas with sarcomatoid differentiation are rare. Our aim was to review the clinicopathologic and immunohistochemical features of a large cohort of sarcomatoid chromophobe renal cell carcinomas.

Design: Twenty-one cases were identified over a 25-year period (1995-2021). The clinicopathologic data was compiled and a retrospective review was undertaken. Immunohistochemical stains PAX8, cytokeratin 7, CD117, and GATA3 were performed on 4 µm sections on Dako automated platform along with appropriate controls.

Results: Thirteen cases (62%) occurred in males and the mean age at diagnosis was 55 years (range 44-78 years). Follow up data was available for 17 cases (mean 31.2 months, range 0-227 months). Fifteen cases presented with metastatic disease; 11

cases had distant metastatic disease. Thirteen patients died of disease. Median time to death was 7 months (range 2-90 months). All primary tumors were >7.0 cm in greatest dimension (average 15.0 cm, range 7.4-31.5 cm) and had identifiable conventional chromophobe renal cell carcinoma. Sarcomatoid differentiation ranged from 5 to 95%. Fifteen cases had the sarcomatoid component available for immunohistochemical evaluation. CD117 was lost in 100% of the cases, cytokeratin 7 in 73%, and PAX8 in 53%. GATA3 was expressed in 20% of the conventional components and 27% of the sarcomatoid components. Twenty percent of cases lost PAX8 and expressed GATA3.

Conclusions: Sarcomatoid chromophobe renal cell carcinomas have a high propensity for metastases and cancer progression. The median survival in this cohort was less than 1 year. The sarcomatoid portion was the dominant component in the majority of the cases and had frequent loss of expression of multiple immunohistochemical markers, including CD117, cytokeratin 7, and PAX8. A high proportion of sarcomatoid chromophobe renal cell carcinomas exhibited GATA3 expression.

646 Using Next-Generation Sequencing to Characterize Unclassified Oncocytic Renal Cell Tumors

Joshua Wong[1], William Lam[2], Evelyne Kouame[2], Li Li[3], George Haines III[2], Meenakshi Mehrotra[4], Jane Houldsworth[1], Qiusheng Si[1]

[1]Icahn School of Medicine at Mount Sinai, New York, NY, [2]Mount Sinai Hospital, New York, NY, [3]Thomas Jefferson University Hospital, Philadelphia, PA, [4]Mount Sinai Medical Center, New York, NY

Disclosures: Joshua Wong: None; William Lam: None; Evelyne Kouame: None; Li Li: None; George Haines III: None; Meenakshi Mehrotra: None; Jane Houldsworth: None; Qiusheng Si: None

Background: Renal cell tumors with oncocytic features can present as a diagnostic challenge. Immunohistochemical (IHC) studies are used to provide further classification, but many times a definitive diagnosis cannot be determined. Some renal cell tumors show morphologic features overlapping with renal oncocytoma (RO) and eosinophilic variant of chromophobe renal cell carcinoma (e-ChRCC), but do not correspond with established histology or IHC profiles. These tumors have often remained as unclassified oncocytic renal tumors with low-grade cytologic features. With the advent of next-generation sequencing (NGS), rapid molecular profiling can be conducted to better classify the clinicopathological and molecular characteristics of these unclassified oncocytic renal tumors.

Design: A retrospective review of 13 oncocytic renal cell tumors from 2014 to 2021 was performed. Tumors were selected based on unclassifiable cytomorphology and IHC. NGS was performed using the ThermoFisher OCAv3 and OncominePlus panels on the Ion S5XL sequencing platform. NGS results were evaluated for both genetic alterations and whole chromosome gains and losses.

Results: Among the 13 cases, the median age was 65 years and the male to female ratio was 5:8. Of the 10 patients sequenced, three presented with lower urinary tract symptoms, while 7 were asymptomatic on diagnosis. All cases had unifocal tumors which localized to the right in eight of ten cases, and tumors ranged in size from 1.6 cm to 11 cm. NGS was performed on 10 cases. Three cases showed frameshift mutations in KMT2A, PTEN, and TSC2. These mutations were deemed likely oncogenic with likely loss-of-function. Five cases showed copy number alterations ranging from 1 to 9 chromosomes lost. Out of these five cases, one case only showed loss of chromosome 1, suggestive of RO. Chromosomes 1, 6, 9, and 17 were amongst the most commonly lost chromosomes, suggestive of e-ChRCC despite ambiguous histology. Three cases identified either no genetic alterations or only VUS with no copy number alterations which may suggest the diagnosis of RO.

Conclusions: NGS can be used to provide subclassification of unclassified oncocytic renal tumors when immunohistochemical studies are ambiguous. Results also suggest tumors may be reclassified to existing categories based on molecular profiling techniques such as NGS, providing additional guidance for treatment selection in these patients.

647 ApoL1 Genotype in African American Patients with Kidney Neoplasm

Dongling Wu[1], Opeyemi Olabisi[2], Zachary Kozel[3], Oksana Yaskiv[4], Yihe Yang[5], Vanesa Bijol[6]

[1]Long Island Jewish Medical Center/Northwell Health, Manhasset, NY, [2]Duke Medical Center, Durham, NC, [3]Donald and Barbara Zucker School of Medicine at Hofstra/Northwell, Lake Success, NY, [4]Northwell Health System, New York, NY, [5]Donald and Barbara Zucker School of Medicine at Hofstra/Northwell, Riverhead, NY, [6]Donald and Barbara Zucker School of Medicine at Hofstra/Northwell, Manhasset, NY

Disclosures: Dongling Wu: None; Opeyemi Olabisi: None; Zachary Kozel: None; Oksana Yaskiv: None; Yihe Yang: None; Vanesa Bijol: None

Background: African Americans (AA) may carry high risk Apolipoprotein L1 (*APOL1)* genetic variants (termed G1 and G2) that predispose them to significantly higher incidence of chronic kidney disease (CKD). About 13% of AA carry 2 *APOL1* high-risk variants, while 1 *APOL1* high-risk variant is found in 45% of AA. Epidemiologic studies have also shown that AA had a significantly higher incidence rate and lower survival rate of renal cell cancer (RCC), and they were also diagnosed at a younger age. This overlapping raised the question of potential impact of *APOL1* genotype on RCC. The objective of this study was to examine the associations of *APOL1* nephropathy risk alleles in AA patients with RCC.

Design: This retrospective cohort study included all patients with nephrectomy procedure for kidney neoplasms. AA patients were retrospectively studied for *APOL1* genotype.

Results: In the total of 361 tumor nephrectomy cases, we identified 36 (10%) specimens had APOL1 genotype. Of these, 16 (44%) patients carried no *APOL1* risk alleles (G0); 13 (36%) patients carried one *APOL1* risk allele and 7 (19%) patients carried two *APOL1* risk alleles. ESKD prevalence in zero, one and two risk allele groups were 3 (19%), 3 (23%) and 5 (71%), respectively. The odds ratio of ESKD in those carrying two risk alleles is 3.45 compared with zero or one risk allele. On histopathology examination, a total of 17 papillary renal cell carcinomas (PRCC) were identified, with 10 type 1, 2 type 2 and 5 mixed type. For patients carrying two *APOL1* risk alleles, 5 of which (71%) had papillary carcinoma; 2 were type 1, 1 was type 2, and 2 were mixed type. In a median follow-up of 250 days, no disease progression was observed in these patients. In AA patients with end stage kidney disease (ESKD) (n=6), 2 (33%) had type 1 PRCC. In AA with 0 or 1 risk alleles without ESKD (n=29), 8 (28%) patients had PRCC (6 type 1, 1 type 2 and 1 mixed). Among the non-AA patients (n=319), 7 (2.2%) patients presented with ESKD, of which 2 (33%) had PRCC, mixed type. On IHC examination, there was no significant staining in any of the tumors except one showed focal cytoplasmic staining, while non-neoplastic kidney tissue showed variable staining either on endothelial or podocytes. Detailed results listed in Table.

	AA with 2 risk alleles	*AA with 0 or 1 risk alleles, ESKD*	*AA with 0 or 1 risk alleles*	*Non-AA with ESKD*	***Total Population***
N	7	6	29	7	**361**
Male	2 (29%)	6 (100%)	18 (62%)	7 (100%)	**221 (61.2%)**
Age (year)	58±14	64±14	64±14	68±8	**63 ± 12**
BMI(kg/m^2)	30±5	25±4	28±5	31±4	**36 ± 115**
Tumor size (cm)	4.0±2.5	3.0±2.8	4.9±3.1	3.6±0.9	
Multifocal	1 (15%)	2 (33%)	3 (11%)	5 (71%)	
HTN	7 (100%)	6 (100%)	24 (83%)	6 (86%)	**234 (65%)**
DM	3 (43%)	2 (33%)	7 (24%)	4 (57%)	**90 (25%)**
Proteinuria	5/5 (100%)	3/3 (100%)	14/20 (70%)	3/3 (100%)	62/205 (30%)
ESKD	5 (71%)		6 (21%)	7 (100%)	**18 (5%)**
Tumor size (cm)	4.0±2.5	3.0±2.8	4.8±2.9	3.6±0.9	4.4±2.7
TUMOR TYPE					
Papillary 1	2 (29%)	2 (33%)	6 (21%)		**37 (10%)**
Papillary 2	1(14%)		1 (3%)		**9 (3%)**
Papillary RCC, mixed or unknown type	2 (29%)		1 (3%)	2 (29%)	
Papillary RCC present as a secondary component	ccPRCC n =1		PRCC n =1; ccPRCC n =1		PRCC type 2, n=1
RCC, unclassified	1(14%)		1 (3%)	1(14%)	**21 (6%)**
Urothelial ca	1(14%)			1(14%)	**32 (9%)**
Clear cell RCC		3 (50%)	12 (41%)	2 (29%)	**203 (56%)**
AML		1 (17%)	1 (3%)		**16 (4%)**
Acquired cystic disease associated RCC		Presented as a 2nd component n=1	Presented as a 2nd component n=1 (3%)		
Chromophobe		Presented as a 2nd component n=1	Primary component n = 2 (8%) Secondary component n = 1 (3%)		
Oncocytoma			1 (3%)	1(14%)	**18 (5%)**
Radical nephrectomy	7 (100%)	6 (100%)	19 (66%)	6 (86%)	174 (48%)

Conclusions: We observed a cluster phenomenon in APOL1 high-risk genotype, ESKD, and kidney neoplasm. We observed significantly more frequent papillary RCC prevalence in AA patients with high-risk *APOL1* genotype.

648 Detection of Clinically Significant Prostate Cancer by Transperineal Multiparametric Magnetic Resonance Imaging-Ultrasound Fusion Targeted Prostate Biopsy in Smaller Prostate

Shulin Wu[1], Douglas Dahl[1], Michelle Kim[2], Sharron Lin[1], Rory Crotty[1], Kristine Cornejo[1], Mukesh Harisinghani[1], Adam Feldman[1], Chin-Lee Wu[1]
[1]Massachusetts General Hospital, Boston, MA, [2]Massachusetts General Hospital, Harvard Medical School, Boston, MA

Disclosures: Shulin Wu: None; Douglas Dahl: None; Michelle Kim: None; Sharron Lin: None; Rory Crotty: None; Kristine Cornejo: None; Mukesh Harisinghani: None; Adam Feldman: *Consultant*, Olympus America, Inc; *Speaker*, Janssen Pharmaceuticals; *Advisory Board Member*, Vessi Medical; Chin-Lee Wu: None

Background: Transperineal (TP) multiparametric magnetic resonance imaging (MRI)-targeted biopsy (TBx) has shown to detect more clinically significant (cs) prostate cancer (PCa) than standard template biopsies (SBx). Current data support the inclusion of both TBx and SBx in obtaining an optimal csPCa detection rate. We compared PCa and csPCa detection rates in patients with different prostate volumes to examine the benefit of performing targeted biopsy in smaller prostates through the TP approach.

Design: We identified PCa patients who underwent transperineal TBx (3-core) and concomitant SBx (20-core) from September 2019 to February 2021. Clinical, MRI and biopsy pathological characteristics were evaluated and compared between TBx and SBx. csPCa was defined as grade group 2 or greater prostate adenocarcinoma.

Results: Three hundred and one (n=301) patients underwent TBx and SBx concomitant procedures. The median prostate volume by MRI was 45 ml (IQR, 33-61 ml). The patients were divided by prostate volume into three groups: ≤30ml group (n=60, 19.9%), 30-45 ml group (n=94, 31.3%) and >45ml group (n=147, 48.8%). Patients in the ≤30ml group showed significantly higher frequency of combined (both TBx and/or SBx) cancer detection rate (CDR) (90.0%) and csPCa detection rate (65.0%) than the >45ml group (73.5% and 39.5%, respectively) but similar frequency to the 30-45 ml group (80.8% and 54.2%, respectively). By TBx only, both the ≤30ml group (55.0%) and the 30-45ml group (42.6%) showed significantly higher rates of csPCa detection than the>45 ml group (27.9%). On the other hand, by SBx only, the ≤30ml group (56.7%) showed significant higher csPCa rate compared to the other two groups (35.1% and 34.0%, respectively). In the ≤30ml group, the detection rate of csPCa was similar by targeted biopsy (55.0%), template biopsy (56.7%) and when combined (65.0%). csPCa in the four cases missed by targeted biopsy but detected by template biopsy (n=6) were present at the base location by template biopsy.

TABLE 1: Differences of clinically significant (cs) prostate cancer detection rate by prostate volume groups in 301 men with identifiable target(s) on prostate mpMRI who underwent MRI-US fusion targeted and standard 20-core template transperineal biopsy

Variables/Total (n=301)	≤30ml (group a, n=60)	30-45ml (group b, n=94)	>45ml (group c, n=147)	p
Combined SBx/TBx				**0.008(a vs c)**
negative for PCa (n=63)	6 (10.0)	18 (19.2)	39 (26.5)	
non-csPCa PCa only (n=90)	15 (25.0)	25 (26.6)	50 (34.0)	
csPCa (n=148)	39 (65.0)	51 (54.2)	58 (39.5)	
SBx only				**0.026(a vs b, a vs c)**
negative for PCa (n=78)	6 (15.0)	24 (25.5)	45 (30.6)	
non-csPCa PCa only (n=106)	17 (28.3)	37 (39.4)	52 (35.4)	
csPCa (n=117)	34 (56.7)	33 (35.1)	50 (34.0)	
TBx only				**0.001(a vs c, b vs c)**
negative for PCa (n=110)	11 (18.3)	30 (31.9)	69 (46.9)	
non-csPCa PCa only (n=77)	16 (26.7)	24 (25.5)	37 (25.2)	
csPCa (n=114)	33 (55.0)	40 (42.6)	41 (27.9)	

SBx: standard 20-core template transperineal biopsy; TBx: MRI-US fusion targeted transperineal biopsy; Combined: with diagnosis by SBx and/or TBx; PCa: prostate cancer; csPCa: Grade Group 2 disease or above; ( ) of p: post hoc test significance.

Conclusions: Our data suggests PCa patients with smaller prostates (≤30 ml), who undergo targeted biopsy only, will likely detect a satisfactory number of csPCa cases, similar to template biopsy only or a combination of the two. Therefore, targeted biopsy with limited additional cores may potentially achieve the same csPCa detection as the combined template and targeted biopsy.

649 Nonlinear Microscopy: A Tool to Assess Intraoperative Radical Prostatectomy Margins

Yubo Wu[1], Tadayuki Yoshitake[2], Lucas Cahill[3], Seymour Rosen[1], Leo Wu[4], Dimitra Pouli[4], Timothy Weber[2], Sagar Doshi[2], Peter Chang[4], Andrew A. Wagner[1], James Fujimoto[2], Yue Sun[5]
[1]Beth Israel Deaconess Medical Center, Boston, MA, [2]Massachusetts Institute of Technology, Cambridge, MA, [3]Massachusetts Institute of Technology, Harvard University, Cambridge, MA, [4]Beth Israel Deaconess Medical Center, Harvard Medical School, Boston, MA, [5]Beth Israel Deaconess Medical Center, MA

Disclosures: Yubo Wu: None; Tadayuki Yoshitake: None; Lucas Cahill: None; Seymour Rosen: None; Leo Wu: None; Dimitra Pouli: None; Timothy Weber: None; Sagar Doshi: None; Peter Chang: None; Andrew A. Wagner: None; James Fujimoto: None; Yue Sun: None

Background: Nonlinear microscopy (NLM) is a fluorescence microscopy technique that allows rapid generation of images resembling H&E histology in freshly excised tissue without the need to freeze or microtome section. The aim of this study is to show the feasibility of NLM imaging for rapid margin evaluation of radical prostatectomies. Prostate specimens were grossed fresh and margins were analyzed with NLM in simulated real-time conditions by a genitourinary pathologist.

Design: Twenty-one fresh radical prostatectomy specimens were collected and postoperatively evaluated. Inking following standard in-house protocol was performed. The neurovascular bundles, when included, were then dissected off by the surgeon, and the newly created margins were inked a separate color. The prostates were then grossed fresh into 3-5 mm thickness slices, stained for 2 min in nuclear and cytoplasmic/stromal fluorophores (acridine orange/sulforhodamine), and then rinsed with saline for 30 seconds. Based on gross appearance and prior biopsy information, slices were selected and placed in a holder for NLM evaluation.

Time to gross and ink the specimen, NLM evaluation for the slices, gross measurements, basic specimen description, and margin status for each evaluated slice were recorded. After imaging, the specimens were submitted for standard H&E processing.

Results: Median time to ink and gross a prostate was 12.8 min; median evaluation time was 23.0 min. Total median and average time from grossing to evaluation was 36 min.

Of the 21 prostate specimens, 7 had overtly positive margins and 8 had overtly negative margins. 5 cases were deemed equivocal by NLM – tumor approached the margin – but were ultimately negative on H&E. 1 case had a falsely negative margin by NLM that was focally positive on H&E.

Thus, 8/21 patients would have been converted to a nerve-sparing procedure. It is important to note that NLM visualizes tissue three-dimensionally, up to 100 microns tissue depth. NLM images larger, more intact areas than tissue processed for H&E evaluation, which can contribute to discordances.

Figure 1 - 649

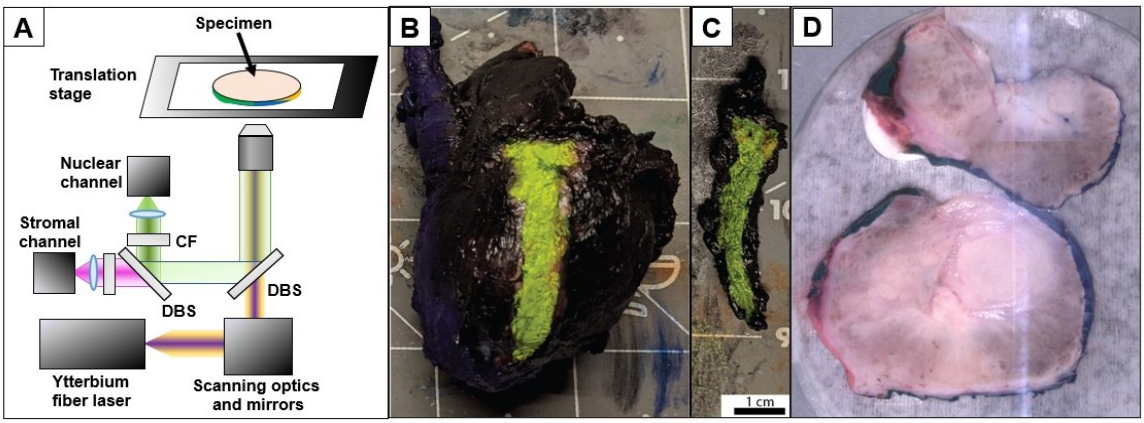

Figure 1. A. Schematic of NLM. Images are generated by a scanned short pulse laser which excites fluorescence only in the focal plane. Specimens are rapid stained with nuclear and stromal fluorophores and images displayed in an H&E color scale. Regions of interest are imaged by 3D translation of the specimen holder. (DBS-dichroic beam splitter, CF-chromatic filter). B. Radical prostatectomy specimen. Black = right, blue = left, yellow = neurovascular bundle margin inked after resection; C. Neurovascular bundle dissected by surgeon, corresponding surface to the main resection is also inked yellow. D. Gross white light image of tissue in a specimen holder. Orange ink was used for this neurovascular margin.

Figure 2 – 649

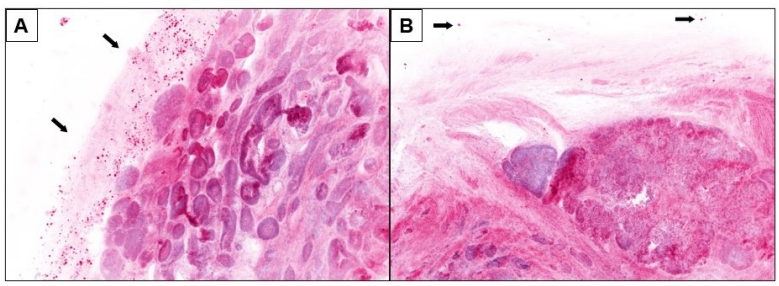

Figure 2. A. NLM images of radical prostatectomy slice with frank adenocarcinoma at the inked margin. Red pigment-like particles (black arrows) in NLM image are the applied ink. B. NLM images of radical prostatectomy slice with negative margin. Again, red pigment-like particles (black arrows) in image are the applied ink.

Conclusions: This study suggests the feasibility of NLM as a novel method for rapid intraoperative evaluation of margins in radical prostatectomies.

650 Reclassifying pT3 Renal Pelvic Urothelial Carcinoma with Renal Parenchyma Invasion to pT2 Improves Correlation with Overall Survival

Douglas Wu[1], Debra Zynger[2]
[1]The Ohio State University Medical Center, Columbus, OH, [2]The Ohio State University Wexner Medical Center, Columbus, OH

Disclosures: Douglas Wu: None; Debra Zynger: None

Background: The American Joint Cancer Committee pT categorization in renal pelvic carcinoma is used for prognostication and adjuvant treatment recommendations. Renal pelvic pT3 is defined as invasion of renal parenchyma, invasion of peripelvic fat, or both. However, survival heterogeneity within the pT3 category has been demonstrated. This investigation sought to compare survival between pT categories of renal pelvic urothelial carcinoma and identify modifications to improve correlation with survival.

Design: Pathology reports from nephroureterectomies performed at our institution from 2010-2019 were analyzed to identify primary renal pelvic urothelial carcinoma. Cases with previous or concurrent higher pT tumors of the bladder or ureter, history of neoadjuvant chemotherapy, and non-urothelial tumors were excluded. Slide review was performed. Tumors (n=146) were stratified based on pT, pN, and invasion of renal parenchyma vs invasion of peripelvic fat (with or without renal parenchyma invasion). Kaplan Meier survival curves and Cox regression multivariate analysis were used to compare overall survival.

Results: The prognostic value of pT classification was confirmed, demonstrating a stepwise decrease in overall survival as pT increased, with pT3 and pT4 having the worst prognosis (5-year overall survival: pT3, 37.4%; pT4, 0%) (p<0.0001). pT3 was the largest pT category (43.2%). Similar survival curves were observed for pT2 and pT3 and multivariate analysis confirmed overlapping hazard ratios [pT2: HR=1.67, 95% CI (0.46, 6.01); pT3: HR=3.52, 95% CI (1.86, 6.66)]. Survival heterogeneity was identified within the pT3 category. pT3 tumors with peripelvic fat invasion, regardless of renal parenchyma involvement, had a 2.9-fold worse overall survival than pT3 tumors with only renal parenchyma involvement. Comparing pT3 subcategories to other pT categories revealed that renal parenchyma invasion (without peripelvic fat invasion) had similar overall survival as pT2, whereas peripelvic fat invasion was worse (p=0.0013). Additionally, reclassifying renal parenchyma invasion as pT2 yielded greater survival curve separation and greater difference in hazard ratios.

Conclusions: We present the novel finding that reclassifying pT3 renal pelvic urothelial tumors with only renal parenchyma invasion to pT2 improves pT correlation with overall survival. Therefore, restricting the pT3 category to tumors with peripelvic fat invasion and modifying the pT2 category to include renal parenchyma invasion is recommended.

651 Molecular Correlates of Male Germ Cell Tumors with Overgrowth of Components Resembling "Somatic" Malignancies: Multi-Platform Analysis of a Collaborative Series

Nicolas Wyvekens[1], Lynette Sholl[2], Brendan Dickson[3], Muhammad Idrees[4], Katrina Collins[4], Khaleel Al-Obaidy[5], Jennifer Gordetsky[6], Andres Matoso[7], Fiona Maclean[8], Christopher Fletcher[9], Jason Hornick[1], Nicholas Baniak[10], Chia-Sui (Sunny) Kao[11], Michelle Hirsch[9], Sara Wobker[12], Andres Acosta[1]

[1]Brigham and Women's Hospital, Harvard Medical School, Boston, MA, [2]Harvard Medical School, Boston, MA, [3]Mount Sinai Health System, Toronto, Canada, [4]Indiana University School of Medicine, Indianapolis, IN, [5]Cleveland Clinic Foundation, Cleveland, OH, [6]Vanderbilt University Medical Center, Nashville, TN, [7]Johns Hopkins Medical Institutions, Baltimore, MD, [8]Douglass Hanly Moir Pathology, Melbourne, Australia, [9]Brigham and Women's Hospital, Boston, MA, [10]University of Saskatchewan, Saskatchewan Health Authority, Saskatoon, Canada, [11]Stanford Medicine/Stanford University, Stanford, CA, [12]The University of North Carolina at Chapel Hill, Chapel Hill, NC

Disclosures: Nicolas Wyvekens: None; Lynette Sholl: *Consultant*, Genentech; *Grant or Research Support*, Genentech; *Consultant*, Lilly; Brendan Dickson: None; Muhammad Idrees: None; Katrina Collins: None; Khaleel Al-Obaidy: None; Jennifer Gordetsky: *Consultant*, Jansen; Andres Matoso: None; Fiona Maclean: None; Christopher Fletcher: None; Jason Hornick: *Consultant*, Aadi Biosciences; *Consultant*, TRACON Pharmaceuticals; Nicholas Baniak: None; Chia-Sui (Sunny) Kao: None; Michelle Hirsch: *Consultant*, Janssen Pharmaceuticals; Sara Wobker: None; Andres Acosta: None

Background: Germ cell tumors (GCTs) rarely demonstrate overgrowth of components that resemble somatic malignancies. These "somatic" components can arise in primary or metastatic GCTs, and their presence has been associated with resistance to systemic treatment and poor outcomes, especially in the post-chemotherapy setting. Although the clinicopathologic features of GCTs with "somatic" transformation have been described previously, their molecular characteristics remain largely unknown.

Design: Next generation DNA sequencing (solid tumor panel; 447 genes) was performed on a series of 24 GCTs with "somatic" transformation (19 testicular; 5 primary mediastinal) after enrichment of the "somatic" components by macrodissection. RNA sequencing was performed on 9 tumors. Eight GCTs without "somatic" components identified in our institutional molecular database were used as a comparator.

Results: The median age was 34 years (range 16-61 yrs). Metastatic disease (lymph nodes or distant) was noted in 19 cases. A history of chemotherapy was present in 3 cases, absent in 14 cases, and unknown in 7 cases. The "somatic" components included: embryonic-type neuroectodermal tumor (42%, 10/24), unclassified sarcoma (29%, 7/24), rhabdomyosarcoma (21%, 5/24), unclassified small round blue cell tumor (4%, 1/24) and nephroblastoma (4%, 1/24). Twenty-two tumors (92%, 22/24) had 12p gains. Widespread loss of heterozygosity (LOH) suggestive of whole-genome doubling (WGD) events, as well as numerous copy number (CN) imbalances spanning whole chromosomes and chromosomal arms were invariably found in these cases (96%, 23/24). Focal amplification of *MDM2* and homozygous *RB* deletion were each seen in two tumors (8%, 2/24). Besides in *KRAS* (29%, 7/24) and *TP53* (25%, 6/24), recurrent mutations were largely absent. Overall, molecular events leading to cell cycle dysregulation (loss of *RB* or *TP53* and *MDM2* amplifications) were seen in 38% of the cases (9/24). RNA sequencing

revealed only stochastic gene fusions. Eight conventional GCTs (i.e., without "somatic" components) used as a comparator also demonstrated widespread LOH suggestive of WGD. However, except for 12p gains, they largely lacked additional CN imbalances.

Conclusions: "Somatic" malignant components of GCTs harbor chromosomal imbalances and frequent mutations in cell cycle regulatory genes that set them apart from conventional GCTs. Analysis of additional cases and paired SNP-array of "conventional" and "somatic" components of GCTs from individual patients are ongoing.

652 TSC/MTOR-associated Eosinophilic Renal Tumors Exhibit Heterogenous Clinicopathologic Spectrums: A Targeted Next-generation Sequencing and Gene Expression Profiling Study

Qiuyuan Xia[1], Xiaotong Wang[2], Ming Zhao[3], Huiying He[4], Qiu Rao[5]
[1]Jinling Hospital, Nanjing University School of Medicine, Shanghai, China, [2]Jinling Hospital, Nanjing University School of Medicine, Nanjing, China, [3]Zhejiang Provincial People's Hospital, People's Hospital of Hangzhou Medical College, Hangzhou, China, [4]Peking University Health Science Center, Beijing, China, [5]Jinling Hospital, Nanjing, China

Disclosures: Qiuyuan Xia: None; Xiaotong Wang: None; Ming Zhao: None; Huiying He: None; Qiu Rao: None

Background: Several emerging subsets of *TSC1/2* or *MTOR* mutated eosinophilic renal tumors have recently been proposed, including eosinophilic solid and cystic renal cell carcinoma (ESC RCC), eosinophilic vacuolated tumors (EVT) and low-grade oncocytic tumor (LOT). Furthermore, there still exist a group of “unclassified renal tumors with *TSC/MTOR* mutations” failing to meet the criteria for any of the previously recognized histo-molecular subtype. Whether these known or unknown entities could represent a continuum of the same disease associated with *TSC1/2* and *MTOR* mutations remains to be further determined.

Design: We collected 39 eosinophilic renal tumors that had molecular confirmation of *TSC/MTOR* mutations by targeted DNA sequencing. The clinicopathologic and IHC profiles were further evaluated. To obtain the transcriptional profile, twenty-eight of the series, together with 6 chRCC, 5 RO, 5 ccRCC, 7 MiT RCC and 6 normal renal tissues were submitted to RNA sequencing analysis.

Results: According to previous described morphological and IHC features, 39 cases were reclassified into 4 groups: 12 ESC RCCs, 9 EVT, 8 LOT, and 10 cases which fail to meet the morphologic criteria for either type, hence characterized as *TSC*-mutated RCC not otherwise specified (*TSC*-mt RCC-NOS). The mutation types existed distinct tendency that ESC RCC (12/12) demonstrated consistent *TSC* mutations, while the majority of LOT (7/8) demonstrated *MTOR* mutations. 10 *TSC*-mt RCC-NOS exhibited heterogenous morphology, arising a differential diagnosis with other renal tumors including MiT RCC, PRCC and epithelioid PEComa. RNA sequencing-based clustering analysis segregated ESC RCC, EVT and LOT from each other, as well distinct from other renal tumor types, suggesting that they are independent entities on expression profile level. Nine of 10 *TSC*-mt RCC-NOS cases formed a mixed cluster with ESC RCC, suggesting a largely similar expression signature; the remaining one with unusual morphology mimicking MiT RCC, clustered within the branch of EVT.

Figure 1 - 652

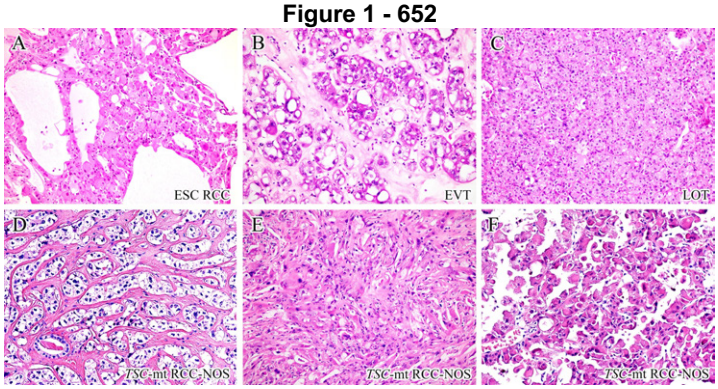

Figure 2 – 652

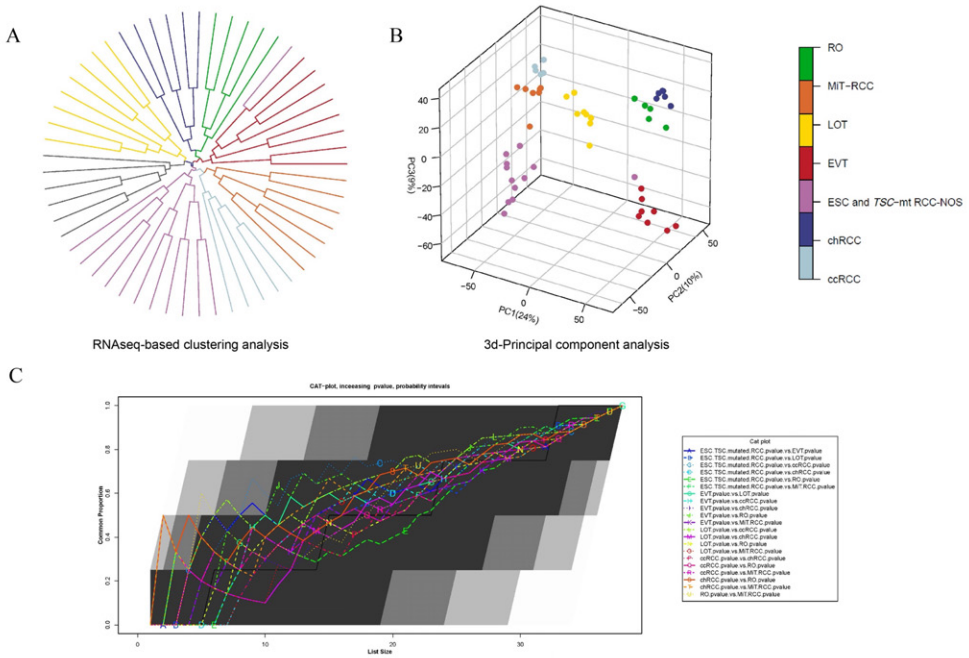

Conclusions: We expanded the morphologic spectrum and identified the gene mutation type of *TSC/MTOR*-associated eosinophilic renal tumors and further highlighted the challenge in differential diagnosis with other renal tumors, especially with MiT RCC. On expression profile level, ESC RCC, EVT, and LOT are distinctive entities and *TSC*-mt RCC-NOS could be clustered within these recognized *TSC/MTOR*-associated entities.

653 Classification of Flat Urothelial Lesions Using A Commercial Deep Learning Enabled Image Analysis Tool

Hongzhi Xu[1], Fang-Ming Deng[2], David Bacsa[3], Ming Zhou[4]
[1]Tufts Medical Center, Boston, MA, [2]New York University Medical Center, New York, NY, [3]Cognex, Natick, MA, [4]Tufts University School of Medicine, Boston, MA

Disclosures: Hongzhi Xu: None; Fang-Ming Deng: None; David Bacsa: None; Ming Zhou: None

Background: Artificial intelligence (AI) has been increasingly used in surgical pathology to assist pathologists for diagnosis, grading and staging purposes. We describe in this report a proof of concept study that pathologists themselves could use a commercial deep learning software to develop an AI model to assist the classification of flat urothelial lesions.

Design: 227 flat urothelial lesions including normal (N) (66), benign reactive (BR) (53), dysplasia (D) (49) and carcinoma in situ (CIS) (59) from one institution (TMC) were reviewed, and representative H&E micrographs of taken at 10X magnification by pathologists on various cameras attached to microscopes. Fifty % of these images were imported into Cognex VisionPro Deep Learning 2.0 software tool, which was trained to develop a flat urothelial classifier (Model 1) to distinguish between N, BR, D and CIS. The classifier comprised of a chain of 3 deep learning models to first remove the blank space in the images, to identify urothelial regions and finally to classify the urothelial regions. An F-score was used to measure the accuracy of the model to classify the images of flat urothelial lesions. 191 micrographs of flat urothelial lesions from a different institution (NYU), including N (35), BR (52), D (47) and CIS (57), were used as validation cases. Fifty % of latter images were used to train a new model (Model 2) based on the Model 1.

Results: The F-score for Model 1 on TMC cases was 96.1%. 97.1%, 85.2%, 100% and 100% of cases in N, BR, D and CIS were correctly classified. When Model 1 was used on NYU cases, the overall F-score was 44.9%. Model 1 was retrained using 50% of NYU images to generate Model 2. The F-score for Model 2 on NYU images improved to 86.8%, while it was 88.9% on TMC images.

Conclusions: This proof of concept study confirms that a pathologist with little background in deep learning software development can use a commercially available deep learning software to develop a robust AI model to assist the classification of flat urothelial lesions. While a model developed using one set of images from one lab may not be directly applied to images from a different lab, it could nevertheless be retrained using the images from the second lab to achieve high classification accuracy. Studies are underway to develop AI models for flat urothelial classification on whole slide images.

654 Renal Cell Carcinomas with Clear cells, Papillae, and Unusual Presentation: A Molecular Analysis of Nine Cases

Yunshin Yeh[1], Catherine Chaudoir[1], Anthony Tanner[1], Tajammul Fazili[1], Xiuping Yu[2], Michael Constantinescu[1]
[1]Overton Brooks VA Medical Center, Shreveport, LA, [2]Louisiana State University Health Sciences Center, Shreveport, LA

Disclosures: Yunshin Yeh: None; Catherine Chaudoir: None; Anthony Tanner: None; Tajammul Fazili: None; Xiuping Yu: None; Michael Constantinescu: None

Background: Clear cell and papillary renal cell carcinomas (RCCs) are the two most common histologic subtypes of RCC and account for 70% and 15%, respectively of all kidney cancers. It has been shown that clear cell RCC harbors *VHL* alterations and papillary RCC bears +7,+17,-Y chromosomal changes. We evaluated for molecular changes in nine cases of RCC with clear cells, papillary fronds, and unusual morphologic features.

Design: Nine cases of RCCs were retrieved from the case archives of Pathology and Laboratory Medicine. The H&E and immunohistochemically stained slides were reviewed. Next-generation sequencing (NGS) was performed. Cytogenetics was obtained for one case.

Results: All the patients were males aged from 49 to 68 (mean 61.4) years. There were 6 radical and 3 partial nephrectomies. Seven tumors involved the left kidney and 2 occurred in the right kidney. Tumor sizes ranged from 0.8 to 15.2 cm. Carcinoma cells stained positively for the immunomarkers RCC (6/9), CAIX (3/4), CD10 (6/6), and CK7 (5/9). Cytogenetics studies performed on case #5 revealed 50,X,-Y,+3,+7,+16, +17,+20 [20].

Next-Generation Sequencing of Renal Cell Carcinomas

#	Diagnosis before NGS	Molecular Alterations	Diagnosis after NGS
1	Clear cell RCC with papillary features	*VHL, APC, EGFR, mTOR, NTRK, PTPN11*	Clear cell RCC
2	RCC unclassified	*VHL, PTEN, MSH6*	Clear cell RCC
3	Clear cell RCC with smooth muscles	*mTOR*	Clear cell RCC with leiomyomatous stroma
4	Papillary RCC with clear cell changes	*FANCA*	Papillary RCC, type 2
5	RCC unclassified	*JAK, MLH3, TET2,* (see cytogenetics)	Papillary RCC, type 2
6	Clear cell RCC with sarcomatous cells	*PBRM1, SETD2, NFE2L2, TP53*	Clear cell RCC with sarcomatous elements
7	Clear cell RCC	No reportable mutations (no *VHL* changes)	Clear cell papillary RCC
8	Clear cell RCC	*VHL, PBRM1, SF3B1, TERT, TP53*	Clear cell RCC
9	Clear cell RCC with sarcomatous cells	*VHL, PBRM1, SET2, TP53*	Clear cell RCC with sarcomatous elements

Conclusions: NGS is a useful tool for subclassifying RCC with clear cells, papillary fronds, sarcomatous and leiomyomatous components. In addition to *VHL*, recurrent *PBRM1* alteration is found in clear cell RCC. Furthermore, *PBRM1* alterations may serve as a therapeutic target for precision therapy in clear cell RCC and its variants.

655 Cribriform Pattern Prostate Cancer and Associated Genomic Classifier (GC) Risk Scores in Asian Men

Joe Yeong[1], Adelene Sim[2], Enya Ong[2], Amanda Lau[2], Kar Low[2], Tian Wong[2], Nicole Tan[2], Alexander Hakansson[3], Yang Liu[3], Elai Davicioni[3], Kae Jack Tay[4], Chien Sheng Tan[5], Melvin Chua[2], Lui Lee[4], Li Yan Khor[4]
[1]Singapore General Hospital, Singapore, Singapore, [2]National Cancer Centre Singapore, Singapore, Singapore, [3]Veracyte, Inc., South San Francisco, CA, [4]Singapore General Hospital and Duke-NUS Medical School, Singapore, Singapore, [5]Changi General Hospital, SINGHEALTH, Singapore, Singapore

Disclosures: Joe Yeong: None; Adelene Sim: None; Enya Ong: None; Amanda Lau: None; Kar Low: None; Tian Wong: None; Nicole Tan: None; Alexander Hakansson: *Employee*, Veracyte; Yang Liu: *Employee*, Veracyte; Elai Davicioni: *Employee*, Veracyte; Kae Jack Tay: None; Chien Sheng Tan: None; Melvin Chua: *Grant or Research Support*, Decipher Biosciences; *Speaker*, Janssen; *Speaker*, Astellas; *Speaker*, Varian; *Speaker*, Pfizer; *Speaker*, Bayer; *Advisory Board Member*, MSD; *Consultant*, Immunoscape; *Consultant*, Telix pharmaceuticals; *Grant or Research Support*, EVYD technology, MedLever; Lui Lee: None; Li Yan Khor: None

Background: Cribriform pattern (CP) and intraductal carcinoma (IDC) subpathologies in prostate cancer harbor a constellation of adverse features like hypoxia and genomic instability, and are associated with distant metastasis and poor prognosis following radical prostatectomy or radiotherapy. Here, we searched for similar associations in a cohort of East Asian men using limited biopsy material.

Design: We performed a 22-gene genomic classifier (GC, Decipher Biosciences Inc., CA) on diagnostic biopsies of men at a single institution (N=251). Majority of men were treated with radiotherapy +/- hormonal therapy (N=215; 85.7%). The core with the highest ISUP Grade Group (GG) was selected for RNA extraction from 2 x 2.0-mm tumor cores using Qiagen AllPrep DNA/RNA FFPE Kit (Qiagen, Germany) and gene expression was performed on Affymetrix Human Exon 1.0 ST Array (ThermoFischer, CA). Presence of CP on histology (invasive and/or IDC) was recorded. Survival analysis by metastasis-free survival (MFS) was performed.

Results: Of the 251 patients, 94 (37.5%) were NCCN low- to intermediate-, 138 (55.0%) were NCCN high- and very-high-risk prostate cancers. The remainder (N=19; 7.6%) were regional risk. The CP-IDC cohort comprised of 109 (43.4%) cases. We observed a positive association between presence of CP-IDC and higher GG tumors; 25.6%, 54.0%, and 64.2% of GG2, 3 and 4-5 tumors harbored CP-IDC, respectively. Patients with CP-IDC+ve tumors also had higher PSA at diagnosis (10.6 vs 21.7 ng/mL, P<0.001; Table 1). 81 of 251 (32.3%) patients had GC data; among them, CP-IDC+ve tumors had a higher GC score than CP-IDC-ve tumors (median of 0.54 vs 0.35, P=0.009; Figure 1), and higher proportion of GC high risk (42.5% vs 19.5%; P=0.046). In the overall cohort (N=251) and when stratified by NCCN risk group, CP cases showed no significant relationships to MFS (median follow-up time = 42.5 months). Interestingly, GC was significantly associated with MFS when stratified by GC low-/intermediate- and high-risk (HR 4.7; 95% CI: 1.1 – 20, P=0.034).

Table 1: Cohort summary statistics.

Clinical characteristics	**Cribriform absent N=142**	**Cribriform present N=109**	**p**
Median age at diagnosis, yr (IQR)	69 (64–74)	70 (65–75)	0.14
PSA at diagnosis, ng/mL (IQR)	10.6 (7.1–20.5)	21.7 (10.1–59.3)	**<0.001**
Race Chinese Others	130 (91.5%) 12 (8.5%)	104 (95.4%) 5 (4.6%)	0.52
NCCN risk groups Low/Fav. intermediate Unfav. Intermediate High Very High Regional	51 (35.9%) 25 (17.6%) 25 (17.6%) 34 (23.9%) 7 (4.9%)	3 (2.8%) 15 (13.8%) 40 (36.7%) 39 (35.8%) 12 (11.0%)	**<0.001**
ISUP Grade Group 1 2 3 4 5	17 (12.0%) 67 (47.2%) 29 (20.4%) 12 (8.5%) 17 (12.0%)	0 (0.0%) 23 (21.1%) 34 (31.2%) 30 (27.5%) 22 (20.2%)	**<0.001**

Conclusions: We show that GC, performed on limited biopsy material, confirms CP-IDC is associated with higher risk scores in a predominantly NCCN high-risk cohort of Asian men. Despite their associations, CP-IDC and GC scores are prognostic indices that may be jointly applied for treatment decision making in localized prostate cancer.

656 A Comparative Analysis of Muscle-Invasive Urothelial Carcinoma Subtypes Using NanoString and Immunohistochemistry Markers

Yan Hong (Shirley) Yu[1], Ekaterina Olkhov-Mitsel[2], Christopher Sherman[2], Michelle Downes[2]
[1]Sunnybrook Health Sciences Centre, University of Toronto, Toronto, Canada, [2]Sunnybrook Health Sciences Centre, Toronto, Canada

Disclosures: Yan Hong (Shirley) Yu: None; Ekaterina Olkhov-Mitsel: None; Christopher Sherman: None; Michelle Downes: None

Background: Molecular subtypes of muscle invasive bladder cancer (MIBC) have distinct clinical behaviors and sensitivities to chemotherapy and immunotherapy. However, these molecular classifiers are based on multiomic technologies, which limits their utility and applicability to daily practice. In this study, we investigate NanoString-based and immunohistochemical (IHC) markers that would permit simple and cost-effective molecular classification of MIBC in a clinical setting.

Design: IHC classification was performed on MIBC radical cystectomy cohort (n=98) tissue microarrays sequentially stained with signature basal (CK5/6) and luminal (GATA-3) markers, with the latter subdivided into genomically unstable (GU, p16+) and urothelial like (Uro, p16-) subgroups. NanoString-based classification was performed on the same cohort using a novel 23-gene panel curated from the literature.

Results: IHC identified 64.3% luminal (CK5/6-, GATA3+), 30.6% basal (CK5/6+, GATA3-) and 5.1% double negative (CK5/6-, GATA3-) cases in our cohort. Within the luminal subgroup (n=63), 30 cases were classified as GU and 33 as Uro. Unsupervised hierarchical and consensus clustering performed on NanoString gene expression data identified two groups as the optimal number of molecular subtypes, with cluster I consisting of 29 of the 30 IHC basal cases and 8 luminal cases (4 Uro + 4 GU) while cluster II included 55 luminal (26 GU+29 Uro), 1 basal and 5 DN cases (Figure 1). Concordance between IHC classification and NanoString-based molecular subtypes was good ($\kappa = 0.791$, $p<0.001$). Differentially expressed genes identified between luminal and basal subtypes included upregulation of FOXA1, GATA3, KRT20, SNX31, UPK1A, UPK2 and UPK3A in the luminal subtype and DSG3, KRT5, KRT6C, KRT14, KRT16, KRT17 in the basal subtype. The technical cost of the custom NanoString panel was $148.14/sample while the cost of the 3 antibody IHC panel was $43.86/sample.

Figure 1 - 656

Figure 1. Hierarchical clustering heatmap of MIBC radical cystectomy cohort (n=98). Gene expression profiling was performed via NanoString custom panel of 23 genes. Values are log2-transformed, normalized mRNA counts.

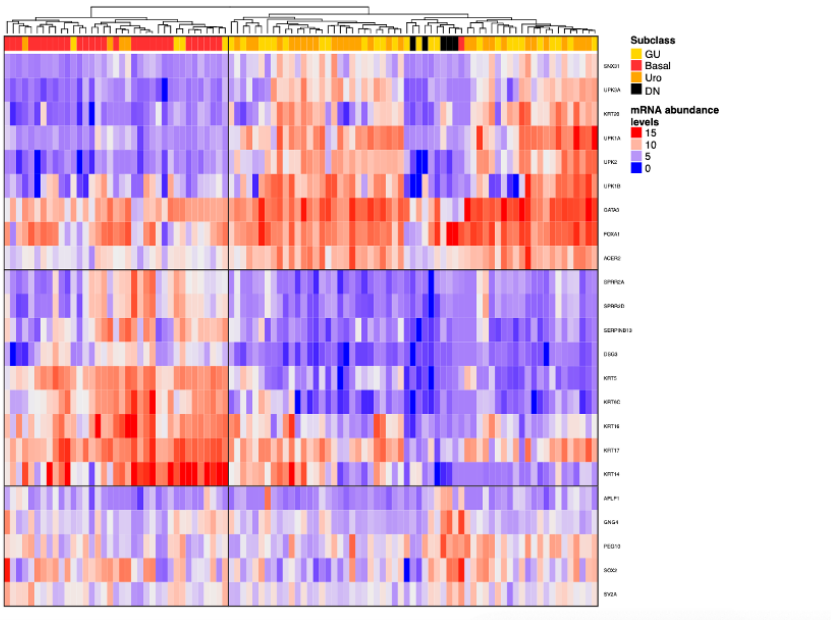

Conclusions: We report good concordance between a novel 23-gene transcriptomic panel and conventional IHC which could serve as less expensive alternatives to whole RNA sequencing for MIBC molecular subtyping in routine clinical practice.

657 The Impact of Cribriform Pattern 4 and Intraductal Prostatic Carcinoma on NCCN and CAPRA Patient Stratification

Yan Hong (Shirley) Yu[1], Katherine Lajkosz[2], Theodorus Van Der Kwast[3], Michelle Downes[4]
[1]Sunnybrook Health Sciences Centre, University of Toronto, Toronto, Canada, [2]Laboratory Medicine Program, Toronto General Hospital/University Health Network, Toronto, Canada, [3]University Health Network, Toronto, Canada, [4]Sunnybrook Health Sciences Centre, Toronto, Canada

Disclosures: Yan Hong (Shirley) Yu: None; Katherine Lajkosz: None; Theodorus Van Der Kwast: None; Michelle Downes: None

Background: Pretreatment classification tools using biopsy data are used in prostate cancer to inform patient management. Data suggests nomograms such as CAPRA outperform D'Amico- and D'Amico derived (e.g. NCCN) in predicting prostate cancer death. The effect of cribriform architecture pattern 4 (CC) and intraductal carcinoma (IDC) on such nomograms is still unknown. We analyzed the CAPRA and NCCN nomograms in cases with and without CC/IDC to assess impact on biochemical (BCR) and metastases/death of prostate cancer (event free survival-EFS) after prostatectomy.

Design: A matched biopsy- prostatectomy cohort (2010-2017) was reviewed for CC/IDC. Age, serum PSA, biopsy grade group, number of cores, prostatectomy grade and stage and clinical follow up were collected. CAPRA and NCCN scores were calculated. CAPRA score 0-2 were deemed "low", 3-5 "intermediate" and 6-10 "high". NCCN scores 1-2 "very low/low", 3 "favorable intermediate", 4 "unfavorable intermediate", 5-6 "high/very high". Cases were stratified by presence of CC/IDC. BCR and EFS probabilities were estimated using the Kaplan-Meier method. Prognostic performance was evaluated using log-rank tests and Harrell's concordance index.

Results: 496 patients with mean age 63.2 years and mean follow up of 4.9 (range 0-10.8) years were included. 133/496 (27%) biopsies had CC/IDC. The biopsy grade groups were as follows: GG1 (77-16%), GG2 (278-56%), GG3 (80-16%), GG4 (34-7%) and GG5 (25-5%). There were 87 (18%) BCR and 38 (8%) events (Table 1). CAPRA discriminated 3 distinct risk categories for BCR ($p<0.001$) while only high risk separated significantly for EFS ($p<0.001$). NCCN distinguished only two prognostic groups for BCR ($p<0.001$) and three for EFS ($p<0.001$). Addition of CC/IDC to CAPRA mainly impacted scores 3-5 both for both BCR and

EFS (Table 1) and improved the overall concordance index (BCR: 0.66 vs. 0.71; EFS: 0.74 vs. 0.80). Addition of CC/IDC to NCCN mainly impacted score 4 (Table 1) and also improved the concordance index (BCR: 0.62 vs. 0.68; EFS: 0.75 vs. 0.81). Regarding EFS, NCCN score 4 CC/IDC+ behaved more unfavourably then NCCN scores 5-6 that were CC/IDC-.

Table 1: Survival estimates at 8 years:

Stratification Tool	BCR (8 year survival)		P value	EFS (8 year survival)		P value
	CC/IDC+	CC/IDC-		CC/IDC+	CC/IDC-	
CAPRA 0-2	NA	0.95 (0.90-1.00)	<0.0001	NA	1.00 (1.00-1.00)	<0.0001
CAPRA 3-5	0.61 (0.47-0.79)	0.80 (0.73-0.89)		0.83 (0.71-0.98)	0.94 (0.89-1.00)	
CAPRA 6-10	0.47 (0.33-0.68)	0.49 (0.26-0.94)		0.60 (0.46-0.78)	0.79 (0.64-0.99)	
NCCN 1-2	NA	0.84 (0.72-0.99)	0.0037	NA	1.00 (1.00-1.00)	<0.0001
NCCN 3	0.69 (0.49-0.99)	0.91 (0.85-0.98)		0.93 (0.83-1.00)	0.95 (0.88-1.00)	
NCCN 4	0.54 (0.42-0.71)	0.79 (0.70-0.89)		0.79 (0.67-0.92)	0.94 (0.88-1.00)	
NCCN 5-6	0.47 (0.27-0.82)	0.62 (0.39-0.98)		0.62 (0.45-0.85)	0.85 (0.74-0.99)	

Conclusions: The CAPRA nomogram allows better outcome stratification than NCCN. Addition of CC/IDC status particularly improves patient stratification for CAPRA scores 3-5 and NCCN score 4.

658 Sarcomatoid and Rhabdoid Differentiation in Renal Cell Carcinoma

Bassel Zein-Sabatto[1], Brian Ceballos[1], Sofia Canete-Portillo[1], Soroush Rais-Bahrami[1], Cristina Magi-Galluzzi[1]
[1]*The University of Alabama at Birmingham, Birmingham, AL*

Disclosures: Bassel Zein-Sabatto: None; Brian Ceballos: None; Sofia Canete-Portillo: None; Soroush Rais-Bahrami: None; Cristina Magi-Galluzzi: None

Background: Renal cell carcinoma (RCC) with sarcomatoid (SARC) or rhabdoid (RHAB) differentiation is considered as ISUP/WHO grade 4 and associated with poor outcome. We aim to evaluate the histologic subtypes of RCCs associated with SARC and/or RHAB features and assess the relationship with clinical outcome in different ethnic groups.

Design: RCC with SARC and/or RHAB differentiation diagnosed at one institution between 2000 and 2020 were reviewed. Cases were classified based on histologic subtypes, race, and differentiation (SARC, RHAB, or SARC+RHAB). Patients' charts were reviewed for clinical outcome. Kaplan-Meier analysis was used to assess survival.

Results: A total of 88 cases were included in the study. Mean patient age was 61 years (range: 32-88) with 2:1 male-to-female ratio. 62 (70%) patients were Caucasian, 10 (11%) Black/African American (B/AA), and 16 (18%) of unknown ethnicity. Mean tumor size was 9.7 cm (range: 1.5-25). Most cases (n=70, 80%) presented with advanced stage pT3 and pT4. Clear cell RCC (CCRCC) was the most common histologic subtype with 68 (77%) cases; 6 (7%) and 4 (5%) cases were papillary RCC (PRCC) and chromophobe RCC (ChRCC), respectively. Ten (11%) cases were unclassified RCC, 3 of which occurred in B/AA patients. Clinical and histologic characteristics are summarized in Table 1.

SARC features were seen in 55 (63%) patients, RHAB features in 16 (18%), and 17 (19%) showed SARC+RHAB. RHAB without SARC differentiation was not observed in B/AA. RHAB without SARC differentiation was associated with either CCRCC or unclassified RCC, but not with ChRCC or PRCC. Although 7 (44%) patients with RHAB differentiation alone presented with metastasis, and 4 (25%) developed metastases later in the disease course, they were all alive at follow-up (median: 12 months; range: 2-43) (Figure 1).

	Chromophobe	*Clear*	*Papillary*	*Unclassified*	*Total*
N (%)	4 (5)	68 (77)	6 (7)	10 (11)	**88 (100)**
Mean age, years *(range)*	64 (42-84)	61 (32-86)	57 (34-88)	60 (47-76)	**61 (32-88)**
Female *N (%)*	2 (7)	20 (69)	2 (7)	5 (17)	**29 (33)**
Male *N (%)*	2 (3)	48 (81)	4 (7)	5 (8)	**59 (67)**
B/AA *N (%)*	1 (10)	4 (40)	2 (20)	3 (30)	**10 (11)**
Caucasian *N (%)*	1 (2)	53 (85)	2 (3)	6 (10)	**62 (70)**
Unknown *N (%)*	2 (13)	11 (69)	2 (13)	1 (6)	**16 (18)**
Mean size, cm *(range)*	11.7 (4.7-16)	9.9 (1.5-25)	8.6 (3.9-15)	8.6 (4-12)	**9.7 (1.5-25)**
SARC *N (%)*	3 (5)	41 (75)	6 (11)	5 (9)	**55 (63)**
RHAB *N (%)*	0 (0)	14 (88)	0 (0)	2 (12)	**16 (18)**
SARC+RHAB *N (%)*	1 (6)	13 (76)	0 (0)	3 (18)	**17 (19)**
AWD *N (%)*	1 (2)	46 (79)	4 (7)	7 (12)	**58 (66)**
DOD *N (%)*	2 (17)	8 (67)	1 (8)	1 (8)	**12 (14)**
NED *N (%)*	1 (6)	14 (78)	1 (6)	2 (11)	**18 (20)**
Mean F/U, months (range)	17 (0-42)	18 (0.1-126)	16 (1-69)	10 (2-21)	**17 (0-126)**
pT1	0 (0)	7 (70)	2 (20)	1 (10)	**10 (11)**
pT2	0 (0)	6 (86)	0 (0)	1 (14)	**7 (8)**
pT3	4 (6)	49 (75)	4 (6)	8 (12)	**65 (75)**
pT4	0 (0)	5 (100)	0 (0)	0 (0)	**5 (6)**
LN+ at presentation	0 (0)	7 (78)	1 (11)	1 (11)	**9 (10)**
Metastasis at presentation	3 (6)	38 (79)	2 (4)	5 (10)	**48 (55)**
Additional metastasis at F/U	2 (4)	41 (73)	5 (9)	8 (14)	**56 (64)**
Treatment (immunotherapy or chemotherapy)	1 (2)	32 (76)	3 (7)	6 (14)	**42 (48)**
No treatment	3 (7)	36 (78)	3 (7)	4 (9)	**46 (52)**

Table 1. Clinical and histologic characteristics; **AWD**: alive with disease, **DOD**: dead of disease, **NED**: No evidence of disease, **LN+**: positive lymph nodes, **F/U**: Follow-up.

Figure 1 - 658

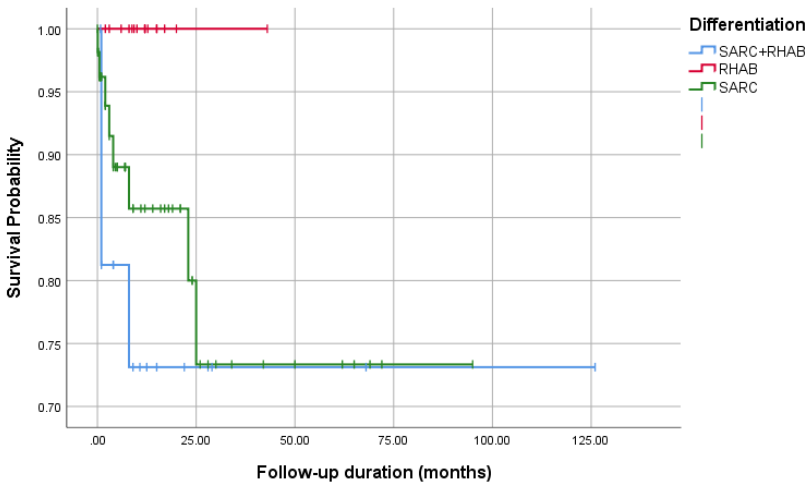

Conclusions: CCRCC was the most common RCC associated with SARC/RHAB differentiation. Unclassified RCC with SARC/RHAB differentiation was more common in B/AA patients than in Caucasians. RHAB without SARC differentiation was not observed in B/AA patients. Although the sample is small, our findings suggest that SARC differentiation appears to drive the aggressive behavior rather than RHAB differentiation, especially in B/AA population. Further studies are needed to assess the impact of RHAB differentiation in absence of SARC differentiation.

659 Significance of Extraprostatic Extension (EPE) on Needle Core Biopsy of Grade Groups 1-3 Prostatic Adenocarcinoma (PCa)

Jianping Zhao[1], Jonathan Epstein[2]
[1]Johns Hopkins Hospital, Baltimore, MD, [2]Johns Hopkins Medical Institutions, Baltimore, MD

Disclosures: Jianping Zhao: None; Jonathan Epstein: None

Background: EPE on prostate needle biopsy is uncommon and typically associated with extensive Grade Groups (GG) 4-5 prostatic adenocarcinoma on biopsy such that the EPE typically doesn't add prognostic information. No study has specifically addressed the rare scenario of EPE on biopsy with GG 1-3 prostatic adenocarcinoma.

Design: We retrieved 38 cases where GG1-3 prostatic adenocarcinoma was the highest grade in the case with EPE on needle biopsy from our consultation files between 2019 and 2021, consisting of ~9,000 prostate cancers per year.

Results: The highest grade part in the case was: GG1 (n=4); GG2 (n=15), and GG3 (n=19). The mean (range) age of the patients was 66 (45–83) years. The mean (range) serum PSA level was 12 (1.6–78.9) ng/mL. The mean % of cores with PCa was 76%. The mean % of PCa in each involved core per case was 51.6%, and in the core(s) with EPE was 59.5%. Perineural invasion was identified in 32 cases (84%) and cribriform pattern 4 was documented in 23 out of 29 cases (79%) with available information. Of 37 men with clinical follow-up data, 18 (49%) received radiation and/or hormonal therapy (RT),13 patients (35%) either underwent (n=11) or are planning (n=2) radical prostatectomy (RP), and 6 patients (16%) received either ablation therapy or active surveillance. Of 10 RP cases, 8 were GG2, one GG3 with tertiary pattern 5, and one GG3. Only one had more advanced stage than seen on the biopsy with pT3bN1 disease. Of the 10 RP cases, 6 cases had positive margins. We evaluated whether the favorable findings at RP could result from a selection bias where men with more favorable pre-operative findings underwent RP and men with worse disease underwent RT. The only difference between the 2 groups in their pre-treatment parameters was the mean age of the RP patients was 61 compared to 69 for the RT men (p=0.02). There were no differences between the 2 groups in terms of serum PSA levels, % positive cores, % PCa per core, percent Gleason pattern 4, or Grade Group.

Figure 1 - 659

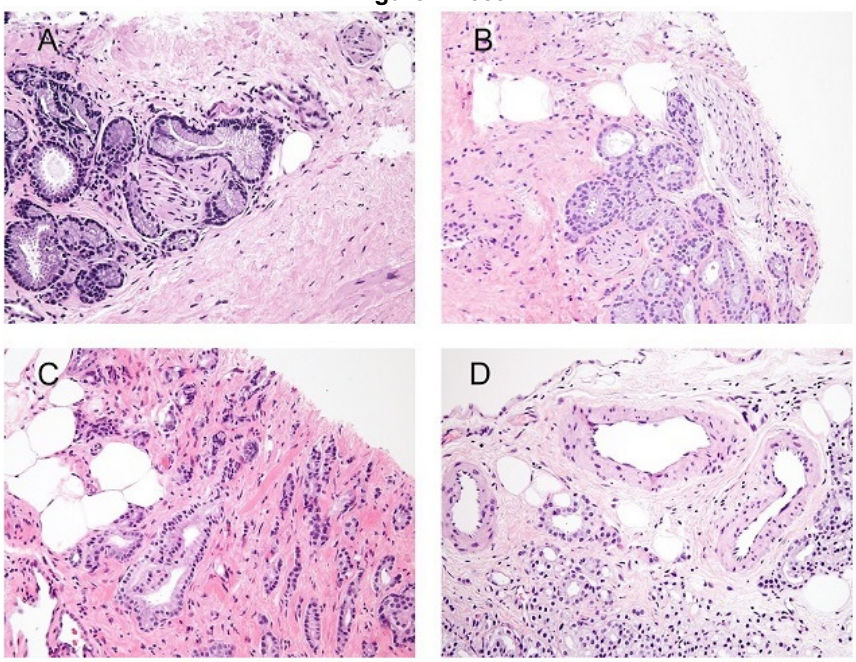

Prostatic adenocarcinoma involving peri-prostatic adipose tissue on needle biopsy with GG1 (A-B), GG2 (C), and GG3 (D).

Conclusions: Our findings suggest that despite EPE on biopsy, most had relatively favorable findings at radical prostatectomy, and radical prostatectomy is a viable treatment option in this setting. Additional follow up will be needed to determine the prognosis for patients with EPE who had radiation and/or hormonal therapy.